

A Thesis for the Degree of Ph.D. in Engineering

Hierarchical Modeling of Tactile Sensation
based on Human Perception and
Augmentation of Thermal Perception using
Spatial Summation

June 2021

Graduate School of Science and Technology
Keio University

Iza Husna Binti Mohamad Hashim

Acknowledgements

بِسْمِ اللَّهِ الرَّحْمَنِ الرَّحِيمِ

In the name of Allah, the most gracious and the most merciful

Alhamdulillah, first of all, I would like to express my gratitude to the Almighty for blessing me with strength and courage to complete this thesis. From the beginning till the end of this thesis, I have so many people who stood by me; given me guidance for every obstacle that stand in my way. Therefore, I would like to express my deepest appreciation to those involved in this thesis.

First and foremost, I would like to express my gratitude and millions of thanks to my thesis supervisor, Prof. Dr. Kenjiro Takemura, who always been very helpful and encouraging through the whole year. Thank you for supporting me with ideas and guidance consistently till the last second. I would also like to express my appreciation to Prof. Takashi Maeno for the endless guidance for the research. I take this chance to express my appreciation towards colleagues from Asahi Kasei Corporation, Sumi Nakamura, Narumi Saegusa and others for collaborating and assisting me in every way possible to conduct this research. I am also profoundly grateful to everyone in Takemura Laboratory: Kiho Kobayashi, Asuka Kobari, Kyohei Hosoda, Kazuki Takahashi, Yuta Kurashina, Shogo Kumamoto, Shosho Ou, Yuki Shiyama, Toshiyuki Wada, Takuma Ueyama, Ayana Hoshi, Chikahiro Imashiro, Hiroki Eguchi and Yoshiki Iijima for augmenting this project with their priceless guidance, ideas and critics to make the best of this thesis. My deepest appreciation also goes out to the tactile and haptic team in Graduate School of System Design and Management for their bright ideas, critics, and insights in the area. I would like to express my appreciation to my beloved parents Salmah Binti Omar and Mohamad Hashim Bin Abdul Latiff for the unconditional love and support that let me through the toughest days in my life. Then, for my beloved siblings, Siti Farhana and Iza Shafinaz, for helping me with love. Last but not least, for my partner until the life hereafter, Abdul Raziz bin Junaidi for always be encouraging and supportive. For those who are not stated here, I would like to thank for their help, friendship and countless support to me.

7th May 2021

Iza Husna Binti Mohamad Hashim
Keio University, Faculty of Science and Technology

ABSTRACT

The interest in haptic technology has been growing exponentially in recent years due to its capabilities in accelerating product development cycles especially in analysis and design stage. It is primarily due to the significance in tactile sensations in consumer. By introducing haptic technology in the manufacturing industry, new products can be developed rapidly, thus allowing higher rate of production to satisfy the booming market demand. The integration of haptic technology, namely tactile rendering will be a great aid in product development industries as it can manipulate the prototype's touch sensation to the chosen material's touch sensation without producing a sample of the product. Furthermore, to evaluate new products, manufacturers need to conduct a sensory evaluation which is a time consuming and costly process. Therefore, a need to quantify tactile sensation is explored to accelerate the product development.

In this research, we investigate the significance of tactile rendering and sensation technologies in manufacturing industry. For tactile rendering, we focus on the impact of spatial summation for augmentation of thermal sense in AR thermal display. The proposed display is used to replicate the material identification, in order to allow users experience various materials without changing the material of an object. In tactile sensation, we present a novel quantification method of human tactile sense evaluation for fabrics to provide a reliable quality assessment method for textile industry. We hierarchically classify adjectives into three groups called as low-order of tactile sensation (LTS), high-order of tactile sensation (HTS) and desired tactile sensation (DTS). We then perform a multiple regression analysis to discover the correlations between each extracted LTS factor and all measured physical quantities. We express DTS adjectives in terms of physical quantities by computing equations. From the proposed quantification, we are able to predict or evaluate unknown samples' tactile sensation.

CONTENTS

CHAPTER 1 Introduction	1
1.1 Background.....	1
1.2 Related Works.....	5
1.2.1 Tactile Rendering Technologies.....	5
1.2.2 Tactile Sensing Technologies.....	12
1.3 Objective.....	17
CHAPTER 2 Human Somatosensory Mechanism	19
2.1 Mechanoreceptors.....	20
2.1.1 Meissner’s Corpuscle.....	21
2.1.2 Pacinian Corpuscle.....	22
2.1.3 Merkel’s Corpuscle.....	22
2.1.4 Ruffini Ending.....	23
2.2 Thermoreceptors.....	24
2.3 Nocireceptors.....	24
CHAPTER 3 Modelling of Tactile Sensation	25
3.1 Concept for Modelling of Tactile Sensation.....	25
3.1.1 Human Tactile Sense Evaluation.....	25
3.1.2 Modelling of Tactile Sensation.....	28
3.2 Modelling of Tactile Sensation for Door Armrest.....	30
3.2.1 Classification of Adjectives.....	30
3.2.2 Sensory Evaluation.....	31
3.2.2.1 Principal Component Analysis.....	33
3.2.2.2 Multiple Regression Analysis.....	35
3.2.3 Discussions.....	46
3.3 Modelling of Tactile Sensation for Fabrics.....	48
3.3.1 Classification of Adjectives.....	48
3.3.2 Sensory Evaluation by Hand.....	52
3.3.2.1 Principal Component Analysis.....	53

3.3.2.2 Multiple Regression Analysis	57
3.3.3 Sensory Evaluation by Forearm	66
3.3.3.1 Principal Component Analysis	67
3.3.3.2 Multiple Regression Analysis	71
3.3.4 Discussions.....	83
CHAPTER 4 Quantification for Human Tactile Sensation	85
4.1 Quantification Tactile Sensation for Door Armrest	86
4.1.1 Data Collection of Physical Quantities	86
4.1.1.1 Vibration.....	86
4.1.1.2 Bulk Displacement.....	88
4.1.1.3 Thermal Properties	88
4.1.1.4 Friction Force	89
4.1.2 Quantification of Tactile Sense Evaluation	90
4.1.2.1 Principal Component Analysis.....	90
4.1.2.2 Multiple Regression Analysis	91
4.1.2.3 Discussions.....	92
4.1.2.4 Verification Test of Quantified Tactile Sense Evaluation	94
4.2 Quantification Tactile Sensation for Fabrics	95
4.2.1 Data Collection of Physical Quantities	96
4.2.1.1 Physical Properties of Fabrics.....	97
4.2.1.2 Physical Quantities Measured by using Commercialized Tactile Sensor	100
4.2.1.3 Physical Quantities Measured by using Proposed Tactile Sensor.....	101
4.2.2 Quantification of Tactile Sense Evaluation by Hand	112
4.2.2.1 Multiple Regression Analysis	112
4.2.2.2 Discussions.....	121
4.2.2.3 Verification Test of Quantified Tactile Sense Evaluation	123
4.2.3 Quantification of Tactile Sense Evaluation by Forearm	126
4.2.3.1 Multiple Regression Analysis	126
4.2.3.2 Discussions.....	134
4.2.3.3 Verification Test of Quantified Tactile Sense Evaluation	136
4.2.4 Summary	138
CHAPTER 5 Augmented Reality Thermal Display	140
5.1 Concept for Thermal Display	140

5.1.1 Thermal Perception	140
5.1.2 Spatial Summation	141
5.1.3 Method of Display	142
5.1.4 Proposed AR Thermal Display.....	142
5.2 Development of Augmented Reality Thermal Display	144
5.2.1 Design and Hardware Implementation of Display System	145
5.2.1.1 Peltier Device Driver Circuit	147
5.2.1.2 Thermal Sensor Circuit	152
5.2.1.3 Microcontroller Board.....	154
5.2.2 Peltier Device's Temperature Feedback Control	155
5.2.3 Structure of Program	158
5.3 Experiment of Spatial Summation.....	158
5.3.1 Back of Hand Stimulated in Advance	160
5.3.1.1 Apparatus	160
5.3.1.2 Methods.....	162
5.3.1.3 Results and Discussions	166
5.3.2 Back of Hand and Palm Stimulated Simultaneously	169
5.3.2.1 Apparatus	169
5.3.2.2 Methods.....	169
5.3.2.3 Results and Discussions	171
5.4 Discussions	181
CHAPTER 6 Conclusion	182
References	186
Appendix	196

Chapter 1

INTRODUCTION

1.1 Background

Human has five traditionally recognized senses: sight, hearing, taste, smell, and touch (Hellier, 2016). Through these senses, we can perceive the surroundings' changes and respond to the particular physical phenomenon. Each of the senses has a specific organ that runs specific tasks. There are sensory receptors in the sensory organs that will produce signals, and the signal will be sent via networks of neurons to the brain, where the signals are being processed and interpreted.

Among all these senses, touch has the most prominent organ called the skin that covers every part of the body. Furthermore, skin also acts as the first line of defense from the intrusion of viruses and bacteria. Skin is so vital that it is the first natural instinct of living for us from newborns, as touch appears not just to soothe and relax us but also to enhance our growth and comfort level. For example, Dr. Harry Harlow had conducted an experiment where infant monkeys were separated from their mothers a few hours after birth and provided with a folded gauze diaper on their cage floor (Harry, 1959). From this experiment, the infant monkeys have deep personal attachments towards diaper pads and exhibited distress when the pads were removed once a day for sanitation purposes. Furthermore, the discovery shows impressive enlightenment that the sense of touch is inevitable in our daily life, although we do not personally realize and appreciate it.

Haptics is a study field that is related to the sense of touch. This word derives from the Greek, which means “being able to come into contact” (Mudit Ratana, Harsh Vardhan, & Anand Vardhan, 2010). After the rise of the nuclear industry in the 1950s, the first haptic feedback master-slave telemanipulation system was developed in the United States. Then, this haptic

technology was used in military flight simulators in the 1960s to imitate the tactile and kinesthetic cues of real flight. From the late 1970s, visual and audio media developed tremendously fast, and now, the interfaces are widely used in everyday life. However, the haptic interface is far behind compared to the visual and audio interfaces as haptics is complex and challenging to synthesize (Iwata, 2008). Until now, haptic technology has been applied in various fields, including entertainment, medical, military, communication, aviation, and many more. Currently, new product development in the manufacturing industry has become a promising application area for haptic technology (Pingjun, 2016).

In recent years, the competition in the world market for manufactured products has intensified enormously. The rapid development of new products has become the top priority in many manufacturing industries to commercialize emerging technology and satisfy customer needs. Hence, it is essential for new products to shorten product design to the market as fast as possible (Y. Chen, Yang, & Lian, 2005). Besides shorter time-to-market, affordable prices and high quality of a product are also crucial factors for the manufacturing industry to compete effectively in the world market. Consequently, the processes involved in the design, test, manufacture, and market of the product have been squeezed regarding time and cost. Figure 1.1 shows one of the primary product development cycles, which starts from the analysis and design stage (Seeram, Lingling, Charlene, Susan, & Wee Eong, 2015). This cycle adopts multiple

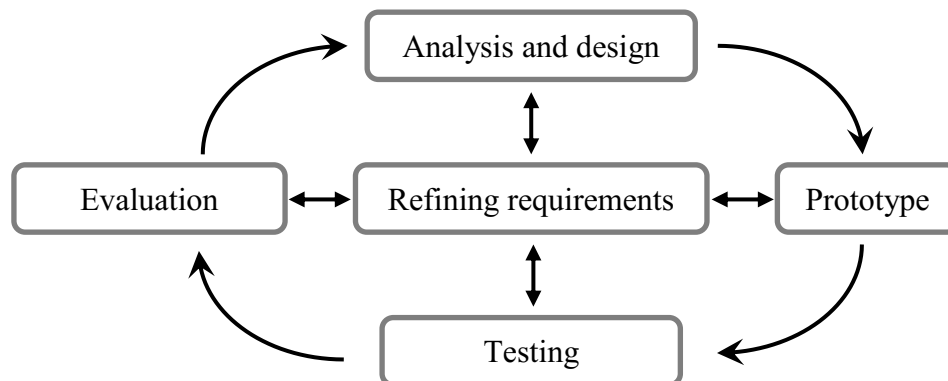


Figure 1.1 Product development cycle

iterations of the products from customer feedback at the early stage of the development. Hence, this may help the manufacturing industry to survive in rapidly changing markets.

There have been many efforts introduced and developed to shorten the product development cycle time. Recently, haptic technology has been introduced in the manufacturing industry, especially in the analysis and design stage. Haptic technology is practically used to aid computer-aided engineering, CAE (Y. Chen et al., 2005). As the high power of computing technologies, there are many aspects of work that can be done in a virtual environment, such as shape modeling and reverse engineering. For this task, a commercial haptics device like Touch X from 3D System Corporation is commonly used ("3D Systems: Scanners and Haptics," 2017). By using haptic shape modeling, the designers can trace, touch, feel, deform or grasp virtual objects. Moreover, the product can be evaluated some of the functional performances in the early stage. For example, when designing a toothbrush, the designer may want to make sure the toothbrush is not too hard, mainly when used by children. From the haptic modeling, the designer can feel the stiffness of a toothbrush's neck and change the material or geometry of the brush neck. Hence, the designer may iterate the product's design on the tactile aspect from building and testing the product virtually compared to traditional product simulation.

Currently, haptic technology has also become one of the promising approaches for prototype and evaluation stages to reduce time-taken for a product to reach the market. For the prototyping stage, rapid prototyping has been developed over the past few decades and proven to shorten the lead time by 60 % compared to conventional technologies such as numerical control milling (Lan, 2009). Rapid prototyping is a novel technology in forming process where physical parts are fabricated layer by layer to form three-dimensional computer-aided design, 3D CAD models in a short time (Lan, 2009). Rapid prototyping can also be referred to as solid free-form manufacturing, computer automated manufacturing, and layered manufacturing.

The prototypes are generally used for market research, typically to acquire customers' requirements. Besides, the prototypes can also be powerful communication tools among designers for better understanding (Lan, 2009). Also, through prototypes, any mistake is easy to be discovered and corrected, and most importantly, modifications can also be made while the prototypes are still inexpensive. Although the materials used for rapid prototyping usually are

affordable compared to conventional technologies, the range of materials is limited and mostly available for plastic. As a result, in order to use other materials, the prototypes have to be made by using conventional technologies, and eventually, it will lengthen development time and also increase the cost. Even though the product's appearance and function are vital factors for a product, touch sensation also gives an added value with significant impact in the highly competitive market (Grohmann, Spangenberg, & Sprott, 2007; Peck & Childers, 2002, 2003, 2006). In addition, Citrin et al. demonstrate that individuals with a higher need for tactile input when making decision of product will be less likely to purchase products over the Internet as tactile cues are absent (Citrin, Stem, Spangenberg, & Clark, 2003). Although the need for tactile cues will vary across consumers, it is clear that tactile cues are essential in decision making. Therefore, the integration of tactile rendering technologies in rapid prototyping is a new approach to rendering various touch or tactile sensations. The related research on tactile rendering technologies will be introduced in Section 1.2.1.

On the other hand, for the evaluation stage, customer feedback on a product is essential to review the product's acceptance or preference. There are many perspectives of the feedbacks such as appearance, durability, functionality, expected price, and many more. Besides, touch or tactile sensation also plays a crucial role in determining the preference of a product (Grohmann et al., 2007; Schmitt, Falk, Stiller, & Heinrichs, 2015), as mentioned in the previous paragraph. Although the impact of tactile sensation will vary across the types of products, the tactile sensation can affect the evaluation of the product's quality (Grohmann et al., 2007).

Besides, McCabe and Nowlis also prove that tactile cues significantly affect impulse purchasing. Buying impulsiveness refers to the tendency of a customer to buy spontaneously (McCabe & Nowlis, 2003). Peck and Childers also reported that there is a positive and significant correlation between the need for tactile input and buying impulsiveness (Peck & Childers, 2003); increment of the necessity for tactile input will increase the buying impulsiveness of the customer. Apart from that, the confidence level in product evaluations increases with tactile input (Peck & Childers, 2002, 2003). Generally, tactile input will lead to positive consumer responses; acceptable quality level.

Additionally, Grohman et al. reveal the effects of tactile input on product evaluation. Furthermore, the tactile input can also result in the quality of a product. In the experiment, for high-quality products, tactile input positively affects the evaluation of products and vice versa (Grohmann et al., 2007). Overall, tactile cues play an important role in making product evaluations, whether in the perception of product quality or decision making.

Conventionally, most manufacturing industries use sensory evaluation to evaluate a product as this method gives direct feedback from the customers, and it is the most comprehensive method (Kemp, Hollowood, & Hort, 2009). Sensory evaluation is a scientific method used to measure, analyze, and interpret qualitative responses from our senses (Stone, Bleibaum, & Thomas, 2012). Unfortunately, the feedback from this method may not be applicable for newly modified or developed products. Furthermore, this method can be a time-consuming and costly process (Lawless & Heymann, 2010). Consequently, a quantification method of tactile sensation is crucial in improving the conventional way of manufacturing industries evaluate their product at low cost and fast in time. Thus, introducing tactile sensing technologies in the product's evaluation method is a new and worthwhile practice. This may also help manufacturing industries to understand the main factors that correlate with customers' preferences. The related research on tactile sensing technologies will be presented in Section 1.2.2.

1.2 Related Works

In this section, based on the fundamental knowledge of the human sense of touch, haptics technologies including tactile rendering and sensing that have been developed will be introduced.

1.2.1 Tactile Rendering Technologies

In general, tactile rendering or display can be divided according to the type of tactile information such as roughness/smoothness, hardness/softness, stickiness/slipperiness, and warmness/coldness (Shirado & Maeno, 2014; Yamauchi et al., 2010). Besides, tactile display can

also be classified by the display method of tactile information; Virtual Reality (VR) and Augmented Reality (AR) technologies. VR is a computer-simulated environment where the user is totally immersed in. This utterly synthetic world may mimic the properties of real world environment either fictional or nonfictional (Milgram & Kishino, 1994). On the other hand, AR is a novel human-machine interaction that allows the user to see the real world with the superimposed upon or composited with the real world (Rekimoto, 1997). AR blurs the boundary between reality and computer-generated by enhancing what we see, hear, feel and smell and has been found as fine potential applications in many fields (Ong, Yuan, & Nee, 2008).

Roughly, as shown in Table 1.1, this clause will explore conventional tactile display based on two types of tactile stimuli: mechanical (roughness, hardness, and friction) and thermal information, and display method of the information.

In general, tactile displays are used to provide roughness and hardness information of an

Table 1.1 Classification of tactile rendering or display

Receptors included	Display method	Related works
Mechanoreceptor	VR	<ul style="list-style-type: none"> • Tactile feedback for teleoperation (Sarakoglou, Garcia-Hernandez, Tsagarakis, & Caldwell, 2012) • Tendon electrical stimulation (Kajimoto, 2012) • ExoInterfaces (Tsetserukou, Sato, & Tachi, 2010)
	AR	<ul style="list-style-type: none"> • Fingertip display system (Ando et al., 2007) • REVEL (Bau & Poupyrev, 2012) • High precision AR haptics display (Bianchi, Knörlein, Székely, & Harders, 2006) • TeslaTouch (Bau, Poupyrev, Israr, & Harrison, 2010) • Force feedback AR haptics display (Zhao, Huang, Lu, & Liu, 2017)
Mechanoreceptor and thermoreceptor	VR	<ul style="list-style-type: none"> DGIS (Caldwell et al., 1996) TELESAR V (Fernando et al., 2012) VITAL (Khoudja & Hafez, 2004)

object in virtual environment. Consequently, the integration of thermal feedback into tactile displays is a relatively new concept. Several studies have shown how thermal cues can provide information about the object's temperature and thermal properties that assist in object identification and material discrimination when other cues, such as surface texture are minimized (Dyck, Curtis, Bushek, & Offord, 1974; Ho & Jones, 2006; L. A. Jones & Berris, 2003). As a result, a more realistic image can be created with thermal information in a virtual environment. Therefore, the integration of thermal information into conventional tactile displays can improve the tactile displays that only have the mechanical information: roughness, hardness, and friction.

In this research, using this new concept of the tactile display, the tactile information of a certain material can be manipulated or deluded to any materials. In other words, this proposed tactile display can solve the limitation of materials in rapid prototyping technologies. As a result, this research proposes a tactile display that can provide all of the tactile information in rapid prototyping technologies and at the same time, reduces lead time and cost, which have been significant factors in determining the success in product development.

a) Mechanical Stimulated Tactile Display for VR

In the past decades, VR tactile displays which create stimulation of roughness and friction that are mechanically stimuli have enormously developed. This clause will introduce two methods of displaying mechanical stimuli: (i) mechanical and (ii) electrical actuation.

(i) VR Tactile Display using Mechanical Actuation

Sarakoglou et al. (2012) developed a compact tactile: roughness, friction and hardness, and force feedback display for integration in teleoperation (Sarakoglou et al., 2012). The tactile display contains of a fingertip display module, a flexible tendon transmission, and the actuation unit. The fingertip module houses 16 vertically moving tactors that are cylindrical with flat top end and round edge. These tactors move perpendicularly to the skin surface and typically convey information on roughness, friction, and roughness. This information is perceived by slowly

adapting and rapidly adapting mechanoreceptors. It is integrated on Omega7 ("Force Dimension: Products," 2017) force feedback device.

This tactile display achieves a compact design with superior performance in terms of spatiotemporal resolution, force, and amplitude. Furthermore, the ergonomic design of this tactile display makes it suitable for integration on haptic devices in teleoperation. However, this device does not provide visual and thermal feedback for teleoperation. It would need a further study on visual feedback for exploration and recognition of remote surfaces, and thermal feedback for assisting in material identification.

(ii) VR Tactile Display using Electrical Actuation

Kajimoto proposed to use electrical stimulations to tendons in order to create a kinesthetic illusion (Kajimoto, 2012). The illusion was generated by the activity of the muscle spindles, which are indirectly stimulated by vibratory input to the tendon. However, it would inevitably stimulate muscle efferent nerves that cause motion. Electrodes are placed on the Golgi tendon organ, which is at least partially responsible for the illusion without stimulating muscles.

In the experiment, a current-controlled rectangular pulse with 200 μ s pulse width, up to 20 mA pulse height, and 100 Hz pulse frequency. The voltage is depending on the conditions on the skin, ranged from 0 to around 150 V. When the biceps electrode was the cathode, the arm felt to move outwards. Conversely, when the triceps electrode was the cathode, the arm felt to move inwards. Consequently, as the electrode positions were close to the elbow joint, the stimulation of the muscle spindles is not possible.

b) Mechanical Stimulated Tactile Display for AR

Recently, a novel technology, AR tactile display mostly creates stimulation of roughness and friction that are mechanically stimuli. Same as VR tactile display, this clause will explore two methods of displaying mechanically stimuli: (i) mechanical and (ii) electrical actuation.

(i) AR Tactile Display using Mechanical Actuation

Ando et al. (2007) had developed a tactile device that presents tactile information (roughness and friction) to the fingertips (Ando et al., 2007). The methods of tactile sensation presentation are utilized not only in the virtual space but also in AR, where artificial sensation is superimposed on the real environment. Ando et al. (2007) proposed an adequate vibration stimulus is applied from above of the nail to generate the virtual undulation sensation, as shown in Figure 1.2 (Ando et al., 2007). Therefore, the device was not interposed between the real environment and did not block tactile sensations from the real environment. The vibration sensation will be produced more strongly in the finger pads in contact with the object than on the nail side since the tactile receptors are concentrated on the finger pads (McGlone & Reilly, 2010). This device is small and can be attached as a wristwatch, including the power supply and the control circuits. This tactile sensation can be realized over a wide range of applications, for example, adding tactile sensation to the contour of a picture, providing interaction through tactile sensation in combination with a large-scale monitor, adding click sensation to a touch panel (Fukumoto & Sugimura, 2001), and many more.

(ii) AR Tactile Display using Electrical Actuation

REVEL is an AR tactile technology that allows us to change the tactile feeling of real world objects by augmenting them with virtual tactile texture (Bau & Poupyrev, 2012). The user feels virtual tactile textures on a real object while observing them through an AR display. It is based on the principle of reverse electrovibration where a weak electrical signal is injected anywhere on the user's body, creating an oscillating electrical field around the user's finger. Reverse electrovibration is a novel use of the fundamental physical effect of electrovibration,

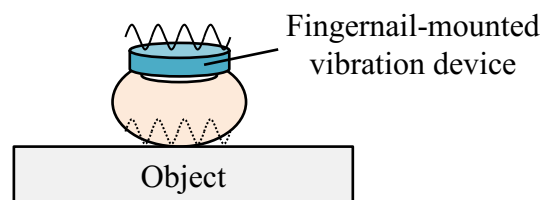


Figure 1.2 Proposed tactile display (Ando, Watanabe, Inami, Sugimito, & Maeda, 2007)

which is an electrically-induced mechanical skin vibration. When alternating current is injected into a conductive object covered by a thin insulator, a distinctive rubbery tactile sensation is perceived by a finger sliding on the surface of the object (Bau & Poupyrev, 2012). This is due to the AC signal creates an intermittent electrostatic force $\vec{F}_e(t)$ that attracts the finger to the conductive surface. When the finger is static, this force is too weak to be perceived, but it does modulate friction $\vec{F}_r(t)$ between the surface and sliding finger. Thus this creating a strong friction-like tactile sensation. By using this new concept of tactile display, it allows for the design of intrinsic tactile displays by instrumenting the user with a small wearable tactile signal generator that can be attached anywhere on the user's body.

The signal generator creates various tactile sensations by injecting an AC electrical signal into the user's body. Properties of the generated signal have a significant effect on the nature of the tactile sensations' quality and intensity. This tactile display is lightweight, inexpensive, can be used anywhere and at anytime to add tactile sensations to both virtual and real objects, but at the same time, it has some limitations. The skin condition affects the operation, for example, excessive sweating because REVEL has to be operated by dry clean hands.

c) Mechanical-Thermal Stimulated Tactile Display for VR

In previous researches, the thermal display is capable of simulating materials that cover a broad range of thermal properties and becomes an important element for telexistence, virtual reality, and virtual environments (Caldwell et al., 1996; Ho & Jones, 2007). Thus, there are many researches that integrate thermal display with their present mechanical stimulated tactile display. This section will explore some researches which include thermal information in a tactile display by using Peltier device.

(i) Multi-modal Cutaneous Feedback Systems

Recently, an advanced realistic user interface that included five key sensor elements; vision, audition, smell, taste, and touch, is needed for telexistence, virtual reality, and virtual environments. In Caldwell's research, a combined multi-modal mechanical and thermal output system, Data Glove Input System (DGIS) has been designed and constructed which is proposed to be applied to a remote operator working in a telexistence environment (Caldwell et al., 1996).

This haptic interface provides force, tactile and thermal feedback. The thermal feedback unit is a Peltier device that makes contact with the dorsal surface of the index finger. Thermal feedback tests were conducted with objects at temperatures ranging from 0 °C to more than 45 °C. Subjects achieved a 90% success rate in identifying the various materials (ice, boiling kettle, foam, aluminium) based only on these thermal cues. In their research, the combination of different types of feedback (mechanical and thermal) can be achieved. However, further developments will be required, which include:

- a) better spatial resolution,
- b) simulation of frictional forces,
- c) combination with kinesthetic sensation derived from joint and muscle position and force inputs.

(ii) TELESAR V

Fernando et al. proposed a telexistence surrogate anthropomorphic robot called Telesar, composed of a head-mounted display, a mechanism for sensing and rendering fingertip haptic as well as thermal sensation. In telexistence, the operator should be able to move freely and feel the slave robot as an expansion of his bodily consciousness.

The robot's fingers are installed with a vision-based cutaneous sensor to sense both force vector and temperature. The force vector is detected by tracking green and red markers placed on a transparent elastic body. In addition, a layer of thermo sensitive ink is wafered between the elastic body and outer surface.

Furthermore, on the master's side, the vertical and shearing forces generated by motor driven belt mechanism. Peltier devices are placed on the bottom side of operator's fingertips to reproduce the temperature.

1.2.2 Tactile Sensing Technologies

Currently, the evaluation on product quality is now largely depending on human tactile sensory evaluation which is the most logical method as people's preferences rely on numerous factors; physiological, perceptual, social factors and etc. Besides, the sensory evaluation gives the direct answer on consumers' perception of product quality. However, the sensory evaluation method may not be reliable for many cases as the arrival of new products are very quick. Moreover, the sensory evaluation can be a time consuming and costly process (Lawless & Heymann, 2010).

Hence, a quantification method of tactile sense evaluation, as the foundation of developing tactile sensing technologies is required to help product industry to evaluate their products without consuming too much time and cost. Moreover, quantification of tactile sense evaluation may help product industry and us in understanding the relationship between physical stimuli and physiological with psychological and perceptual response.

Beginning from 1930, started by Peirce, there was a number of trials in quantifying tactile sensation according to physical quantities (Pan, 2007). In 1970's, a KES-F system (Kawabata's Hand Evaluation System for Fabric) for tactile sense evaluation/sensing was developed by Kawabata et al. to the prior of quantification of tactile sensation. The system is used to measure fabric's surface properties and low stress mechanical such as fabric bending, shear, extension, compression, surface friction and roughness by applying simple scientific principles.

From the recorded values and curves obtained from each tester in warp and weft direction, a characteristic Table 1.2 shown below is hereby calculated and tabulated. Same apparatus is used to measure both the tensile properties (force-strain curve) and shear properties (force-angle curve) to measure the bending properties (torque-angle curve) are achieved by bending first its reverse sides against each other and later the face sides against each other. A compression tester is used to measure the pressure-thickness values. Same apparatus with different detectors measurements are done for surface friction (friction coefficient variation curve) and surface roughness (thickness variation curve).

Table 1.2 Characteristic values in KES-F system (Kawabata, 1980; Mäkinen, Meinander, & Mag, 2005)

Type of system	Surface properties	Characteristics measured
KES-FB1	Tensile	Linearity of load-extension curve Tensile energy Tensile resilience
	Shearing	Shear rigidity Hysteresis of shear force at 0.5° shear angle Hysteresis of shear force at 5° shear angle
KES-FB2	Bending	Bending rigidity Hysteresis of bending moment
KES-FB3	Compression	Linearity of pressure-thickness curve Compressional energy Compressional resilience
KES-FB4	Surface	Coefficient of friction Mean deviation of MIU, frictional roughness Geometrical roughness
Fabric construction	Weight	Weight per unit area
	Thickness	Thickness at 0.5 gf/cm ²

Kawabata and Niwa (Kawabata, 1980; Mäkinen, Meinander, & Mag, 2005; Niwa, 1975) had put forward Empirical equations for calculating primary hand value and total hand values from the measurement of quantified tactile sensation properties.

Fabric properties is measured by the system which then correlate the measurements with the subjective assessment of handle (Niwa, 1975) . Nonetheless, the system needs professionals to interpret the resulting data and very costly too. These drawbacks brought to the development of different testing device called the FAST (Hu, 2004). Australian CSIRO has introduced FAST (Fabric Assurance by Simple Testing) in 1990 to provide easier alternative than KES system.

FAST is designed and developed by the Australian CSIRO which is better in terms of testing speed and practicality than the KES system. Other than that, the FAST system met the requirements of garment makers, finishers and is reliable, inexpensive, accurate, robust and easy to operate. Compared to KES-F system, FAST only measures the resistance of fabric to deformation; not the recovery of fabric from deformation (Behery, 2005; Shishoo, 1995).

Similar information on the aesthetic characteristics of fabric is observed from FAST as compared to KES-F. However, it is even simpler and more suited to a mill environment. The FAST system can be categorized as follows: FAST-1 for thickness, FAST-2 for bending, FAST-3 for extensibility and FAST-4 for dimensional stability (refer to Table 1.3). Based on the objective measurement of fabric and ‘fingerprint’ or data set on a chart, manufacturer will be able to localize fabric faults, make predictions of the consequences of the faults found and look for other alternative routes or possible changes in the production process (Hu, 2008).

As the sensation is very much related to physical properties of the material, thus the data obtained through physical measurements will significantly portray an objective evaluation results. Complicated measuring systems posed major disadvantages such as high costs, complexity in

Table 1.3 List of fabric properties measured using FAST (Saville, 1999)

Type of system	Surface properties	Characteristics measured
FAST-1	Compression	Total thickness Surface thickness
FAST-2	Bending	Bending length
FAST-3	Tensile	Warp elongation Weft elongation Crosswise elongation
FAST-4	Dimensional stability	Relaxation shrinkage Hygral expansion
Fabric construction	Weight	Weight per unit area

maintenance and reparation. Studies to improve simpler and individual instruments was then conducted for each handle related objective fabric properties (Kayseri et al., 2012).

Asaga et al., based on human tactile perception mechanism proposed a new tactile evaluation method. The evaluation used vibration information acquired during active touch (Asaga, Takemura, Maeno, Ban, & Toriumi, 2013). First, sensory evaluation was carried out to extract same potential factors of each adjective on 16 samples that are made of fabrics and leathers. Two factors relating to softness and surface roughness are extracted according to factor analysis. Therefore, by quantifying the two factors, the evaluation of tactile sensation on leather/fabric samples may be conducted.

To imitate human active touch a concept of tactile measuring system will need to be devised. Human touches an object in order to perceive tactile sense. Human perceives the texture of an object using the kinesthetic and tactile information obtained by several receptors in his/her body while touching the object (Hollins, Aldowski, Rao, & Young, 1993; Lederman, 1983; Lederman, Loomis, & Williams, 1982; Taylor et al., 1973). In perceiving surface roughness or slipperiness of an object, “active touch” or “stroking the surface” is suitable to be applied, while “passive touch” or “just pressing an object” is the best way to perceive stiffness and thermal feel of the object. To detect minute surface roughness, active touch is known to be effective (Lederman, 1974).

Therefore, a system, which is known as the tactile measurement system, is capable of measuring vibration information during actively touching an object was then developed. The ability to control the tracing velocity and normal force during measurement was its key main function. Later the vibration information during actively touching the samples shall be used in sensory evaluation from the measurement system developed. Two factors extracted are surface softness and roughness were quantified by comparing the vibration information and tactile receptors properties. The tactile evaluation indices obtained would then be able to provide close approximation values of the softness and roughness correlation coefficient of 0.47 and 0.54 respectively. A preference index can be defined by combining the softness and roughness index. The index value was observed to be higher when the object is softer and smoother. Thus preference with correlation coefficient of 0.69 is able estimate successfully (Asaga et al., 2013).

This system has a concrete concept on quantifying tactile sensation. However, the system has a low correlation coefficient that leads to large error when estimating unknown samples. Therefore, there is a necessity to increase the accuracy of this system to quantify tactile sensation.

Moreover, a tactile-haptic interface was developed by Shen et al. to quantify surface texture properties such as roughness, softness, and veins of automobile interior (Shen et al., 2006). The interface will aid the designer to quantify and group the comfort index of automobile interior design for quality control, and allow customers to experience the surface textures in order to determine the preferable surface characteristics for each customer. A high-resolution optical tactile sensor is developed to accurately capture the interior surface textures in order to realize the aim. The tactile sensor is designed based on total internal reflection optical principle.

The pattern of the surface that differs from a nominal surface is called the surface texture. The differences may be random or repetitive, and result from lay, flaws, roughness and waviness. The seat surface textures could be quantified by executing the 3-D surface textures from the tactile sensing. To quantify one of the required parameters of the seat surface texture, surface roughness is used as it affects a few of functional attributes of the seat surface textures; for example, contact causing heat transmission, light reflection, surface friction and others. As a result, both samples of Majesty-B-Loose5 and Provence-A-Loose5 possess the similar surface roughness. The two samples' roughness curves which have the same surface roughness in real life are close in both the column and row axis as observed from the quantified roughness curves. The effectiveness of the quantification method and the sensor performance are verified by the analysis of the roughness curves.

Furthermore, softness of the non-identical leathers of the seats were quantified with the aid from ATI-FT05900 force/torque sensor i.e the tactile sensor used to make contact with the three different leather surfaces to increase the difference of the pressure force. The larger bright area of the 2-D tactile image shall indicate that the distension of the leather is more (due to more contact area involved). Therefore, we could determine the softness of the leathers by calculating the increased bright area, where the larger the increased bright area, the softer the leather. The softness order of the three samples (from soft to hard) is determined and matched the real circumstances (Shen et al., 2006). This system shows that surface roughness and softness could

be quantified by the proposed method. However, Shen et al. did not show the accuracy of this system quantitatively. Furthermore, there is a need to relate this quantified results with subjective sensory by human to verify this system.

1.3 Objective

The integration of tactile display into rapid prototyping will be a great help in product development industries and a novel device that can manipulate the prototype's touch sensation to any material's touch sensation without making a sample of the product. Previous researches have shown that tactile display can be categorized based on how the tactile information is displayed: (1) Realized tactile information to obtain real-world sensation, (2) Emphasize or restraint certain tactile information, (3) Display a completely different tactile information based on purpose (Shimojo, 2014). Furthermore, in order to display tactile information onto a rapid prototyping model, the tactile display should not block the user to touch the prototype directly. Therefore, this research proposes AR technology as the method to display tactile information which is nearer to real material sensation. In previous studies have shown that in virtual environment, thermal displays could assist in material identification and discrimination. The absence of thermal tactile feedback does not allow us to take advantage of the powerful mechanisms of the human sense of touch and diminishes the quality of experience. Thus, for tactile rendering, this research proposes an AR thermal display that can augment the thermal sensation.

From section 1.2.2, most of the previous works attempted to quantify the component in basic tactile sense classification, as generally, tactile sense can be expressed as roughness/smoothness, hardness/softness, friction, and warmness/coldness (Yamauchi et al., 2010). There is almost no work that attempt to quantify the complex sense of touch such as, elegant, refreshing, comfortable, etc. This is because of human tactile perception is very complex that involves many other factors. However, it is also important to the manufacturers to grasp this kind of complex tactile sensation too, in order to evaluate their products. Thus, this research

proposes a new method to quantify the complex tactile sensation by hierarchically classifying tactile sensation for better interpretation and understanding.

Furthermore, presently, most of the previous works were using one physical quantity to quantify one tactile sensation. This is because this method is very simple and comprehensible; however, it does not give high accuracy in quantification of tactile sensation. This may be due to the existence of multiple correlations between one tactile sensation with multiple physical quantities (Shimojo, 2014). Thus, this research proposes to quantify one tactile sensation by using multiple physical quantities.

This research also focuses on quantification of tactile sensation for fabrics. This is because, Citrin et al. thus deduced that clothing/fabrics do have a much higher need for tactile as compared to other products (Citrin et al., 2003). In conclusion, for tactile sensing, this research proposes a novel quantification method of human tactile sense evaluation for fabrics to provide a reliable quality assessment method for textile industry.

Chapter 2

HUMAN SOMATOSENSORY MECHANISM

Haptic information can be classified basically into two kinds of information: kinesthetic and tactile information. Kinesthetic information refers to the sensation acquired from the internal sensing inside muscles, tendons, and joints. On the other hand, tactile information refers to the sensation received from the receptors inside our skin.

Most of the early works on haptic devices are primarily related to kinesthetic sensation. As a result, the studies on kinesthetic sensation are quite established (Bergamasco et al., 1994; Hannaford, Wood, McAfee, & Zak, 1991; Okamura, Richard, & Cutkosky, 2002; Shimoga, 1993), and currently, a vast variety number of devices that are commercially available ("3D Systems: Scanners and Haptics," 2017; "Force Dimension: Products," 2017; "Haption: Products," 2017). On the contrary, the studies on tactile devices are immature compared to kinesthetic devices. As haptics is associated with both kinesthetic and tactile sensation, this research will address mostly on tactile sensation to help in enhancing the haptic technologies as overall.

In general, tactile information can be expressed as roughness/smoothness, hardness/softness, stickiness/slipperiness, and warmness/coldness (Shirado & Maeno, 2014; Yamauchi et al., 2010). However, these expressions may vary depending on the type of object that it is being evaluated. These sensations are perceived through cutaneous receptors located inside our skin. The skin can be divided into two; glabrous skin and hairy skin (Schmidt, 1986), and the area of hairy skin is larger compared to glabrous skin. This research will focus on the glabrous skin as the tested skin area is restricted only to the hand. There are three layers of skin; epidermis, dermis, and subcutaneous (Kandel, Schwartz, Jessell, Siegelbaum, & Hudspeth, 2012). The cutaneous receptors consist of mechanoreceptor, thermoreceptor, chemoreceptor, polymodal receptor, and nociceptor (Miyaka, 2010a).

2.1 Mechanoreceptors

Mechanoreceptor is an enclosed dendrite in a capsule that senses touch, pressure, vibration, and skin tension. In other words, the stimuli received from mechanoreceptors can correspond to tactile information of roughness, hardness, and stickiness. There are four types of mechanoreceptors in the glabrous skin, which are Meissner's corpuscle, Pacinian corpuscle, Merkel's disk, and Ruffini ending (Miyaoka, 2010a).

Mechanoreceptors in the glabrous skin can also be classified by the size and structure of the receptive field and sensitivity to static and dynamic events, as shown in Table 2.1 (Vallbo & Johansson, 1984). Meissner's corpuscle, Pacinian corpuscle, Merkel's disk, and Ruffini ending can be identified as fast adapting I (FA I), fast adapting II (FA II), slow adapting I (SA I), and slow adapting II (SA II). In addition, each mechanoreceptor has its own frequency range of the

Table 2.1 Types of tactile afferent units in the glabrous skin of the human hand and their properties. Graphs show schematically the impulse discharge (lower trace) to perpendicular ramp indentation of the skin (upper trace) for each unit type. (Vallbo & Johansson, 1984)

Mechanoreceptor	Adaptation	Presence of static response	Receptive fields	Impulse discharge graph
FA I (Meissner's corpuscle)	Fast	No	Small, sharp borders	
FA II (Pacinian corpuscle)	Fast	No	Large, obscure borders	
SA I (Merkel's disk)	Slow	Yes	Small, sharp borders	
SA II (Ruffini ending)	Slow	Yes	Large, obscure borders	

tuning curve (A. Gescheider, Bolanowski, & Hardick, 2001).

2.1.1 Meissner's Corpuscle

The Meissner's corpuscle is found in glabrous hairless skin within the dermal papillae. It consists of an elongated, encapsulated stack of flattened epithelial cells with the first afferent terminal fibers interdigitated between the cells.

A force applied to non-hairy skin causes the laminar cells in the Meissner corpuscle to slide past one another. This distorts the membranes of the axon terminals located between these cells. When the force is maintained, the laminar cells remain in a fixed, displaced position, and the shearing force on the axon terminals' membranes disappears. Consequently, the first afferent axons produce a transient, rapidly adapting response to a sustained mechanical stimulus.

When a force is applied to the dermal papilla containing the Meissner's corpuscle, the laminar cells in the corpuscle slide past one another. This shearing force distorts the membranes of the axon terminals located between the laminar cells, which depolarizes the axon terminals. When the force is sustained on the dermal papilla, the laminar cells remain in their displaced positions and no longer produce a shearing force on the axon terminals. Consequently, the sustained force on the dermal papilla is transformed into a transient force on the axon terminals of the Meissner's corpuscle. The first afferent axon response of a Meissner's corpuscle is rapidly adapting, and action potentials are only generated when the force is first applied.

The Meissner's first afferent discharges follow low frequency vibrating (30-50Hz) stimuli, which produces the sensation of flutter. Because a single afferent axon forms many dispersed Meissner's corpuscles, the first afferent can detect and signal small movements across the skin. Stimulation of a sequence of Meissner's corpuscles has been described to produce the perception of localized movement along the skin.

Besides that, Meissner's corpuscles are also considered to be the discriminative touch system's flutter and movement detecting receptors in non-hairy skin.

2.1.2 Pacinian Corpuscle

Pacinian corpuscle is found in subcutaneous tissue beneath the dermis and the connective tissues of bone, the body wall, and the body cavity. Therefore, they can be cutaneous, proprioceptive, or visceral receptors, depending on their location.

The Pacinian corpuscle is football-shaped, encapsulated, and contains the concentrically layered epithelial cell. The Pacinian corpuscle looks like a slice of onion in the cross-section, with a single first afferent terminal fiber located in its center. The outer layers of laminar cells contain fluid that is displaced when a force is applied to the corpuscle.

When a force is first applied on the Pacinian corpuscle, it initially displaces the laminar cells and distorts the axon terminal membrane. If the external pressure is maintained on the corpuscle, the displacement of fluid in the outer laminar cells dissipates the applied force on the axon terminal. Consequently, a sustained force on the corpuscle is transformed into a transient force on the axon terminal, and the Pacinian corpuscle's first afferent produces a fast adapting response.

Pacinian corpuscles' first afferent axons are most sensitive to vibrating stimuli at 100Hz to 300Hz and unresponsive to steady pressure. The sensation is elicited when cutaneous Pacinian corpuscles are stimulated by vibration or tickle. Pacinian corpuscles in the skin are considered to be the vibration-sensitive receptors of the discriminative touch system.

2.1.3 Merkel's Corpuscle

Merkel's disk is found in both hairy and non-hairy skin and is located in the basal layer of the epidermis. The Merkel's disk is non-encapsulated and consists of a specialized receptor cell, the Merkel cell, and a first afferent terminal ending, the Merkel's disk. Thick, short, finger-like protrusions of the Merkel cell are coupled tightly to the surrounding tissue. The Merkel cell is a modified epithelial cell, which contains synaptic vesicles that appear to release neuropeptides

that modulate the activity of the first afferent terminal. Each first afferent axon often innervates only a few Merkel cells in a discrete patch of skin.

A force applied to the overlying skin distorts the Merkel cell, which releases a stream of neuropeptides at its synaptic junctions with the Merkel disk. As the Merkel cell is mechanically coupled to the surrounding skin, it remains distorted for the duration of the force applied on the overlying skin. As a result, the action potential discharges produced by the Merkel complex afferent are slowly adapting.

Merkel's disk is considered to be the fine tactile receptors of the discriminative touch system that provide cues used to localize tactile stimuli and to perceive the edges of objects.

2.1.4 Ruffini Ending

Ruffini ending is found deep in the skin, as well as in joint ligaments and joint capsules, and can function as cutaneous or proprioceptive receptors depending on their location. The Ruffini ending is cigar-shaped, encapsulated, and contains longitudinal strands of collagenous fibers that are continuous with the connective tissue of the skin or joint. Within the capsule, the first afferent fiber branches repeatedly, and its branches are intertwined with the encapsulated collagenous fibers.

The Ruffini ending is oriented with its long axes parallel to the surface of the skin and is most sensitive to skin stretch. Stretching the skin stretches the collagen fibers within the Ruffini ending, which compresses the axon terminals. As the collagen fibers remain stretched and the axon terminals remain compressed during the skin stretch, the Ruffini ending afferent axon produces a sustained slowly adapting discharge to maintained stimuli.

Ruffini endings in the skin are considered to be skin stretch-sensitive receptors of the discriminative touch system. They also work with the proprioceptors in joints and muscles to indicate the position and movement of body parts.

2.2 Thermoreceptors

Thermoreceptors are free dendrite endings without any special structure. Thermoreceptors can be divided into two types; warm and cold thermoreceptors (Hensel, 1973b). Cold thermoreceptors respond only to cooling, whereas warm thermoreceptors respond to warming. Neither the thermoreceptors respond to mechanical stimulation. (Patapoutian et al., 2003). The density of thermoreceptors may vary at different sites on the body. However, the density of cold thermoreceptors is higher than warm thermoreceptors in all sites. The resting temperature of the skin on the hand ranges from 25 °C to 36 °C (Verrillo et al., 1998). However, the neutral skin temperature ranges from 30 °C to 36 °C. This is because when the skin temperature is maintained at the neutral skin temperature, there will be no thermal sensation is sensed; despite that, both types of thermoreceptors exhibit spontaneous firing.

The response of both cold and warm thermoreceptors changes according to the skin temperature (Patapoutian, Peier, Story, & Viswanath, 2003). The warm thermoreceptor's firing frequency increases when the skin temperature increased from 30 °C to 50 °C and reached a maximum at 45 °C. On the other hand, the cold thermoreceptor responds at the range of 5 °C to 43 °C and at the maximum when the skin temperature ranges 22 °C to 28 °C (Ho & Sato, 2014; Spray, 1986). In addition, when the skin temperature increases above 45 °C and decreases below 15 °C, nociceptor is also stimulated, and the thermal sensation change to pain sensation (Ian Darian-Smith & Johnson, 1977; Ho & Sato, 2014; L. a Jones & Ho, 2008).

2.3 Nocireceptors

Nociceptor is free dendrite endings without any special structure and responds to pain caused by physical or chemical injury to body tissues. For example, pain can be divided into sharp, pricking, cutting pain, dull, burning pain, and deep aching pain.

Chapter 3

MODELING OF TACTILE SENSATION

As described in Chapter 1, quantification of tactile sense evaluation may help industries to evaluate their new products without conducting a sensory evaluation. In order to realize this objective, there are several steps that are indispensable. First, to understand on how human perceps and evaluates tactile sensation. Next, to determine the approach on how to define or model tactile sensation that will be discussed in this chapter. Lastly, to propose the method to quantify the tactile sensation and suggest physical quantities for the quantification (will be discussed in Chapter 4).

In Section 3.1, the concept for modeling of tactile sensation will be discussed. Specifically, in Section 3.1.1, human tactile cognition and evaluation of tactile sensation will be explained, and a novel approach for defining tactile sensation will be proposed in Section 3.1.2.

Next, by using the concept explained, modeling of tactile sensation for door armrests and fabrics will be discussed in Section 3.2 and 3.3, respectively. Lastly, an improved way of modeling tactile sensation will be introduced in Section 3.4.

3.1 Concept for Modeling of Tactile Sensation

3.1.1 Human Tactile Sense Evaluation

The perception of touch sensation does not normally come from the simple stimulus patterns or from the stimulation of single receptors. The complexity of the stimulation of the various senses through coordinated variation in the outputs of logically independent receptors

shall need to be sought out. The information obtained from patterns of motion kinesthetically sensed in combination with the pattern of motion visually, auditorily, and tactually sensed.

According to Taylor, the interaction between an object's surface and skin may consider as same as a transducer (Taylor et al., 1973). A transducer is a device that changes energy from one form to another. For example, a speaker is a transducer as it converts electrical energy into sound and heat. Although heat is usually ignored, it is actually as much a part of the output. During the interaction between a fingertip and an object, the inputs of the transducer are the relative motions of the object and skin and the force between the hand and the object. The outputs are skin deformation, vibration, lateral (friction) and vertical (resistance) forces, bulk deformation of the fingertip, thermal effects, and sound. The transducer function, which relates the input and output, can be defined as the texture. It is determined by the properties of the object and skin. In other

Table 3.1 Postulated links between knowledge about objects and EPs (Lederman & Klatzky, 1987)

Knowledge about object	Exploratory procedure
Substance-related properties	
Texture	Lateral motion
Hardness	Pressure
Temperature	Static contact
Weight	Unsupported holding
Structure-related properties	
Weight	Unsupported holding
Volume	Enclosure Contour following
Global shape	Enclosure
Exact shape	Contour following
Functional properties	
Part motion	Part motion test
Specific function	Function test

words, the transducer function is a joint function of object and skin properties. The simple transducer function explained above represents only a small part of multimodal texture perception system.

Regarding the input of texture perception, the hand movements are purposively related to object properties. The typical movements (i.e., exploratory procedure) such as lateral movements, unsupported holding, etc., are used to identify object properties (Lederman & Klatzky, 1987). The object properties and exploratory procedures are summarized in Table 3.1. This study presents the nature of haptic object recognition. In the other study, when the object is focused on fabrics, the exploratory procedures are as shown in Figure 3.1. Table 3.2 shows the properties



(a) Touch stroke



(b) Rotating cupped



(c) Multiple finger



(d) Two handed rotation

Figure 3.1 Handle techniques

Table 3.2 Properties evaluated by different handle techniques (Moody, Morgan, Dillon, Baber, & Wing, 2001)

	Handle technique	Properties evaluated
(a)	Touch-stroke	Surface quality (texture), temperature
(b)	Rotating cupped action	Stiffness, weight, temperature, comfort, overall texture, creasing
(c)	Multiple finger pinch: Rotating between the finger action with one hand (thumb and 1 or 2 fingers)	Texture, stiffness, temperature, fabric structure, both sides of a fabric, friction, stretch (force-feedback)
(d)	Two handed rotation action	Stretch, sheerness

evaluated for each exploratory procedure (Moody et al., 2001).

3.1.2 Modeling of Tactile Sense Evaluation

After detecting physical quantities by the cutaneous receptors, human perceives these tactile senses after in-depth data analysis and integration done (Maeno, Kobayashi, & Yamazaki, 1998). From psychological aspect, the tactile sensation is usually evaluated qualitatively by humans (Shirado & Maeno, 2014). Generally, human uses adjectives to express the tactile sensation of an object. As the evaluation of tactile sensation is complicated (Shimojo, 2014), it is important to use the right expression for describing the tactile sensation to ensure the assessment reliability (Mäkinen et al., 2005).

Therefore, this research proposes to hierarchically classify adjectives into three groups called as low-order of tactile sensation, high-order of tactile sensation, and desired tactile sensation. This concept is based on the flow of human tactile perception (refer to Figure 3.2), i.e., from the interaction between object and skin, the stimuli are perceived by the receptor, and then the signals are interpreted in the brain. As shown in Figure 3.3, low-order of tactile sensation

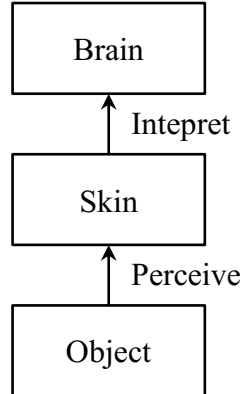


Figure 3.2 Summary on flow of human tactile perception

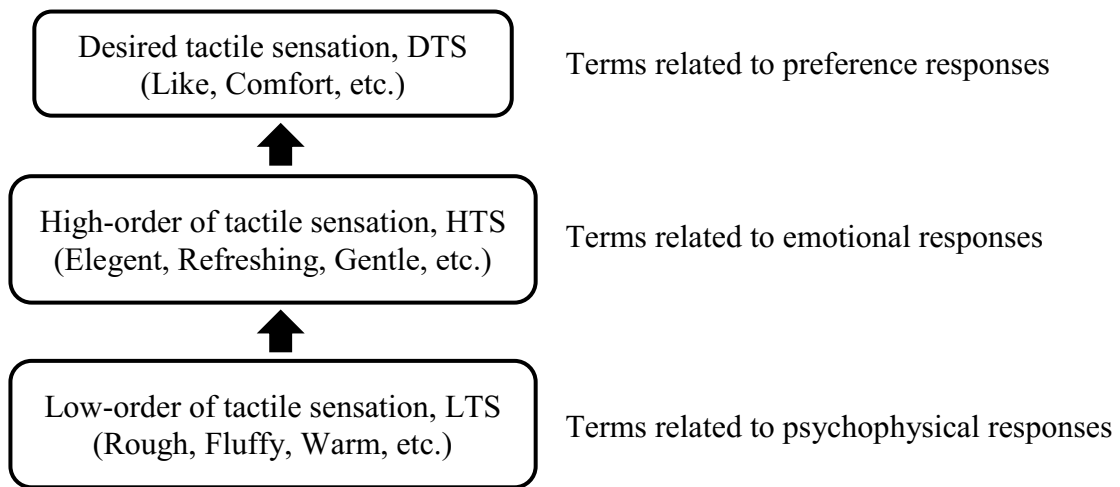


Figure 3.3 Proposed concept of hierarchically classified tactile sensation

(LTS) is a group of adjectives that directly describe the texture/property of the object, in other words, tactile-related adjectives. On the other hand, high-order of tactile sensation (HTS) is a group of adjectives that describe the object by associating LTS adjectives with psychological impressions and past experiences. Desired tactile sensation (DTS) means adjectives that are related to one's preference which majorly affect the purchase decision-making process. By using this concept, better understanding and interpretation of tactile sensation could be achieved. In order to acquire the main components in LTS, HTS, and DTS, and the relationship between LTS and HTS, and HTS and DTS, a sensory evaluation is conducted. After clarifying the definition of tactile sensation, the method to quantify may be determined in Chapter 4.

3.2 Modeling of Tactile Sensation for Door Armrest

This section mainly explores the hierarchical structure of tactile sensation for door armrest. First, in Section 3.2.1, the tactile sensation is classified into two groups; low-order of tactile sensation (LTS) and high-order of tactile sensation (HTS). Then, two adjectives are selected as the desired tactile sensation (DTS). Then, a sensory evaluation is conducted and explained in section 3.2.2.

3.2.1 Classification of Adjectives

In the sensory evaluation, there were 22 items of adjectives listed and classified into LTS, HTS, and DTS as shown in Table 3.3. The adjectives were selected by referring to previous works (Asaga, 2012; Guest et al., 2009; Nagano, Okamoto, & Yamada, 2014; Okamoto, Nagano, Kidoma, & Yamada, 2016; Shirado & Maeno, 2014) and discussion with door-armrest developers.


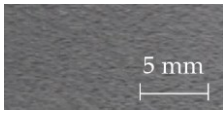





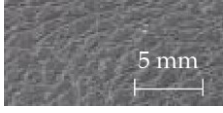
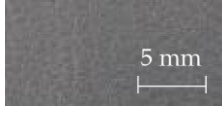
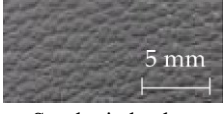
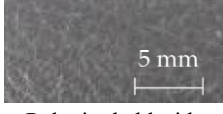

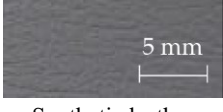
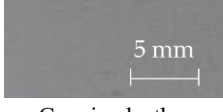
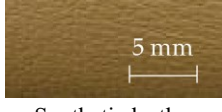

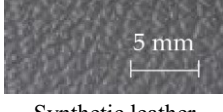
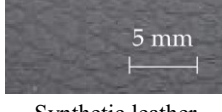
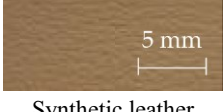

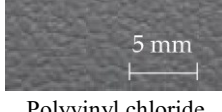
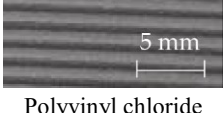
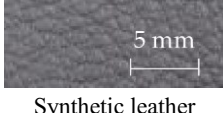
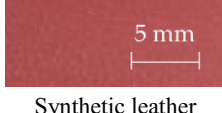
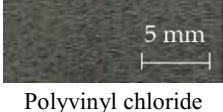
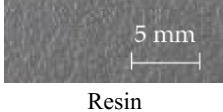
Table 3.3 List of adjectives

	Adjective		Adjective
	Wet		Fit
	Damp		Embraceable
	Chilly		Reviving
	Cold		Refreshing
	Smooth	HTS	Exciting
LTS	Silky		Exhilarating
	Rough		Cheap
	Bumpy		Luxury
	Tough		
	Hard		Prefer
	Brittle	DTS	Pleasant
	Hollow		

3.2.2 Sensory Evaluation

A sensory evaluation with a semantic differential method was carried out. 15 adults with age between their twenties and forties were asked to touch freely with their hands. Then, they were asked to evaluate 26 samples of door armrest on a seven-point unipolar scale. The unipolar scale is used to avoid translation problems between opposite adjectives (Tuorila et al., 2008). Moreover, the scale is only defined at the endpoints to prevent varying interpretations of verbal anchors and unevenness between anchors (Cantin & L. Dubé, 1999).

Table 3.4 List of door armrest samples.

#1		#2		#3	
	Genuine leather Type A		Resin Type E		Synthetic leather Type A
#4		#5		#6	
	Synthetic leather Type B		Synthetic leather Type A		Synthetic leather Type B
#7		#8		#9	
	Fabric Type A		Resin Type B		Synthetic leather Type C
#10		#11		#12	
	Synthetic leather Type A		Polyvinyl chloride Type C		Genuine leather Type C
#13		#14		#15	
	Synthetic leather Type C		Genuine leather Type A		Synthetic leather Type A
#16		#17		#18	
	Fabric Type D		Synthetic leather Type C		Synthetic leather Type A
#19		#20		#21	
	Synthetic leather Type A		Fabric Type A		Polyvinyl chloride Type C
#22		#23		#24	
	Polyvinyl chloride Type C		Synthetic leather Type A		Synthetic leather Type A
#25		#26			
	Polyvinyl chloride Type C		Resin Type E		

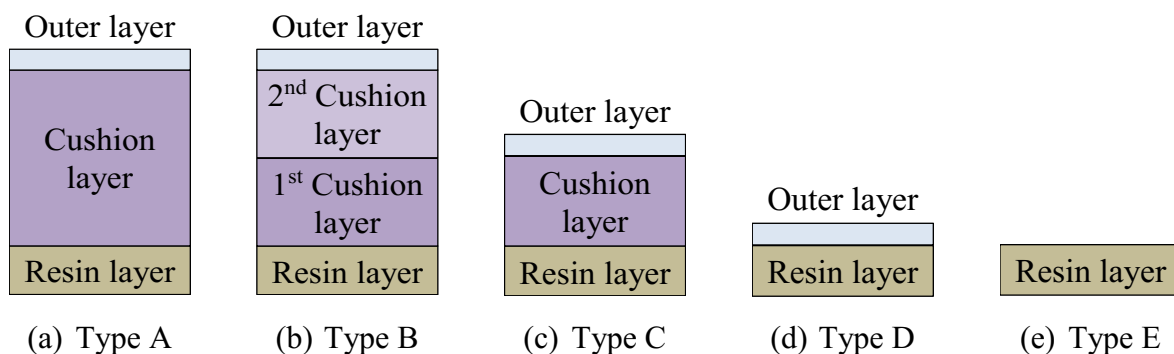


Figure 3.4 Cross-sectional structure types of door armrest samples.

The experiment was carried out as a blind test with samples' details undisclosed in order to exclude visual effects from the sensory evaluation. Table 3.4 shows the outer layer samples (synthetic leather, genuine leather, fabric, polyvinyl chloride, and resin) and the cross-sectional structure types of each sample; there are five types, as shown in Figure 3.4. The participants are informed in advance of what objects that they are going to evaluate.

3.2.2.1 Principal Component Analysis

From the survey data of sensory evaluation, principal component analysis with varimax rotation was carried out using statistical analysis software (SPSS Ver. 22, IBM) to reduce the number of variables by grouping the adjectives that have a strong correlation to each other into an independent semantic variable or principal component (PC). Previous research (X. Chen, Barnes, Childs, Henson, & Shao, 2009; Okamoto, Nagano, & Yamada, 2013; Sakamoto & Watanabe, 2017) has shown that the adjectives can be grouped and one of the methods used is principal component analysis. By reducing the number of variables, they become practical and easy for interpreting the data. Tables 3.5 and 3.6 show the results of principal component analysis for LTS and HTS, respectively. All components that have loadings higher than 0.50 are in bold (this is an arbitrary limit).

Table 3.5 Result of principal component analysis for low-order of tactile sensation (LTS).

Adjective	Principal Components					
	1	2	3	4	5	6
Wet	0.971	0.091	0.081	-0.014	-0.057	-0.010
Damp	0.967	0.098	0.125	-0.018	-0.053	-0.028
Chilly	0.088	0.966	0.091	0.066	0.067	0.084
Cold	0.104	0.963	0.091	0.066	0.112	0.038
Smooth	0.100	0.106	0.915	-0.176	-0.105	-0.057
Silky	0.118	0.084	0.908	-0.127	-0.199	0.000
Rough	-0.019	0.105	-0.093	0.917	0.219	0.006
Bumpy	-0.014	0.031	-0.227	0.886	0.216	0.100
Tough	-0.023	0.140	-0.131	0.239	0.893	-0.129
Hard	-0.102	0.061	-0.193	0.220	0.887	-0.143
Brittle	-0.101	0.069	-0.139	0.144	-0.024	0.900
Hollow	0.063	0.052	0.084	-0.052	-0.223	0.892
Eigen value	3.430	2.513	1.899	1.490	0.983	0.693
Cumulative contribution ratio	16.22	32.39	47.74	62.84	77.86	91.74

Table 3.6 Result of principal component analysis for high-order of tactile sensation (HTS)

Adjective	Principal Components			
	1	2	3	4
Fit	0.920	0.025	0.188	0.241
Embraceable	0.887	0.108	0.272	0.245
Reviving	0.075	0.945	0.173	0.049
Refreshing	0.057	0.865	0.378	0.039
Exciting	0.287	0.314	0.858	0.160
Exhilarating	0.256	0.322	0.858	0.194
Cheap	-0.216	0.018	-0.115	-0.941
Luxury	0.501	0.203	0.287	0.695
Eigen value	4.369	1.741	0.708	0.570
Cumulative contribution ratio	26.09	49.82	72.94	92.35

There were six principal components for LTS extracted with 91.7% of the total variance. PC1 was interpreted as “dampness” dimension, with high loadings on *damp* and *wet*, PC2 was “coldness” dimension, with high loadings on *chilly* and *cold*. PC3 was “micro-roughness” dimension, with high loadings on *smooth* and *silky*. PC4 was “macro-roughness” dimension, with high loadings on *rough* and *bumpy*. PC5 was “hardness” dimension, with high loadings on *tough* and *hard*. Lastly, PC6 was “hollowness” dimension, with high loadings on *brittle* and *hollow*.

On the other hand, there were four principal components for HTS extracted with 92.3% of the total variance. PC1 was identified as “embracingness” dimension, with high loadings on *fit* and *embraceable*. PC2 was “refreshingness” dimension, with high loadings on *reviving* and *refreshing*. PC3 was “excitingness” dimension, with high loadings on *exciting* and *exhilarating*. Lastly, PC4 was “expensiveness” dimension, with high loadings on *cheap* (negative sign) and *luxury*. Here, *luxury* was seen to have slightly loading on PC1, in other words, *luxury* had a combination of *not cheap* and *fit*.

3.2.2.2 Multiple Regression Analysis

Multiple regression analysis is generally used when a statistician thinks there are several independent variables contributing to the variation of the dependent variable. Furthermore, this analysis could determine whether there is a significant relationship exists between the independent variables and dependent variables (Bluman, 2014).

In multiple regression, the strength of the relationship between independent variables and the dependent variable is presented by multiple correlation coefficient, R . This R is computed from individual correlation coefficients of all independent variables. The multiple coefficient of determination, R^2 is a better indicator of the strength of the relationship compared with R . Yet, adjusted R^2 considers the sampling error and controls overestimation of R^2 . The R^2 represents the amount of variation explained by the regression model. By identifying the significance of R^2 , one could determine whether the regression model is a good fit for the data. If a multiple regression equation fits the data well, it can be used to make predictions (Bluman, 2014).

Moreover, multiple regression equation can be generally represented as below.

$$y = a + b_1x_1 + b_2x_2 + \dots + b_kx_k \quad (3.1)$$

The x's are the independent variables, and y is the dependent variable. The value for a is more or less an intercept, although a multiple regression equation with two independent variables constitutes a plane rather than a line. The b's are called as partially regression coefficients. Each regression coefficient represents the amount of change dependent variable for one unit of change in corresponding to one independent variable when the other independent variables are held constant. The probability value (p-value) of the regression coefficient shows the amount of contribution of the independent variable to the regression model.

However, the regression coefficient could not represent the correlation between a dependent variable and independent variables individually. Here, the correlation should be computed to determine whether a positive/negative linear relationship exists between a dependent variable with independent variables individually, and each probability value (p-value) of correlation shows the strength of the individual correlation.

In this section, multiple regression analysis was conducted to determine and examine the relationship between all components in LTS and each component in HTS, and between all components in HTS and each adjective in DTS by using SPSS software [IBM Corporation]. Before conducting the multiple regression analysis, bivariate Pearson correlation was conducted for all explanatory variables to make sure that there is no multicollinearity occurred between the variables. All the correlations showed values below 0.65.

Table 3.7 shows the correlation and multiple regression analysis results when the dependent variable is HTS component of “embracingness” and the independent variables are LTS components of “dampness”, “coldness”, “micro-roughness”, “macro-roughness”, “hardness” and “hollowness”. As shown in Table 3.7 (a), “dampness”, “micro-roughness” and “hollowness” had a positive and significantly correlation with “embracingness”. However, “macro-roughness” and “hardness” had a negative and significantly correlation with the “embracingness”. Moreover, “coldness” had a weak negative correlation with “embracingness”.

The multiple regression model with the two predictors (“macro-roughness” and “hardness”) produced $R^2 = 0.961$, $F(2, 23) = 284.494$, $p < .001$, thus, the multiple regression model had a very good fit of data, indicating that the “embracingness” scores were related to two

Table 3.7 Result for multiple regression analysis (HTS-“Embracingness” with all LTS principal components)

(a) Correlations		
	“Embracingness”	
	Pearson correlation	Sig.
“Dampness”	0.341**	.044
“Coldness”	-0.147	.236
“Micro-roughness”	0.633****	2.575E-04
“Macro-roughness”	-0.443**	.012
“Hardness”	-0.954****	2.208E-14
“Hollowness”	0.493***	.005

*p < .1 **p < .05 ***p < .01 ****p < .001

(b) Model Summary			
R	R Square	Adjusted R Square	Std. Error of the Estimate
.980 ^a	0.961	0.958	0.143

a. Predictors: (Constant), “Hardness”, “Macro-roughness”

(c) ANOVA ^a					
Model	Sum of Squares	df	Mean Square	F	Sig.
Regression	11.689	2	5.845	284.494*	.000 ^b
Residual	0.473	23	0.021		
Total	12.162	25			

*p < .001

a. Dependent variable: “Embracingness”

b. Predictors: (Constant), “Hardness”, “Macro-roughness”

Table 3.7 Result for multiple regression analysis (HTS-“Embracingness” with all LTS principal components)

Model	(d) Coefficients ^a			Sig.
	Unstandardized Coefficients		Standardized Coefficients	
	B	Std. Error	Beta	
(Constant)	-0.002	0.028	-	.945
“Hardness”	-0.846	0.040	-0.900*	.000
“Macro-roughness”	-0.231	0.042	-0.231*	.000

*p < .001

a. Dependent variable: “Embracingness”

LTS components: “macro-roughness” and “hardness”.

According to the standardized regression coefficients, the “hardness” had the most contribution to the HTS component of “embracingness”, followed by “macro-roughness”. “Hardness” and “macro-roughness” had negative regression coefficients, indicating that the higher score of “hardness” and “macro-roughness”, i.e. the softer and smoother sample was expected to have a higher score of “embracingness”. From Table 3.7 (d), a multiple regression equation can be obtained as the equation below.

$$H_{embracingness} = (-0.846 \times L_{hardness}) + (-0.231 \times L_{macro-roughness}) - 0.002 \quad (3.2)$$

Table 3.8 shows the correlation and multiple regression analysis results when the dependent variable is HTS component of “refreshingness” and the independent variables are LTS components of “dampness”, “coldness”, “micro-roughness”, “macro-roughness”, “hardness” and “hollowness”. As shown in Table 3.8 (a), “dampness” had a negative and significantly correlation with the “refreshingness”. However, “hardness” had a positive and significantly correlation with the “refreshingness” and others LTS components had weak correlations with “refreshingness”.

Table 3.8 Result for multiple regression analysis (HTS-“Refreshingness” with all LTS principal components)

(a) Correlations		
“Refreshingness”		
	Pearson correlation	Sig.
“Dampness”	-0.751****	5.001E-06
“Coldness”	-0.178	.192
“Micro-roughness”	0.024	.454
“Macro-roughness”	0.090	.331
“Hardness”	0.579***	.001
“Hollowness”	0.073	.361

*p < .1 **p < .05 ***p < .01 ****p < .001

(b) Model Summary			
R	R Square	Adjusted R Square	Std. Error of the Estimate
.819 ^a	0.670	0.642	0.127

b. Predictors: (Constant), “Dampness”, “Hardness”

(c) ANOVA ^a					
Model	Sum of Squares	df	Mean Square	F	Sig.
Regression	0.762	2	0.381	23.391*	.000 ^b
Residual	0.375	23	0.016		
Total	1.136	25			

*p < .001

c. Dependent variable: “Refreshingness”

d. Predictors: (Constant), “Dampness”, “Hardness”

Table 3.8 Result for multiple regression analysis (HTS-“Refreshingness” with all LTS principal components)

Model	(d) Coefficients ^a			Sig.
	Unstandardized Coefficients		Standardized Coefficients	
	B	Std. Error	Beta	
(Constant)	0.002	0.025	-	.939
“Dampness”	-0.443	0.092	-0.622*	.000
“Hardness”	0.101	0.037	0.351*	.012

*p < .001

b. Dependent variable: “Refreshingness”

The multiple regression model with the two predictors produced $R^2 = 0.670$, $F(2, 23) = 23.391$, $p < .001$, thus, the multiple regression model had a very good fit of data, indicating that the “refreshingness” scores were related to two LTS components: “dampness” and “hardness”.

According to the standardized regression coefficients, the “dampness” had the most contribution to the HTS component of “refreshingness”, followed by “hardness”. “Dampness” had a negative and “hardness” had positive regression coefficients, indicating that the higher score of “dampness” and “hardness”, i.e., the drier and softer sample was expected to have a higher score of “refreshingness”. From Table 3.8 (d), a multiple regression equation can be obtained as the equation below.

$$H_{refreshingness} = (-0.443 \times L_{dampness}) + (0.101 \times L_{hardness}) + 0.002 \quad (3.3)$$

Table 3.9 shows the correlation and multiple regression analysis results when the dependent variable is HTS component of “expensiveness” and the independent variables are LTS components of “dampness”, “coldness”, “micro-roughness”, “macro-roughness”, “hardness” and “hollowness”. As shown in Table 3.9 (a), “dampness”, “micro-roughness” and “hollowness” had positively and significantly correlations with the “expensiveness”. However, “macro-

Table 3.9 Result for multiple regression analysis (HTS-“Expensiveness” with all LTS principal components)

(a) Correlations		
“Expensiveness”		
	Pearson correlation	Sig.
“Dampness”	0.293*	.073
“Coldness”	-0.129	.265
“Micro-roughness”	0.672****	8.510E-05
“Macro-roughness”	-0.443**	.012
“Hardness”	-0.747****	5.863E-06
“Hollowness”	0.394**	.023

*p < .1 **p < .05 ***p < .01 ****p < .001

(b) Model Summary			
R	R Square	Adjusted R Square	Std. Error of the Estimate
0.815 ^a	0.664	0.634	0.202

c. Predictors: (Constant), “Hardness”, “Micro-roughness”

(c) ANOVA ^a					
Model	Sum of Squares	df	Mean Square	F	Sig.
Regression	1.852	2	0.926	22.681*	.000 ^b
Residual	0.939	23	0.041		
Total	2.791	25			

*p < .001

e. Dependent variable: “Expensiveness”

f. Predictors: (Constant), “Hardness”, “Micro-roughness”

roughness” and “hardness” had positively and significantly correlations with the “expensiveness”, and “coldness” had a weak correlation with “expensiveness”.

Table 3.9 Result for multiple regression analysis (HTS-“Expensiveness” with all LTS principal components)

(d) Coefficients ^a				
Model	Unstandardized Coefficients		Standardized Coefficients	Sig.
	B	Std. Error	Beta	
(Constant)	-0.004	0.040	-	.922
“Hardness”	-0.245	0.064	-0.543**	.001
“Micro-roughness”	0.346	0.129	0.384*	.013

*p < .05 **p < .01

c. Dependent variable: “Expensiveness”

The multiple regression model with the two predictors produced $R^2 = 0.664$, $F(2, 23) = 22.681$, $p < .001$, thus, the multiple regression model had a very good fit of data, indicating that the “expensiveness” scores were related to two LTS components: “hardness” and “micro-roughness”.

According to the standardized regression coefficients, the “dampness” had the most contribution to the HTS component of “expensiveness”, followed by “hardness”. “Hardness” had a negative and “micro-roughness” had positive regression coefficients, indicating that the higher score of “hardness” and “micro-roughness”, i.e., the softer and smoother sample was expected to have a higher score of “expensiveness”. From Table 3.9 (d), a multiple regression equation can be obtained as the equation below.

$$H_{expensiveness} = (-0.245 \times L_{hardness}) + (0.346 \times L_{micro-roughness}) - 0.004 \quad (3.4)$$

Table 3.10 shows the correlation and multiple regression analysis results when the dependent variable is DTS component of “prefer” and the independent variables are HTS components of “embracingness”, “refreshingness”, “excitingness” and “expensiveness”. As shown in Table 3.10 (a), “embracingness”, “excitingness” and “expensiveness” had positively

and significantly correlation with the “prefer”. However, “refreshingness” had a negatively and significantly correlation with the “prefer”.

Table 3.10 Result for multiple regression analysis (DTS-“Prefer” with all HTS principal components)

(a) Correlations		
	“Prefer”	
	Pearson correlation	Sig.
“Embracingness”	0.943****	2.667E-13
“Refreshingness”	-0.344**	0.043
“Excitingness”	0.308*	0.063
“Expensiveness”	0.795****	6.272E-07
*p < .1 **p < .05 ***p < .01 ****p < .001		

(b) Model Summary			
R	R Square	Adjusted R Square	Std. Error of the Estimate
0.959 ^a	0.919	0.912	0.315

d. Predictors: (Constant), “Embracingness”, “Refreshingness”

(c) ANOVA ^a					
Model	Sum of Squares	df	Mean Square	F	Sig.
Regression	25.979	2	12.990	130.566*	.000 ^b
Residual	2.288	23	0.099		
Total	28.267	25			

*p < .001

g. Dependent variable: “Prefer”

h. Predictors: (Constant), “Embracingness”, “Refreshingness”

Table 3.10 Result for multiple regression analysis (DTS-“Prefer” with all HTS principal components)

(d) Coefficients ^a				
Model	Unstandardized Coefficients		Standardized Coefficients	Sig.
	B	Std. Error	Beta	
(Constant)	3.776	0.062	-	.000
“Embracingness”	1.596	0.106	1.047**	.000
“Refreshingness”	0.995	0.346	0.199*	.009

*p < .01 **p < .001

d. Dependent variable: “Prefer”

The multiple regression model with the two predictors produced $R^2 = 0.919$, $F(2, 23) = 130.566$, $p < .001$, thus, the multiple regression model had a very good fit of data, indicating that the “prefer” scores were related to two HTS components: “embracingness” and “refreshingness”.

According to the standardized regression coefficients, the “embracingness” had the most contribution to the DTS component of “prefer”, followed by “refreshingness”. “Embracingness” and “Refreshingness” had positive regression coefficients, indicating that the higher score of “embracingness” and “refreshingness”, i.e. the more embracing and refreshing sample was expected to have higher score of “prefer”. From Table 3.10 (d), a multiple regression equation can be obtained as the equation below.

$$D_{prefer} = (1.596 \times H_{embracingness}) + (0.995 \times H_{refreshingness}) + 3.776 \quad (3.5)$$

Table 3.11 shows the correlation and multiple regression analysis results when the dependent variable is DTS component of “pleasant” and the independent variables are HTS components of “embracingness”, “refreshingness”, “excitingness” and “expensiveness”. As shown in Table 3.11 (a), “embracingness”, “excitingness” and “expensiveness” had positively and significantly correlation with the “pleasant”. However, “refreshingness” had a negatively and significantly correlation with the “pleasant”.

The multiple regression model with the two predictors produced $R^2 = 0.964$, $F(3, 22) = 96.164$, $p < .001$, thus, the multiple regression model had a very good fit of data, indicating that

Table 3.11 Result for multiple regression analysis (DTS-“Pleasant” with all HTS principal components)

(a) Correlations		
“Pleasant”		
	Pearson correlation	Sig.
“Embracingness”	0.939****	6.795E-13
“Refreshingness”	-0.330*	.050
“Excitingness”	0.276*	.086
“Expensiveness”	0.824****	1.187E-07

*p < .1 **p < .05 ***p < .01 ****p < .001

(b) Model Summary			
R	R Square	Adjusted R Square	Std. Error of the Estimate
.964 ^a	0.929	0.919	0.283

e. Predictors: (Constant), “Embracingness”, “Refreshingness”, “Expensiveness”

(c) ANOVA ^a					
Model	Sum of Squares	df	Mean Square	F	Sig.
Regression	23.078	3	7.693	96.164	.000 ^b
Residual	1.760	22	0.080		
Total	24.838	25			

*p < .001

- i. Dependent variable: “Pleasant”
- j. Predictors: (Constant), “Embracingness”, “Refreshingness”, “Expensiveness”

Table 3.11 Result for multiple regression analysis (DTS-“Pleasant” with all HTS principal components)

(d) Coefficients ^a				
Model	Unstandardized Coefficients		Standardized Coefficients	Sig.
	B	Std. Error	Beta	
(Constant)	3.907	0.055	-	.000
“Embracingness”	1.272	0.145	0.890***	.000
“Refreshingness”	0.917	0.313	0.196**	.008
“Expensiveness”	0.574	0.274	0.192*	.048

*p < .05 **p < .01 ***p < .001

e. Dependent variable: “Pleasant”

the “pleasant” scores were related to three HTS components: “embracingness”, “refreshingness” and “expensiveness”.

According to the standardized regression coefficients, the “embracingness” had the most contribution to the DTS component of “pleasant”, followed by “refreshingness” and “expensive”. “Embracingness”, “refreshingness” and “expensiveness” had positive regression coefficients, indicating that the higher score of “embracingness”, “refreshingness” and “expensiveness”, i.e. the more embracing, refreshing and expensiveness sample was expected to have higher score of “pleasant”. From Table 3.11 (d), a multiple regression equation can be obtained as the equation below.

$$D_{pleasant} = (1.272 \times H_{embracingness}) + (0.917 \times H_{refreshingness}) + (0.574 \times H_{expensiveness}) + 3.907 \quad (3.6)$$

3.2.3 Discussions

From the principal component analysis and multiple regression analysis results, the hierarchical structure of tactile sensation for door armrest can be summarized as shown in Figure

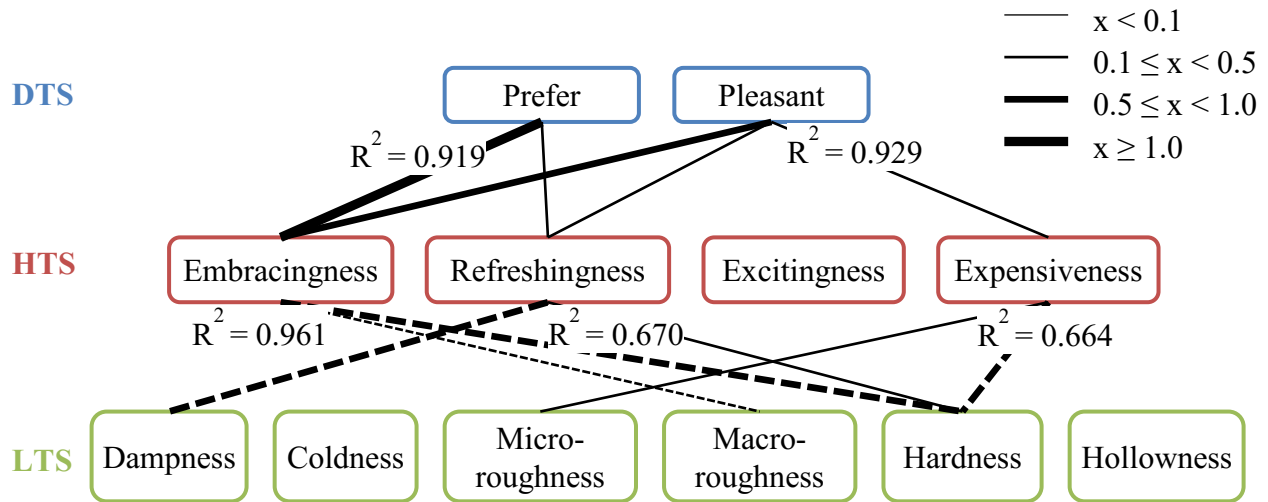


Figure 3.5 Multiple regression analysis result.

3.5. The thickness of the lines corresponds to the standardized coefficients. Moreover, the solid and dash lines indicate the positive and negative coefficients, respectively.

There was one component in HTS (the “excitingness” dimension) that could not successfully construct its multiple regression with components in LTS because the correlations between the “excitingness” dimension with components in LTS were not significantly strong. Therefore, the “excitingness” dimension was not included during the construction of multiple regressions between DTS and HTS.

By using the multiple regression equations, DTS adjectives can be expressed by LTS components. In order to express DTS adjectives for hand in terms of LTS components, the equations (3.2), (3.3), and (3.4) are substituted in equations (3.5) and (3.6). The computed equations are as shown below.

$$D_{prefer} = (-1.250 \times L_{hardness}) + (-0.369 \times L_{macro-roughness}) + (-0.441 \times L_{dampness}) + 3.775 \quad (3.7)$$

$$D_{pleasant} = (-1.124 \times L_{hardness}) + (-0.294 \times L_{macro-roughness}) + (-0.406 \times L_{dampness}) + (0.199 \times L_{micro-roughness}) - 0.003 \quad (3.8)$$

3.3 Modeling of Tactile Sensation for Fabrics

This section mainly explores on the hierarchical structure of tactile sensation for fabrics. First, in Section 3.3.1, the tactile sensation is classified into two groups; low-order of tactile sensation (LTS) and high-order of tactile sensation (HTS). Then, two adjectives are selected as the desired tactile sensation (DTS). Next, a sensory evaluation by using hand and forearm are conducted and explained in section 3.3.2 and section 3.3.3, respectively. The sensory evaluation is conducted using hand and forearm to understand the difference of tactile perception in both types of skin; glabrous skin (hand) and hairy skin (forearm). Besides, the tactile sensation by hand may represent the tactile sensation when the consumer firstly touches the fabric during the evaluation for purchasing. On the other hand, the tactile sensation by forearm may represent the tactile sensation when the consumer actually wears the fabric. Lastly, in section 3.3.4, the summary of analysis results will be presented.

3.3.1 Classification of Adjectives

There are 15 adjectives that are used in this research, as shown in Table 3.12. The original Japanese terms of these adjectives' definitions together with English meanings are provided as well. These adjectives were selected by referring to previous works (Asaga et al., 2013; Shirado & Maeno, 2014) and discussion with tactile-related experts and experienced textile-related workers.

Table 3.12 List of adjectives in Japanese and English translation

Japanese	Roman alphabets	English translation
ヒヤッと ⇔ 温かい	<i>Hiya' / Atataikai</i>	<i>Hiya'</i> means the feel of chilly. <i>Atataikai</i> means the feel of warm.

Table 3.12 List of adjectives in Japanese and English translation (continued from previous page)

Japanese		Roman alphabets	English translation
軽い	⇔ 重い	<i>Karui/ Omoi</i>	<i>Karui</i> means light or not heavy. <i>Omoi</i> means heavy or weighty.
ざらざら	⇔ すべすべ	<i>Zara-zara/ Sube-sube</i>	<i>Zara-zara</i> means the feel of rough like sandy, gritty or granular. <i>Sube-sube</i> means the feel of smooth but not slippery.
きめが粗い	⇔ きめが細かい	<i>Kimega arai/ Kimega komakai</i>	<i>Kimega arai</i> means rough texture. <i>Kimega komakai</i> means fine texture.
硬い	⇔ 柔らかい	<i>Katai/ Yawarakai</i>	<i>Katai</i> means hard. <i>Yawarakai</i> means soft.
ふんわりする	⇔ ふんわりしない	<i>Funwari</i>	<i>Funwari</i> means spongy, fluffy and soft in an airy manner.
しっとりする	⇔ しっとりしない	<i>Shittori</i>	<i>Shittori</i> means moist and damp
さらさらする	⇔ さらさらしない	<i>Sara-sara</i>	<i>Sara-sara</i> means the feel of smooth and dry with no stickiness or moistness
落ち着く	⇔ 落ち着かない	<i>Ochitsuku</i>	<i>Ochitsuku</i> means relaxing and calm
さわやか	⇔ さわやかでない	<i>Sawayaka</i>	<i>Sawayaka</i> means the feel of refreshing
すっきり	⇔ すっきりしない	<i>Sukkiri</i>	<i>Sukkiri</i> means the feel of be refreshed or clear
優しい	⇔ 優しくない	<i>Yasashi</i>	<i>Yasashi</i> means delicate or gentle

Table 3.12 List of adjectives in Japanese and English translation (continued from previous page)

Japanese		Roman alphabets	English translation
上品	⇔ 下品	<i>Jouhin</i>	<i>Jouhin</i> means elegant or stylish
心地良い	⇔ 心地良くない	<i>Kokochiyoi</i>	<i>Gokochiyoi</i> means pleasant, cozy or comfortable
好き	⇔ 嫌い	<i>Suki</i>	<i>Suki</i> means prefer or like

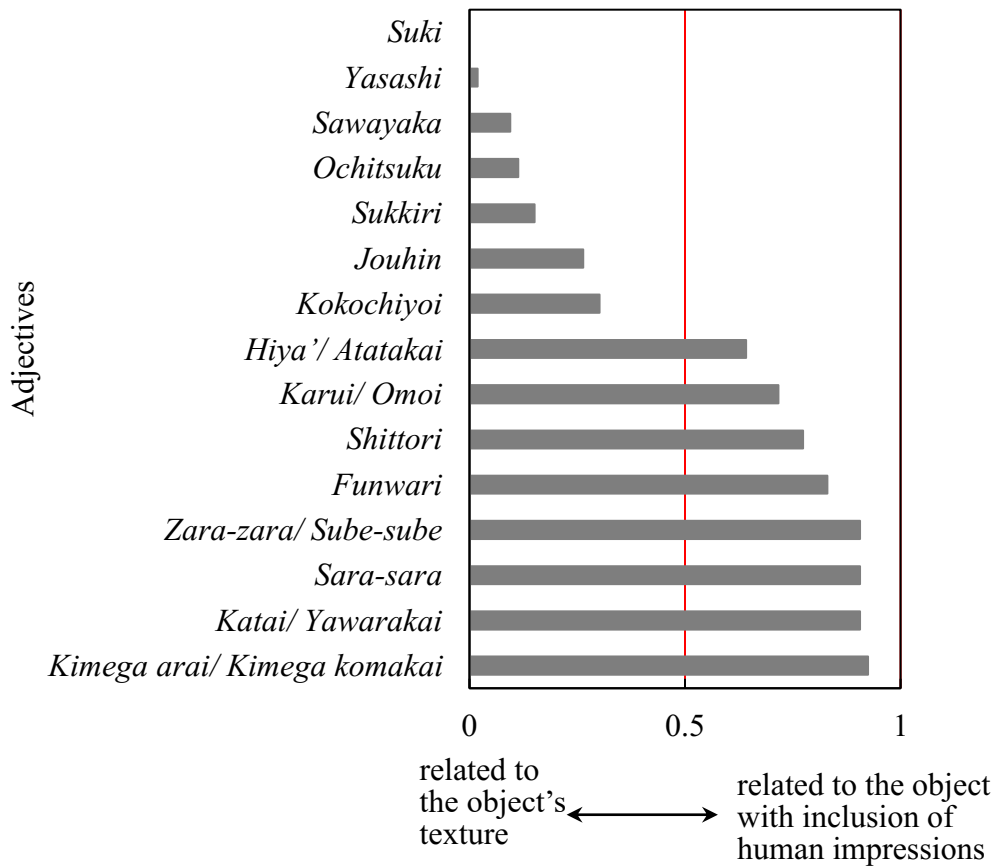


Figure 3.6 Grouping of adjectives

Table 3.13 Classification of adjectives

Adjectives		Adjectives	
LTS	<i>Hiya' / Atatakai</i>	HTS	<i>Ochitsuku</i>
	<i>Karui/ Omoi</i>		<i>Sawayaka</i>
	<i>Zara-zara/ Sube-sube</i>		<i>Sukkiri</i>
	<i>Kimega arai/ Kimega komakai</i>		<i>Yasashi</i>
	<i>Katai/ Yawarakai</i>		<i>Jouhin</i>
	<i>Funwari</i>	DTS	<i>Kokochiyoi</i>
	<i>Shittori</i>		<i>Suki</i>
	<i>Sara-sara</i>		

In order to classify tactile sensation into LTS and HTS, a survey was carried out. 53 males and females in their twenties participated in this survey. They were asked whether the listed adjectives in Table 3.12 are related to the object's texture or related to the object with inclusion of human emotions.

The result is as shown in Figure 3.6. From the result, the tactile sensation is classified in LTS, HTS and two adjectives, i.e. "comfort" and "preference" are selected for DTS. "Preference" is selected for DTS because it directly describes the one's preference towards an object. Nevertheless, "comfort" is selected for DTS because it has the same tendency as preference, since generally, only comfortable fabrics that will be preferable. The classification of adjectives is summarized in Table 3.13.

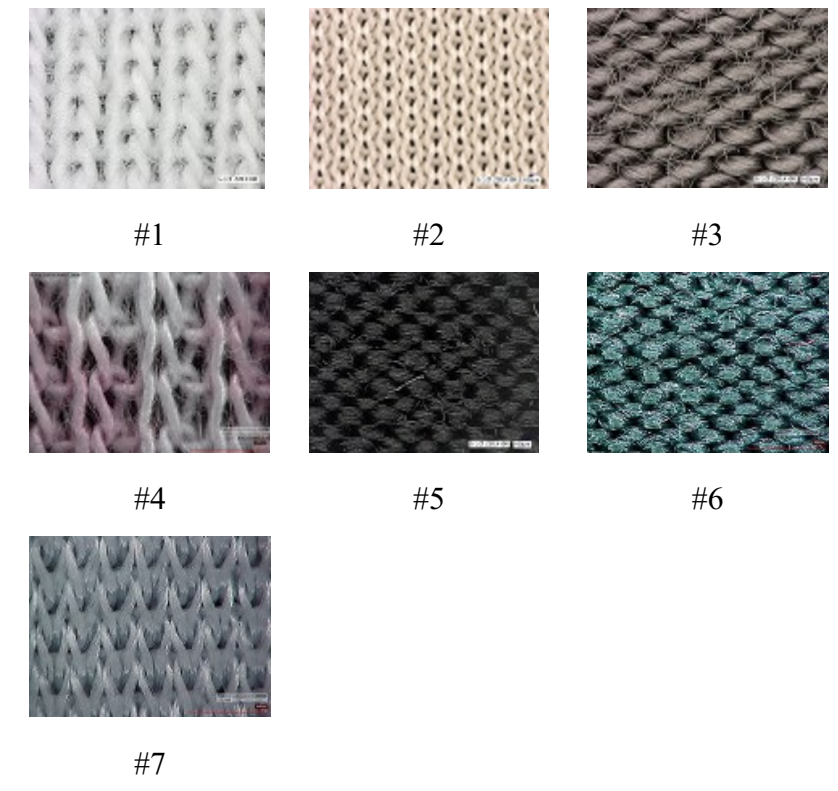
3.3.2 Sensory Evaluation by Hand

In this section, a sensory evaluation is carried out to model the tactile sensation by human evaluation. A paired comparison method was used for this sensory evaluation. 13 adult females around twenties and thirties were asked to touch with their hands in wale direction of fabrics and evaluate 7 samples of fabrics on a seven-point scale with Sample #1 which is made of 100 % cotton as the standard sample. In order to exclude non-tactile effects in the sensory evaluation, the experiment was carried out as blind test with samples' details undisclosed. The participants are informed in advance of what objects that they are going to evaluate.

The sensory evaluation included 15 items of adjectives as mention in section 3.3.1. The room temperature and humidity were controlled to 24 °C and 50 % respectively. The list of

Table 3.14 List of fabric samples

(a) Materials and knitted method		
#	Material	Knitted method
1	Cotton 100 %	Rib stitch
2	Polyester 100 %	Interlock stitch
3	Rayon 95 %, Polyurethane 5 %	Plain stitch
4	Acryl 100 %	Rib stitch
5	Cupro 59 %, Nylon 34 %, Polyurethane 7 %	Plain stitch
6	Cupro 53 %, Nylon 39 %, Polyurethane 8 %	Plain stitch
7	Cupro 60 %, Nylon 30 %, Polyurethane 10 %	Rib stitch

Table 3.14 List of fabric samples (continued from previous page)(b) Picture of fabrics ($\times 100$ magnification)

samples with the material, knitted method and picture are as shown in Table 3.14. The samples are undergarments which are designed for summer season.

This sensory evaluation is participated by only female. This is because Citrin et al. discovered that female requires tactile input more than male to evaluate or purchase a product (Citrin et al., 2003). Thus, by limiting participants to female, this research expects to reduce the errors in evaluation caused from gender difference.

3.3.2.1 Principal Component Analysis

Principal component analysis with varimax rotation is performed to extract the common potential components of adjectives from each group, i.e. LTS and HTS.

Before conducting component analysis, all of the sensory evaluation values are normalized by each participant by using below equation.

$$x'_{ij} = \frac{x_{ij} - \bar{x}}{s} \quad (3.9)$$

x'_{ij} : Normalized sensory value for each item of a sample

x_{ij} : Sensory value for each item of a sample

\bar{x} : Mean for all sensory values of a participant

s : Standard deviation for all sensory values of a participant

As the results, there were 4 principal components extracted with 72.0% of cumulative contribution rate as shown in Table 3.15. According to Shirado et al., the cumulative contribution is preferable to be around 70 to 80 %, so that most of the tactile sensations could be explained by the extracted components (Shirado & Maeno, 2014). The scree plot was as presented in Figure 3.7. PC1 was interpreted as “surface texture” because high loadings were shown by items such as “*kimega arai/ kimega komakai*”, “*zara-zara/ sube-sube*” and “*katai/ yawarakai*”. PC2 was interpreted as “dryness” because high loadings were shown by items such as “*shittori*” and “*sara-sara*”. PC3 was interpreted as “downiless” because high loadings of items “*funwari*” and “*karui/ omoi*”. PC4 was interpreted as “coolness” because high loading of item “*atatakai/ hiyak*”.

Table 3.15 Result for principal component analysis of LTS

Adjective	Principal Components			
	1	2	3	4
<i>Katai/ Yawarakai</i>	0.900	-0.118	0.126	-0.207
<i>Zara-zara/ Sube-sube</i>	0.796	-0.029	0.048	0.207
<i>Kimega arai/ Kimega komakai</i>	0.774	0.197	-0.150	0.071
<i>Shittori</i>	0.036	0.853	-0.029	-0.151
<i>Sara-sara</i>	-0.090	0.690	0.160	0.163
<i>Funwari</i>	0.014	-0.013	0.998	-0.009
<i>Karui/ Omoi</i>	0.066	0.131	0.407	0.027
<i>Hiya'/ Atatakai</i>	-0.008	-0.043	0.004	1.027
Eigenvalue	3.206	1.509	1.290	0.686
Cumulative contribution rate	18.971	39.811	63.307	71.994

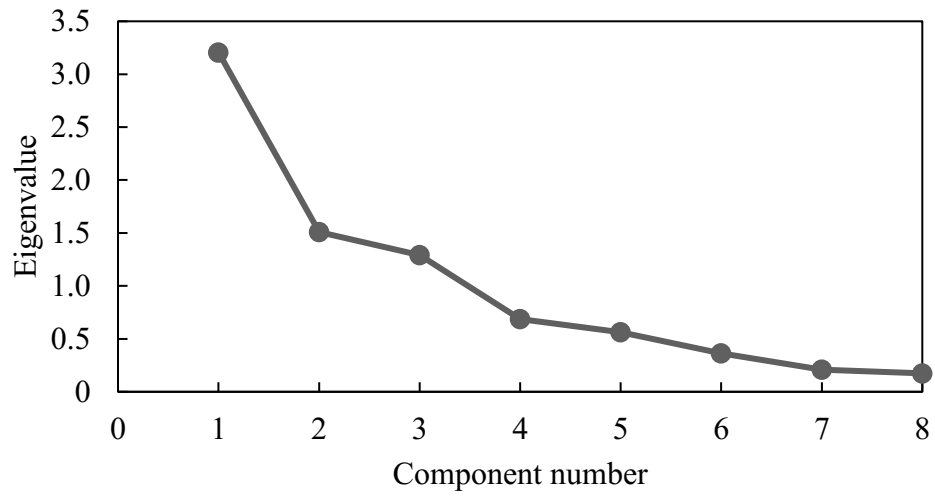


Figure 3.7 Scree plot for principal component analysis of LTS

Table 3.16 Result for principal component analysis of HTS

Adjective	Principal Components	
	1	2
<i>Yasashi</i>	0.937	-0.030
<i>Ochitsuku</i>	0.844	-0.034
<i>Jouhin</i>	0.482	0.334
<i>Sawayaka</i>	0.002	0.878
<i>Sukkiri</i>	-0.020	0.783
Eigenvalue	3.167	0.862
Cumulative contribution rate	56.939	68.751

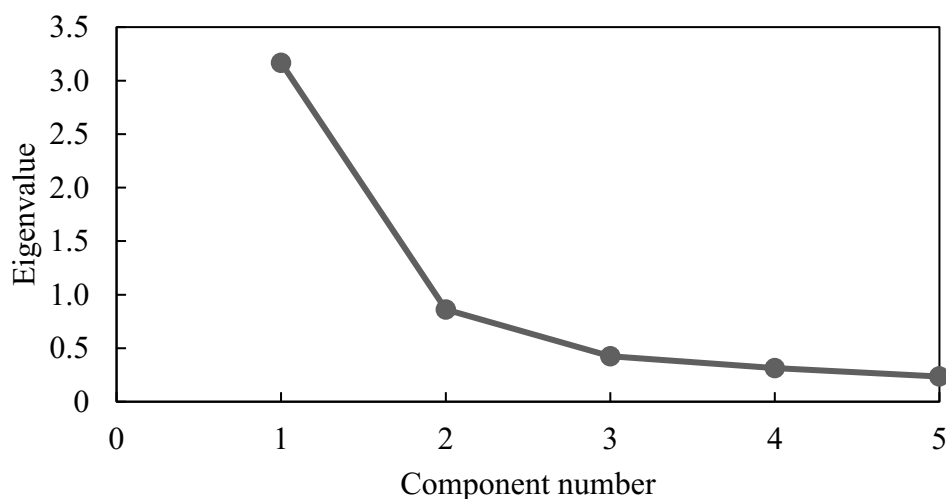


Figure 3.8 Scree plot for principal component analysis of HTS

On the other hand, there were 2 principal components extracted with 68.8% of cumulative contribution rate as shown in Table 3.16 and the scree plot was as presented in Figure 3.8. Although the cumulative contribution ratio is lower than 70 %, the number of extracted components can also be determined by the curve of scree plot. PC1 was interpreted as “relaxation” because high loadings were shown by items such as “*yasashii*”, “*ochitsuku*” and “*jouhin*”. PC2 was interpreted as “refreshingness” because high loadings were shown by items such as “*sawayaka*” and “*sukkiri*”.

3.3.2.2 Multiple Regression Analysis

In this section, multiple regression analysis was conducted to determine and examine the relationship between all components in LTS and each component in HTS, and between all components in HTS and each adjective in DTS by using SPSS software [IBM Corporation]. Before conducting multiple regression analysis, bivariate Pearson correlation was conducted for all explanatory variables to make sure that there is no multicollinearity occurred between the variables. All the correlations showed values below 0.65.

Table 3.17 Result for multiple regression analysis (HTS-“relaxation” with all LTS components)

(a) Correlations					
“relaxation”					
			Pearson correlation		Sig.
“surface texture”			0.984****		.000
“dryness”			0.948***		.001
“downiless”			0.631*		.064
“coolness”			0.714**		.036
*p < .1	**p < .05	***p < .01	****p < .001		

(b) Model Summary			
R	R Square	Adjusted R Square	Std. Error of the Estimate
0.998 ^a	0.996	0.989	0.074478

a. Predictors: (Constant), “surface texture”, “dryness”, “downiless”, “coolness”

(c) ANOVA ^a					
Model	Sum of Squares	df	Mean Square	F	Sig.
Regression	2.942	4	0.736	132.605*	.007 ^b
Residual	0.011	2	0.006		
Total	2.953	6			

*p < .01
a. Dependent variable: “relaxation”
b. Predictors: (Constant), “surface texture”, “dryness”, “downiless”, “coolness”

Table 3.17 Result for multiple regression analysis (HTS-“relaxation” with all LTS principal components)

(d) Coefficients ^a				
Model	Unstandardized Coefficients		Standardized Coefficients	Sig.
	B	Std. Error	Beta	
(Constant)	-8.577E-7	0.028	-	1.000
“surface texture”	1.497	0.561	1.281	.117
“dryness”	-0.109	0.796	-0.097	.904
“downiless”	0.016	0.162	0.012	.932
“coolness”	-0.308	0.372	-0.252	.494

a. Dependent variable: “relaxation”

Table 3.17 shows the correlation and multiple regression analysis results when the dependent variable is HTS component of “relaxation” and the independent variable are LTS components of “surface texture”, “dryness”, “downiless” and “coolness”. As shown in Table 3.17 (a), “surface texture”, “dryness” and “coolness” had a positively and significantly correlation with the “relaxation”. However, “downiless” had a weak positive correlation with “relaxation”. This indicates that when all LTS components values increase, the “relaxation” component value tends to increase too.

The multiple regression model with all four predictors produced $R^2 = 0.996$, $F(4, 2) = 132.605$, $p < .01$, thus, the multiple regression model had a good fit of data, indicating that the “relaxation” scores were related to all four LTS components. According to the standardized regression coefficients, the “surface texture” had the most contribution to the HTS component of “relaxation”, followed by “coolness”. “Surface texture” had a positive regression coefficient, indicating that the higher score of “surface texture”, i.e. the smoother sample was expected to have higher score of “relaxation”, i.e. more relaxation. On the other hand, “coolness” had a negative regression coefficient (opposite in sign from its correlation with “relaxation”), indicating that after accounting for “surface texture”, the higher score of “coolness”, i.e. the cooler sample was expected to have lower score of “relaxation”, i.e. less relaxation. However,

“dryness” and “downiless” had the least contribution to this multiple regression model because the p-value of both LTS components was not significant and nearly 1 (if p-value equals to 1 indicates that the independent variable does not contribute to the regression model at all). From Table 3.17 (d), a multiple regression equation can be obtained as the equation below.

$$H_{relaxation} = (1.497 \times L_{surface}) + (-0.109 \times L_{dryness}) + (0.016 \times L_{downiless}) + (-0.308 \times L_{coolness}) - 8.577 \times 10^{-7} \quad (3.10)$$

Table 3.18 shows the correlation and multiple regression analysis results when the dependent variable is HTS component of “refreshingness” and the independent variable are LTS components of “surface texture”, “dryness”, “downiless” and “coolness”. As shown in Table 3.18 (a), “surface texture”, “dryness” and “coolness” had a positively and significantly correlation with the “relaxation”. However, “downiless” had a weak positive correlation with “refreshingness”. This indicates that when all LTS components values increase, the “refreshingness” component value tend to increase too.

Table 3.18 Result for multiple regression analysis (HTS-“refreshingness” with all LTS principal components)

(a) Correlations		
	“refreshingness”	
	Pearson correlation	Sig.
“surface texture”	0.922***	.002
“dryness”	0.948***	.001
“downiless”	0.209	.326
“coolness”	0.942***	.001

*p < .1 **p < .05 ***p < .01 ****p < .001

Table 3.18 Result for multiple regression analysis (HTS-“refreshingness” with all LTS principal components)

(b) Model Summary					
R	R Square	Adjusted R Square	Std. Error of the Estimate		
0.983 ^a	0.967	0.901	0.21560		

f. Predictors: (Constant), “surface texture”, “dryness”, “downiless”, “coolness”

(c) ANOVA ^a					
Model	Sum of Squares	df	Mean Square	F	Sig.
Regression	2.712	4	0.678	14.584*	.065 ^b
Residual	0.093	2	0.046		
Total	2.805	6			

*p < .1
k. Dependent variable: “refreshingness”
l. Predictors: (Constant), “surface texture”, “dryness”, “downiless”, “coolness”

(d) Coefficients ^a				
Model	Unstandardized Coefficients		Standardized Coefficients	Sig.
	B	Std. Error	Beta	
(Constant)	2.769E-8	0.081	-	1.000
“surface texture”	1.833	1.625	1.610	.376
“dryness”	-1.586	2.303	-1.450	.562
“downiless”	-0.014	0.470	-0.011	.979
“coolness”	1.085	1.076	0.912	.419

a. Dependent variable: “refreshingness”

The multiple regression model with all four predictors produced $R^2 = 0.901$, $F(4, 2) = 14.584$, $p < .1$, thus, the multiple regression model had not so good fit of data compared to “relaxation” regression model. According to the standardized regression coefficients, the “surface texture” had the most contribution to the HTS component of “refreshingness”, followed by “coolness” and “dryness”. “Surface texture” and “coolness” had positive regression coefficients, indicating that the higher score of “surface texture” and “coolness”, i.e. the smoother and cooler sample was expected to have higher score of “refreshingness”, i.e. more refreshing. On the other hand, “dryness” had a negative regression coefficient (opposite in sign from its correlation with “refreshingness”), indicating that after accounting for “surface texture” and “coolness”, the higher score of “dryness”, i.e. the drier sample was expected to have lower score of “refreshingness”, i.e. less refreshing. However, “downiless” had the least contribution to this multiple regression model because the p-value of the LTS component was not significant and nearly 1. From Table 3.18 (d), a multiple regression equation can be obtained as the equation below.

$$H_{refreshingness} = (1.833 \times L_{surface}) + (-1.586 \times L_{dryness}) + (-0.014 \times L_{downiless}) + (1.085 \times L_{coolness}) + 2.769 \times 10^{-8} \quad (3.11)$$

Table 3.19 shows the correlation and multiple regression analysis results when the dependent variable is DTS adjective of “comfort” and the independent variable are HTS

Table 3.19 Result for multiple regression analysis (DTS-“comfort” with all HTS principal components)

(a) Correlations		
	“comfort”	
	Pearson correlation	Sig.
“relaxation”	0.988****	.000
“refreshingness”	0.856***	.007

*p < .1 **p < .05 ***p < .01 ****p < .001

Table 3.19 Result for multiple regression analysis (DTS-“comfort” with all HTS principal components)

(b) Model Summary					
R	R Square	Adjusted R Square	Std. Error of the Estimate		
0.988 ^a	0.977	0.965	0.09127		
a. Predictors: (Constant), “relaxation”, “refreshingness”					
(c) ANOVA ^a					
Model	Sum of Squares	df	Mean Square	F	Sig.
Regression	1.411	2	0.706	84.714*	.001 ^b
Residual	0.033	4	0.008		
Total	1.445	6			
*p < .01					
a. Dependent variable: “comfort”					
b. Predictors: (Constant), “relaxation”, “refreshingness”					
(d) Coefficients ^a					
Model	Unstandardized Coefficients		Standardized Coefficients	Sig.	
	B	Std. Error	Beta		
(Constant)	0.559	0.034	-	.000	
“relaxation”	0.657	0.101	0.940*	.003	
“refreshingness”	0.041	0.103	0.057	.713	
*p < .01					
f. Dependent variable: “comfort”					

components of “relaxation” and “refreshingness”. As shown in Table 3.19 (a), “relaxation” and “refreshingness” were positively and significantly correlated with the “comfort”. This indicates that when all HTS components values increase, the “comfort” adjective sensory evaluation value tend to increase too.

The multiple regression model with all two predictors produced $R^2 = 0.965$, $F(2, 4) = 84.714$, $p < .01$, thus, the multiple regression model had a good fit of data, indicating that the

“comfort” adjective sensory evaluation value was related to all two HTS components. According to the standardized regression coefficients, the “relaxation” had the most contribution to “comfort” adjective sensory evaluation value. “Relaxation” had a positive regression coefficient, indicating that the higher score of “relaxation”, i.e. the more relaxation of sample was expected to have higher value of “comfort” adjective sensory evaluation, i.e. more comfort. However, “refreshingness” had the least contribution to this multiple regression model because the p-value was not significant and nearly 1. From Table 3.19 (d), a multiple regression equation can be obtained as the equation below.

$$D_{comfort} = (0.657 \times H_{relaxation}) + (0.041 \times H_{refreshingness}) + 0.559 \quad (3.12)$$

Table 3.20 shows the correlation and multiple regression analysis results when the dependent variable is DTS adjective of “preference” and the independent variable are HTS components of “relaxation” and “refreshingness”. As shown in Table 3.20 (a), “relaxation” and “refreshingness” were positively and significantly correlated with the “preference”. This indicates that when all HTS components values increase, the “preference” adjective sensory evaluation value tends to increase too.

Table 3.20 Result for multiple regression analysis (DTS-“preference” with all HTS principal components)

(a) Correlations		
	“preference”	
	Pearson correlation	Sig.
“relaxation”	0.993****	.000
“refreshingness”	0.901***	.003

*p < .1 **p < .05 ***p < .01 ****p < .001

Table 3.20 Result for multiple regression analysis (DTS-“preference” with all HTS principal components)

(b) Model Summary					
R	R Square	Adjusted R Square	Std. Error of the Estimate		
0.999 ^a	0.998	0.997	0.02923		
a. Predictors: (Constant), “relaxation”, “refreshingness”					
(c) ANOVA ^a					
Model	Sum of Squares	df	Mean Square	F	Sig.
Regression	1.784	2	0.892	1043.876*	.000 ^b
Residual	0.003	4	0.001		
Total	1.787	6			
*p < .001					
a. Dependent variable: “preference”					
b. Predictors: (Constant), “relaxation”, “refreshingness”					
(d) Coefficients ^a					
Model	Unstandardized Coefficients		Standardized Coefficients	Sig.	
	B	Std. Error	Beta		
(Constant)	0.305	0.011	-	.000	
“relaxation”	0.639	0.032	0.821**	.000	
“refreshingness”	0.162	0.033	0.203*	.008	
*p < .01 **p < .001					
a. Dependent variable: “preference”					

The multiple regression model with all two predictors produced $R^2 = 0.997$, $F(4, 2) = 1043.876$, $p < .001$, thus, the multiple regression model had a better fit of data compared to “comfort” regression model. According to the regression coefficients, the “relaxation” had the most contribution to the DTS adjective of “preference”, followed by “refreshingness”. “Relaxation” and “refreshingness” had significantly positive regression coefficients, indicating that the higher score of “relaxation” and “refreshingness”, i.e. the more relaxation and refreshing sample was expected to have higher value of “preference” adjective sensory evaluation, i.e. more

preferable. From Table 3.20 (d), a multiple regression equation can be obtained as the equation below.

$$D_{preference} = (0.639 \times H_{relaxation}) + (0.162 \times H_{refreshingness}) + 0.305 \quad (3.13)$$

3.3.3 Sensory Evaluation by Forearm

A sensory evaluation is conducted with similar conditions in the section 3.3.2. However, this section focuses to discover the tactile sensation by forearm. As shown in Figure 3.9, both forearms of the participants are placed on a table and an examiner uses a jig to place the fabric samples on the participants' both forearms or stroke in wale direction of fabrics. The touch behavior is set differently according to the adjectives (refer to Table 3.21). The touch behavior will differ depending on the tactile information that one would like to know (Lederman & Klatzky, 1987). The stroking velocity and the placing weight are set as around 50 mm/s and 3 g respectively. Asaga et al. had discovered that human strokes around 52.4 mm/s when one is simply asked to touch an object (Asaga et al., 2013). In order to exclude non-tactile effects in the sensory evaluation, the experiment was carried out as blind test with samples' details undisclosed. The participants are informed in advance of what objects that they are going to evaluate.

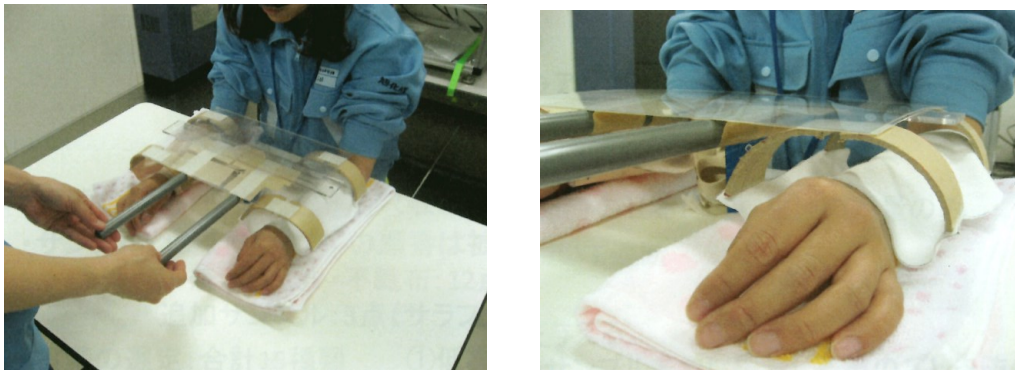


Figure 3.9 Sensory evaluation by forearm [received permission from Asahi Kasei Corporation]

Table 3.21 Adjectives and touch behavior

	Adjectives	Touch behavior
	<i>Hiya' / Atataakai</i>	<i>Overlay on</i>
	<i>Karui/ Omoi</i>	
LTS	<i>Zara-zara/ Sube-sube</i>	<i>Touch stroke</i>
	<i>Kimega arai/ Kimega komakai</i>	
	<i>Katai/ Yawarakai</i>	
	<i>Funwari</i>	
	<i>Shittori</i>	
	<i>Sara-sara</i>	
HTS	<i>Ochitsuku</i>	<i>Touch stroke</i>
	<i>Sawayaka</i>	
	<i>Sukkiri</i>	
	<i>Yasashi</i>	
	<i>Jouhin</i>	
DTS	<i>Kokochiyoi</i>	<i>Touch stroke</i>
	<i>Suki</i>	

3.3.3.1 Principal Component Analysis

Similarly to section 3.2.1, all of the sensory evaluation values were normalized by using equation (1) and varimax rotation was used to extract the principal components in each group, i.e. LTS and HTS.

From the results, there were 3 principal components extracted with 54.9% of cumulative contribution rate as shown in Table 3.22 and the scree plot was as presented in Figure 3.10. Although the cumulative contribution ratio is lower than 70 %, the number of extracted components can also be determined by the curve of scree plot. PC1 was interpreted as “surface texture” because high loadings were shown by items such as “*zara-zara/ sube-sube*”, “*atatakai/ hiyak*”, “*shittori*”, “*kimega arai/ kimega komakai*” and “*sara-sara*”. PC2 was interpreted as

Table 3.22 Result of LTS principal component analysis

Adjective	Principal Components		
	1	2	3
<i>Zara-zara/ Sube-sube</i>	1.015	-0.115	0.163
<i>Kimega arai/ Kimega komakai</i>	0.571	0.015	0.005
<i>Sara-sara</i>	0.490	-0.059	-0.014
<i>Hiya'/ Atatakai</i>	0.481	0.223	-0.115
<i>Shittori</i>	0.448	0.269	-0.225
<i>Katai/ Yawarakai</i>	-0.034	1.010	0.146
<i>Karui/ Omoi</i>	-0.015	-0.029	0.858
<i>Funwari</i>	0.020	0.261	0.486
Eigenvalue	2.922	1.529	0.930
Cumulative contribution rate	20.865	41.073	54.876

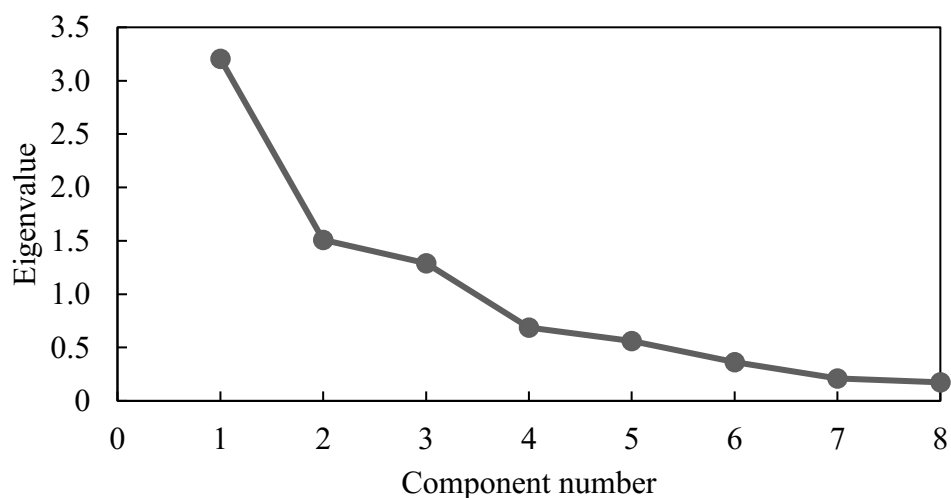


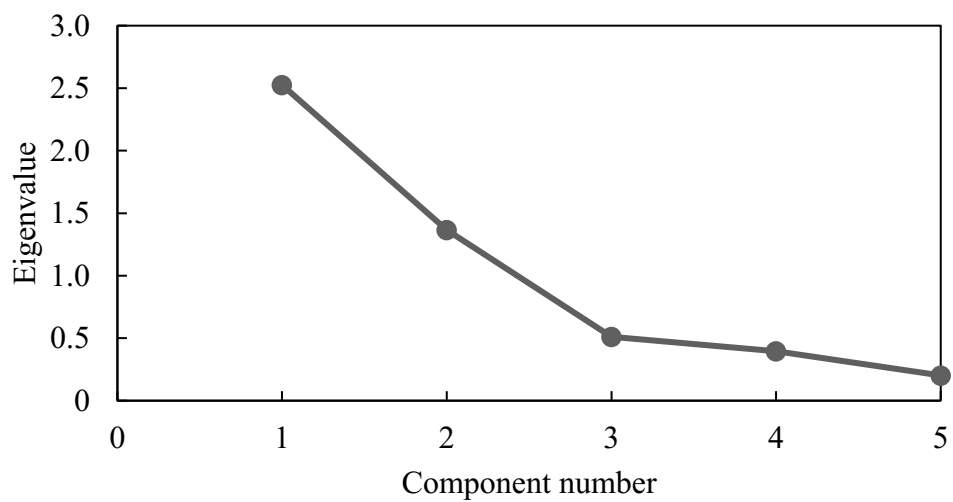
Figure 3.10 Scree plot for principal component analysis of LTS

“softness” because high loading was shown by item of “*katai/ yawarakai*”. PC3 was interpreted as “downless” because high loadings of items “*karui/ omoi*” and “*funwari*”.

On the other hand, there were 3 principal components extracted with 88.0% of cumulative contribution rate as shown in Table 3.23. The scree plot was as shown in Figure 3.11. PC1 was interpreted as “refreshingness” because high loadings were shown by items such as “*sawayaka*” and “*sukkiri*”. PC2 was interpreted as “relaxation” because high loadings were shown by items such as “*ochitsuku*” and “*yasashii*”. PC3 was interpreted as “elegant” because high loading of item “*jouhin*”.

Table 3.23 Result for principal component analysis of HTS

Adjective	Principal Components		
	1	2	3
<i>Sawayaka</i>	0.947	-0.029	0.016
<i>Sukkiri</i>	0.906	0.085	0.055
<i>Ochitsuku</i>	0.103	1.004	-0.123
<i>Yasashi</i>	-0.177	0.530	0.496
<i>Jouhin</i>	0.111	-0.094	0.971
Eigenvalue	2.525	1.365	0.511
Cumulative contribution rate	50.508	77.818	88.044

**Figure 3.11** Scree plot for principal component analysis of HTS

3.3.3.2 Multiple Regression Analysis

Similarly to section 3.3.2, multiple regression analysis was conducted to determine and examine the relationship between all components in LTS and each component in HTS, and between all components in HTS and each adjective in DTS. Before conducting multiple

Table 3.24 Result for multiple regression analysis (HTS-“relaxation” with all LTS principal components)

(a) Correlations					
“relaxation”					
	Pearson correlation	Sig.			
“surface texture”	0.937***	.001			
“softness”	0.808**	.014			
“downiless”	-0.173	.355			
*p < .1 **p < .05 ***p < .01 ****p < .001					
(b) Model Summary					
R	R Square	Adjusted R Square	Std. Error of the Estimate		
0.949 ^a	0.901	0.803	0.16018		
a. Predictors: (Constant), “surface texture”, “softness”, “downiless”					
(c) ANOVA ^a					
Model	Sum of Squares	df	Mean Square	F	Sig.
Regression	0.703	3	0.234	9.138*	.051 ^b
Residual	0.077	3	0.026		
Total	0.780	6			
*p < .1					
a. Dependent variable: “relaxation”					
b. Predictors: (Constant), “surface texture”, “softness”, “downiless”					

Table 3.24 Result for multiple regression analysis (HTS-“relaxation” with all LTS principal components)

(d) Coefficients ^a				
Model	Unstandardized Coefficients		Standardized Coefficients	Sig.
	B	Std. Error	Beta	
(Constant)	-3.258E-7	0.061	-	1.000
“surface texture”	0.531	0.267	1.004	.141
“softness”	-0.007	0.293	-0.011	.983
“downiless”	0.167	0.315	0.170	.633

a. Dependent variable: “relaxation”

regression analysis, bivariate Pearson correlation was conducted for all explanatory variables to make sure that there is no multicollinearity occurred between the variables. All the correlations showed values below 0.65.

Table 3.24 shows the correlation and multiple regression analysis results when the dependent variable is HTS component of “relaxation” and the independent variable are LTS components of “surface texture”, “softness” and “downiless”. As shown in Table 3.24 (a), “surface texture” and “softness” were positively and significantly correlated with the “relaxation”, indicating that when all LTS components values increase, the “relaxation” component value tends to increase too. However, “downiless” had a weak negative correlation with “relaxation”.

The multiple regression model with all three predictors produced $R^2 = 0.803$, $F(3, 3) = 0.803$, $p < .1$, thus, the multiple regression model did have not so good fit of data, indicating that the “relaxation” scores may be related to all three LTS components. According to the standardized regression coefficients, the “surface texture” had the most contribution to the HTS component of “relaxation”, followed by “downiless”. “Surface texture” and “downiless” had positive regression coefficient, indicating that the higher score of “surface texture” and “downiless”, i.e. the smoother and not too downy sample was expected to have higher score of “relaxation”, i.e. more relaxation. However, “dryness” had the least contribution to this multiple

regression model because the p-value of both LTS components was not significant and nearly 1. From Table 3.24 (d), a multiple regression equation can be obtained as the equation below.

$$H_{relaxation} = (0.531 \times L_{surface}) + (-0.007 \times L_{softness}) + (0.167 \times L_{downiless}) - 3.258 \times 10^{-7} \quad (3.14)$$

Table 3.25 shows the correlation and multiple regression analysis results when the dependent variable is HTS component of “refreshingness” and the independent variable are LTS components of “surface texture”, “softness” and “downiless”. As shown in Table 3.25 (a), “surface texture” was positively and significantly correlated with the “relaxation”. On the other hand, “downiless” was negatively and significantly correlated with the “refreshingness”. However, “softness” had a weak positive correlation with “refreshingness”. This indicates that “surface texture” component value increases, the “refreshingness” component value tend to

Table 3.25 Result for multiple regression analysis (HTS-“refreshingness” with all LTS principal components)

(a) Correlations			
	“refreshingness”		
	Pearson correlation	Sig.	
“surface texture”	0.885***	.004	
“softness”	0.436	.164	
“downiless”	-0.612*	.072	
*p < .1 **p < .05 ***p < .01 ****p < .001			
(b) Model Summary			
R	R Square	Adjusted R Square	Std. Error of the Estimate
.977 ^a	.954	.907	.20304
a. Predictors: (Constant), “surface texture”, “softness”, “downiless”			

Table 3.25 Result for multiple regression analysis (HTS-“refreshingness” with all LTS principal components)

(c) ANOVA ^a					
Model	Sum of Squares	df	Mean Square	F	Sig.
Regression	2.545	3	0.848	20.579*	.017 ^b
Residual	0.124	3	0.041		
Total	2.669	6			

*p < .05

a. Dependent variable: “refreshingness”

b. Predictors: (Constant), “surface texture”, “softness”, “downiless”

(d) Coefficients ^a				
Model	Unstandardized Coefficients		Standardized Coefficients	Sig.
	B	Std. Error	Beta	
(Constant)	-1.232E-6	0.077	-	1.000
“surface texture”	1.368	0.339	1.398	.141
“softness”	-0.733	0.371	-0.656	.983
“downiless”	-0.007	0.399	-0.004	.633

a. Dependent variable: “refreshingness”

increase too, and when the “softness” component value increases, the “refreshingness” component value tend to decrease.

The multiple regression model with all three predictors produced $R^2 = 0.907$, $F(3, 3) = 20.579$, $p < .05$, thus, the multiple regression model had a better fit of data compared to “relaxation” regression model. According to the standardized regression coefficients, the “surface texture” had the most contribution to the HTS component of “refreshingness”, followed by “softness”. “Surface texture” had a positive regression coefficient, indicating that the higher score of “surface texture”, i.e. the smoother sample was expected to have higher score of “refreshingness”, i.e. more refreshing. On the other hand, “softness” had a negative regression

coefficient (opposite in sign from its correlation with “refreshingness”), indicating that after accounting for “surface texture”, the higher score of “softness”, i.e. the softer sample was expected to have lower score of “refreshingness”, i.e. less refreshing. However, “downiless” had the least contribution to this multiple regression model because the p-value of the LTS component was not significant and nearly 1. From Table 3.25 (d), a multiple regression equation can be obtained as the equation below.

$$H_{refreshingness} = (1.368 \times L_{surface}) + (-0.733 \times L_{softness}) + (-0.007 \times L_{downiless}) - 1.232 \times 10^{-6} \quad (3.15)$$

Table 3.26 shows the correlation and multiple regression analysis results when the dependent variable is HTS component of “elegant” and the independent variable are LTS components of “surface texture”, “softness” and “downiless”. As shown in Table 3.26 (a),

Table 3.26 Result for multiple regression analysis (HTS-“elegant” with all LTS principal components)

(a) Correlations			
	“elegant”		
	Pearson correlation	Sig.	
“surface texture”	0.864***	.006	
“softness”	0.931***	.001	
“downiless”	0.162	.364	

*p < .1 **p < .05 ***p < .01 ****p < .001

(b) Model Summary			
R	R Square	Adjusted R Square	Std. Error of the Estimate
0.991 ^a	0.982	0.965	0.11717

a. Predictors: (Constant), “surface texture”, “softness”, “downiless”

Table 3.26 Result for multiple regression analysis (HTS-“elegant” with all LTS principal components)

(c) ANOVA ^a					
Model	Sum of Squares	df	Mean Square	F	Sig.
Regression	2.287	3	0.762	55.534*	.004 ^b
Residual	0.041	3	0.014		
Total	2.329	6			

*p < .05

a. Dependent variable: “elegant”

b. Predictors: (Constant), “surface texture”, “softness”, “downiless”

(d) Coefficients ^a				
Model	Unstandardized Coefficients		Standardized Coefficients	Sig.
	B	Std. Error	Beta	
(Constant)	2.658E-7	0.044		1.000
“surface texture”	0.867	0.196	0.948*	.021
“softness”	0.099	0.214	0.095	.676
“downiless”	0.788	0.230	0.466*	.042

*p < .05

a. Dependent variable: “elegant”

“surface texture” and “softness” were positively and significantly correlated with the “elegant”. However, “softness” had a weak positive correlation with “elegant”. This indicates that when all LTS components values increase, the “elegant” component value tends to increase too.

The multiple regression model with all three predictors produced $R^2 = 0.965$, $F(3, 3) = 55.534$, $p < .01$, thus, the multiple regression model had a quite better fit of data compared to “relaxation” and “refreshing” regression model. According to the standardized regression coefficients, the “surface texture” had the most contribution to the HTS component of “elegant”, followed by “downiless”. “Surface texture” and “downiless” had significantly positive regression coefficients, indicating that the higher score of “surface texture” and “downiless”, i.e. the

smoother and not too downy sample was expected to have higher score of “elegant”, i.e. more elegant. On the other hand, “softness” had the least contribution to this multiple regression model, and it was not significantly positive regression coefficient, indicating that the higher score of “softness”, i.e. the softer sample may not expect to have higher score of “elegant”, i.e. more elegant. From Table 3.26 (d), a multiple regression equation can be obtained as the equation below.

$$H_{elegant} = (0.867 \times L_{surface}) + (0.099 \times L_{softness}) + (0.788 \times L_{downiness}) + 2.658 \times 10^{-7} \quad (3.16)$$

Table 3.27 shows the correlation and multiple regression analysis results when the dependent variable is DTS adjective of “comfort” and the independent variable are HTS components of “relaxation”, “refreshingness” and “elegant”. As shown in Table 3.27 (a), “relaxation”, “refreshingness” and “elegant” were positively and significantly correlated with the “comfort”. This indicates that when all HTS components values increase, the “comfort” adjective

Table 3.27 Result for multiple regression analysis (DTS-“comfort” with all HTS principal components)

(a) Correlations			
	“comfort”		
	Pearson correlation	Sig.	
“relaxation”	0.779**	.020	
“refreshingness”	0.896***	.003	
“elegant”	0.952****	.000	
*p < .1 **p < .05 ***p < .01 ****p < .001			
(b) Model Summary			
R	R Square	Adjusted R Square	Std. Error of the Estimate
0.982 ^a	0.964	0.928	0.12554
a. Predictors: (Constant), “relaxation”, “refreshingness”, “elegant”			

Table 3.27 Result for multiple regression analysis (DTS-“comfort” with all HTS principal components)

(c) ANOVA^a

Model	Sum of Squares	df	Mean Square	F	Sig.
Regression	1.268	3	0.423	26.827*	.011 ^b
Residual	0.047	3	0.016		
Total	1.316	6			

*p < .05

a. Dependent variable: “comfort”

b. Predictors: (Constant), “relaxation”, “refreshingness”, “elegant”

(d) Coefficients^a

Model	Unstandardized Coefficients		Standardized Coefficients	Sig.
	B	Std. Error	Beta	
(Constant)	0.315	0.047		.007
“relaxation”	0.219	0.117	0.312	.157
“refreshingness”	-0.020	0.355	-0.015	.959
“elegant”	0.580	0.173	0.772*	.044

*p < .05

a. Dependent variable: “comfort”

sensory evaluation value tends to increase as well.

The multiple regression model with all three predictors produced $R^2 = 0.928$, $F(3, 3) = 26.827$, $p < .05$, thus, the multiple regression model had a good fit of data, indicating that the “comfort” adjective sensory evaluation value was related to all three HTS components. According to the standardized regression coefficients, the “elegant” had the most contribution to “comfort” adjective sensory evaluation value, followed by “refreshing”. “Elegant” had a significantly positive regression coefficient, indicating that the higher score of “elegant”, i.e. the more elegant sample was expected to have higher value of “comfort” adjective sensory evaluation, i.e. more comfort. Furthermore, “refreshing” had a positive regression coefficient,

indicating that the higher score of “refreshingness”, i.e. the more refreshing sample was expected to have higher value of “comfort” adjective sensory evaluation, i.e. more comfort. However, “relaxation” had the least contribution to this multiple regression model because the p-value was not significant and nearly 1. From Table 3.27 (d), a multiple regression equation can be obtained as the equation below.

$$D_{comfort} = (0.219 \times H_{refreshingness}) + (-0.020 \times H_{relaxation}) + (0.580 \times H_{elegant}) + 0.315 \quad (3.17)$$

Table 3.28 shows the correlation and multiple regression analysis results when the dependent variable is DTS adjective of “preference” and the independent variable are HTS components of “relaxation”, “refreshingness” and “elegant”. As shown in Table 3.28 (a),

Table 3.28 Result for multiple regression analysis (DTS-“preference” with all HTS principal components)

(a) Correlations			
	“preference”		
	Pearson correlation	Sig.	
“relaxation”	0.845***	.008	
“refreshingness”	0.936***	.001	
“elegant”	0.935***	.001	

*p < .1 **p < .05 ***p < .01 ****p < .001

(b) Model Summary			
R	R Square	Adjusted R Square	Std. Error of the Estimate
0.997 ^a	0.993	0.986	0.05272

a. Predictors: (Constant), “relaxation”, “refreshingness”, “elegant”

Table 3.28 Result for multiple regression analysis (DTS-“preference” with all HTS principal components)

(c) ANOVA ^a					
Model	Sum of Squares	df	Mean Square	F	Sig.
Regression	1.209	3	0.403	145.051*	.001 ^b
Residual	0.008	3	0.003		
Total	1.218	6			

*p < .01

a. Dependent variable: “preference”

Predictors: (Constant), “relaxation”, “refreshingness”, “elegant”

(d) Coefficients ^a				
Model	Unstandardized Coefficients		Standardized Coefficients	Sig.
	B	Std. Error	Beta	
(Constant)	0.320	0.020		.001
“relaxation”	0.255	0.049	0.377*	.014
“refreshingness”	0.207	0.149	0.165	.259
“elegant”	0.402	0.073	0.556*	.012

*p < .05

a. Dependent variable: “preference”

“relaxation”, “refreshingness” and “elegant” were positively and significantly correlated with the “preference”. This indicates that when all HTS components values increase, the “preference” adjective sensory evaluation value tends to increase too.

The multiple regression model with all three predictors produced $R^2 = 0.986$, $F(3, 3) = 145.051$, $p < .01$, thus, the multiple regression model had a quite better fit of data compared to “comfort” regression model. According to the standardized regression coefficients, the “elegant” had the most contribution to the DTS adjective of “preference”, followed by “refreshingness”. “Elegant” and “refreshingness” had significantly positive regression coefficients, indicating that the higher score of “elegant” and “refreshingness”, i.e. the more elegant and refreshing sample was expected to have higher value of “preference” adjective sensory evaluation, i.e. more

preferable. On the other hand, “relaxation” had the least contribution to this multiple regression model, and it was not significantly positive regression coefficient, indicating that the higher score of “relaxation”, i.e. the more relaxation sample may not expect to have higher value of “preference” adjective sensory evaluation, i.e. more preferable. From Table 3.28 (d), a multiple regression equation can be obtained as the equation below.

$$D_{preference} = (0.255 \times H_{refreshingness}) + (0.207 \times H_{relaxation}) + (0.402 \times H_{elegant}) + 0.320 \quad (3.18)$$

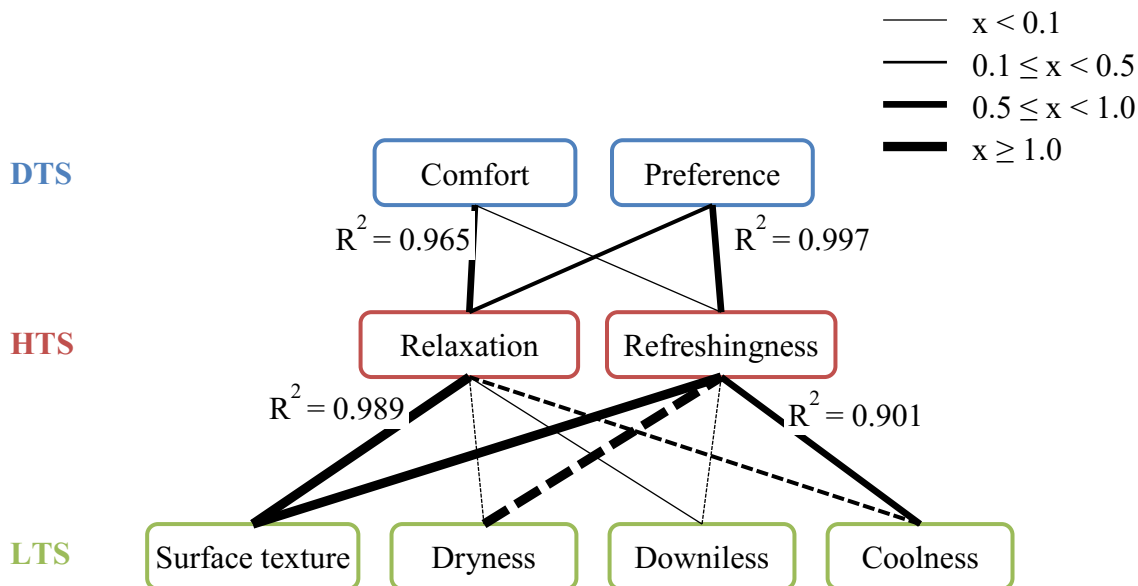


Figure 3.12 Results of principal component analysis and multiple regression analysis (tactile sensation of hand)

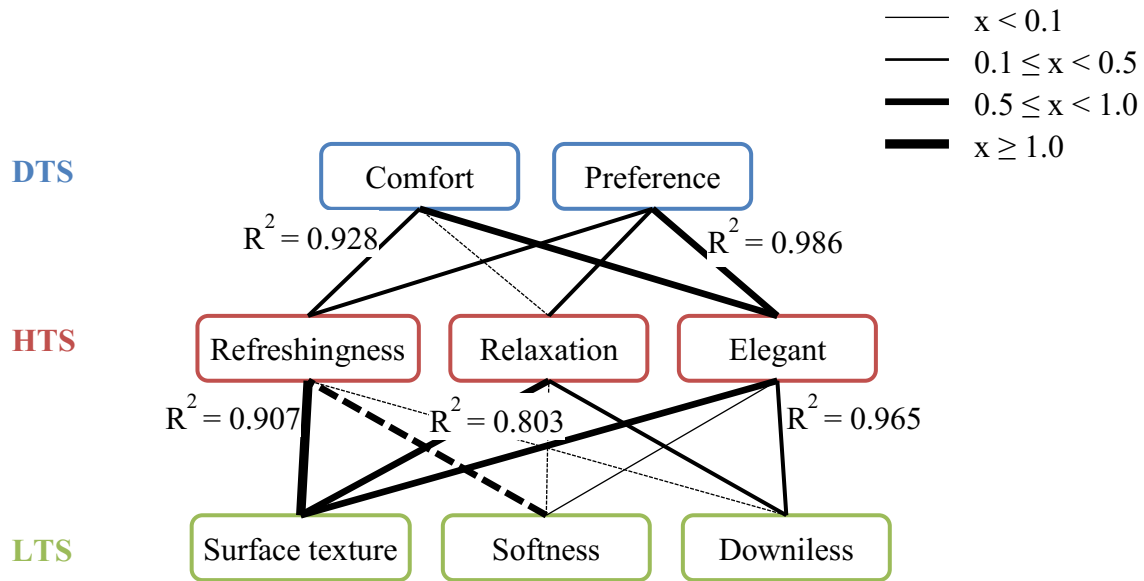


Figure 3.13 Results of principal component analysis and multiple regression analysis (tactile sensation of forearm)

3.3.4 Discussions

From the principal component analysis and multiple regression analysis results, the hierarchical structure of tactile sensation for hand and forearm can be summarized as shown in Figure 3.12 and Figure 3.13 respectively.

By using the multiple regression equations, DTS adjectives for hand and forearm can be expressed by LTS principal components. In order to express DTS adjectives for hand in terms of LTS principal components, the equations (3.10) and (3.11) are substituted in equation (3.12) and (3.13). The computed equations are as shown below.

$$D_{comfort,hand} = (1.059 \times L_{surface}) + (-0.137 \times L_{dryness}) + (0.010 \times L_{downliness}) + (-0.158 \times L_{coolness}) + 0.559 \quad (3.18)$$

$$D_{preference,hand} = (1.254 \times L_{surface}) + (-0.327 \times L_{dryness}) + (0.008 \times L_{downliness}) + (-0.021 \times L_{coolness}) + 0.305 \quad (3.19)$$

On the other hand, DTS adjectives for forearm can be expressed in terms of LTS principal components, when the equations (3.14), (3.15) and (3.16) are substituted in equation (3.17) and (3.18). The computed equations are as shown below.

$$D_{comfort,forearm} = (0.792 \times L_{surface}) + (-0.103 \times L_{dryness}) + (0.452 \times L_{downiless}) + 0.315 \quad (3.20)$$

$$D_{preference,forearm} = (0.807 \times L_{surface}) + (-0.149 \times L_{dryness}) + (0.350 \times L_{downiless}) + 0.320 \quad (3.21)$$

From the above summary, there are some points that show the differences in tactile perception of hand and forearm. First, in principal component analysis of LTS, in the case of hand, there are 4 principal components were extracted, i.e. “surface properties”, “dryness”, “downiless” and “coolness”. However, in the case of forearm, there are 3 principal components were extracted, i.e. “surface properties”, “softness” and “downiless”.

From the principal component analysis results, hand was able to discover “dryness” and “coolness” better than forearm. During the evaluation by forearm, the adjectives that represent “dryness” and “coolness” were not extracted as principal components but the adjectives were included inside “surface texture” principal component. This shows that one could evaluate the dryness and coolness of fabric by using hand. This may be due to the difference in receptors exist in hand (glabrous skin) and forearm (hairy skin), and the greater sensitivity of touch by hand compared to forearm.

Next, this analysis also found that the forearm could distinguish between “softness” and “downiless” compared to hand. During the evaluation by hand, the adjective that represents “softness” was not extracted and was included in the principal component called “surface texture”. This may be due to the difference in the way of handling the fabric. In order to evaluate “downiless”, one may press the fabric, however, to evaluate “softness” one may not only press

the fabric, but also crumple the fabric or overlay the fabric on the skin. For example, the softer the fabric, the easier the fabric will overlay according to the shape of an object.

Then, in principal component analysis of HTS, in the case of hand, there are 2 potential principal components were extracted, i.e. “relaxation” and “refreshingness”. However, in the case of forearm, there are 3 potential principal components were extracted, i.e. “relaxation”, “refreshingness” and “elegant”. The results present that forearm could evaluate “elegant” compared to hand. During the evaluation by hand, the adjective that represents “elegant” was not extracted and was included in the principal component of “relaxation”. This may be interpreted as when one wears the fabric, one could evaluate the elegant of the fabric; indicating that elegant is one of the important principal components during the evaluation.

In this chapter, all DTS adjectives have been expressed in terms of LTS principal components. By quantifying the LTS principal components by using physical quantities which will be discussed in Chapter 4, DTS adjectives can be quantified by physical quantities as highlighted in this research.

Chapter 4

QUANTIFICATION FOR HUMAN TACTILE SENSATION

By using the modeling result of tactile sensation in Chapter 3, the method to quantify may be determined in this chapter. This research proposes to quantify the LTS as LTS is easier to relate with physical quantities. This is due to the fact that LTS describes directly the texture/property of the object. As shown in Figure 4.1, by quantifying LTS with physical quantities, DTS can also be quantified.

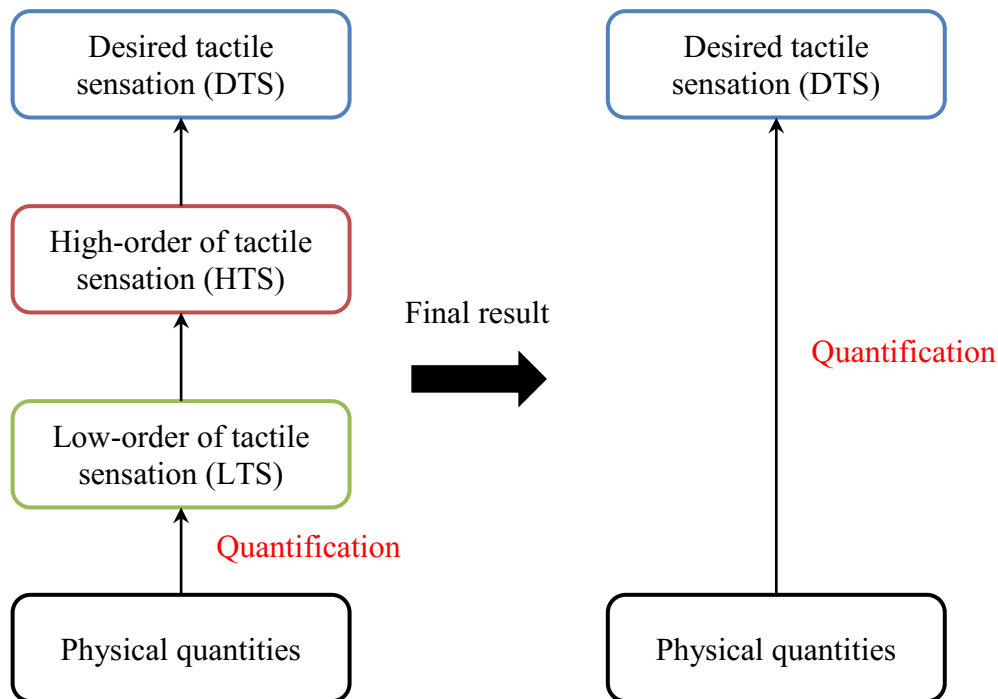


Figure 4.1 Proposed concept of quantification of tactile sensation

4.1 Quantification Tactile Sensation for Door Armrest

For quantification tactile sensation for door armrest, this research suggests using physical quantities from the transducer's outputs (refer to Section 3.1.1) which represent the physical effects of the skin from skin-object interaction, such as, deformation, vibration, thermal effects, etc. These physical effects are the stimuli that are perceived by the cutaneous receptors, not the object's physical properties.

4.1.1 Data Collection of Physical Quantities

There will be four physical measures (vibration, bulk displacement for surface deformation, thermal property, and friction) for each sample that are acquired in this section by a proposed tactile sensor for vibration and commercialized tactile sensors for others.

4.1.1.1 Vibration

During interaction between skin and object, vibration is one of the physical effects that are evoked. There are four kinds of mechanoreceptors in human glabrous skin that perceived vibration or mechanical stimuli: fast adapting, FA I (Meissner corpuscle), slow adapting, SA I (Merkel's disc), FA II (Pacinian corpuscle) and SA II (Ruffini ending) (Miyaoaka, 2010b). Furthermore, each mechanoreceptor has its individual frequency band of vibrating stimuli. Moreover, they have their own perceptible frequency range up to 1000 Hz (A. Gescheider, 2001).

This research referred to previous research on the method of collecting and indexing vibrational data. Asaga et al. had collected vibrational data by tracing on the surface of samples with a piezoelectric element. Then, the vibrational data was compared with mechanoreceptors properties. As a result, two vibratory stimuli values, $I_{FA I}$ and $I_{FA II}$, which correspond to the firing status of FA I and FA II, were determined and used to quantify roughness (Asaga et al., 2013). Here, a 15 mm × 22 mm × 3 mm acrylic resin plate with a piezoelectric element attached to was fabricated as shown in Figure 4.2. Piezoelectric element is mostly used for actuating or sensing vibration in numerous researches as it has simple mechanism so that it is easy to implement in any design (Dargahi & Payandeh, 1998; Klatzky, Pawluk, & Peer, 2013; Xie & Livermore, 2016,

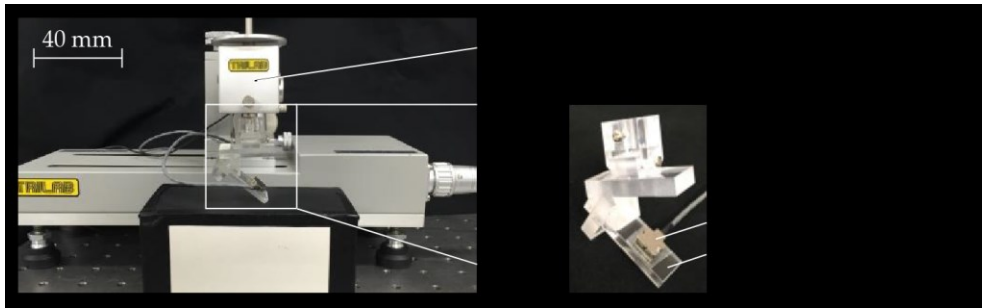
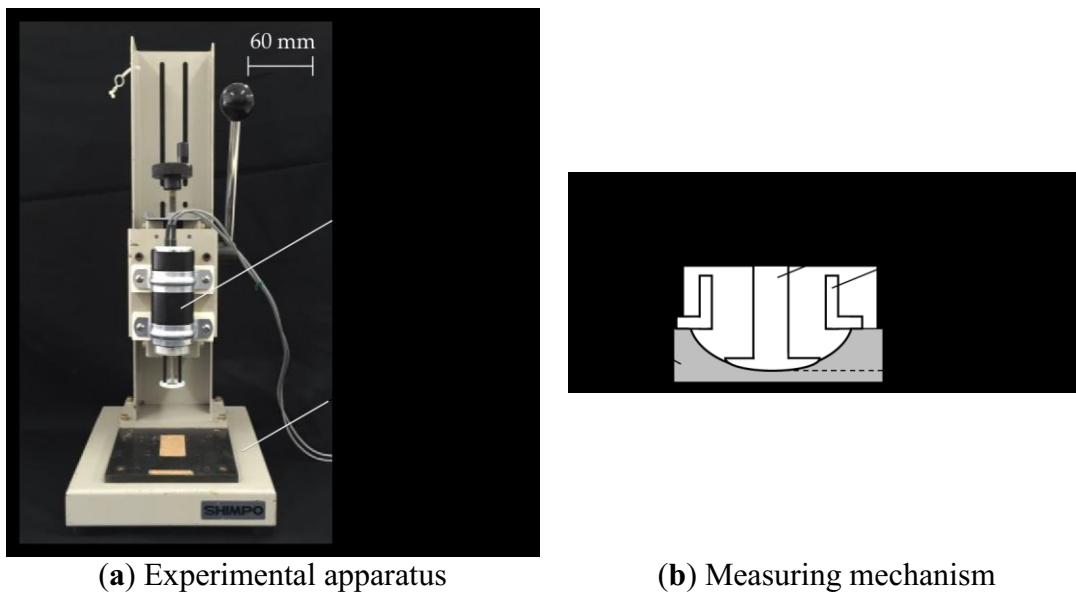


Figure 4.2 Experimental apparatus for measuring vibration.



(a) Experimental apparatus

(b) Measuring mechanism

Figure 4.3 Measurement of bulk displacement.

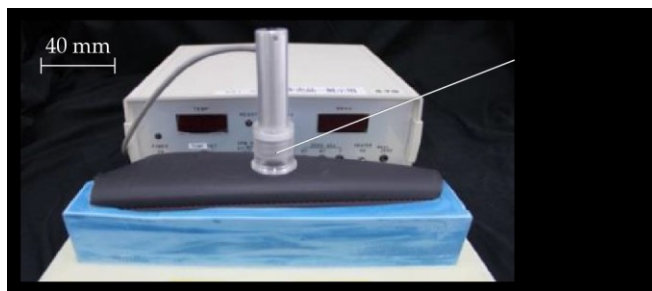
2017; Xie, Zaitsev, Velásquez-García, Teller, & Livermore, 2014). The sensor was placed 45° to the door armrest sample and traced on with a velocity of 50 mm/s under a load of 0.49 N. Then, two values of vibratory stimuli, $I_{FA I}$ and $I_{FA II}$ [$V^2 \cdot Hz$] which corresponded to mechanoreceptor FA I and FA II were estimated and will be used in correlating with LTS in the next section.

4.1.1.2 Bulk Displacement

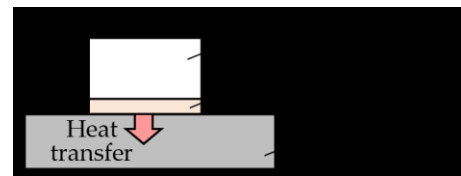
Compliance or softness is perceived when skin is pressed on an object, and both the finger and the object deform as well as change their profile/pressure distributions (Klatzky et al., 2013). However, the deformation of skin will not be measured because previous research (Bergmann Tiest & Kappers, 2009) proved that 90 percent of the information in perceiving compliance is associated with the perception of surface deformation. Consequently, this research proposes to measure bulk displacement when a fixed force is applied. By using an indentation hardness tester (TK-HS100, Tokushu-Keisoku. Co., Ltd, Yokohama, Japan) as shown in Figure 4.3, a sample was pressed with loads from 5 N to 30 N, with an interval of 5 N and the corresponding bulk displacements, d [mm] were measured.

4.1.1.3 Thermal Properties

Coldness or warmth is perceived when heat is transferred from or to our skin when we touch them (L. a Jones & Ho, 2008). Perception of temperature is attributed to the thermal property between skin and an object (Okamoto et al., 2013). By using Thermo Labo II B (FR-07, Kato Tech. Co., Ltd., Kyoto, Japan) which is a heat flux sensor, the silicone rubber surfaced sensor with dimension of $\phi 35 \times 122$ mm was preheated to 33°C which was the average finger skin temperature, and then it was placed on the sample as shown in Figure 4.4. The peak heat



(a) Experimental apparatus



(b) Measuring mechanism

Figure 4.4 Measurement of thermal property

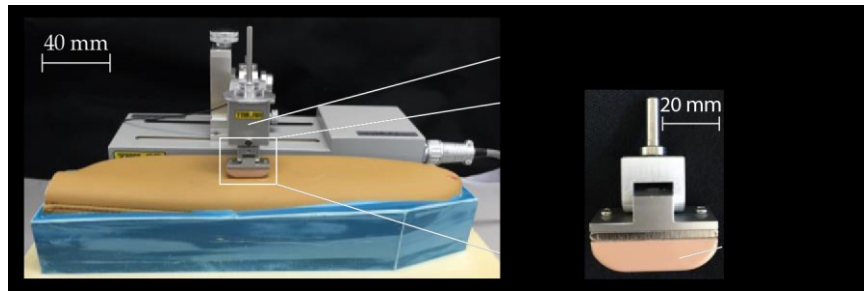


Figure 4.5 Experimental apparatus for measuring frictional force

transfer speed, q_{max} [-] was determined. Note that the sample was left in a room with temperature of 23 °C.

4.1.1.4 Friction Force

Slipperiness or stickiness is a perception when skin slides over on an object's surface, and the skin stretches and adheres to the surface (Okamoto et al., 2013). Furthermore, according to previous research, this perception is mainly attributed to friction forces or friction coefficients (Guest et al., 2012; Shirado, Maeno, & Nonomura, 2006; Smith, Scott, Smith, & Scott, 1996). Hence, by using Built-up Static-Dynamic Friction Measuring Device (TL201Ts, Trinity-Lab. Co., Ltd., Tokyo, Japan) with a skin-like urethane pad as shown in Figure 4.5, frictional force was measured and its variance, A_{fric} was computed to represent the magnitude of fluctuation of the frictional force. The sensor was placed on a sample with a preload of 1.47 N and traced with a velocity of 5 mm/s.

4.1.2 Quantification of Tactile Sense Evaluation

4.1.2.1 Principal Component Analysis

Principal component analysis with varimax rotation was performed to group physical quantities that had strong correlation, and ensured no multicollinearity between independent variables. The result is as shown in Table 4.1. There were four principal components extracted with 94.9% of the total variance; PC1 was associated with bulk displacements for all load conditions, PC2 with vibratory stimuli values of I_{FAI} and I_{FAII} , PC3 with peak heat transfer speed, q_{max} , and PC4 with variance of dynamic frictional force, A_{fric} . This result supports the concept of four main aspects of haptic information which are vibration, bulk displacement for surface

Table 4.1 Result of principal component analysis for physical quantities

Physical quantities	Principal Components			
	1	2	3	4
d_{20N}	0.920	0.347	-0.124	0.083
d_{15N}	0.919	0.340	-0.165	0.087
d_{25N}	0.910	0.350	-0.113	0.062
d_{10N}	0.897	0.308	-0.248	0.061
d_{30N}	0.894	0.344	-0.106	0.032
d_{5N}	0.825	0.183	-0.400	-0.021
I_{FAI}	-0.418	-0.840	-0.056	0.114
I_{FAII}	-0.477	-0.765	0.268	-0.103
q_{max}	-0.250	-0.063	0.955	0.040
A_{fric}	0.084	-0.021	0.035	0.992
Eigen value	6.931	1.061	0.951	0.545
Cumulative contribution ratio	52.77	71.77	84.54	94.87

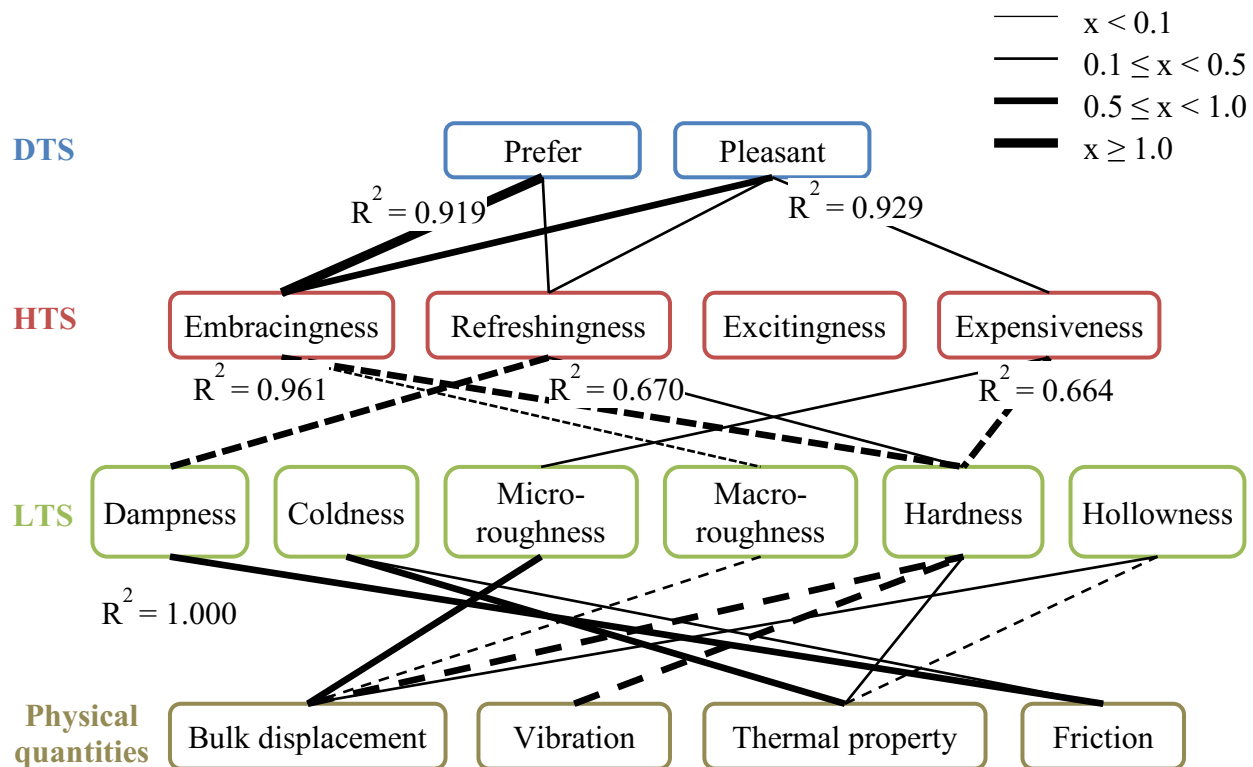


Figure 4.6 Multiple regression analysis result.

deformation,

4.1.2.2 Multiple Regression Analysis

By using principal components scores, multiple linear regression with a stepwise method was conducted three times using statistical analysis software (SPSS Ver. 22, IBM), and Figure 4.6 shows the result. Here, LTS (as dependent variables) and physical quantities (as independent variables). Before conducting multiple linear regression, bivariate Pearson correlation was conducted for all explanatory variables to make sure that there is no multicollinearity occurred between the variables. All the correlations showed values below 0.65. The thickness of the lines corresponds to the standardized coefficients. Moreover, the solid and dash lines indicate the positive and negative coefficients, respectively.

$$D_{prefer} = (0.868 \times \text{Bulk displacement}) + (0.380 \times \text{Vibration}) \\ + (-0.217 \times \text{Thermal property}) + (-0.0821 \times \text{Friction}) + 3.77 \quad (4.1)$$

$$D_{pleasure} = (0.816 \times \text{Bulk displacement}) + (0.342 \times \text{Vibration}) \\ + (-0.195 \times \text{Thermal property}) + (-0.0757 \times \text{Friction}) + 3.90 \quad (4.2)$$

4.1.2.3 Discussions

The above physical measuring and statistical analysis results have shown that the proposed concepts of the developed assessment system can be considered adequate with slight errors. First of all, the concept of hierarchy stages of subjective responses has helped us to easily interpret the main aspect of tactile sensation that is related to the preference or DTS. From Figure 4.6, the “embracingness” dimension seems to have high correlation to both *prefer* and *pleasure*, compared to other HTS components. Furthermore, the “hardness” dimension shows a strong correlation to the “embracingness” dimension. Hence, the biggest influence on the preference layer can be concluded to be the “hardness” dimension in the case of tactile assessment of door armrests. However, the structure is provisional based on the kind of the object. In another study on tactile assessment of film and board materials for confectionery packaging (X. Chen et al., 2009), “roughness” seemed to be the most important principal component to the affective layer (equivalent to HTS in this research).

Besides, this research suggests using the final-end product in the tactile assessment of a product that has layers of different materials. This argument is supported by the result obtained that shows the “hardness” dimension is the most important aspect in tactile assessment of door armrests. The perception of “hardness” involves both the kinesthetic and cutaneous systems (Bergmann Tiest, 2010). This perception may not be evaluated accurately by just using only the outer layer of the sample, as the product had a layered structure.

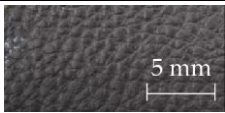
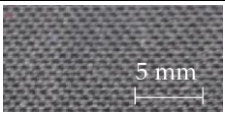

Furthermore, this research suggests correlating LTS with four main aspects of haptic information (roughness, compliance, coldness, and slipperiness). The physical quantities for each aspects of haptic information are selected based on the kind of stimuli that evoked the receptors, and also the physical effects that occurred during the interaction between the skin and the object.

Other than the physical quantities that are selected in this research (i.e. vibration for roughness, bulk displacement for surface deformation for compliance, thermal property for coldness, and friction for slipperiness), there are many other possible physical quantities that are used in other studies. For example, Chen et al. chose three dimensional pictures or topography of a surface's texture for roughness (X. Chen et al., 2009). However, the result is not quite convincing. In addition, the author mentioned that there is a need for further study on the measurement of roughness and it is probably related to vibration, as mentioned in other research (Ekman & Akesson, 1965; Lederman et al., 1982). Thus, the concept proposed in this research may help in selecting suitable physical quantities.

More work is required to find the appropriate physical quantities to correlate with LTS, because in this research, several coefficient of determinations obtained from the multiple regression analysis between LTS (dependent variable) and physical quantities (independent variable) are less than 0.5 (arbitrary lower limit for strong correlation), especially in the case of “micro-roughness”, “macro-roughness” and “hollowness”. Moreover, physical quantity of vibration, which was expected to have correlation with roughness, was found to be not significantly correlated.

In addition, the other work is to classify people by clustering them according to their preference and then construct each group's hierarchy structure of tactile sensation. This may help product developers in targeting their market. Before that, there is a need to increase the number

Table 4.2 List of unknown samples

a		b		c	
	Synthetic leather Type C		Fabric Type D		Genuine leather Type A

of participants and vary the cohorts of people, for example, broaden the age groups.

4.1.2.4 Verification Test of Quantified Tactile Sense Evaluation

In this section, the equations obtained were verified by using unknown samples of a, b, and c (refer Table 4.2). First, a sensory evaluation test for each sample with the same condition and participants in Section 3.2.2 was carried out; however, only adjectives in the preference layer were asked. Next, similar physical quantities as in Section 4.1.1 for unknown samples were measured. Consequently, principal component scores for each principal component in the physical quantities layer were computed by using principal component loadings. Then, the evaluation scores of D_{prefer} and $D_{pleasure}$ were calculated by using estimating Equations (4.1) and (4.2), respectively. Lastly, the actual and estimated scores were compared in Figure 4.7. Gray plots are the 26 samples that are used in the process to derive the estimating equations, and black plots are the unknown samples. Dashed lines indicate one-to-one relationships.

The accuracy of this tactile evaluation feedback system was determined by calculating the percent error for each sample using the following equation.

$$\text{Percent error} = \frac{|\text{Estimated score} - \text{Actual score}|}{\text{Actual score}} \times 100\% \quad (4.3)$$

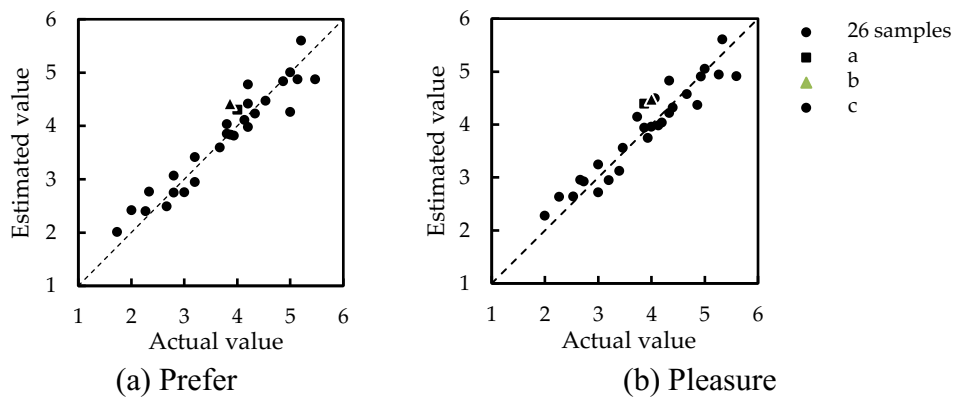


Figure 4.7 Comparison between actual and estimated scores

As a result, the maximum percent error when estimating *prefer* and *pleasure* were 20.8% and 16.2%, respectively. In other words, the developed system has the accuracy of 79% for *prefer* and 84% for *pleasure* in giving feedback on tactile evaluation.

Similarly, the percent errors when estimating *prefer* and *pleasure* for unknown samples a, b and c were computed, and the result was concluded in Table 4.3. Hence, by comparing the percentage error for *prefer* and *pleasure*, both have smaller percent errors compared to the developed system. Thus, this system can give estimation on unknown product's evaluation successfully.

4.2 Quantification Tactile Sensation for Fabrics

Based on the human tactile perception explained in Chapter 3, this research suggests using two types of physical quantities to quantify tactile sensation for fabrics. First, the physical properties of fabrics that determine the transducer function of skin-object interaction. The physical properties of fabrics are physical quantities that indicate or represent the characteristics or properties of the fabrics (Charles, 2003). Second, the physical quantities from the transducer's outputs (refer to Section 3.1.1) which represent the physical effects of the skin from skin-object interaction, such as, deformation, vibration, thermal effects, etc. These physical effects are the stimuli that are perceived by the cutaneous receptors, not the object's physical properties.

From the first types of physical quantities, the relationship between the properties of an object and human tactile sensation could be understood. From the second type of physical quantities, one could comprehend the relationship between physical effects from texture interactions that excite the receptors in human skin and human tactile sensation. Hence, this

Table 4.3 Percent error for unknown samples.

Samples	<i>Prefer</i>	<i>Pleasure</i>
a	7.56%	13.6%
b	14.3%	12.0%
c	6.71%	2.64%

research proposes to use both types of physical properties and quantify human tactile sensations.

Section 4.2.2 and 4.2.3 will discuss on the quantification of tactile sensation for hand and forearm respectively.

4.2.1 Data Collection of Physical Quantities

Section 4.2.1.1 will introduce the physical properties of fabrics that are used for

Table 4.4 List of physical properties of fabrics

Physical properties	Sample						
	#1	#2	#3	#4	#5	#6	#7
Weight, w [g/m ²]	157.12	107.68	184.72	109.77	154.72	147.82	148.59
Thickness, T [mm]	0.698	0.32	0.646	0.522	0.526	0.514	0.61
Course, C	51	70	56	35	65	82	47
Wales, W	30	71	36	30	46	53	57
Permeating resistance, R_{air} [kPa·s/m]	0.072	0.035	0.103	0.031	0.132	0.349	0.096
Compressional linearity, LC	0.613	1.175	0.675	0.559	0.816	0.868	0.847
Compressional work energy, WC [gf/cm]	0.099	0.012	0.080	0.061	0.027	0.031	0.027
Compressional resilience, RC [%]	39.14	48.72	43.38	53.18	31.01	39.14	45.63

quantification. Next, section 4.2.1.2 will present about the commercialized tactile sensors and their measured physical quantities. Then, section 4.2.1.3 will explain on the novel tactile sensors that are proposed by this research and the measured physical quantities.

4.2.1.1 Physical Properties of Fabrics

The descriptions of physical properties that are used for quantification are as written below. All the data of physical properties for 7 fabric samples (refer Table 3.14) are recorded in Table 4.4.

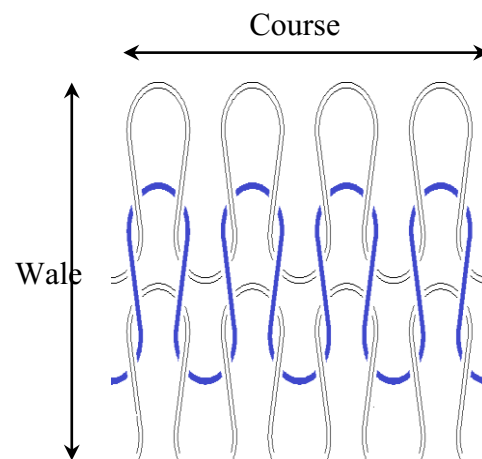


Figure 4.8 Courses and wales

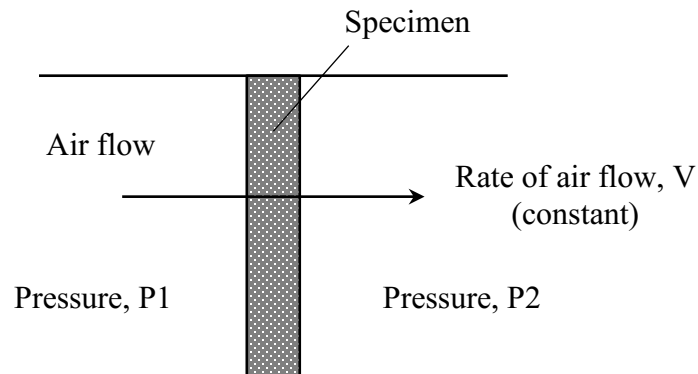


Figure 4.9 Concept of Air Permeability Tester [KES-F8-AP1, Kato Tech Co., Ltd.]

(i) Weight, w

Weight is defined as mass per unit area. The unit is g/m^2 .

(ii) Thickness, T

The unit of the thickness of fabric is mm.

(iii) Course, C and wale, W

Course is the total amount of horizontal rows and wale is the total amount of vertical rows in one inch length (or equal to 25.4 mm). For example, in Figure 4.8, there are 3 courses and 4 wales.

(iv) Airflow permeating resistance, R_{air}

Airflow permeating resistance with the unit of $\text{kPa} \cdot \text{s/m}$ is measured by using Air Permeability Tester [KES-F8-API, Kato Tech Co., Ltd.] . The concept of the device is as shown in Figure 4.9. This device sends air at a constant flow rate, V to the sample by using the reciprocal movement of its plunger and cylinder. The pressure loss, ΔP due to the sample is then measured by using a semiconductor type differential pressure gauge. The permeating resistance, R_{air} can be calculated as below.

$$R_{air} = \frac{\Delta P}{V} \quad (4.4)$$

ΔP : pressure loss, kPa

V : flow rate, $\text{m}^3/\text{m}^2 \cdot \text{s}$

Here, the flow rate, V of this device was 4×10^{-2} $\text{m}^3/\text{m}^2 \cdot \text{s}$. By measuring the pressure loss, the permeating resistance can be calculated.

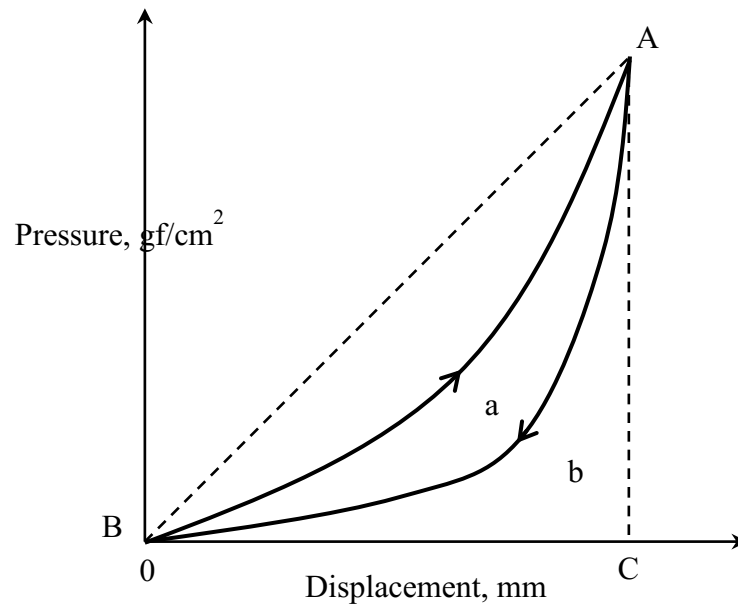


Figure 4.10 Example of compression test results

(v) Compression properties

By using Handy-Type Compression Tester [KES-G5, Kato Tech Co., Ltd.], compression properties such as compressional energy, resilience and rigidity of an object can be measured. The device presses the object with an area of 2.0 cm^2 until the upper limit of force is 10 gf/cm^2 . The graph result obtained is as shown in Figure 4.10. From the graph, there are 3 physical quantities that can be computed. First, by using equation (4.5), compressional linearity, LC can be calculated. Compressional linearity can be interpreted as the hardness of the object and when the value is closer to 1, the object is assumed to be hard.

$$LC = \frac{\text{Area of } a + b}{\text{Area of } \triangle ABC} \quad (4.5)$$

Second, compressional work energy, WC [gf/cm] can be calculated by using equation (4.6) and when the value is bigger, the object is easier to be compressed.

$$WC = \text{Area of } a + b \quad (4.6)$$

Third, by using the equation (4.7), compressional resilience, RC [%] can be calculated and when the value is closer to 100 %, this indicates that the object is good in resilience.

$$RC = \frac{\text{Area of } b}{\text{Area of } a + b} \times 100 \% \quad (4.6)$$

4.2.1.2 Physical Quantities Measured by using Commercialized Tactile Sensor

The descriptions of physical quantities that are measured by using commercialized tactile sensor are as written below. All the data of physical quantities for the fabric samples are recorded in Table 4.5.

(i) Thermal property

By using Thermo Labo II B [KES-F7, Kato Tech. Co., Ltd.], warm or cool feeling through evaluation of q max can be measured. q max represents the peak amount of heat transferred per unit area. As shown in Figure 4.11, first, the contact surface (copper plate) of

Table 4.5 List of physical quantities measured by using commercialized tactile sensor

Physical quantities	Sample						
	#1	#2	#3	#4	#5	#6	#7
Thermal property, q max [W/m ² ·°C]	123.67	137.67	131.67	105.00	136.33	129.67	154.33
Static friction coefficient, μ_{static}	0.671	0.877	0.722	0.596	0.712	1.172	1.086
Dynamic friction coefficient, μ_{dynamic}	0.400	0.450	0.520	0.383	0.359	0.374	0.466

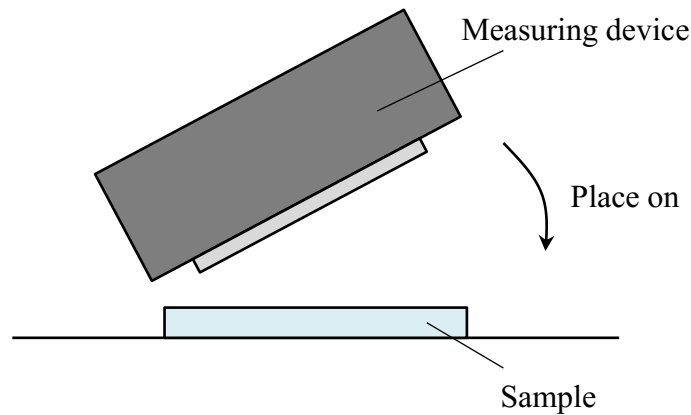


Figure 4.11 Concept of measuring q_{\max}

device with area of 9 cm^2 , mass of 9.79 g and heat capacity of $4.186 \times 10^3 \text{ JK}^{-1}\text{m}^{-2} \text{ }^\circ\text{C}$ is preheated. Then, the copper plate is pressed on the sample with pressure of 10 gf/cm^2 and the stored energy is passed to the lower temperature of sample. The peak value of heat transferred is set as q_{\max} . This simulates the thermal effects of warmth or coolness when the skin touches an object. The thermal effects are one of the physical effects, i.e. the output of skin-object interaction (refer to Figure 3.1). When the measured value of q_{\max} is larger/smaller, the cooler/warmer the feeling of sample is.

(ii) Friction coefficient, μ

The other output of skin-object interaction (refer to Figure 3.1) that is measured is the lateral force which related to friction. By using Built-up Static-Dynamic Friction Measuring Device [TL201Ts, Trinity Lab Co., Ltd], the static and dynamic friction coefficient can be computed. The sample is fixed on the measuring device's table and a skin-like silicon sensor is placed on the sample with a normal force of 3 gf . Then, the sensor traces on the sample with the velocity of 50 mm/s . The measuring length is 100 mm . After that, the lateral force is measured, and the static and dynamic friction coefficient can be calculated.

4.2.1.3 Physical Quantities Measured by using Proposed Tactile Sensor

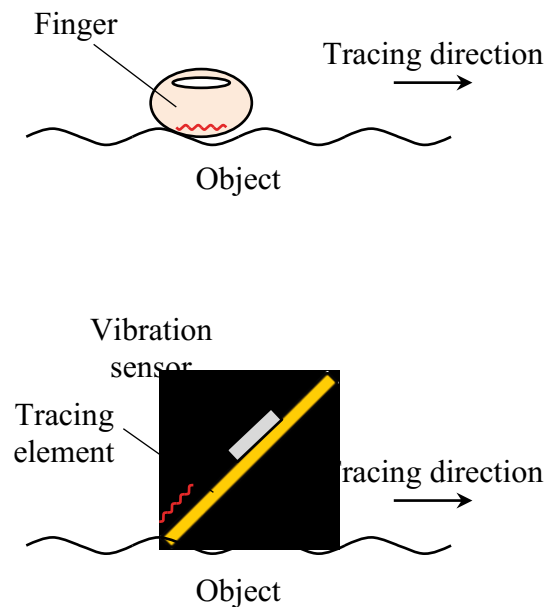


Figure 4.12 Concept of vibration measuring system

As mention in our proposal on physical quantities that are going to be used for quantification of tactile sensation, there are two types of physical quantities; physical properties of object and physical quantities from the effects of skin-object interaction. In the section 4.2.1.2, the latter type of physical quantities such as, thermal effect and lateral force has been discussed and measured. This section will propose to measure two physical effects of skin-object interaction which are the vibration and deformation.

i) Concept of Measuring System

Vibration is one of the physical effects that occurred from tracing on an object. The vibration is then perceived by mechanoreceptors and the signal is sent to the brain. From previous research, Asaga had proposed to collect vibrational data by tracing on the surface of samples. Then, the vibrational data were collected by using piezoelectric element, and the research managed to quantify roughness of samples (Asaga 2012). Thus, this research proposes to a tactile sensor that will collect the vibrational data when tracing fabric samples as one of the

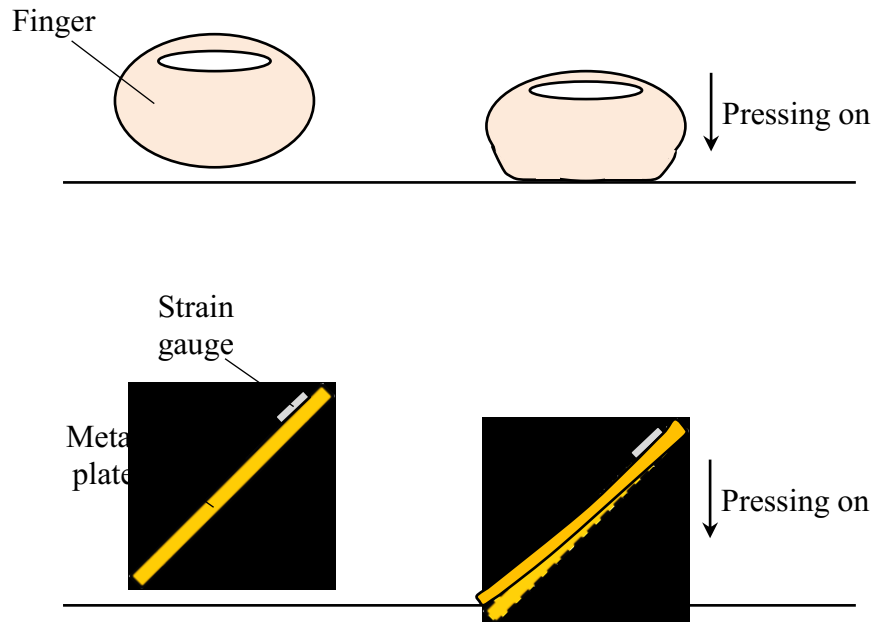


Figure 4.13 Concept of deformation measuring system

physical quantities for quantification of tactile sensation. The concept of the device is as shown in Figure 4.12. This research suggests using a thin metal plate to trace on the surface and collect the vibration by using a vibrational sensor. This is because fabrics have a very soft and small texture, therefore, a sensor that has low rigidity and easy to vibrate is preferable.

Furthermore, deformation of skin is also one of the physical effects when there is skin and object interaction. Asaga had measured the deformation by pressing the developed device and measured the deformation of metal plate by using strain gauge. By using the data from the deformation, the research tried to quantify the softness of samples (Asaga, 2012). Thus, this research also suggests developing a tactile sensor that can measure the deformation of tactile sensor when pressing the object. By using the same structure of tactile sensor as mention in the previous paragraph, this research proposes to use strain gauge to detect the deformation when tactile sensor presses on the fabric. As the tactile sensor is made of thin metal plate, it is easy to bend. The concept of the device is as shown in Figure 4.13.

As a conclusion, this research proposes to measure two physical effects of skin-object interaction which are vibration and deformation.

ii) Design and Fabrication of Measuring System

(i) Vibration Measuring System

The vibration measuring system is divided into two parts; tactile sensor and sample's jig. Figure 4.14 shows the overall system. The tactile sensor is mainly composed of a 0.2 mm thick metal brass plate with a piezoelectric element [VS-BV201, NEC Tokin Co., Ltd] as the vibration sensor as shown in Figure 4.15. The signal from the piezoelectric element will be filtered by a simple low pass filter with cutoff frequency of 4823 Hz. Then, the vibrational signal is recorded in the computer via AD converter known as High-precision analog I/O terminal for USB2.0

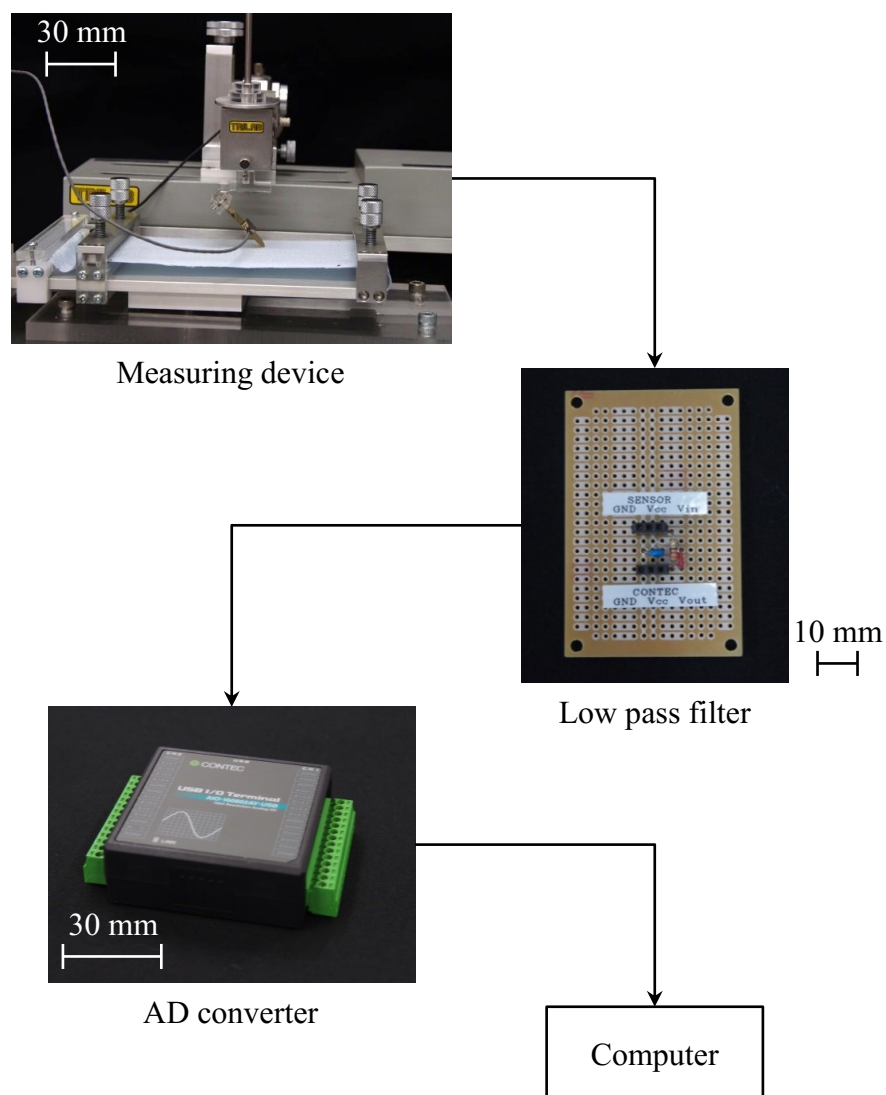


Figure 4.14 Overall view of vibration measuring system

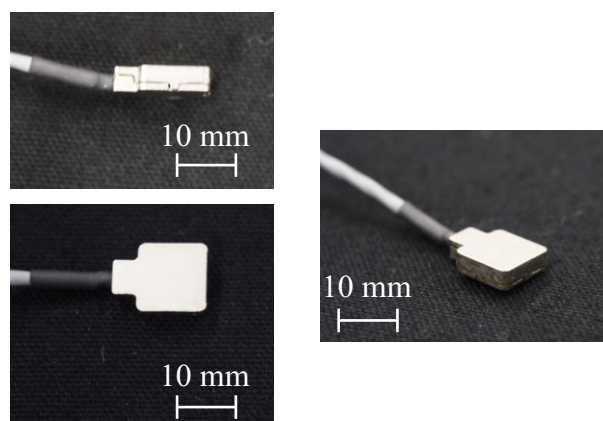


Figure 4.15 Vibration sensor [VS-BV201, NEC Tokin Co., Ltd.]

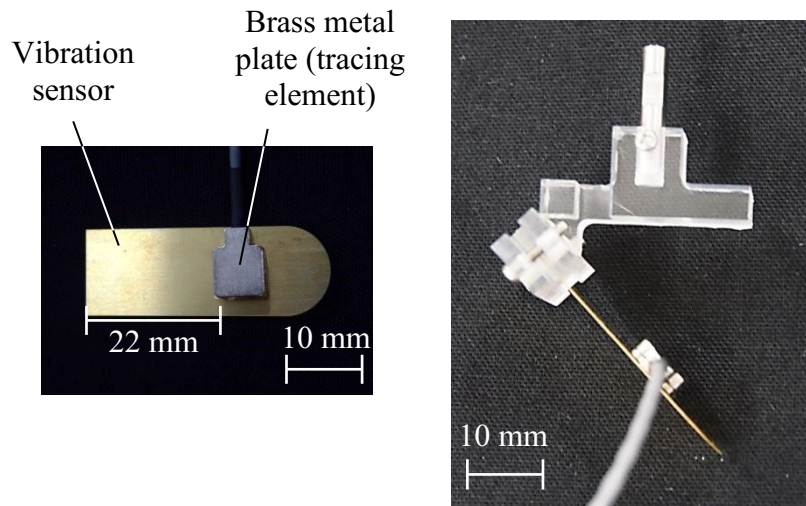


Figure 4.16 Tracing element with a vibration sensor [VS-BV201, NEC Tokin Co., Ltd.]

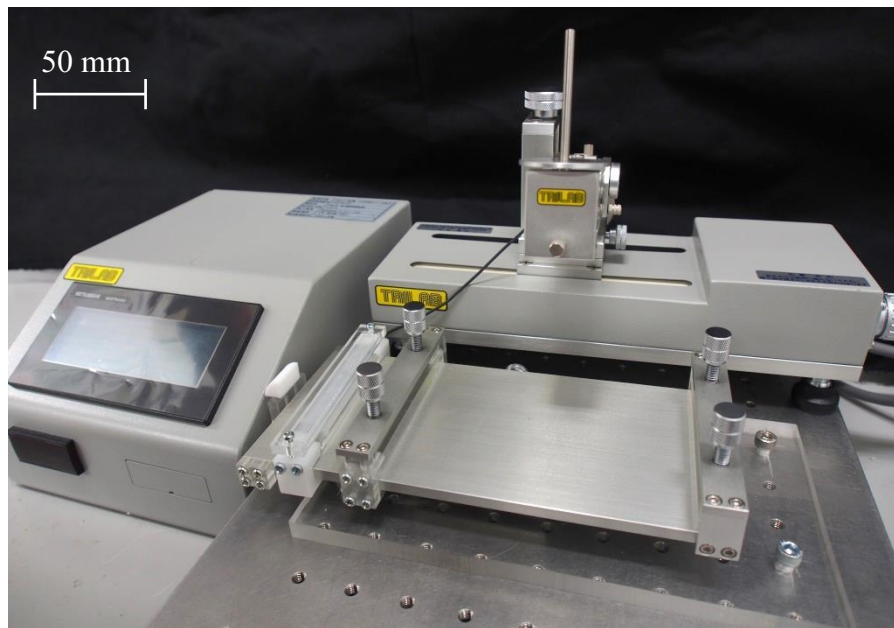


Figure 4.17 Built-up Static-Dynamic Friction Measuring Device [TL201Ts, Trinity Lab Co., Ltd]

[AIO-160802AY-USB, CONTEC Co., Ltd.]. The dimension of the brass plate and the location where the vibration sensor is placed are shown in Figure 4.16. A jig is fabricated so that the sensor is placed 45° to the sample. A Built-up Static-Dynamic Friction Measuring Device [TL201Ts, Trinity Lab Co., Ltd] as shown in Figure 4.17 is used to move the sensor at a constant velocity with a certain length. Besides, by using this device, the load can also be set.

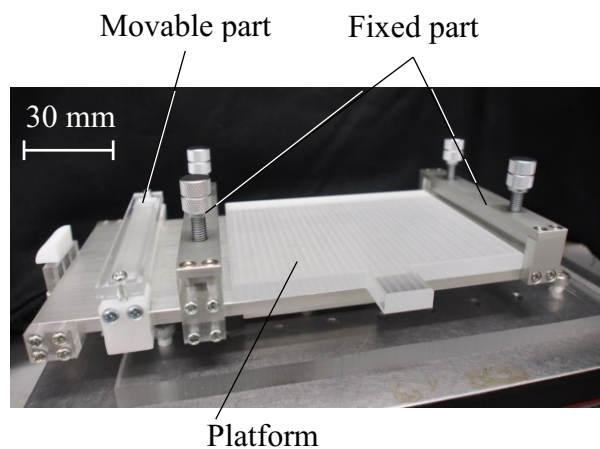
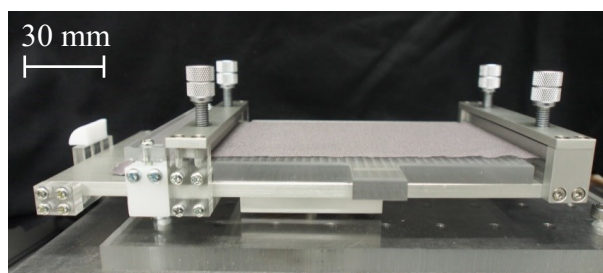
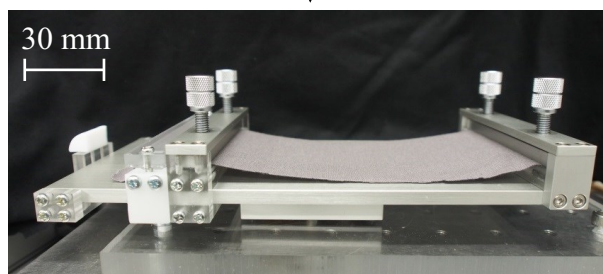


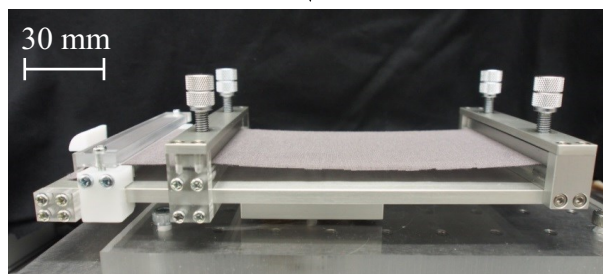
Figure 4.18 Modified sample's jig



The sample is placed on a platform. The sample is fixed at right fixed part and movable part.



The platform is pulled out from the jig.



The movable part slides and pulls the fabric to the fixed extension rate. Lastly, the left fixed part is tightened.

Figure 4.19 Procedures in fixing the fabric sample

Generally, the main purposes of sample's jig are to provide repeatability, accuracy, and interchangeability. The sample's jig is fabricated to make the sample float without touching any surface below. As the sample is very thin, it is easy for the tactile sensor to catch noise from other object too, if there is an object placed below the sample. As shown in Figure 4.18, the jig has two fixed parts and one movable part. The movable part of the jig is used to make sure the

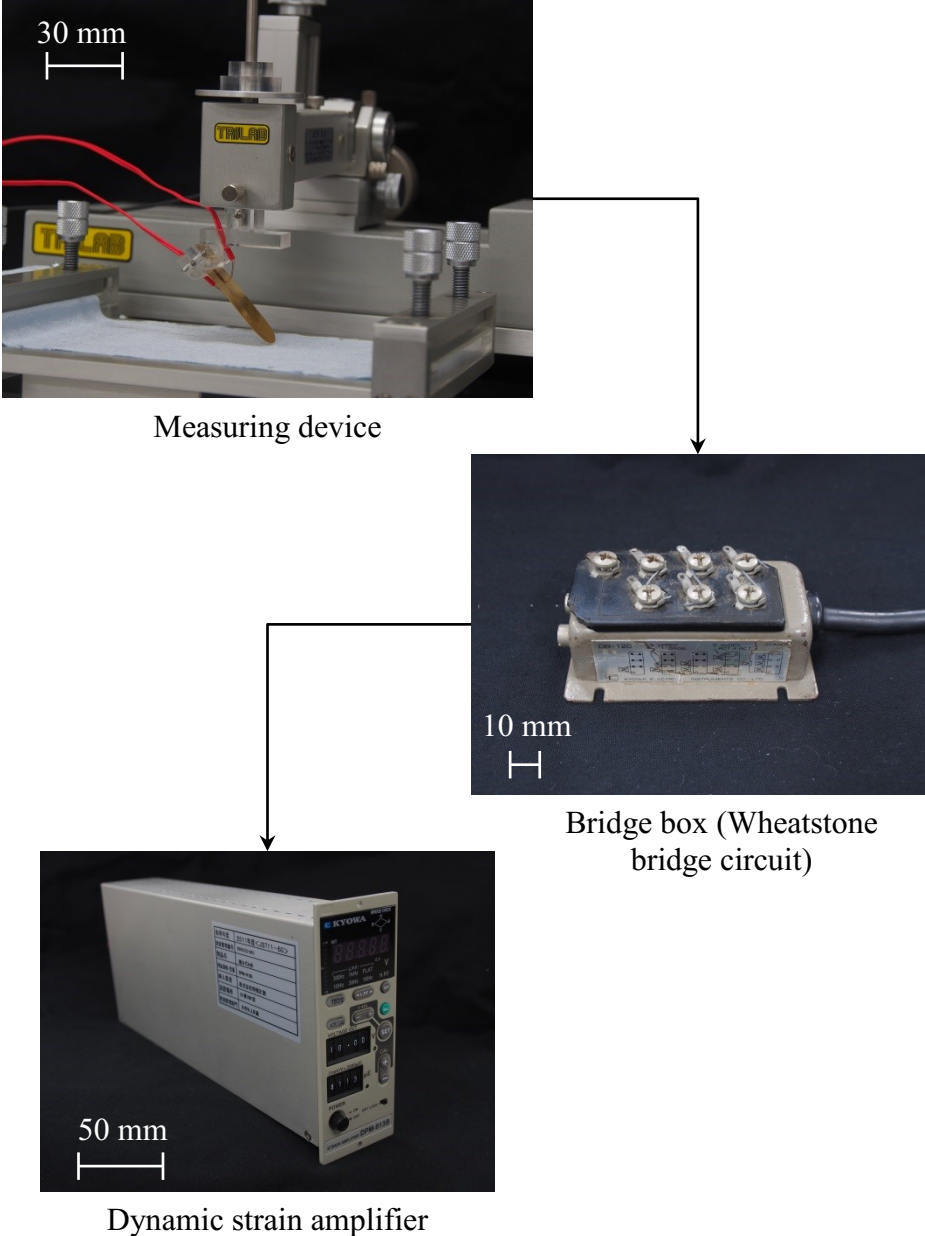


Figure 4.20 Overall view of deformation measuring system

fabric is fixed with the same condition such as, by fixing the extension rate. The sample is fixed by the following procedures (refer to Figure 4.19).

(ii) Deformation Measuring System

The overall system is as shown in Figure 4.20. Similar to the vibration measuring system, the deformation measuring system uses the same dimension of brass plate. However, two strain gauges are used to measure the deformation of the brass plate when it presses on the fabric. A Built-up Static-Dynamic Friction Measuring Device [TL201Ts, Trinity Lab Co., Ltd] is also used in this system because it is easy to set the load. The two-strain gauge is then connected to Wheatstone bridge circuit by using a bridge box [DB-120A, Kyowa Electronic Instruments Co., Ltd.]. After that, the output voltage from the bridge box is amplified by using dynamic strain amplifier [DPM-913B, Kyowa Electronic Instruments Co., Ltd]. The amplified voltage is presented by the monitor indication of strain amplifier. The sample is simply place over a jig.

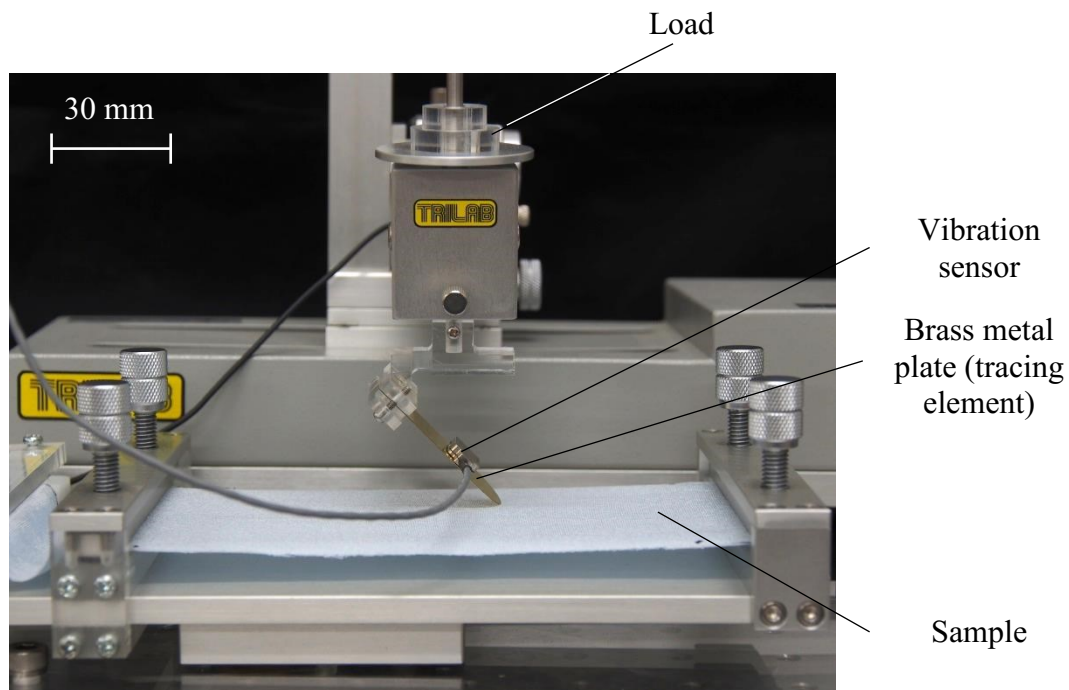


Figure 4.21 Vibration experimental apparatus

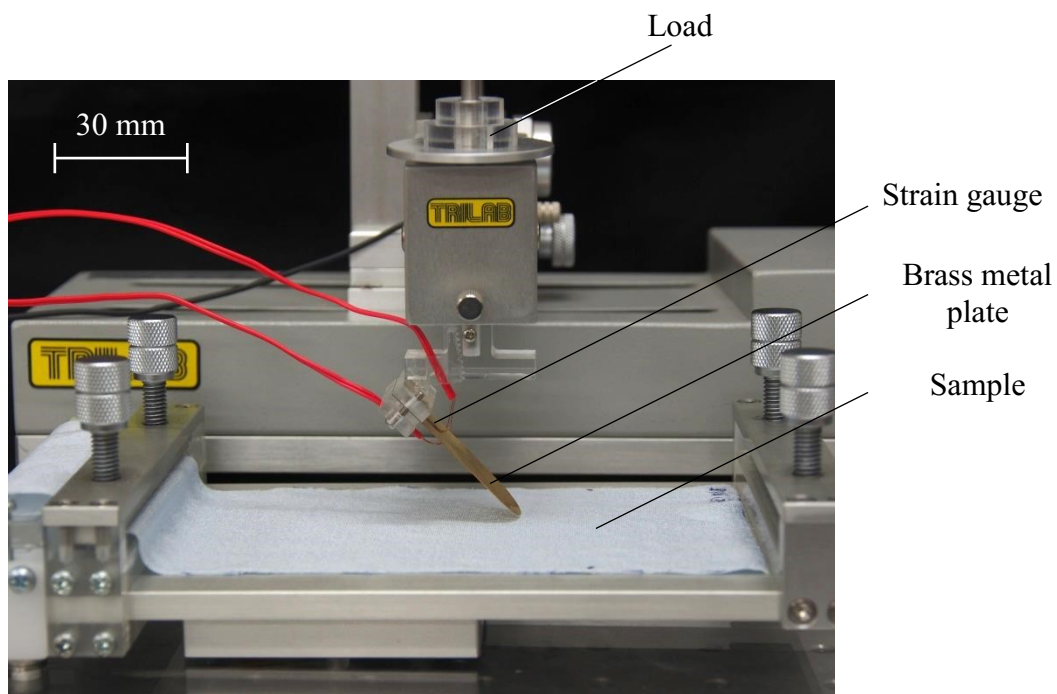
iii) Measuring Experiment

(i) Vibration Measuring Experiment

Samples used are the same as those in the sensory evaluation in Chapter 3 (refer Table 3.14). As shown in Figure 4.21, the sample was fixed by using the sample's jig with the extension rate of 11 %. The velocity, length of measurement and load were set as 50 mm/s, 100 mm and 3 g respectively to the Built-up Static-Dynamic Friction Measuring Device. The sampling frequency of the data was 10000 Hz. The vibrational data from the tracing on sample

Table 4.6 Vibration measuring results

Physical quantities	Sample						
	#1	#2	#3	#4	#5	#6	#7
V _{p-p} [V]	0.474	0.194	0.259	0.245	0.472	1.545	0.188

**Figure 4.22** Deformation experimental apparatus

was measured by the vibration sensor.

From the results, the mean of peak to peak voltage of the vibrational data was calculated for each sample and set as the V_{p-p} (refer to Table 4.6) for the quantification of tactile sensation.

(ii) Deformation Measuring Experiment

Samples used are the same as those in the sensory evaluation in Chapter 3 (refer Table

Table 4.7 Deformation measuring results

Physical quantities	Sample						
	#1	#2	#3	#4	#5	#6	#7
V_{1g} [V]	0.096	0.130	0.165	0.120	0.087	0.131	0.086
V_{2g} [V]	0.280	0.349	0.420	0.359	0.372	0.454	0.339
V_{3g} [V]	0.585	0.544	0.576	0.614	0.616	0.594	0.560
V_{4g} [V]	0.664	0.801	0.851	0.788	0.828	0.812	0.773
V_{5g} [V]	0.983	1.124	0.980	0.878	1.180	0.880	0.960
V_{6g} [V]	1.170	1.286	1.346	1.230	1.218	1.281	1.233
V_{7g} [V]	1.252	1.583	1.435	1.346	1.527	1.568	1.408
V_{8g} [V]	1.540	1.798	1.650	1.631	1.600	1.710	1.650
V_{9g} [V]	1.647	2.082	1.846	1.973	2.049	1.873	1.890
V_{10g} [V]	1.935	2.343	2.109	2.098	2.308	2.212	2.190

3.3). As shown in Figure 4.22, the sample was simply place over the jig. The load was set as 1 g to 10 g with the interval of 1 g on the Built-up Static-Dynamic Friction Measuring Device and then, the output voltage of the strain amplifier was recorded.

The experimental results are as shown in Table 4.7. From the results, the output voltage due to the deformation of tactile sensor when pressed on the fabric was set as V_{1g} to V_{10g} for the quantification of tactile sensation as further to be discuss in Section 4.2.2 and 4.2.3.

4.2.2 Quantification of Tactile Sense Evaluation by Hand

From sensory evaluation for hand in Chapter 3, there were 4 LTS components extracted; “surface texture”, “dryness”, “downiless” and “coolness”. By using the measured physical quantities in previous section, these LTS components will be quantified by using multiple regression analysis.

4.2.2.1 Multiple Regression Analysis

Multiple regression analysis was conducted to determine and examine the relationship between all physical quantities that are listed in previous section and each component in LTS by using SPSS software [IBM Corporation]. Before conducting multiple linear regression, bivariate Pearson correlation was conducted for all explanatory variables to make sure that there is no multicollinearity occurred between the variables. All the correlations showed values below 0.65.

Table 4.8 shows the correlation and multiple regression analysis results when the dependent variable is LTS component of “surface texture” and the independent variables are physical quantities. As shown in Table 4.8 (b), six physical quantities were included; (1) thickness, T (2) thermal property, q_{max} , (3) compressional resilience, RC , (4) deformation at 3 g, V_{3g} , (5) deformation at 6 g, V_{6g} , (6) vibration’s peak-to-peak voltage, V_{p-p} , and others were excluded variables for the multiple regression model. V_{3g} and V_{p-p} had a negatively and

Table 4.8 Result for multiple regression analysis (LTS-“surface texture” with all physical quantities)

(b) Coefficients			
Model	Unstandardized Coefficients		Standardized Coefficients
	B	Std. Error	Beta
(Constant)	-7.775	0.000	
T	-2.140	0.000	-.437
q max	0.025	0.000	.632
RC	0.019	0.000	.232
V _{3g}	4.936	0.000	.220
V _{6g}	1.830	0.000	.174
V _{p-p}	-0.766	0.000	-.617

Dependent variable: “surface texture”

Independent variable: “T”, “q max”, “RC”, “V_{3g}”, “V_{6g}”, “V_{p-p}”

significantly correlation with the “surface texture”. However, q max, RC and V_{6g} had a weak positive correlation with “surface texture”. Moreover, T had a weak negative correlation with “surface texture”.

The multiple regression model with all six predictors produced $R^2 = 1.000$, thus, the multiple regression model had a quite good fit of data, indicating that the “surface texture” scores are strongly related to all six physical quantities. According to the standardized regression coefficients, the q max had the most influence to the LTS component of “surface texture”, followed by V_{p-p}, T, RC, V_{3g} and lastly, V_{6g}. q max, RC and V_{6g} had positive regression coefficients, indicating that the higher values of q max, RC and V_{6g}, the sample was expected to have higher score of “surface texture”, i.e. smoother. On the other hand, T and V_{p-p} had a negative regression coefficient, indicating that the higher values of T and V_{p-p}, the sample was expected to have lower score of “surface texture”, i.e. rougher. However, V_{3g} had a positive regression coefficient (opposite in sign from its correlation with “surface texture”), indicating that after accounting for T, q max, RC, V_{6g} and V_{p-p}, the higher value of V_{3g}, the sample was

expected to have higher score of “surface texture”, i.e. smoother. From Table 4.8 (b), a multiple regression equation can be obtained as the equation below.

$$L_{surface} = (-2.140 \times T) + (0.025 \times q_{max}) + (0.019 \times RC) + (4.936 \times V_{3g}) + (1.830 \times V_{6g}) + (-0.766 \times V_{p-p}) - 7.775 \quad (4.7)$$

Table 4.9 shows the correlation and multiple regression analysis results when the dependent variable is LTS component of “dryness” and the independent variables are physical quantities. As shown in Table 4.9 (b), similar six physical quantities were included in this multiple regression model too. q max had a positively and significantly correlation with the “dryness”. Nevertheless, V_{3g} and V_{p-p} had a negatively and significantly correlation with the “dryness”. Moreover, RC and V_{6g} had a weak positive correlation with “dryness”. However, T had a weak negative correlation with “dryness”.

Table 4.9 Result for multiple regression analysis (LTS-“dryness” with all physical quantities)

(a) Correlations		
“dryness”		
	Pearson correlation	Sig.
T	-0.503	.125
q max	0.639*	.061
RC	0.255	.291
V_{3g}	-0.592*	.081
V_{6g}	0.302	.255
V_{p-p}	-0.619*	.069

*p < .1 **p < .05 ***p < .01 ****p < .001

Table 4.9 Result for multiple regression analysis (LTS-“dryness” with all physical quantities)

Model	(b) Coefficients		
	Unstandardized Coefficients		Standardized Coefficients
	B	Std. Error	Beta
(Constant)	-9.405	0.000	
T	-2.338	0.000	-.459
q max	0.032	0.000	.769
RC	0.015	0.000	.177
V _{3g}	6.845	0.000	.293
V _{6g}	1.752	0.000	.160
V _{p-p}	-0.747	0.000	-.578

Dependent variable: “dryness”

Independent variable: “T”, “q max”, “RC”, “V_{3g}”, “V_{6g}”, “V_{p-p}”

The multiple regression model with all six predictors produced $R^2 = 1.000$, thus, the multiple regression model had a quite good fit of data, indicating that the “dryness” scores are strongly related to all six physical quantities. According to the standardized regression coefficients, the q max had the most influence to the LTS component of “dryness”, followed by V_{p-p}, T, V_{3g}, RC and lastly, V_{6g}. q max, RC and V_{6g} had positive regression coefficients, indicating that the higher values of q max, RC and V_{6g}, the sample was expected to have higher score of “dryness”, i.e. drier. On the other hand, T and V_{p-p} had a negative regression coefficient, indicating that the higher values of T and V_{p-p}, the sample was expected to have lower score of “dryness”, i.e. moister. However, V_{3g} had a positive regression coefficient (opposite in sign from its correlation with “dryness”), indicating that after accounting for T, q max, RC, V_{6g} and V_{p-p}, the higher value of V_{3g}, the sample was expected to have higher score of “dryness”, i.e. drier. From Table 4.9 (b), a multiple regression equation can be obtained as the equation below.

$$L_{dryness} = (-2.338 \times T) + (0.032 \times q_{max}) + (0.015 \times RC) + (6.845 \times V_{3g}) \\ + (1.752 \times V_{6g}) + (-0.747 \times V_{p-p}) - 9.405 \quad (4.8)$$

Table 4.10 shows the correlation and multiple regression analysis results when the dependent variable is LTS component of “downiless” and the independent variables are physical quantities. As shown in Table 4.10 (b), similar six physical quantities were included in this multiple regression model too. V_{p-p} had a negatively and significantly correlation with the “downiless”. Moreover, RC and V_{3g} had a weak positive correlation with “downiless”. However, T, q max and V_{3g} had a weak negative correlation with “downiless”.

The multiple regression model with all six predictors produced $R^2 = 1.000$, thus, the multiple regression model had a quite good fit of data, indicating that the “downiless” scores are strongly related to all six physical quantities. According to the standardized regression coefficients, the V_{p-p} had the most influence to the LTS component of “downiless”, followed by V_{3g} , RC, T, V_{6g} and lastly, q max. RC and V_{3g} had positive regression coefficients, indicating that the higher values of RC and V_{3g} , the sample was expected to have higher score of

Table 4.10 Result for multiple regression analysis (LTS-“downiless” with all physical quantities)

(a) Correlations		
“downiless”		
	Pearson correlation	Sig.
T	-0.095	.420
q max	-0.302	.255
RC	0.550	.100
V_{3g}	0.106	.410
V_{6g}	-0.035	.470
V_{p-p}	-0.844***	.008

*p < .1 **p < .05 ***p < .01 ****p < .001

Table 4.10 Result for multiple regression analysis (LTS-“downiless” with all physical quantities)

(b) Coefficients			
Model	Unstandardized Coefficients		Standardized Coefficients
	B	Std. Error	Beta
(Constant)	-9.269	0.000	
T	-0.579	0.000	-.136
q max	0.003	0.000	.080
RC	0.026	0.000	.361
V _{3g}	12.373	0.000	.631
V _{6g}	1.071	0.000	.117
V _{p-p}	-0.961	0.000	-.888

Dependent variable: “downiless”

Independent variable: “T”, “q max”, “RC”, “V_{3g}”, “V_{6g}”, “V_{p-p}”

“downiless”, i.e. not downy. On the other hand, T and V_{p-p} had a negative regression coefficient, indicating that the higher values of T and V_{p-p}, the sample was expected to have lower score of “downiless”, i.e. downy. However, q max and V_{6g} had a positive regression coefficient (opposite in sign from its correlation with “downiless”), indicating that after accounting for T, RC, V_{3g} and V_{p-p}, the higher values of q max and V_{6g}, the sample was expected to have higher score of “downiless”, i.e. not downy. From Table 4.10 (b), a multiple regression equation can be obtained as the equation below.

$$L_{downiless} = (-0.579 \times T) + (0.003 \times q_{max}) + (0.026 \times RC) + (12.373 \times V_{3g}) + (1.071 \times V_{6g}) + (-0.961 \times V_{p-p}) - 9.269 \quad (4.9)$$

Table 4.11 shows the correlation and multiple regression analysis results when the dependent variable is LTS component of “coolness” and the independent variables are physical quantities. As shown in Table 4.11 (b), similar six physical quantities were included in this

multiple regression model too. q max had a positively and significantly correlation with the “coolness”. Nevertheless, T and V_{3g} had a negatively and significantly correlation with the “coolness”. Moreover, V_{6g} had a weak positive correlation with “coolness”. However, RC and V_{p-p} had a weak negative correlation with “coolness”.

The multiple regression model with all six predictors produced $R^2 = 1.000$, thus, the multiple regression model had a quite good fit of data, indicating that the “coolness” scores were strongly related to all six physical quantities. According to the standardized regression coefficients, the q max had the most influence to the LTS component of “coolness”, followed by T, V_{3g} , V_{p-p} , V_{6g} and lastly, RC. q max and V_{6g} had positive regression coefficients, indicating that the higher values of q max and V_{6g} , the sample was expected to have higher score of “coolness”, i.e. cooler. On the other hand, T and V_{p-p} had a negative regression coefficient, indicating that the higher values of T and V_{p-p} , the sample was expected to have lower score of “coolness”, i.e. warmer. However, RC and V_{3g} had a positive regression coefficient (opposite in sign from its correlation with “coolness”), indicating that after accounting for T, q max, V_{6g} and V_{p-p} , the higher values of RC and V_{3g} , the sample was expected to have higher score of

Table 4.11 Result for multiple regression analysis (LTS-“coolness” with all physical quantities)

(a) Correlations		
“coolness”		
	Pearson correlation	Sig.
T	-0.567*	.092
q max	0.810**	.014
RC	-0.047	.460
V_{3g}	-0.569*	.091
V_{6g}	0.361	.213
V_{p-p}	-0.219	.319

*p < .1 **p < .05 ***p < .01 ****p < .001

Table 4.11 Result for multiple regression analysis (LTS-“coolness” with all physical quantities)

(b) Coefficients			
Model	Unstandardized Coefficients		Standardized Coefficients
	B	Std. Error	Beta
(Constant)	-8.636	0.000	
T	-2.543	0.000	-.543
q max	0.035	0.000	.908
RC	0.002	0.000	.031
V _{3g}	5.705	0.000	.265
V _{6g}	1.724	0.000	.171
V _{p-p}	-0.261	0.000	-.220

Dependent variable: “coolness”

Independent variable: “T”, “q max”, “RC”, “V_{3g}”, “V_{6g}”, “V_{p-p}”

“coolness”, i.e. cooler. From Table 4.11 (b), a multiple regression equation can be obtained as the equation below.

$$L_{cooler} = (-2.543 \times T) + (0.035 \times q_{max}) + (0.002 \times RC) + (5.705 \times V_{3g}) + (1.724 \times V_{6g}) + (-0.261 \times V_{p-p}) - 8.636 \quad (4.10)$$

From the above multiple regression analysis results, the relationship between LTS components and physical quantities by using regression coefficients can be summarized as shown in Figure 4.23.

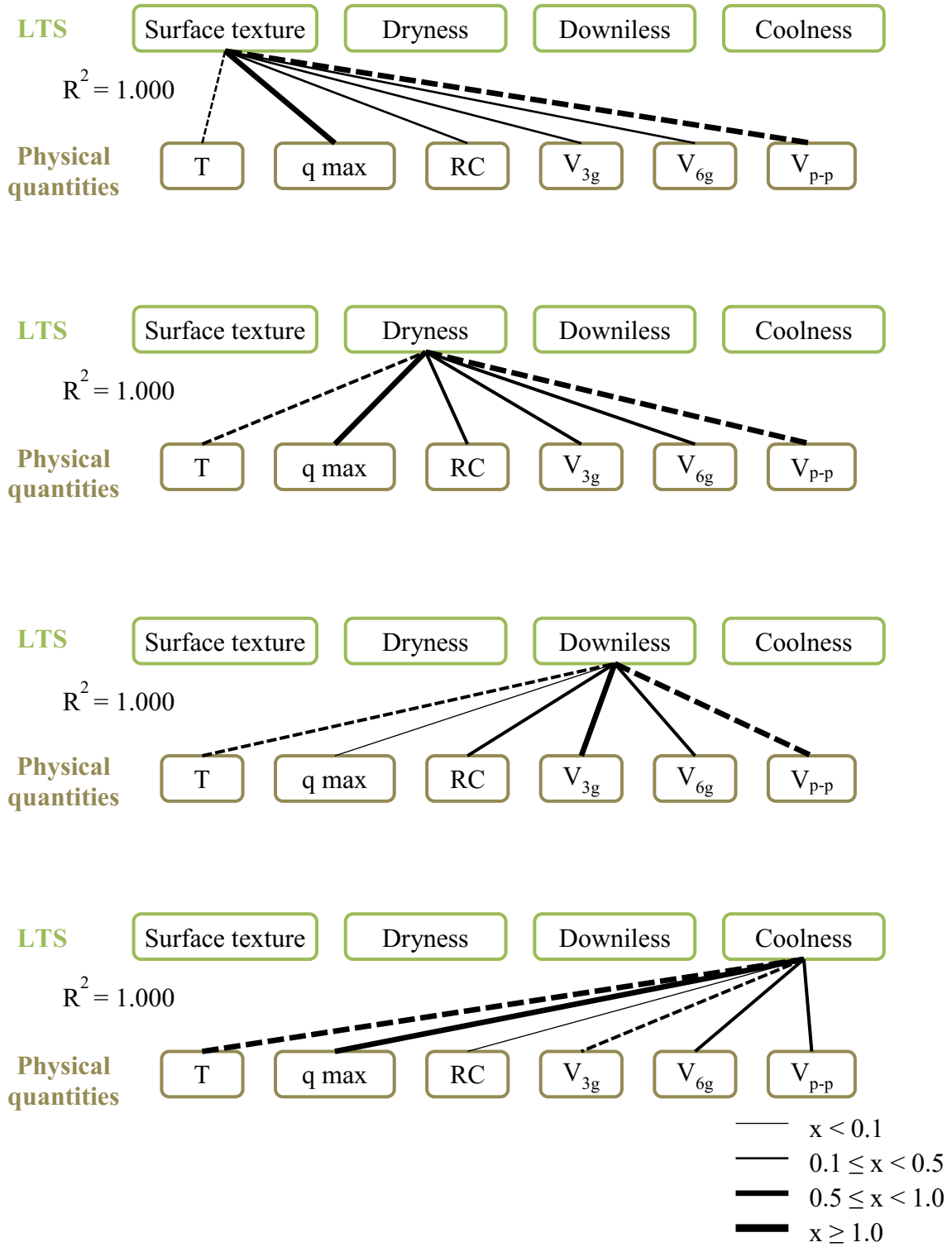


Figure 4.23 Multiple regression analysis results (tactile sensation of hand)

4.2.2.2 Discussions

From the multiple regression equations in section 3.3.2.2 and section 4.2.2.1, DTS adjectives can be expressed by physical quantities. In order to express DTS adjectives in terms of physical quantities, the equations (4.7), (4.8), (4.9) and (4.10) are substituted in equation (3.18) and (3.19). The computed equations are as shown below.

$$D_{comfort,hand} = (-1.550 \times T) + (0.017 \times q_{max}) + (0.018 \times RC) + (3.513 \times V_{3g}) + (1.436 \times V_{6g}) + (-0.677 \times V_{p-p}) - 5.116 \quad (4.11)$$

$$D_{preference,hand} = (-1.870 \times T) + (0.020 \times q_{max}) + (0.019 \times RC) + (3.930 \times V_{3g}) + (1.694 \times V_{6g}) + (-0.718 \times V_{p-p}) - 6.262 \quad (4.12)$$

By using equations (4.11) and (4.12), DTS values for all 7 samples are calculated from the measured physical quantities. The actual values of DTS from sensory evaluation and calculated DTS values from physical quantities are plotted in Figure 4.24, and the absolute errors between the two values are calculated and recorded in Table 4.12.

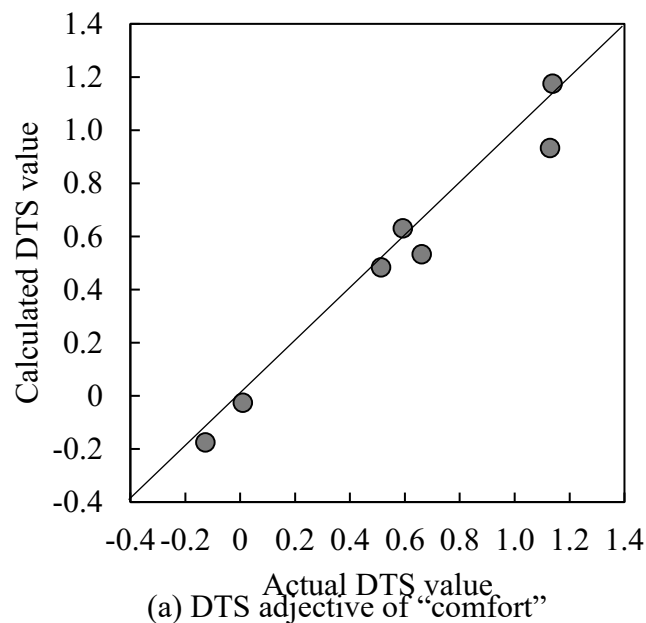
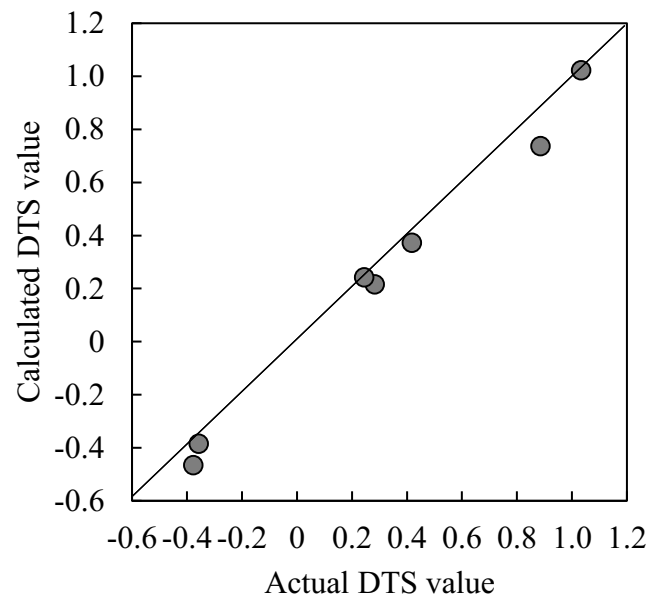


Figure 4.24 Actual and calculated DTS values (tactile sensation for hand)



(b) DTS adjective of “preference”

Figure 4.24 Actual and calculated DTS values (tactile sensation for hand)**Table 4.12** Absolute errors between actual and calculated values of DTS for “comfort” and “preference” (tactile sensation of hand)

Sample	Absolute error between actual and calculated values of DTS	
	“Comfort”	“Preference”
#1	0.035	0.028
#2	0.039	0.011
#3	0.039	0.045
#4	0.128	0.067
#5	0.029	0.002
#6	0.048	0.088
#7	0.195	0.149
Mean	0.073	0.056
Standard deviation	0.059	0.047

Figure 4.24 shows that the actual and calculated values of DTS for “comfort” and “preference”. The mean absolute errors for “comfort” and “preference” are 0.073 ± 0.059 and 0.056 ± 0.047 respectively. In conclusion, the equation (4.11) and (4.12) can be used for prediction of DTS values of “comfort” and “preference” with consideration of the errors. In the next section, the reliability of the above equations will be verified.

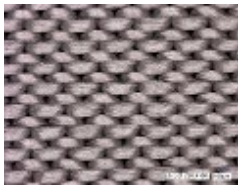
4.2.2.3 Verification Test of Quantified Tactile Sense Evaluation

In this chapter, the computed equations from the quantification of tactile sensation will be verified the reliability by using unknown samples; other than 7 samples in this research. In order to conduct verification test, first, a sensory evaluation of the unknown samples is conducted to determine the actual DTS values. Next, all the physical quantities of the unknown samples needed are measured. Then, by using the measured physical quantities, predicted DTS values are calculated. Lastly, the errors between actual and predicted DTS values are evaluated for the


Table 4.13 List of unknown fabric samples

(a) Materials and knitted method		
#	Material	Knitted method
8	Cupro 93 %, Polyurethane 7 %	Plain stitch
9	Cotton 93 %, Nylon 20 %, Polyurethane 5 %	Half Milano rib

(b) Picture of fabrics ($\times 100$ magnification)



#8



#9

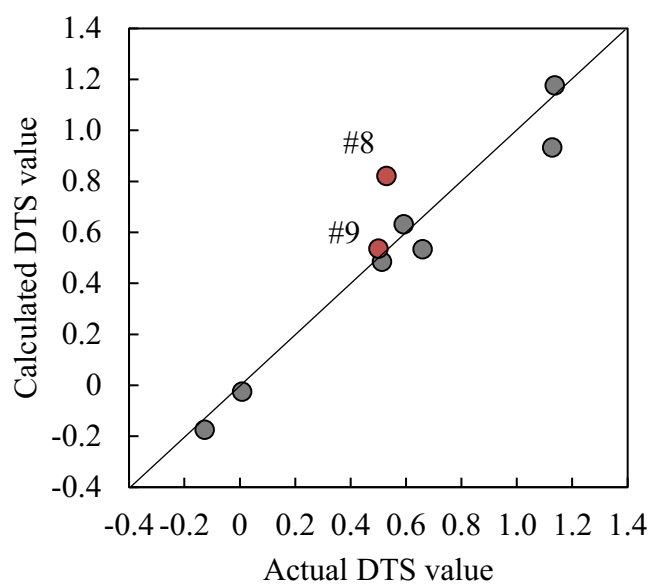
Table 4.14 Physical quantities and DTS values (hand) of unknown samples

	Sample	#8	#9
Physical quantities	T [mm]	0.488	0.574
	q max [W/m ² ·°C]	163.7	108.0
	RC [%]	32.50	42.99
	V _{3g} [V]	0.560	0.612
	V _{6g} [V]	1.212	1.371
	V _{p-p} [V]	0.467	0.212
Actual DTS value	“Comfort”	0.529	0.500
	“Preference”	0.416	0.348
Predicted DTS value	“Comfort”	0.821	0.536
	“Preference”	0.667	0.239

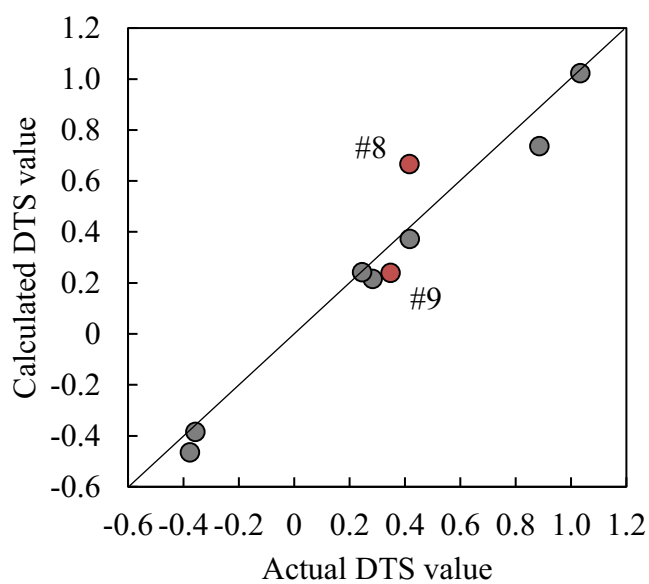
verification of the quantification method proposed by this research.

There are two unknown samples used for the verification. The details on these samples are as shown in Table 4.13. The samples are also undergarments which are designed for summer season; similar to 7 samples used for the quantification.

A sensory evaluation by using the similar methods and conditions as in Chapter 3 was carried out for the two unknown samples. The sensory evaluation was conducted to determine the actual DTS values when human directly evaluates the fabric. Then, six physical quantities which are the variables for the prediction of DTS values were measured with the same condition as in Section 4.2.1 the measured physical quantities, the value of predicted DTS was computed. The actual DTS values from sensory evaluation, measured physical quantities and predicted DTS values were summarized in Table 4.14.



(a) DTS adjective of "comfort"



(b) DTS adjective of "preference"

Figure 4.25 DTS values of unknown samples (hand)**Table 4.15** Error of predictions (hand)

Sample	Error of predictions	
	"Comfort"	"Preference"
#8	0.292	0.251
#9	0.036	0.109

The actual and predicted DTS values of the unknown samples are plotted in Figure 4.25 with 7 other samples. The errors of predictions are as shown in Table 4.15. From the overall results, the errors for DTS value of “comfort” and “preference” in sample #8 is greater than sample #9. The DTS values of “comfort” and “preference” for sample #8 may not be considered to be predictable by using the quantified tactile sensation method because the errors are far greater than the mean errors calculated in Section 4.2.2.2; 0.073 ± 0.059 for “comfort” and 0.056 ± 0.047 for “preference”. Nevertheless, the DTS values of “comfort” and “preference” for sample #9 can be considered to be predictable by using the quantified method because the errors are smaller compared to the mean errors calculated.

4.2.3 Quantification of Tactile Sense Evaluation by Forearm

4.2.3.1 Multiple Regression Analysis

Multiple regression analysis was conducted to determine and examine the relationship between all physical quantities that are listed in Section 4.2.1 and each component in LTS by using SPSS software [IBM Corporation]. Before conducting multiple linear regression, bivariate Pearson correlation was conducted for all explanatory variables to make sure that there is no multicollinearity occurred between the variables. All the correlations showed values below 0.65.

Table 4.16 shows the correlation and multiple regression analysis results when the dependent variable is LTS component of “surface texture” and the independent variable are physical quantities. As shown in Table 4.16 (b), six physical quantities were included; (1) thickness, T (2) thermal property, q max, (3) compressional resilience, RC, (4) deformation at 3 g, V_{3g} , (5) deformation at 6 g, V_{6g} , (6) vibration’s peak-to-peak voltage, V_{p-p} , and others were excluded variables for the multiple regression model. q max had a positively and significantly correlation with the “surface texture”. Nevertheless, T and V_{3g} had a negatively and significantly correlation with the “surface texture”. Moreover, RC and V_{6g} had a weak positive correlation with “surface texture”. However, V_{p-p} had a weak negative correlation with “surface texture”.

Table 4.16 Result for multiple regression analysis (LTS-“surface texture” with all physical quantities)

(a) Correlations			
“surface texture”			
	Pearson correlation	Sig.	
T	-0.780**	.019	
q max	0.597*	.079	
RC	0.122	.397	
V _{3g}	-0.568*	.092	
V _{6g}	0.253	.292	
V _{p-p}	-0.308	.251	

*p < .1 **p < .05 ***p < .01 ****p < .001

(b) Coefficients			
Model	Unstandardized Coefficients		Standardized Coefficients
	B	Std. Error	Beta
(Constant)	-1.006	0.000	
T	-4.377	0.000	-.788
q max	0.024	0.000	.538
RC	-0.006	0.000	-.059
V _{3g}	1.059	0.000	.042
V _{6g}	0.018	0.000	.002
V _{p-p}	-0.431	0.000	-.306

Dependent variable: “surface texture”
Independent variable: “T”, “q max”, “RC”, “V_{3g}”, “V_{6g}”, “V_{p-p}”

The multiple regression model with all six predictors produced $R^2 = 1.000$, thus, the multiple regression model had a quite good fit of data, indicating that the “surface texture” scores

are strongly related to all six physical quantities. According to the standardized regression coefficients, the T had the most influence to the LTS component of “surface texture”, followed by q max, V_{p-p} , RC, V_{3g} and lastly, V_{6g} . q max and V_{6g} had positive regression coefficients, indicating that the higher values of q max and V_{6g} , the sample was expected to have higher score of “surface texture”, i.e. smoother. On the other hand, T and V_{p-p} had a negative regression coefficient, indicating that the higher values of T and V_{p-p} , the sample was expected to have lower score of “surface texture”, i.e. rougher. However, V_{3g} had a positive regression coefficient (opposite in sign from its correlation with “surface texture”), indicating that after accounting for T, q max, RC, V_{6g} and V_{p-p} , the higher value of V_{3g} , the sample was expected to have higher score of “surface texture”, i.e. smoother. Moreover, RC had a negative regression coefficient (opposite in sign from its correlation with “surface texture”), indicating that after accounting for T, q max, V_{3g} , V_{6g} and V_{p-p} , the higher value of RC, the sample was expected to have lower score of “surface texture”, i.e. rougher. From Table 4.15 (b), a multiple regression equation can be obtained as the equation below.

$$L_{surface} = (-4.377 \times T) + (0.024 \times q_{max}) + (0.006 \times RC) + (1.059 \times V_{3g}) + (0.018 \times V_{6g}) + (-0.431 \times V_{p-p}) - 1.006 \quad (4.13)$$

Table 4.16 shows the correlation and multiple regression analysis results when the dependent variable is LTS component of “softness” and the independent variables are physical quantities. As shown in Table 4.17 (b), similar six physical quantities were included in this multiple regression model too. V_{p-p} had a negatively and significantly correlation with the “softness”. Moreover, q max, RC and V_{6g} had a weak positive correlation with “softness”. However, T and V_{3g} had a weak negative correlation with “softness”.

The multiple regression model with all six predictors produced $R^2 = 1.000$, thus, the multiple regression model had a quite good fit of data, indicating that the “softness” scores are strongly related to all six physical quantities. According to the standardized regression coefficients, the V_{p-p} had the most influence to the LTS component of “softness”, followed by T, q max, V_{3g} , V_{6g} and lastly, RC. q max and V_{6g} had positive regression coefficients, indicating

Table 4.17 Result for multiple regression analysis (LTS-“softness” with all physical quantities)

(a) Correlations			
“softness”			
	Pearson correlation	Sig.	
T	-0.534	.108	
q max	0.289	.265	
RC	0.400	.187	
V _{3g}	-0.460	.149	
V _{6g}	0.165	.362	
V _{p-p}	-0.811**	.013	

*p < .1 **p < .05 ***p < .01 ****p < .001

(b) Coefficients			
Model	Unstandardized Coefficients		Standardized Coefficients
	B	Std. Error	Beta
(Constant)	-1.153	0.000	
T	-2.678	0.000	-.550
q max	0.008	0.000	.209
RC	-0.003	0.000	-.041
V _{3g}	1.907	0.000	.085
V _{6g}	0.850	0.000	.081
V _{p-p}	-1.047	0.000	-.848

Dependent variable: “softness”

Independent variable: “T”, “q max”, “RC”, “V_{3g}”, “V_{6g}”, “V_{p-p}”

that the higher values of q max and V_{6g}, the sample was expected to have higher score of “softness”, i.e. softer. On the other hand, T and V_{p-p} had a negative regression coefficient,

indicating that the higher values of T and V_{p-p} , the sample was expected to have lower score of “softness”, i.e. harder. However, V_{3g} had a positive regression coefficient (opposite in sign from its correlation with “softness”), indicating that after accounting for T , q_{max} , RC , V_{6g} and V_{p-p} , the higher value of V_{3g} , the sample was expected to have higher score of “softness”, i.e. softer. Moreover, RC had a negative regression coefficient (opposite in sign from its correlation with “softness”), indicating that after accounting for T , q_{max} , V_{3g} , V_{6g} and V_{p-p} , the higher value of RC , the sample was expected to have lower score of “softness”, i.e. harder. From Table 4.17 (b), a multiple regression equation can be obtained as the equation below.

$$L_{softness} = (-2.678 \times T) + (0.008 \times q_{max}) + (-0.003 \times RC) + (1.907 \times V_{3g}) + (0.850 \times V_{6g}) + (-1.047 \times V_{p-p}) - 1.153 \quad (4.14)$$

Table 4.18 shows the correlation and multiple regression analysis results when the dependent variable is LTS component of “downiless” and the independent variable are physical quantities. As shown in Table 4.18 (b), similar six physical quantities were included in this

Table 4.18 Result for multiple regression analysis (LTS-“downiless” with all physical quantities)

(a) Correlations		
“downiless”		
	Pearson correlation	Sig.
T	0.203	.331
q max	-0.557*	.097
RC	0.703**	.039
V_{3g}	-0.143	.380
V_{6g}	0.091	.423
V_{p-p}	-0.548	.102

*p < .1 **p < .05 ***p < .01 ****p < .001

Table 4.18 Result for multiple regression analysis (LTS-“downiless” with all physical quantities)

(b) Coefficients			
Model	Unstandardized Coefficients		Standardized Coefficients
	B	Std. Error	Beta
(Constant)	5.847	0.000	
T	1.156	0.000	.385
q max	-0.023	0.000	-.920
RC	0.006	0.000	.127
V _{3g}	-8.109	0.000	-.588
V _{6g}	0.872	0.000	.135
V _{p-p}	-0.310	0.000	-.408

Dependent variable: “downiless”

Independent variable: “T”, “q max”, “RC”, “V_{3g}”, “V_{6g}”, “V_{p-p}”

multiple regression model too. RC had a positively and significantly correlation with the “downiless”. Nevertheless, q max had a negatively and significantly correlation with the “downiless”. Moreover, T and V_{6g} had a weak positive correlation with “downiless”. However, V_{3g} and V_{p-p} had a weak negative correlation with “downiless”.

The multiple regression model with all six predictors produced $R^2 = 1.000$, thus, the multiple regression model had a quite good fit of data, indicating that the “downiless” scores are strongly related to all six physical quantities. According to the standardized regression coefficients, the q max had the most influence to the LTS component of “downiless”, followed by V_{3g}, V_{p-p}, T, V_{6g} and lastly, RC. T, RC and V_{3g} had positive regression coefficients, indicating that the higher values of T, RC and V_{3g}, the sample was expected to have higher score of “downiless”, i.e. not downy. On the other hand, q max, V_{3g} and V_{p-p} had a negative regression coefficient, indicating that the higher values of q max, V_{3g} and V_{p-p}, the sample was expected to

have lower score of “downiless”, i.e. downy. From Table 4.18 (b), a multiple regression equation can be obtained as the equation below.

$$\begin{aligned} L_{downiless} = & (1.156 \times T) + (-0.023 \times q_{max}) + (0.006 \times RC) + (-8.109 \times V_{3g}) \\ & + (0.872 \times V_{6g}) + (-0.310 \times V_{p-p}) + 5.847 \end{aligned} \quad (4.15)$$

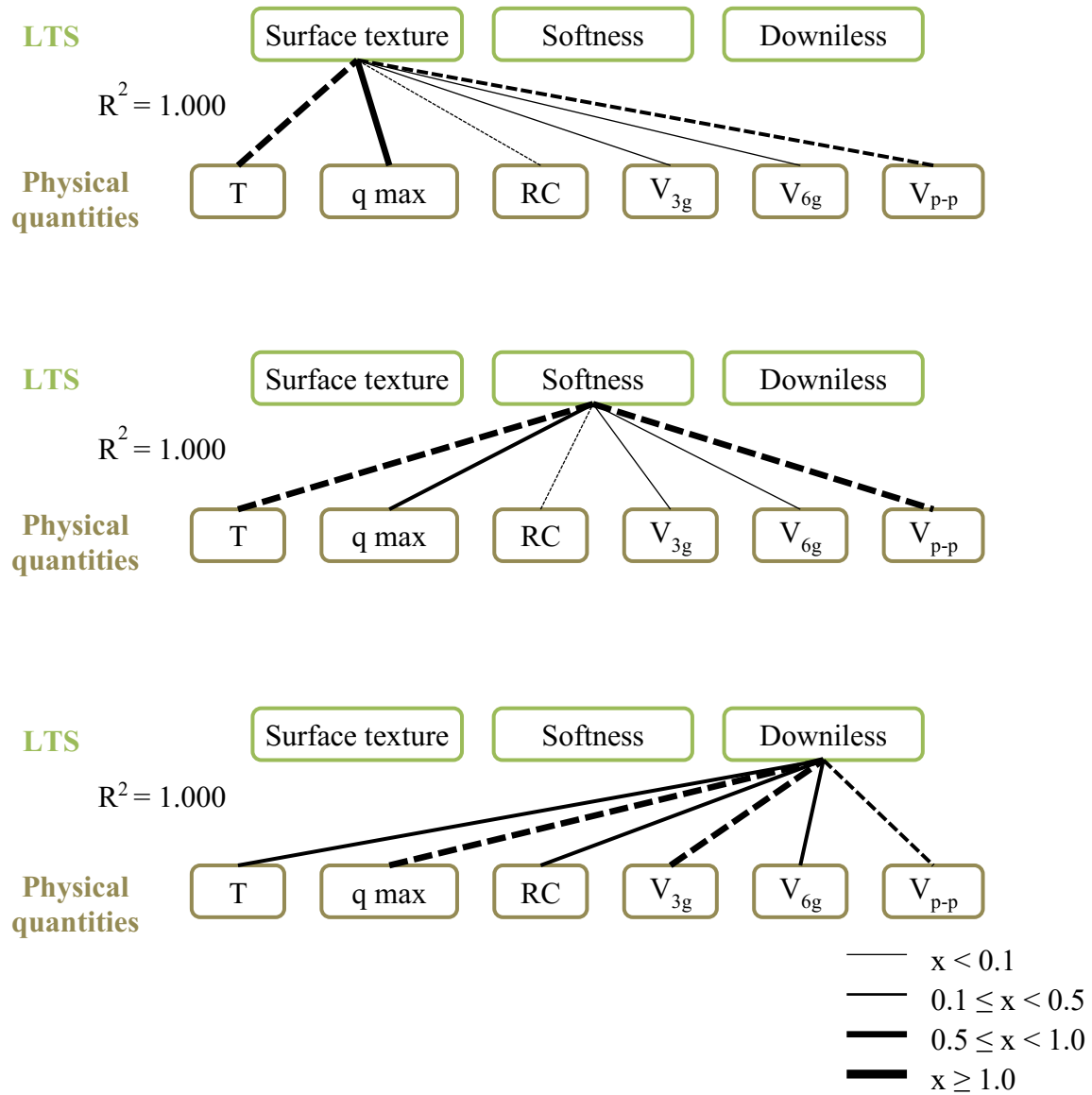


Figure 4.26 Multiple regression analysis results (tactile sensation of forearm)

From the above multiple regression analysis results, the relationship between LTS components and physical quantities by using regression coefficients can be summarized as shown in Figure 4.26.

4.2.3.2 Discussions

From the multiple regression equations in section 3.3.3.2 and section 4.2.3.1, DTS adjectives for forearm can be expressed in terms of physical quantities, when the equations (4.13), (4.14) and (4.15) are substituted in equation (3.20) and (3.21). The computed equations are as shown below.

$$D_{comfort,forearm} = (-2.667 \times T) + (0.008 \times q_{max}) + (-0.002 \times RC) + (-3.024 \times V_{3g}) + (0.321 \times V_{6g}) + (-0.374 \times V_{p-p}) + 2.281 \quad (4.16)$$

$$D_{preference,forearm} = (-2.732 \times T) + (0.008 \times q_{max}) + (-0.002 \times RC) + (-2.263 \times V_{3g}) + (0.193 \times V_{6g}) + (-0.301 \times V_{p-p}) + 1.723 \quad (4.17)$$

By using equations (4.16) and (4.17), DTS values for all 7 samples are calculated from the measured physical quantities. The actual values of DTS from sensory evaluation and calculated DTS values from physical quantities are plotted in Figure 4.27, and the absolute errors between the two values are calculated and recorded in Table 4.19.

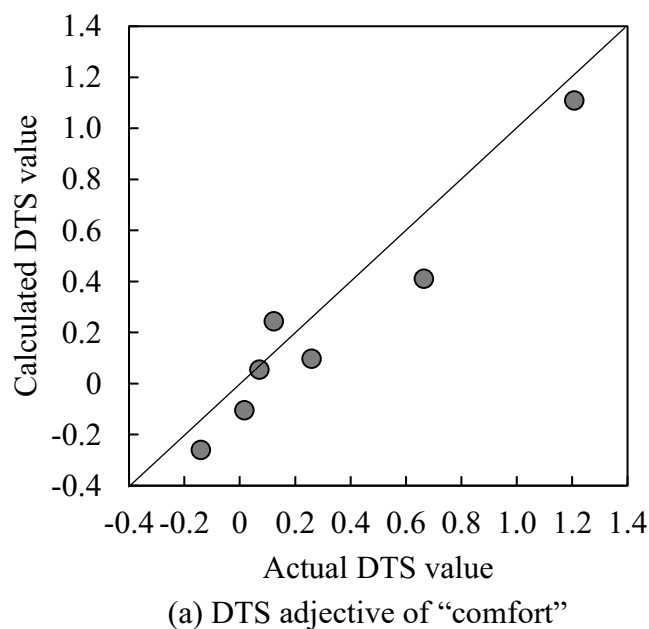
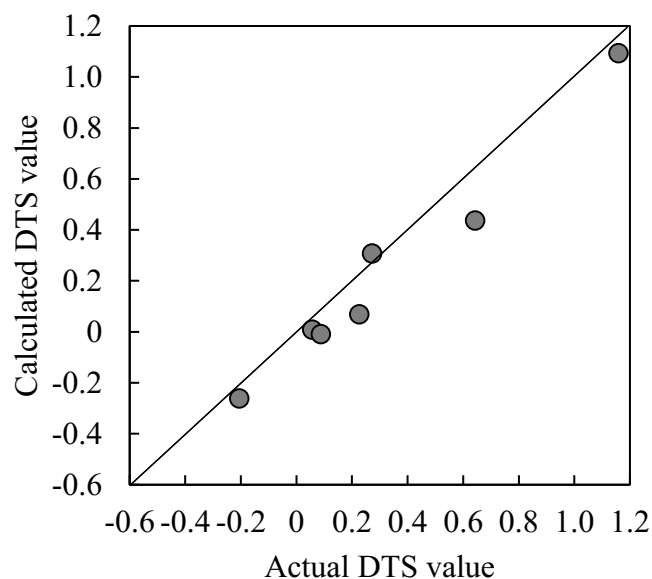


Figure 4.27 Actual and calculated DTS values (tactile sensation for forearm)



(b) DTS adjective of “preference”

Figure 4.27 Actual and calculated DTS values (tactile sensation for forearm)**Table 4.19** Absolute errors between actual and calculated values of DTS for “comfort” and “preference” (tactile sensation of forearm)

Sample	Absolute error between actual and calculated values of DTS	
	“Comfort”	“Preference”
#1	0.119	0.057
#2	0.098	0.065
#3	0.162	0.157
#4	0.016	0.048
#5	0.122	0.035
#6	0.121	0.096
#7	0.254	0.206
Mean	0.128	0.095
Standard deviation	0.066	0.059

Figure 4.27 shows that the actual and calculated values of DTS for “comfort” and

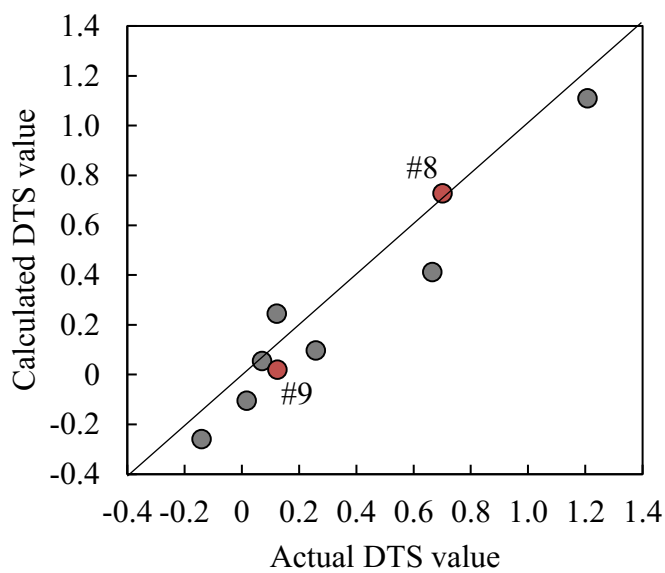
“preference”. The mean absolute errors for “comfort” and “preference” are 0.128 ± 0.066 and 0.095 ± 0.059 respectively. In conclusion, the equation (4.16) and (4.17) can be used for prediction of DTS values of “comfort” and “preference” with consideration of the errors. In the next section, the reliability of the above equations will be verified.

4.2.3.3 Verification Test of Quantified Tactile Sense Evaluation

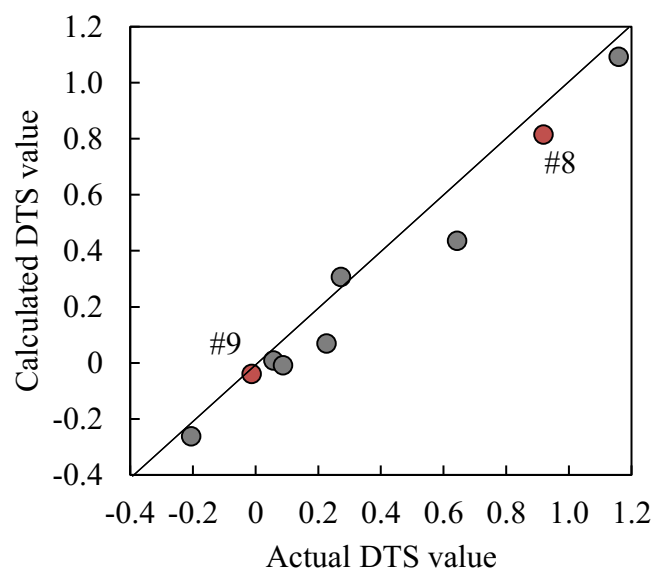
The unknown samples used for the verification are the same as in section 4.2.2.3 (refer Table 4.14). The procedures in verification of quantified tactile sensation of forearm are also similar to quantified tactile sensation of hand in section 4.2.2.3. The actual DTS values from sensory evaluation, measured physical quantities and predicted DTS values were summarized in Table 4.20.

Table 4.20 Physical quantities and DTS values (forearm) of unknown samples

	Sample	#8	#9
Physical quantities	T [mm]	0.488	0.574
	q max [$\text{W}/\text{m}^2 \cdot ^\circ\text{C}$]	163.7	108.0
	RC [%]	32.50	42.99
	V_{3g} [V]	0.560	0.612
	V_{6g} [V]	1.212	1.371
	V_{p-p} [V]	0.467	0.212
Actual DTS value	“Comfort”	0.529	0.500
	“Preference”	0.416	0.348
Predicted DTS value	“Comfort”	0.821	0.536
	“Preference”	0.667	0.239



(a) DTS adjective of "comfort"



(b) DTS adjective of "preference"

Figure 4.28 DTS values of unknown samples (forearm)**Table 4.21** Error of predictions (forearm)

Sample	Error of predictions	
	"Comfort"	"Preference"
#8	0.027	0.103
#9	0.105	0.027

The actual and predicted DTS values of the unknown samples are plotted in Figure 4.28 with 7 other samples. The errors of predictions are as shown in Table 4.21. From the overall results, the errors for DTS value of “comfort” and “preference” in sample #8 is greater than sample #9. The DTS values of “comfort” and “preference” for sample #8 and sample #9 can be considered to be predictable by using the quantified tactile sensation method because the errors are smaller than the mean errors calculated in Section 4.2.3.2; 0.128 ± 0.066 for “comfort” and 0.095 ± 0.059 for “preference”.

4.2.4 Summary

Table 4.22 summarizes the mean absolute errors between actual and calculated values of DTS and for “comfort” and “preference”. In overall, the mean errors of prediction in the case of hand are smaller than forearm. Furthermore, the standard deviations in the case of hand are

Table 4.22 Summary of absolute errors in DTS values

		Tactile sensation	
		Hand	Forearm
DTS	“Comfort”	0.073 ± 0.059	0.128 ± 0.066
	“Preference”	0.056 ± 0.047	0.095 ± 0.059

Table 4.23 Summary of verification results

	“Comfort”		“Preference”	
	Hand	Forearm	Hand	Forearm
Sample #8	△	✓	✓	✓
Sample #9	✓	✓	✓	✓

smaller compared to forearm. Thus, this indicates that the prediction of DTS in the case of hand is more accurate than the forearm.

Moreover, Table 4.23 summarizes the verification results for quantification method of tactile sensation for hand and forearm. As mention previously, the errors of prediction in the case of hand are also smaller than forearm. Therefore, the prediction of unknown samples in the case of hand is much harder compared to forearm.

Chapter 5

AUGMENTED REALITY THERMAL DISPLAY

5.1 Concept for Thermal Display

5.1.1 Thermal Perception

In many research studies, thermal senses of two sensations: cold and warm are considered as separate modalities. The sensations associated with warm and cold stimuli are different (Kenshalo, 1970). The warm sensation feels slow and blooms while the cold sensation feels quick and sharp. Furthermore, in the view of some of the electrophysiological studies, the receptors for warm and cold stimuli are different (Hensel, 1973a, 1973b). These considerations are essential because the operation of one sensation may not apply equally well to the other.

Thermoreceptors respond over a temperature range of 5 °C – 45 °C, but as skin temperature falls below 5 °C – 45 °C or rises above 45 °C, there is a fairly sharp change in the character of thermal sensation to one of pain (Ian Darian-Smith & Johnson, 1977; Spray, 1986). Moreover, the innervation density of thermoreceptors has been analyzed in term of warm and cold spots which varies in density at different sites on the body (B. Green & Cruz, 1998). The warm and cold spots are independently distributed and the cold spots outnumber warm spots has been discovered in previous studies (I. Darian-Smith, Johnson, & Dykes, 1973).

In addition, cold and warm afferent units vary with respect to their conduction velocities. Cold afferent fibers are much faster with conduction velocities of 10 – 20 m/s as compared to 1 – 2 m/s for warm fibers (L. a Jones & Ho, 2008). Thus, the reaction time for the development of cold sensations is significantly shorter than warm sensations (Yarnitsky & Ochoa, 1991).

5.1.2 Spatial Summation

Based on psychophysical measurements of human temperature sensitivity, there are several factors of thermal stimulation: the initial skin temperature, the intensity of the temperature change from the adapted skin temperature, the rate of the temperature change, the body site being stimulated and the area of the skin surface that is stimulated (spatial summation) (Kenshalo et al., 1967). In this research, spatial summation is the subject to be discussed and to be used in method of display, while other parameters are fixed.

A thermal stimulus is becoming more detectable with an increase in the area of stimulation. For warm stimuli, when the area contribution of thermal stimulation increases, the threshold decreases (Joseph C. Stevens & Marks, 1971). On the other hand, for cold stimuli, the perceived threshold grows at nearly constant rate as the contact area increases, regardless of the degree of cooling (Greenspan & Kenshalo, 1985; Kenshalo et al., 1967; Joseph C. Stevens & Marks, 1979). In past research, Hardy et al. found that the threshold was lower when the back of the two hands were stimulated simultaneously than when either hand was stimulated alone (Hardy & Opper, 1937).

Spatial summation not only occurs at a single site of stimulation but has also discovered that it also occurs when two sites symmetrically located on opposite sides of the body are stimulated simultaneously (L. E. Marks, Stevens, & Tepper, 1976; Rózsa & Kenshalo, 1977). However, spatial summation was not observed when the forehead and the dermatomes on the back were simultaneously stimulated (Banks, 1973; Lawrence E. Marks & Stevens, 1973). Although the area of stimulation increases, spatial summation may not occur at certain areas.

In these studies of thermal spatial summation, it has been assumed that the effects of stimulus size on perception solely reflect summation. However, topographic variations in thermal could significantly influence spatial summation and these variations could count much of the increase in sensitivity measured as the stimulation area increases (B. G. Green & Zaharchuk, 2001).

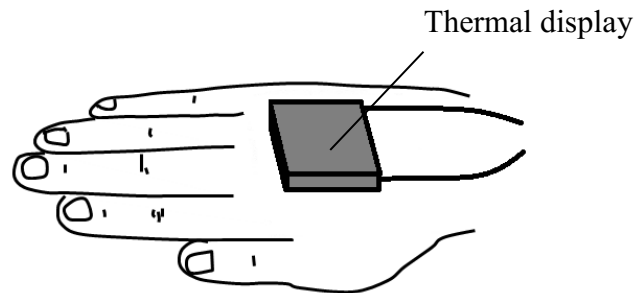


Figure 5.1 Proposed method of display

5.1.3 Method of Display

The AR thermal display in this research is proposed to be placed on the back of hand as shown in Figure 5.1. Thus, the user can touch the object directly without any obstruction on the palm. Moreover, this thermal display is appropriate for AR technology because the device for augmentation of thermal sense does not obstruct the user to feel the object's texture.

By using spatial summation of symmetrical sites, the thermal perception on the palm site is proposed to summate with the thermal perception on the back of hand. For example, when the back of the hand is cooling, the touched object is perceived to be colder than the actual temperature. This phenomenon will be confirmed whether it can be occurred between the back of hand and the palm in Section 5.3. Therefore, when the user's palm touched an object, the AR thermal display presents a certain temperature to delude the object's temperature that leads to material identification.

5.1.4 Proposed AR Thermal Display

As shown in Figure 5.2, the AR thermal display is place on the back of hand and fix by using a wrist supporter. Moreover, there is no obstruction on palm, so the user can touch an

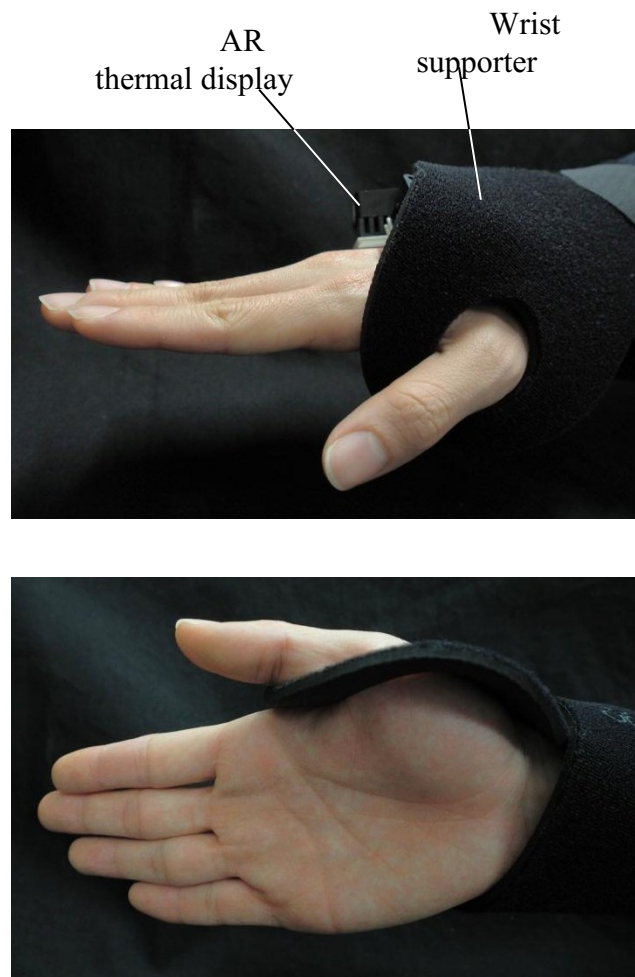


Figure 5.2 Proposed AR thermal display

object directly. The elements of this AR thermal display and the properties will be explained in Section 5.2.

5.2 Development of Augmented Reality Thermal Display

The design and manufacturing of the AR thermal display process can be divided into three different categories. In the first section, all of hardware components for the display are described. Next, in the second section, a Peltier device and a thermal sensor operating circuits and a programmable microcontroller board used for the thermal display are discussed in detail. Then, the third section is allocated to describe the Peltier device's temperature feedback control and palm-object distance feedback control.

AR thermal display

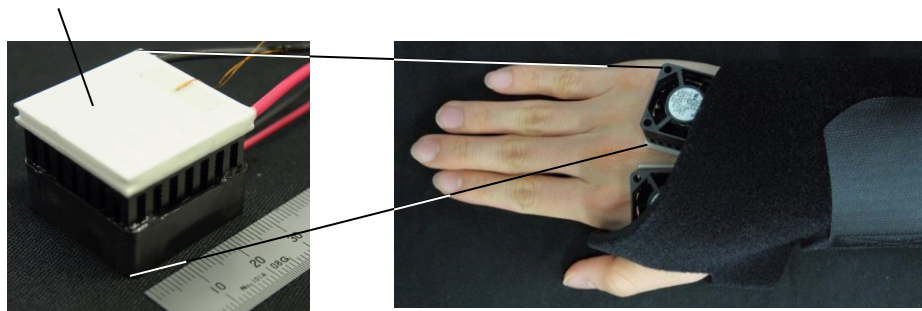


Figure 5.3 AR thermal display on the back of hand

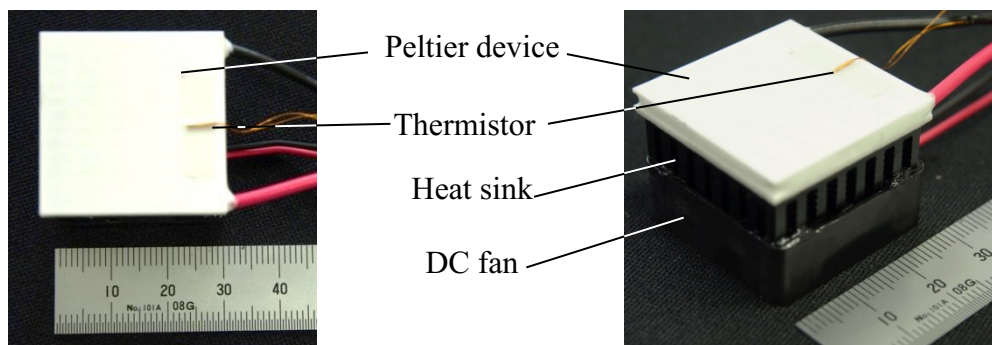


Figure 5.4 AR thermal display

5.2.1 Design and Hardware Implementation of Display System

As shown in Figure 5.3 and Figure 5.4, the hardware implementation of AR thermal display involves a Peltier device, a thermal sensor, a heat sink and a direct current (DC) fan.

A Peltier device with a surface area of 30 mm × 30 mm (TEC1-07108, Nihon Techmo Co., Ltd.) (see Figure 5.5) is selected because it is able to apply localized heating or cooling stimuli to the skin. Peltier devices are the most widely used thermal simulator for thermal displays (Ho & Jones, 2007). Peltier devices pump heat based on the Peltier effect which creates a temperature difference at the junctions of two dissimilar conductors in contact when a direct current passes through them. Unidirectional heat flows between the conductors depending on the

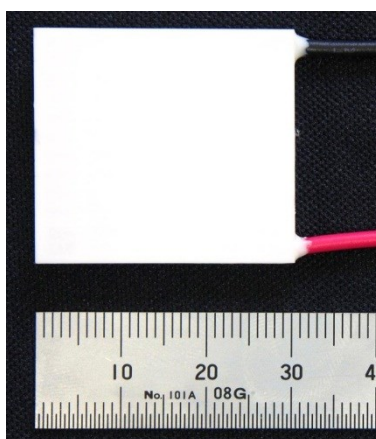


Figure 5.5 Peltier device (30 mm × 30 mm)

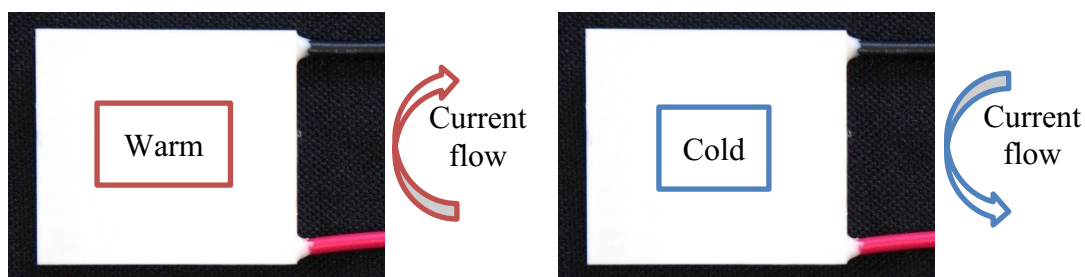


Figure 5.6 Warming or cooling of one side of the Peltier device's surface depending on the direction of the current flow

direction of the current (see Figure 5.6). The temperature difference and the rate of temperature change depend on amplitude of the current passing through the Peltier device.

Next, a thermistor (P1703, Alpha Technics Inc.) (see Figure 5.7) is selected as thermal sensor because the size is small and can be placed between back of hand and Peltier device. The thermistor is used to detect the temperature of the Peltier device. The thermistor is a temperature dependant resistor that varies significantly with temperature compared to a standard temperature and can be divided into two types: positive temperature coefficient and negative temperature coefficient (NTC) thermistor. As shown in Figure 5.8, NTC thermistor is used for this display and the resistance of this thermistor decreases with temperature. This thermistor has a characteristic that the resistance is $10\text{ k}\Omega$ when the temperature is at $25\text{ }^{\circ}\text{C}$.

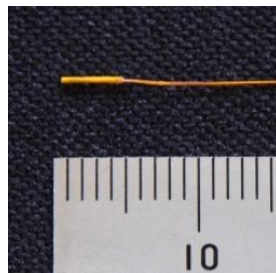


Figure 5.7 Thermistor

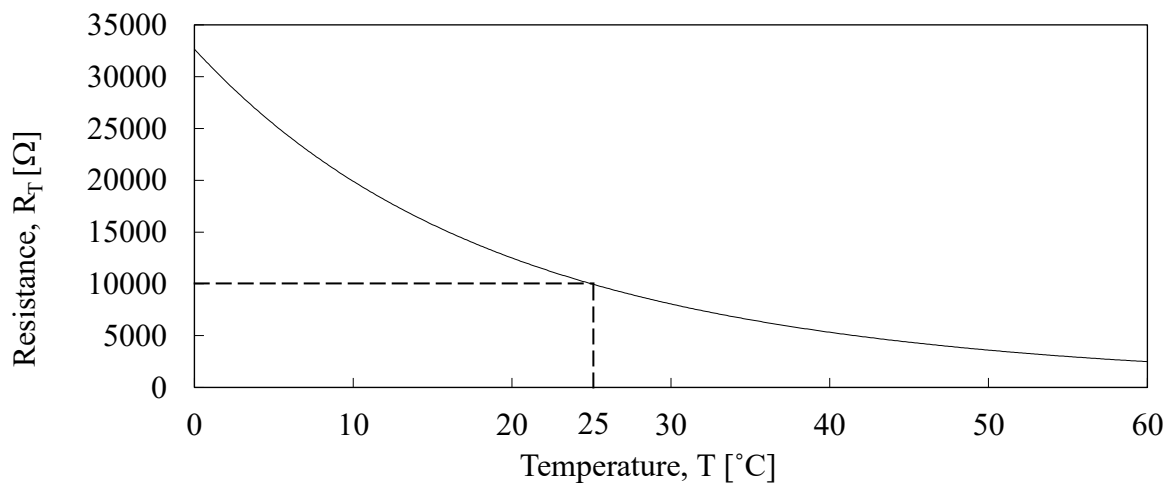


Figure 5.8 The relationship between resistance and temperature

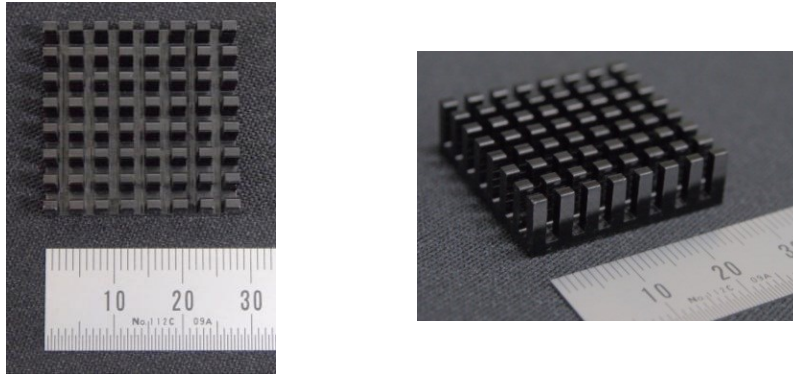


Figure 5.9 Heat sink

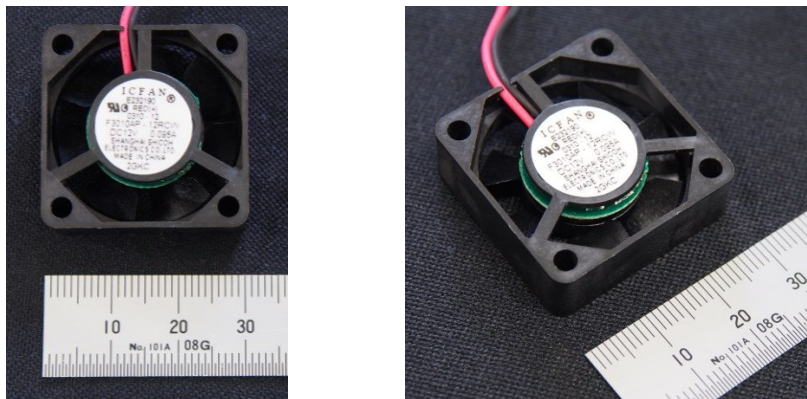


Figure 5.10 DC fan

Furthermore, a 28 mm × 28 mm × 8 mm of heat sink (HS 28288, Comon Co., Ltd.) (see Figure 5.9) and a 30 mm × 30 mm × 10 mm of 12 V DC fan (F3010AP-05PCW, Shicoh Co., Ltd.) (see Figure 5.10) are used for heat radiation of the Peltier device.

5.2.1.1 Peltier Device Driver Circuit

In this research, there are two peltier device driver circuits made. One of the circuits is better in temperature stability and accuracy and the latter is quicker in response time (see Table

Table 5.1 Parameter of Peltier Device Driver Circuit

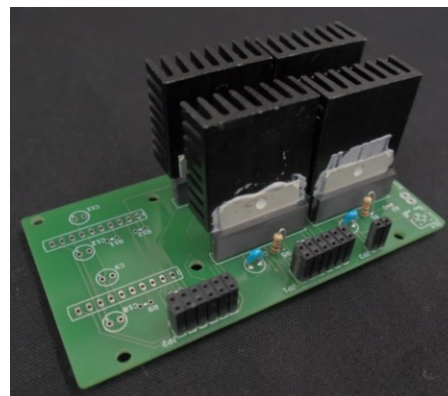
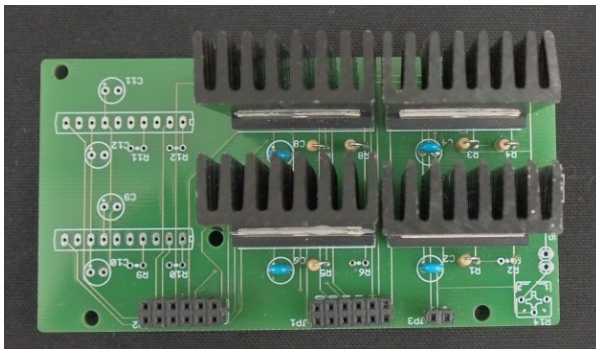
Parameter	Peltier device driver circuit	
	(i)	(ii)
Stability	◎	○
Accuracy	○	×
Response Time	×	◎

Table 5.2 Differences between Bridge Drivers

Differences	Peltier device driver circuit	
	(i)	(ii)
Bridge driver's name	TA7291P	L6203
Operating voltage	5 V	16 V
Output current	1 A(average)	3 A(average)
	2 A(peak)	3.5A(peak)

5.1). The differences between these circuits are the type of bridge driver used (see Table 5.2), the voltage applied to the Peltier device and the amount of current flow through Peltier device.

Both circuits use a bridge driver to control the direction of current flow to the Peltier device. In other words, the bridge driver is used as switching circuit. In order to manipulate the temperature difference between two sides of the Peltier device, pulse width modulation (PWM) is used as the input signal. By changing the duty cycle of PWM, the average voltage applied will vary accordingly; the lesser the duty cycle, the smaller the average voltage applied and vice versa.

**Figure 5.11** Peltier device driver circuit (i)

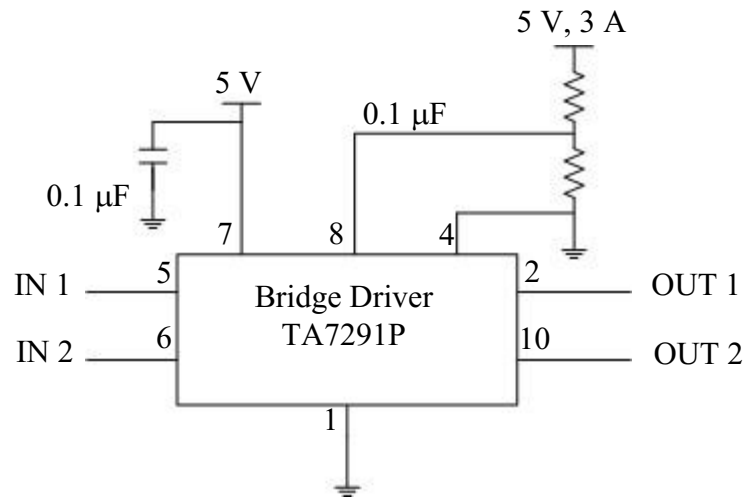


Figure 5.12 Peltier device driver circuit schematic diagram (i)

Table 5.3 Logic states and Peltier device's condition (i)

Input		Output		Peltier device's condition
1	2	1	2	
HIGH	LOW	HIGH	LOW	Hot
LOW	HIGH	LOW	HIGH	Cold
LOW	LOW	LOW	LOW	No change
HIGH	HIGH	∞	∞	No change

∞ : High impedance

(i) Peltier Device Driver Circuit for Better Temperature Stability and Accuracy

In Figure 5.11 and Figure 5.12, the Peltier device driver circuit board and its schematic diagram are shown. A bridge driver (TA7291P) is selected to get a better temperature stability and accuracy because its output current is small, therefore minute tuning can be done. The input and output logic states of the bridge driver are as shown in Table 5.3.

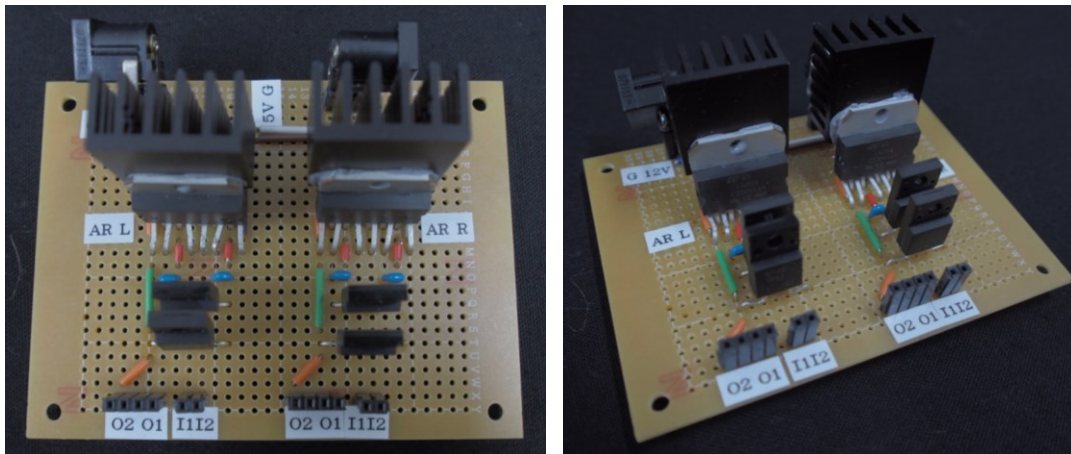


Figure 5.13 Peltier device driver circuit (ii)

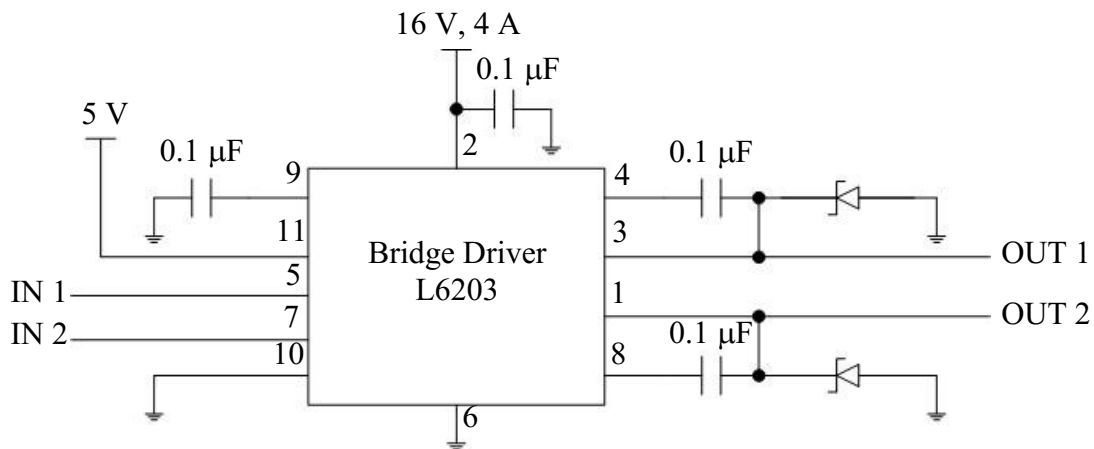


Figure 5.14 Peltier device driver circuit schematic diagram (ii)

Table 5.4 Logic states and Peltier device's condition (ii)

Input		Output		Peltier device's condition
1	2	1	2	
HIGH	LOW	HIGH	LOW	Hot
LOW	HIGH	LOW	HIGH	Cold
LOW	LOW	LOW	LOW	No change
HIGH	HIGH	HIGH	HIGH	No change

(ii) Peltier Device Driver Circuit for Quicker Response Time

In Figure 5.13 and Figure 5.14, the Peltier device driver circuit board and its schematic diagram are shown. A bridge driver (L6203) is used to obtain a quicker response time because its output current is large, thus larger temperature difference of Peltier device can be achieved. The input and output logic states of the bridge driver are as shown in Table 5.4.

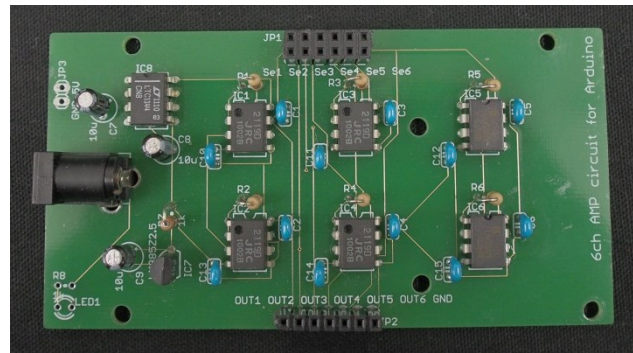


Figure 5.15 Thermal sensor circuit

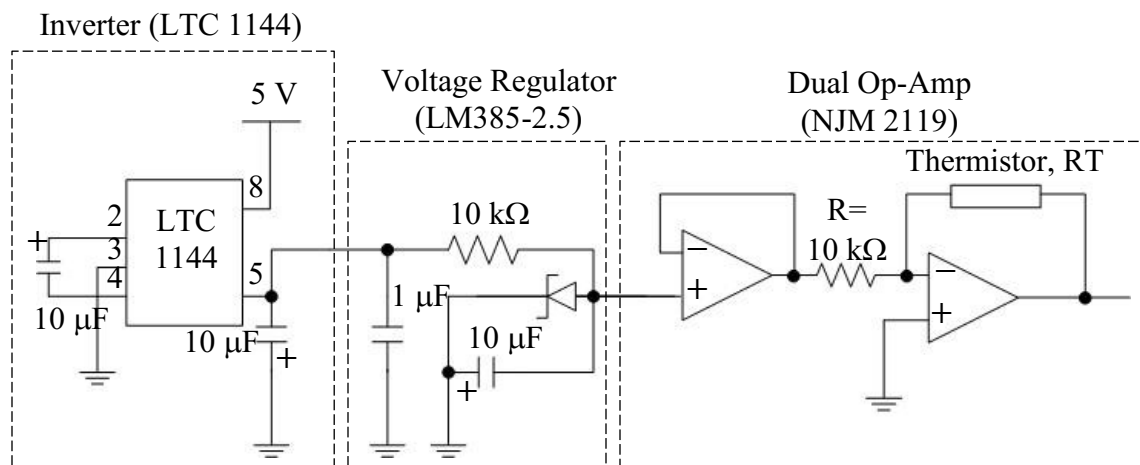


Figure 5.16 Thermal sensor circuit schematic diagram

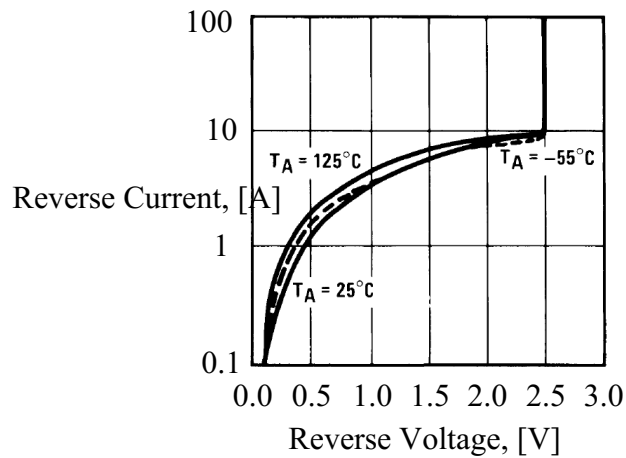


Figure 5.17 Reverse Characteristics [Texas Instruments]

5.2.1.2 Thermal Sensor Circuit

The thermal sensor circuit board and its schematic diagram are as shown in Figure 5.15 and Figure 5.16. According to Figure 5.16, thermal sensor circuit can be divided into three as follows: a) Inverter, b) Voltage regulator and c) Dual operational amplifiers (Op-Amp); first acting as a voltage follower and the second and inverting amplifier.

a) Inverter

This inverter is also called as switched-capacitor voltage converter. It converts voltage from positive to negative from an input range of 2 V to 18 V, resulting in complementary output of -2 V to -18 V . Therefore, in this circuit, the input voltage (pin 8), 5 V is converted into negative voltage (pin 5), -5 V .

b) Voltage regulator

This voltage regulator is used to provide a tight voltage tolerance of -2.5 V . As shown in Figure 5.17, the input voltage is limited to -2.5 V although the current flow increases. Thus, the output voltage of the inverter, -5 V is limited to -2.5 V in this circuit. This voltage regulator can operate at range of micro-power and good temperature stability.

c) Dual Op-Amp

The first Op-Amp is used as a voltage follower, which has the properties of high input impedance and low output impedance. Thus, it prevents the voltage drop before entering the second Op-Amp. The output voltage of the first Op-Amp remained the same as the input voltage.

Next, the second Op-Amp acts as an inverting Op-Amp. The negative input voltage is converted into positive voltage. The output voltage can be expressed by the following equation,

$$V_{out} = -\frac{R_T}{R}V_{in} \quad (5.1)$$

where, V_{out} and V_{in} ($= -2.5$ V) are the output and input voltage of second Op-Amp respectively. Besides, R_T is the thermistor's resistance which varies with temperature and R ($= 10 \Omega$) is a constant.

$$V_{out} = -\frac{R_T}{10 \times 10^3} \times (-2.5) \quad (5.2)$$

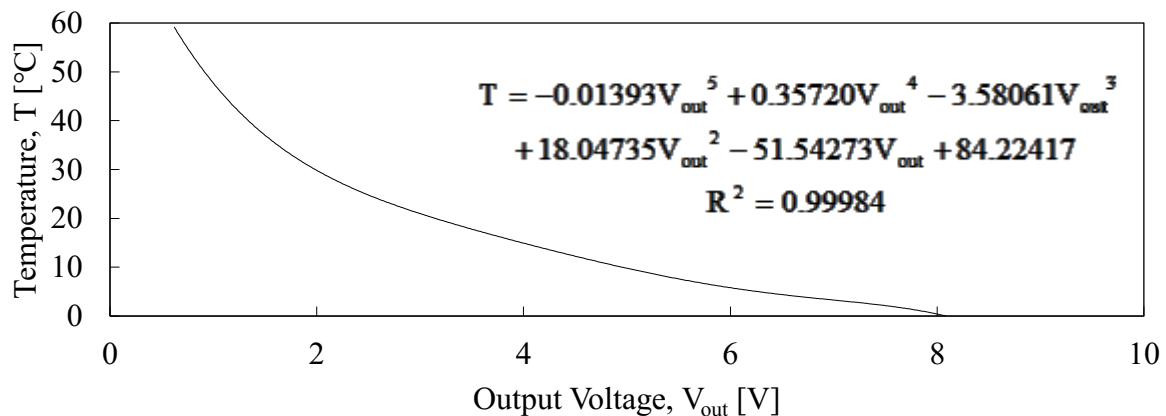


Figure 5.18 Approximation graph of temperature against output voltage

Table 5.5 Inputs and Outputs voltage

Circuit	Input voltage [V]	Output voltage [V]
Inverter	5	-5
Voltage Regulator	-5	-2.5
Dual Op-Amp	-2.5	$-\frac{R_T}{10 \times 10^3} \times (-2.5)$

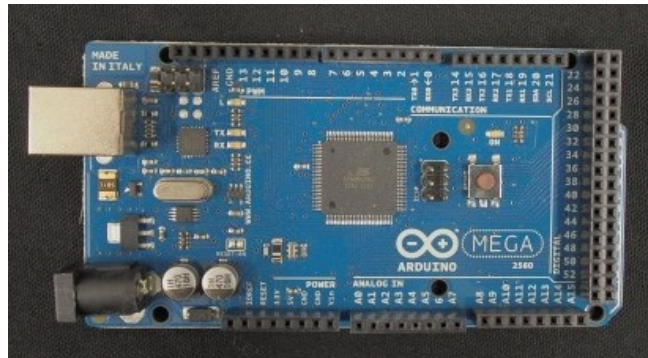


Figure 5.19 Arduino MEGA 2560 R3

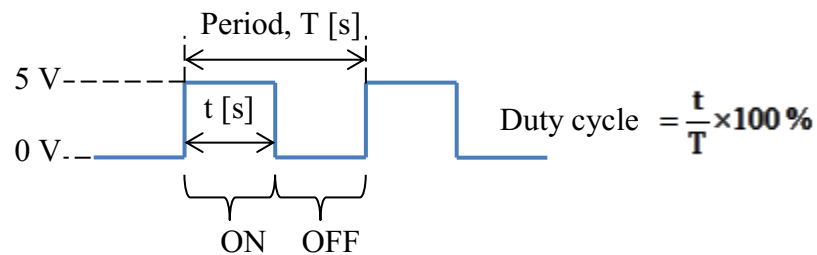


Figure 5.20 PWM signal

From the equation (5.2) and Figure 5.17, the relationship between thermal sensor circuit's output voltage and Peltier device's temperature can be shown as in Figure 5.18.

According to the above explanations, all inputs and outputs voltage are summarized as shown in Table 5.5.

5.2.1.3 Microcontroller Board

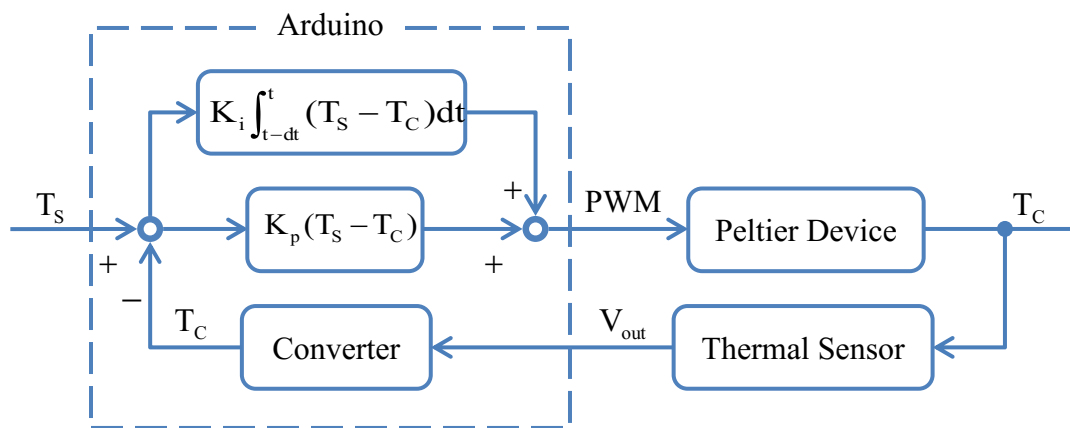
A programmable microcontroller board called Arduino (Arduino MEGA 2560 R3, Strawberry Linux Co.) (see Figure 5.19) is used to control the Peltier device's temperature. This microcontroller board can receive input from a variety of sensors and can give output to lights, motors and other actuators. In this research, Arduino receives the output voltage from the

thermal sensor and sends PWM signal (see Figure 5.20) with a frequency of 500 Hz to the Peltier device.

5.2.2 Peltier Device's Temperature Feedback Control

In this research, a (proportional and integral) PI control loop programmed in Arduino is used to control the surface temperature of Peltier devices. The block diagram of temperature feedback control is as shown in Figure 5.21.

The flow of temperature feedback control is as follows. The current temperature of Peltier device is detected by thermal sensor and the output voltage is converted to temperature in Arduino. Next, the difference between set temperature and current temperature is calculated and inserted in PI elements. Then, PWM signals as the output of Arduino is inserted into Peltier device.

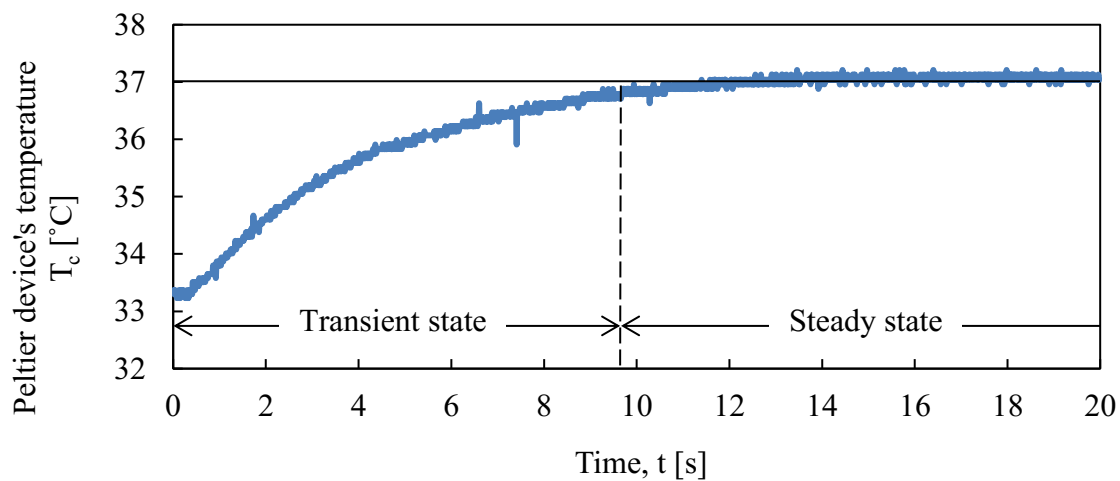


T_s : Set Temperature

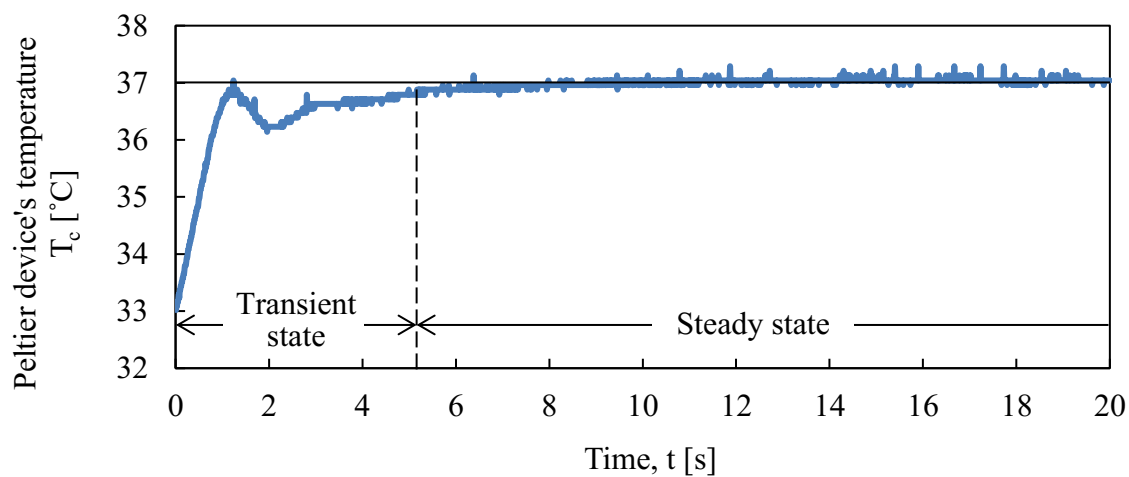
T_c : Current Temperature

V_{out} : Output Voltage

Figure 5.21 Block diagram of temperature feedback control



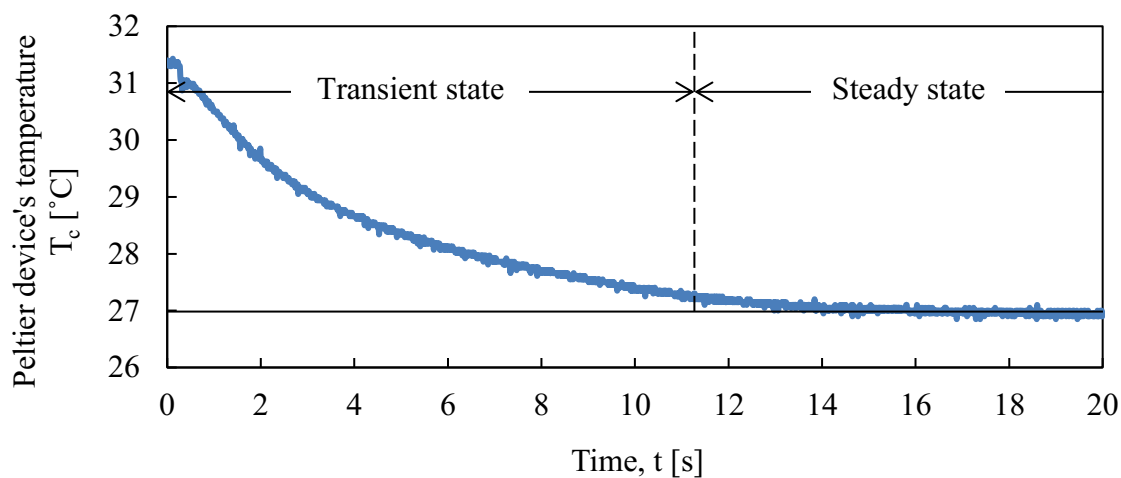
(a) Peltier device driver circuit (i)



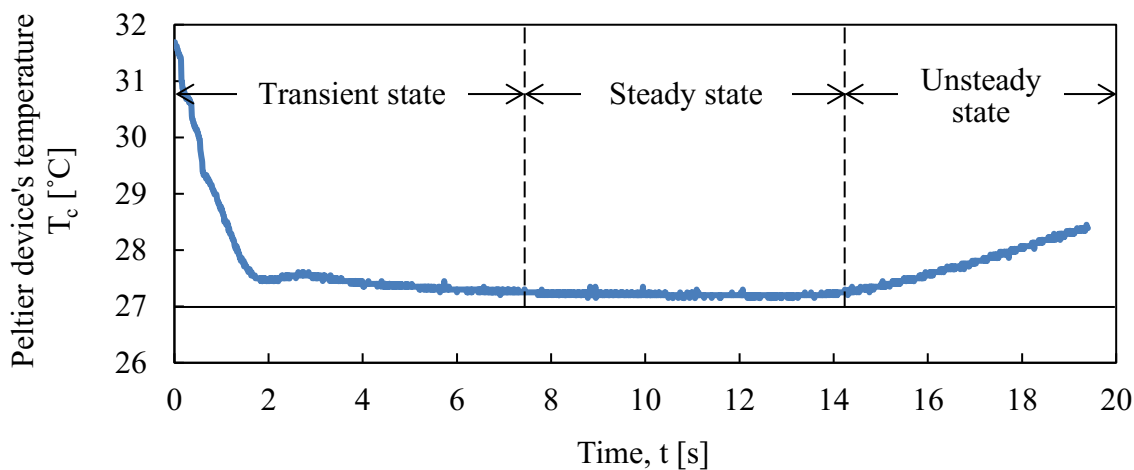
(b) Peltier device driver circuit (ii)

Figure 5.22 Temperature feedback control result for 37 $^{\circ}\text{C}$ **Table 5.6** Temperature feedback control result

Parameter	Peltier device driver circuit			
	(i)	(ii)	(i)	(ii)
Set temperature	37 $^{\circ}\text{C}$		27 $^{\circ}\text{C}$	
Proportional gain, K_p	175	100	200	120
Integral gain, K_i	55	20	40	40
Setting time	9.67 s	5.35 s	11.29 s	7.45 s
Rising time	7.36 s	0.88 s	10.85 s	1.64 s



(a) Peltier device driver circuit (i)



(b) Peltier device driver circuit (ii)

Figure 5.23 Temperature feedback control result for 27 °C

As shown in Table 5.6, the results of temperature feedback control are discussed separately based on used Peltier device driver circuits: (i) Peltier device driver circuit for better temperature stability and accuracy and (ii) Peltier device driver circuit for quicker response time (see Figure 5.22 and Figure 5.23). The set temperatures are 37 °C and 27 °C.

As shown in Figure 5.22, circuit (i) has a longer time to reach steady state than circuit (ii). Both circuits have stability and quality to reach warm temperature; higher than ambient temperature.

On the other hand, as shown in Figure 5.23, when the set temperature was colder than the ambient temperature, circuit (i) has also a longer time to reach steady state than circuit (ii). However, after 14 s, circuit (ii) has lost its stability compared to circuit (i). The reason is as follows. When one surface of Peltier device is cooling, the other surface will become hot and a heat sink and a fan are needed for radiation of heat. In this case, Peltier device for circuit (ii) pumped heat very fast to the heat sink compared to the Peltier device for circuit (i). The heat sink for circuit (ii) did not have time to dissipate out heat. Therefore, the heat from the other side of Peltier device conducted to the cold surface of Peltier device and the temperature increased.

The results can conclude that circuit (i) has a better stability and accuracy than circuit (ii). Nevertheless, circuit (ii) has a quicker respond time compared to circuit (i). In Section 5.3, circuit (i) is used for the first experiment and circuit (ii) is used for the second experiment. In the first experiment, the Peltier device needs to warm/cool the back of hand and has a good stability of temperature for a long time. On the other hand, in the second experiment, the Peltier device needs to reach the set temperature at a very short time (around 2 s). The stability of temperature is not important for the second experiment.

5.2.3 Structure of Program

Figure 5.24 shows a flow chart to illustrate the thermal feedback program in Arduino. This program is used to control the temperature of Peltier device.

5.3 Experiment of Spatial Summation

Two experiments were conducted to determine whether spatial summation occurs between the back of hand and the palm as in the explanation in Section 5.1. In the first experiment, the thermal cues were stimulated on the back of hand in advanced before the participant touched an object. In the second experiment, the back of hand was stimulated at the same time when the participant touched an object.

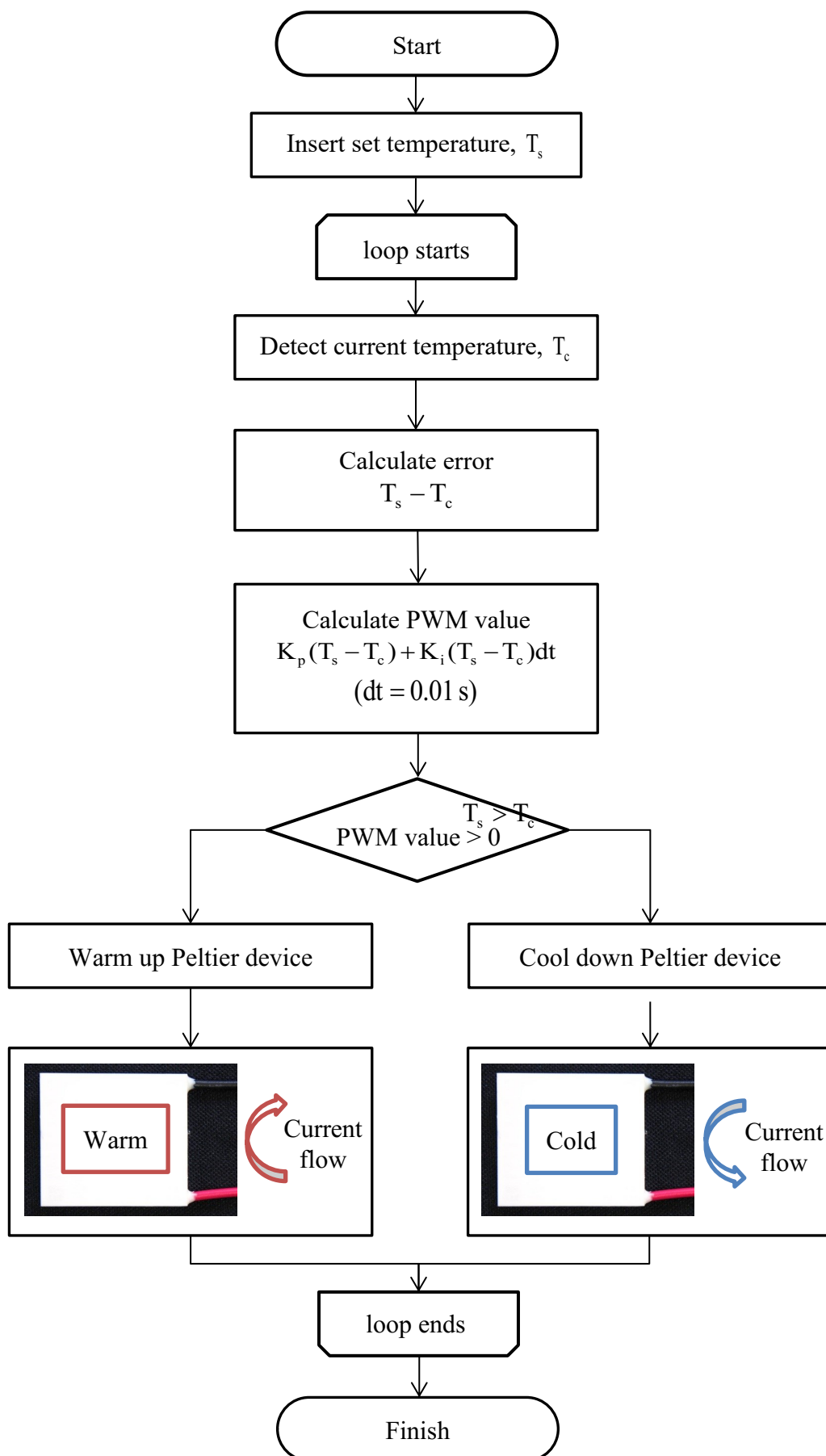


Figure 5.24 Flow chart of thermal feedback program

5.3.1 Back of Hand Stimulated in Advance

In this section, the back of hand was stimulated before the participant touched the object.

5.3.1.1 Apparatus

The experimental apparatus is as shown in Figure 5.25. A thermostat with a surface area of 200 mm × 170 mm (NHP-M20, Nissin Co., Ltd.) (see Figure 5.26) was used for adaptation set.

As shown in experimental apparatus (see Figure 5.26), set A and set B were operated as the objects to be touched. Both Peltier devices have a surface area of 50 mm × 50 mm (TEC1-12714, Nihon Techmo Co., Ltd.) as shown in Figure 5.27(a) were used to display objects' temperature. The structure of set A and set B were similar to AR thermal display as shown in Figure 5.28. A thermistors were used to detect Peltier devices' temperature. Moreover, heat sinks with size of 60 mm × 60 mm × 20 mm (UBH60-20BP, Alpha Co., Ltd.) (see Figure 5.27(b)) and DC fans with size of 60 mm × 60 mm × 25 mm (TUDC12D4, RS Components Co., Ltd.) (see Figure 5.27(c)) were used as heat radiator.

Two AR thermal displays were placed on the right hand of the participant. The augmentation of thermal sense was proposed to be occurred only at the right hand. The AR

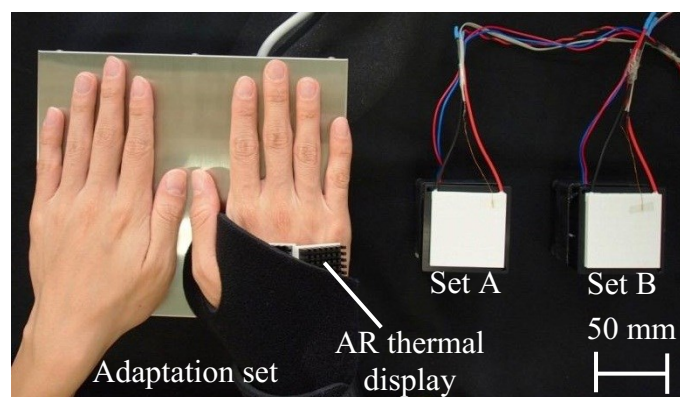


Figure 5.25 Experimental apparatus (Experiment 1)

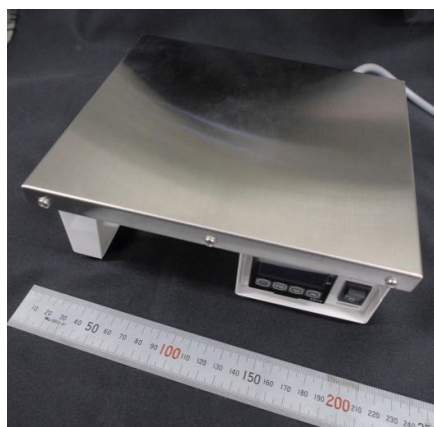
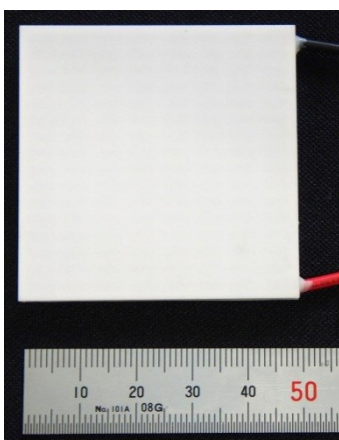
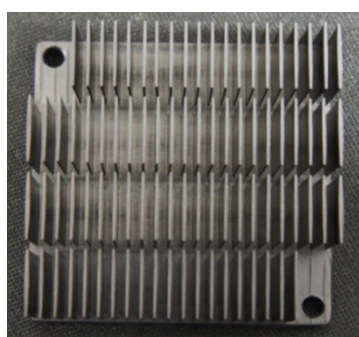


Figure 5.26 Thermostat (200 mm × 170 mm)



(a) Peltier device (50 mm × 50 mm)



(b) Heat sink



(c) DC fan

Figure 5.27 Elements of set A and set B

thermal displays were fixed by using a wrist supporter.

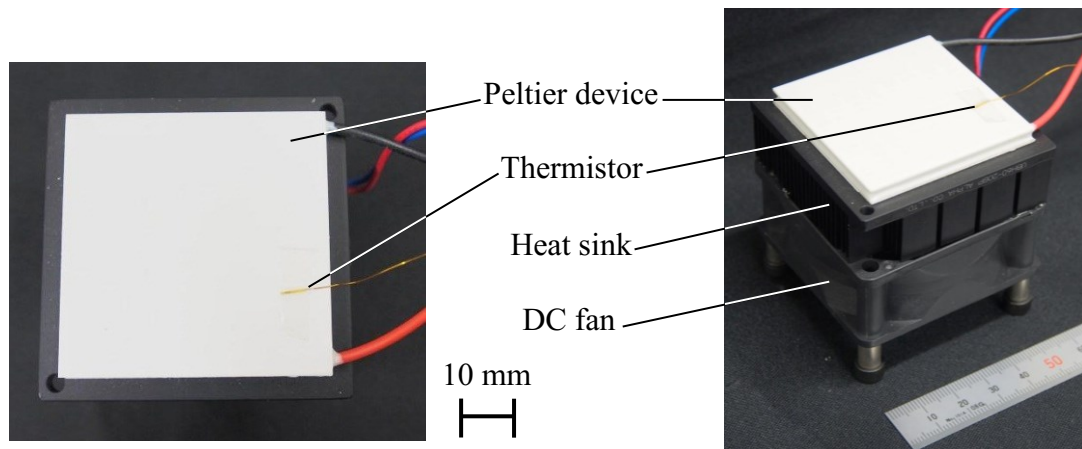


Figure 5.29 The structure of set A and set B

5.3.1.2 Methods

This experiment used the method of constant stimuli which is one of the classical methods for psychophysical experiment. This method is an experiment method which the stimulus is not related from one trial to the next and presented randomly. This is to prevent the participant from being able to predict the level of the next stimulus, and therefore reduces errors of habituation and expectation. Furthermore, the stimuli are usually between five and nine different values; the lower value should be a stimulus that can almost never be detected, and the upper value should be a stimulus that is almost always detected. During the experiment, the participants have to answer whether yes or no and the proportion of yes responses is plotted in a graph called psychometric function. If enough measurements are made, the graph will usually follow a particular S shape called an ogive (G. A. Gescheider, 1985).

The experimental procedures were as follows. Firstly, participants were requested to wear Peltier devices on the back of their right hands. Every participant had to place both hands on the adaptation set about 20 s to make sure the skin temperature at both palms were fixed and the differences between individuals can be minimized.

Next, the participants were required to place the left hands on the set A and right hands on the set B about 3 s. Here, set A was defined as comparison stimulus and set B as standard

stimulus. After 3 s, the participants were asked whether set B is colder than set A and required to answer “Yes” or “No”. Then, the participants were requested to place back both hands on the adaptation set. These processes were repeated for 50 times.

The temperature conditions for all thermal displays were as shown in Table 5.7. The temperature of thermostat for adaptation set was always set at 32 °C. This is because the resting temperature of the skin on the hand ranges from 25 °C to 36 °C (Verrillo et al., 1998) and the skin temperature of all participants in this experiment were at range between 31 °C and 34 °C. On the other hand, the temperature of Peltier device for set A was randomly set up to 25, 26, 27, 28 and 29 °C. All five of the temperatures were displayed 10 trials each. The temperature of set B was always set at 27 °C. There are four temperature conditions: None (no AR thermal display), 27, 32 and 37 °C, for AR thermal displays that placed on the back of the right hand. The time display of these temperatures is as shown in Figure 5.29(a).

Four women participated in this experiment. All of the participants were right-handed, aged between 21 and 23 years, and had no known abnormalities of their tactile and thermal sensory systems. Moreover, all participants did not know about the thermal illusion phenomena. As a result, the error of expectation was reduced.

Table 5.7 Temperature conditions (Experiment 1)

Adaptation set	32 °C	
AR Thermal Display	Left Hand (without augment)	Right Hand (with augment)
	None	Condition 1 : 27 °C Condition 2 : 32 °C Condition 3 : 37 °C Condition 4 : None
Object	Set A (comparison stimulus)	Set B (standard stimulus)
	25, 26, 27, 28, 29 °C (randomly 10 times each)	27 °C

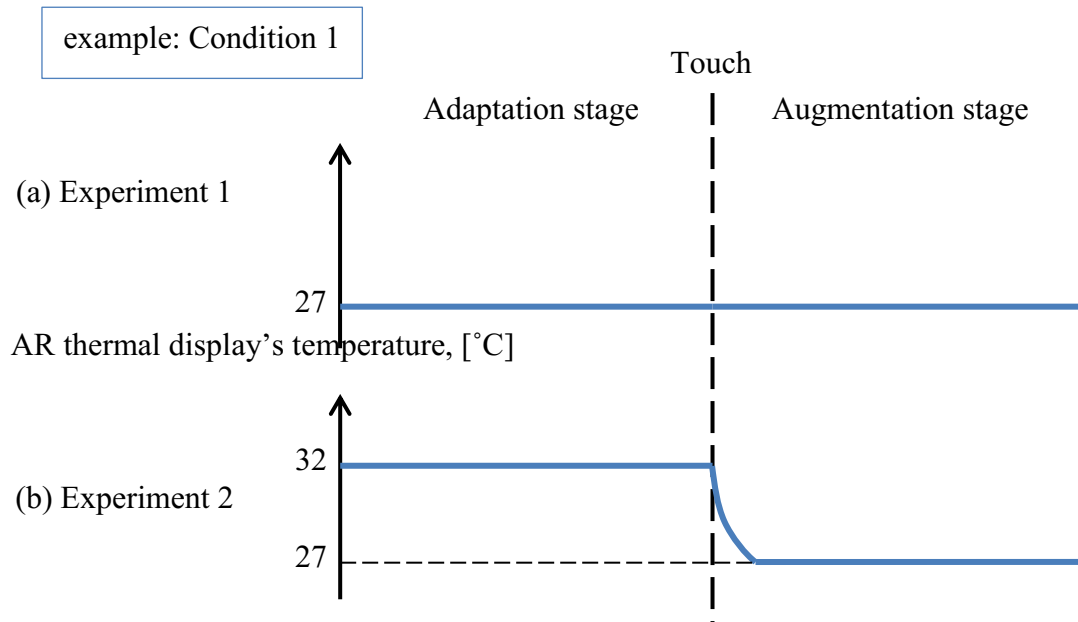
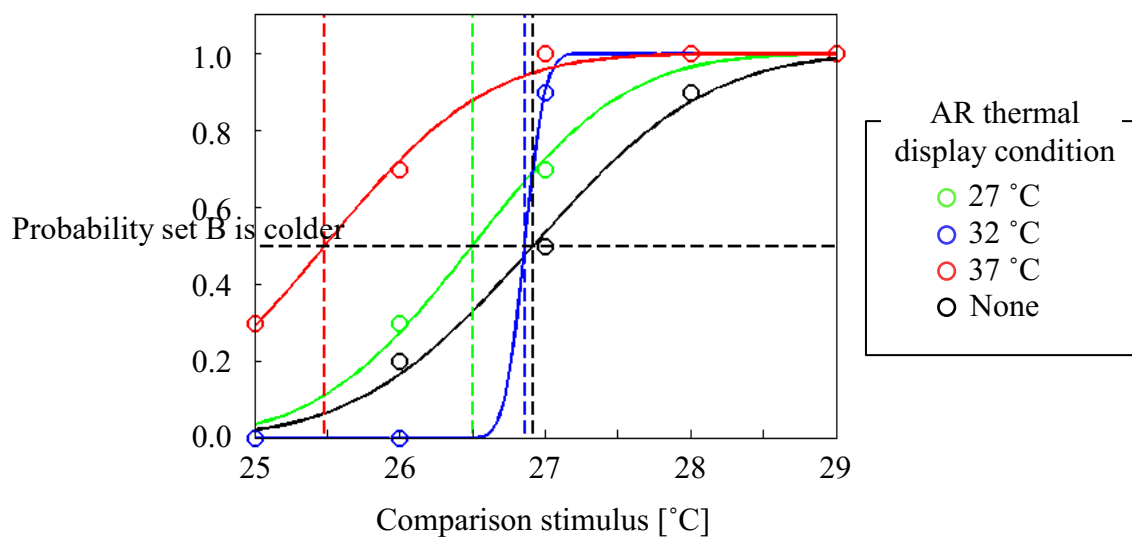
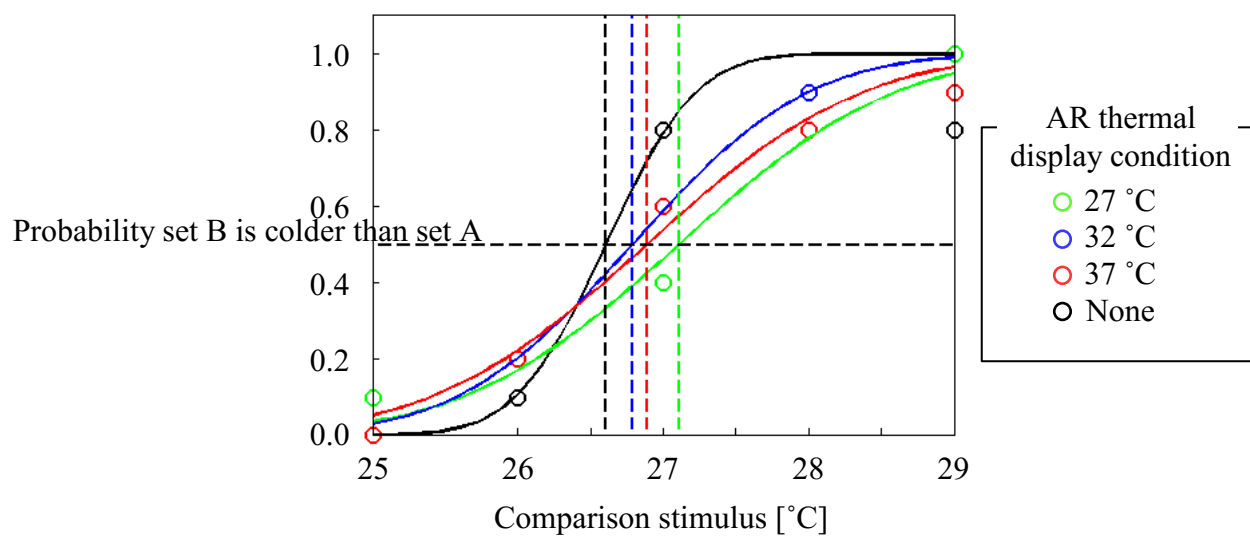


Figure 5.29 Time display of temperature for AR thermal display



(a) Participant 1



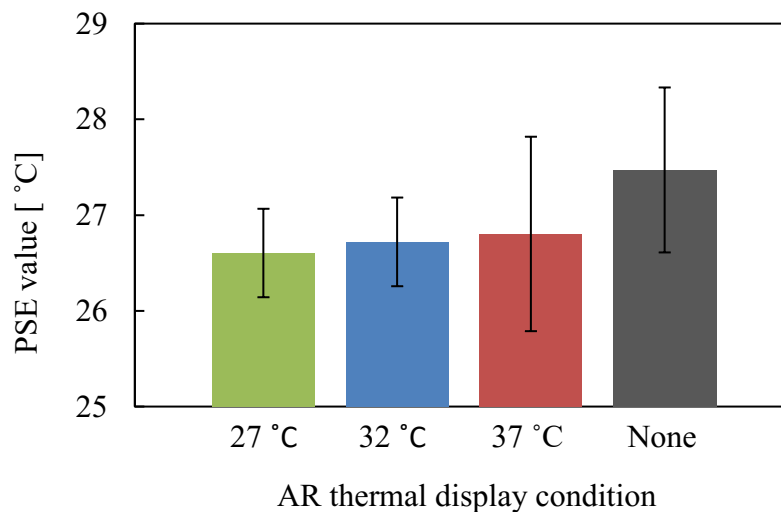
(b) Participant 2

Figure 5.30 Probability set B is colder than set A

Table 5.8 PSE values

Participant	AR thermal display			
	27 °C	32 °C	37 °C	None
1	26.50	26.86	25.49	26.92
2	27.11	26.79	26.89	26.61
3	26.02	26.07	26.88	28.47
4	26.79	27.16	27.96	27.89
Mean	26.60	26.72	26.80	27.47
Standard deviation	0.462	0.463	1.015	0.862

unit: °C

**Figure 5.31** Mean of PSE value

5.3.1.3 Results and Discussions

The coldness of standard stimulus (set B) and comparison stimulus (set A) were compared, and the probability of set B is colder than set A for all participants were shown in Figure 5.30 as follows. The horizontal axis shows the comparison stimulus that was displayed by set A. The fitting curve was computed using maximum likelihood estimation.

Based on Figure 5.31, the point of subjective equality (PSE) was determined for every participant in Table 5.8. PSE is the point where the probability of answer is 50 %. It represents the value of the comparison stimulus which is perceived subjectively as equal to the standard

Table 5.9 Result conclusion for experiment 1

Object	AR thermal display	Augmented thermal perception	Spatial summation
Cool	Cool	Cooler	×
	Warm	Undefined	×

stimulus (G. A. Gescheider, 1985). The mean and standard deviations of PSE were calculated and showed in Figure 5.31.

Then, dependent T-Test with a significant level of 5 % was conducted to find significant different of 27 °C and 37 °C with compared to 32 °C and None. 32 °C is set because it is near to the skin temperature. The results for dependent T-Test are as follows. As a result, the mean difference of PSE values between the conditions of 27 °C and 32 °C was -0.12 °C, which was not statistically significant, $t(3) = -0.71$, $p > 0.05$. Moreover, the mean difference of PSE values between the conditions of 27 °C and None was -0.87 °C, which was not statistically significant, $t(3) = -1.39$, $p > 0.05$. Both results showed that the thermal perception of palm decreased, but they had not significant difference. Thus, the phenomenon of spatial summation cannot be confirmed.

Then, the mean difference of PSE values between the conditions of 37 °C and 32 °C was 0.08 °C, which was not statistically significant, $t(3) = 0.16$, $p > 0.05$. Furthermore, the mean difference of PSE values between the conditions of 37 °C and None was -0.67 °C, which was not statistically significant, $t(3) = -1.36$, $p > 0.05$. These results showed that there is no significant difference between the mean of PSE values for 37 °C with 32 °C and None. Therefore, in this experiment, the thermal perception of palm had no significantly effect by warming up the back of hand.

Furthermore, there was also the same result for the mean difference of PSE values between the conditions of None and 32 °C, which was 0.75 °C and not statistically significant, $t(3) = 1.29$, $p > 0.05$. Thus, this result proved that there is no significant difference between the

mean of PSE values for the conditions of None and 32 °C. All the results were concluded in Table 5.9.

In this research, by displaying thermal information on the back of hand, the thermal perception on the palm can be augmented and deluded based on the concept of the proposed AR thermal display. Spatial summation is a phenomenon which all of thermal threshold in a certain region summate each other. Therefore, according to the hypothesis in this research, when the back of hand is cooled, the thermal perception of the palm become lower, and vice versa. In other words, the object felt colder than the actual temperature.

In this experiment, the back of hand was cooling and warming in advance and then, the palm touched the object. The results showed that there was no significant effect to thermal perception of the palm when the back of hand was cooled or warmed. Therefore, the results for all participants when the back of hand was warmed were irrelevance with each other and large individual differences between participants can be seen.

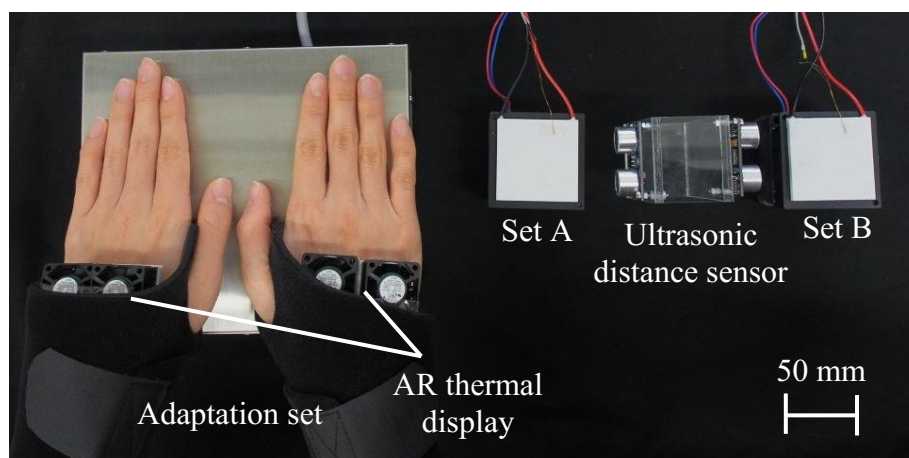


Figure 5.32 Experimental apparatus (Experiment 2)

5.3.2 Back of Hand and Palm Stimulated Simultaneously

In this section, the back of hand was stimulated at the same time when the participant touched the objects: set A and set B.

5.3.2.1 Apparatus

The experimental apparatus is as shown in Figure 5.32. The adaptation set, set A and set B were similar to the first experiment. In this experiment, the back of hand was needed to be stimulated when the participant touched the objects: set A and set B. Thus, two ultrasonic distance sensors (#28015, Akizuki Denshi Tsusho Co., Ltd.) (see Figure 5.33) were used to detect the distance of both hands and the objects. Two AR thermal displays each were placed on both hands of the participant and fixed by using wrist supporters.

5.3.2.2 Methods

The method of this experiment was similar to the first experiment. The participants were requested to wear Peltier devices on the back of their both hands. The experimental procedures were the same as described in Section 5.3.1.2. Every participant had to place both hands on the adaptation set about 20 s and the objects about 5 s alternately. These processes were also

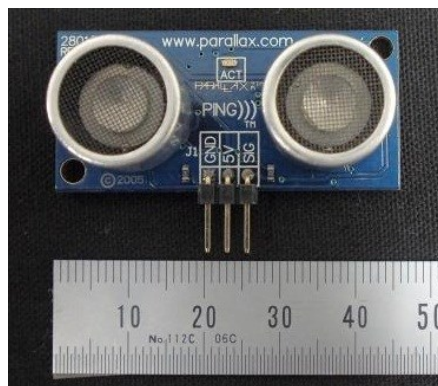


Figure 5.33 Ultrasonic distance sensor

Table 5.10 Temperature conditions (Experiment 2)

Adaptation set	32 °C	
AR Thermal Display	Without augment	With augment
	32 °C	Condition 1 : 27 °C
		Condition 2 : 32 °C
		Condition 3 : 37 °C
Object	Comparison stimulus	Standard stimulus
	25, 26, 27, 28, 29 °C (randomly 10 times each)	27 °C
	35, 36, 37, 38, 39 °C (randomly 10 times each)	37 °C

repeated for 50 times.

The temperature conditions for all thermal displays were as shown in Table 5.10. There are two conditions for object's temperature: cold and warm conditions. For cold condition, the standard stimulus was 27 °C which is colder than the skin temperature and the comparison stimulus was randomly set up to 25, 26, 27, 28 and 29 °C. On the other hand, for warm condition, the standard stimulus was 37 °C which is warmer than the skin temperature and the comparison stimulus was randomly set up to 35, 36, 37, 38 and 39 °C. Set A and set B were randomly set as standard stimulus and comparison stimulus.

For AR thermal displays, there were three temperature conditions: 27 (cold), 32 (skin temperature) and 37 °C (warm). The temperatures of *with* and *without augment* were displayed randomly on the back of right and left hands. When the temperature of *with augment* was displayed on the back of one hand, the object that be touched must be standard stimulus, and vice versa (see Figure 5.34).

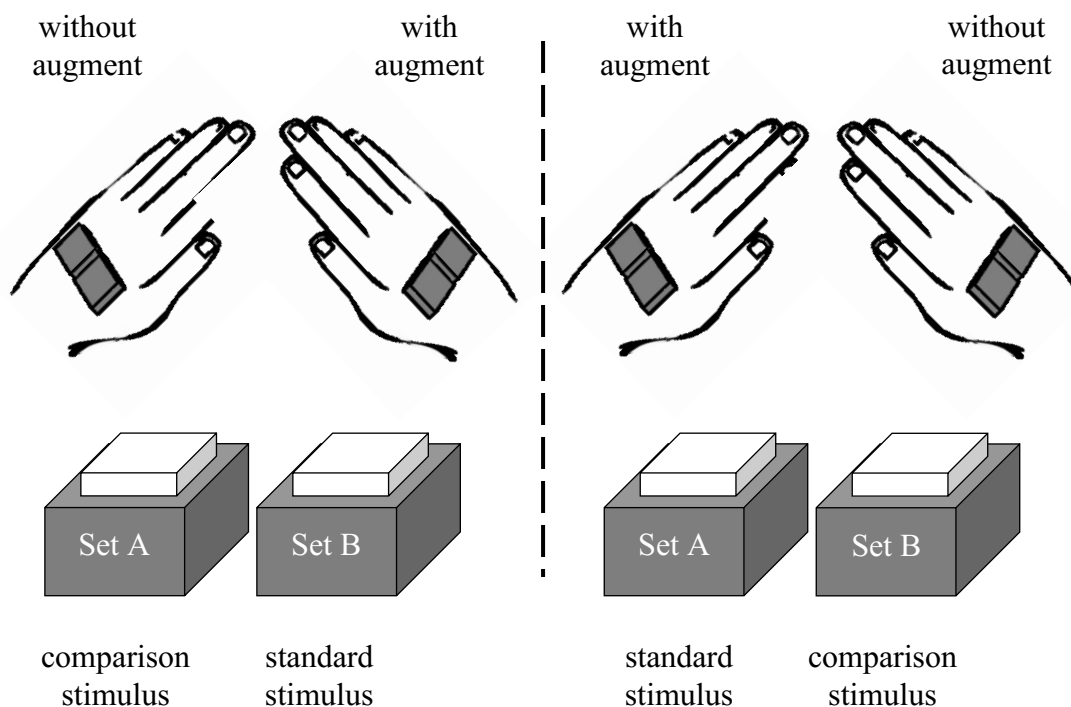


Figure 5.35 The relationship between condition of AR thermal display and type of object's stimulus

The time display of these temperatures is as shown in Figure 5.29(b). The timing of touch was adjusted in order to make sure the rate of change of temperature on the back of both hands was at the same time with the rate of change of temperature on the palms when they touched the objects.

Five women participated in this experiment. The conditions for the participants were similar to the first experiment.

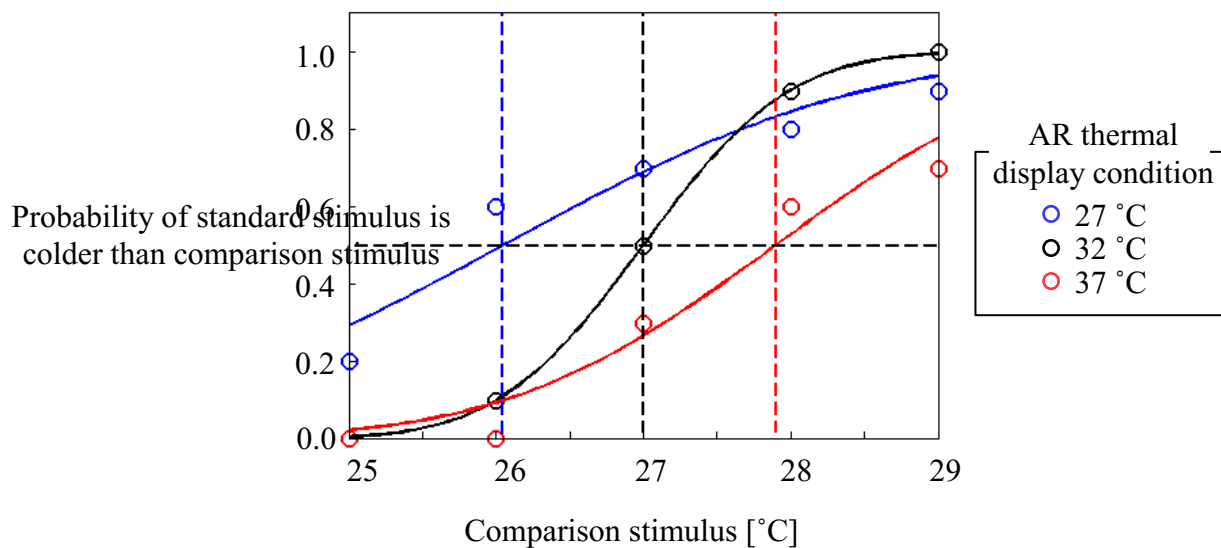
5.3.2.3 Results and Discussions

The results of this experiment are divided according to the touched objects: cold and warm. First, the coldness of standard stimulus and comparison stimulus were compared, and the

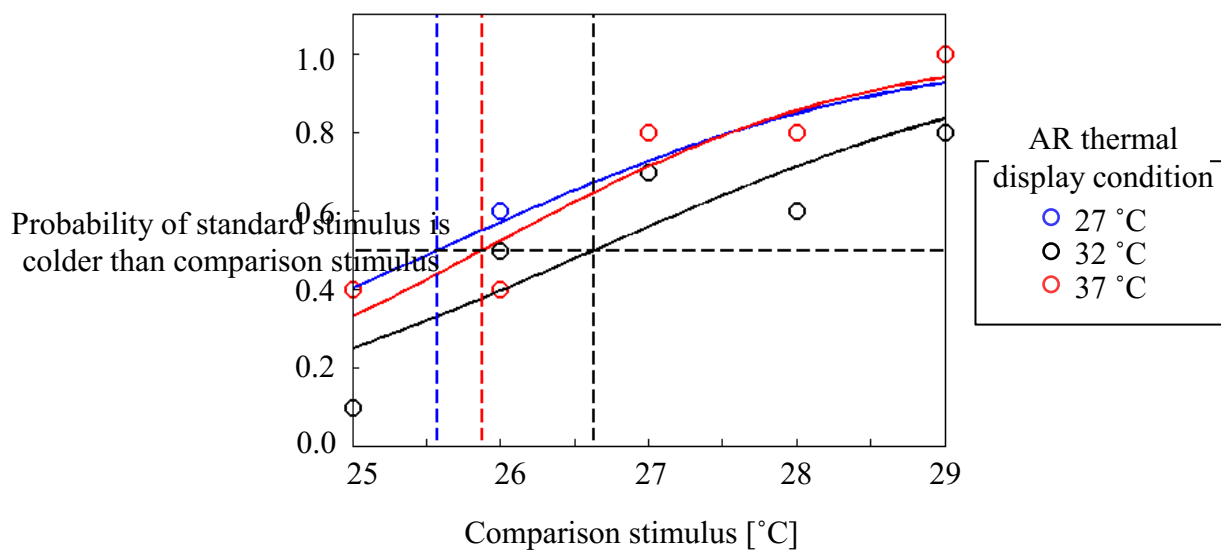
probability of standard stimulus is colder than comparison stimulus for all participants were shown in Figure 5.36 as follows. The horizontal axis shows the comparison stimulus. The fitting curve was computed using maximum likelihood estimation.

Based on Figure 5.35, the point of subjective equality (PSE) was determined for every participant in Table 5.11. Next, the mean and standard deviations of PSE were calculated and showed in Figure 5.36.

Then, dependent T-Test with a significant level of 5 % was conducted to find significant different between all conditions. The result for dependent T-Test is also showed in Figure 5.36. As a result, the mean difference of PSE values between the conditions of 27 °C and 32 °C was – 0.99 °C, which was statistically significant, $t(4) = -45.25$, $p < 0.05$. This result showed that the mean of PSE value for 27 °C to be significantly lower than 32 °C. Thus, this result proved that, when the back of the hand was cooling, the thermal perception of palm became lower; the object felt colder than actual temperature.

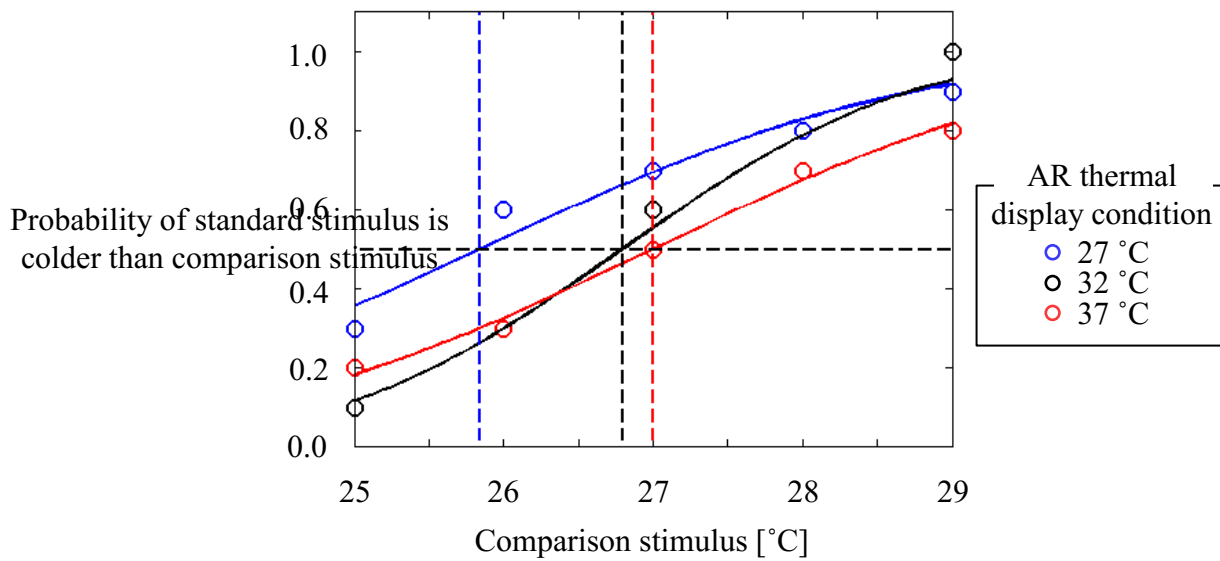


(a) Participant 1

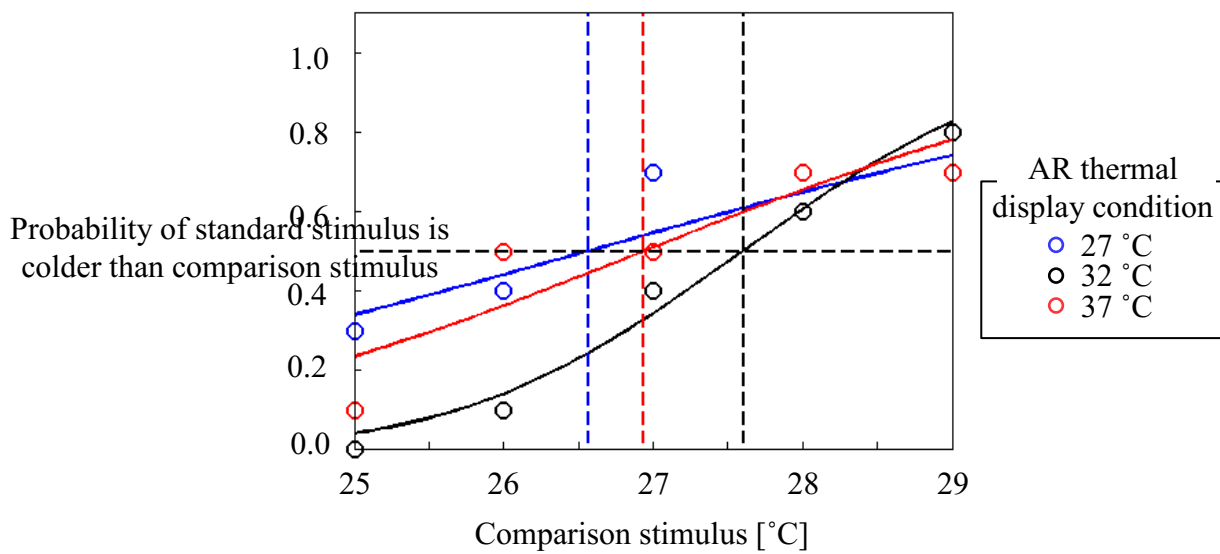


(b) Participant 2

Figure 5.35 Probability of standard stimulus is colder than comparison stimulus

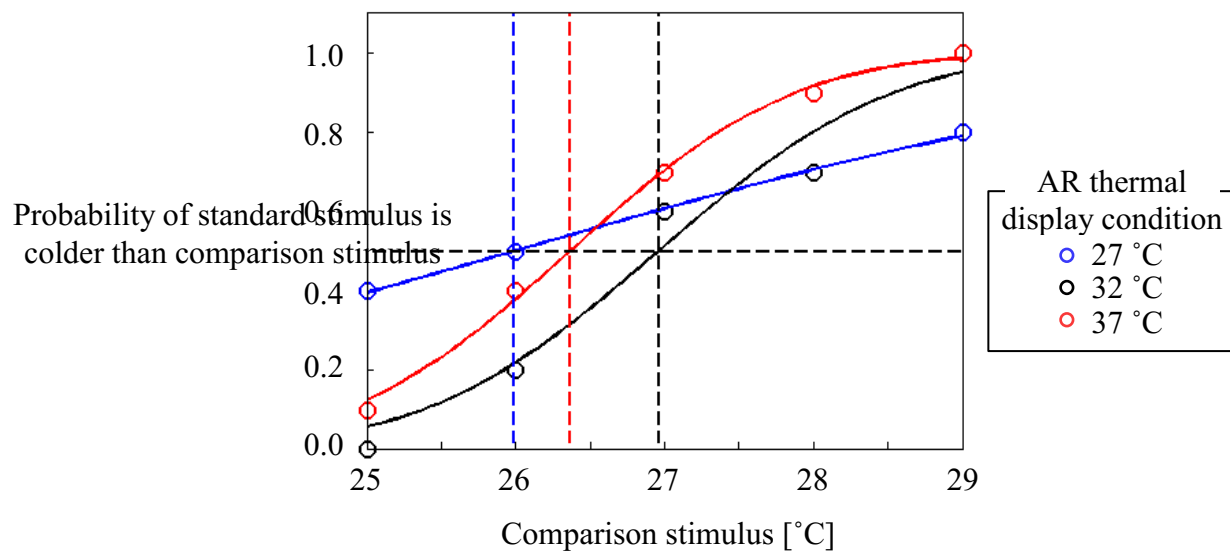


(c) Participant 3



(d) Participant 4

Figure 5.35 Probability of standard stimulus is colder than comparison stimulus



(e) Participant 5

Figure 5.35 Probability of standard stimulus is colder than comparison stimulus**Table 5.11** PSE values (Object: cold condition)

Participant	AR thermal display condition		
	27 °C	32 °C	37 °C
1	26.05	27.00	27.90
2	25.58	26.63	25.88
3	25.84	26.80	27.00
4	26.57	27.60	26.94
5	25.99	26.96	26.37
Mean	26.01	27.00	26.82
Standard deviation	0.363	0.368	0.759

unit: °C

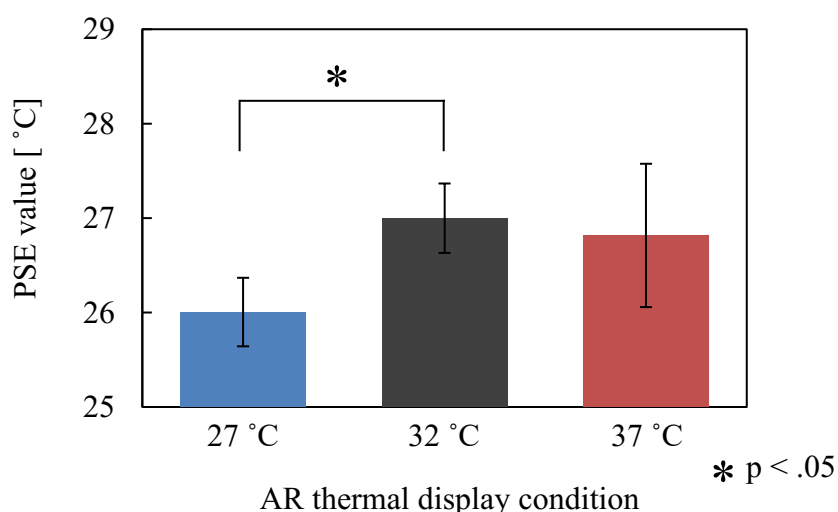


Figure 5.36 Mean of PSE values (Object: cold condition)

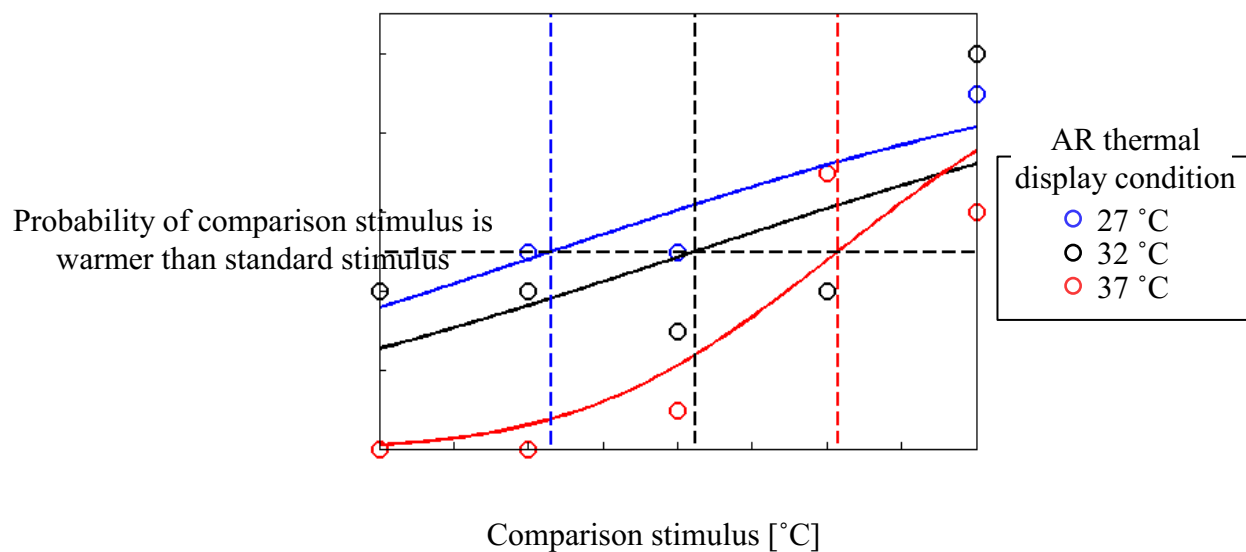
On the other hand, the mean difference of PSE values between the conditions of 37 °C and 32 °C was -0.18 °C, which was not statistically significant, $t(4) = -0.57$, $p > 0.05$. This result showed that there is no significant difference between the mean of PSE values for 37 °C and 32 °C. Therefore, in this experiment, the thermal perception of palm had no significant effect by warming up the back of hand.

Next, the warmth of standard stimulus and comparison stimulus were compared, and the probability of comparison stimulus is warmer than standard stimulus for all participants were shown in Figure 5.37. The horizontal axis and the fitting curve were as same as the former.

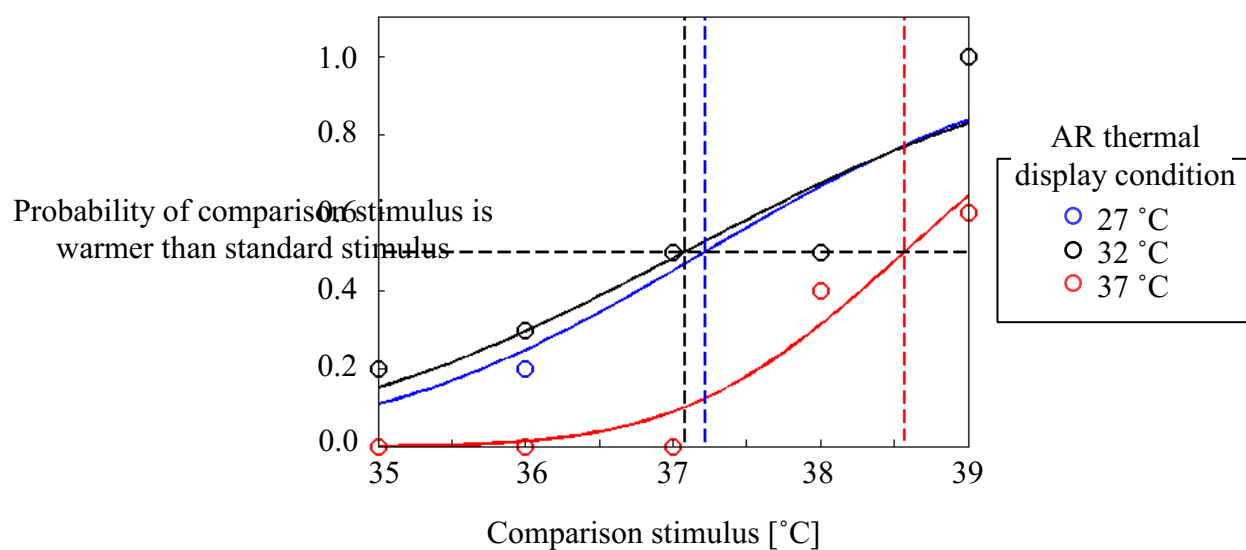
Based on Figure 5.37, the point of subjective equality (PSE) was determined for every participant in Table 5.12. Moreover, the mean and standard deviations of PSE were calculated and showed in Figure 5.38.

Then, dependent T-Test with a significant level of 5 % was conducted to find significant different between all conditions. The result for dependent T-Test is also showed in Figure 5.38. As a result, the mean difference of PSE values between the conditions of 27 °C and 32 °C was -0.39 °C, which was statistically significant, $t(4) = -2.04$, $p < 0.05$. This result showed that the mean of PSE value for 27 °C to be significantly lower than 32 °C. Thus, this result proved that,

when the back of the hand was cooling, the thermal perception of palm became lower; the object felt colder than actual temperature.

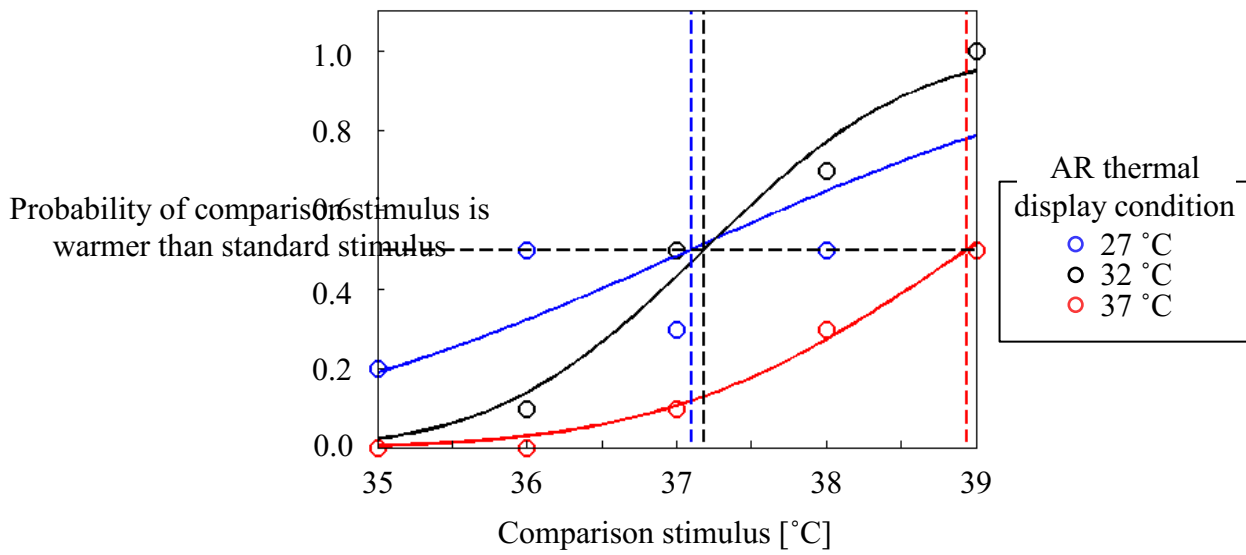


(a) Participant 1

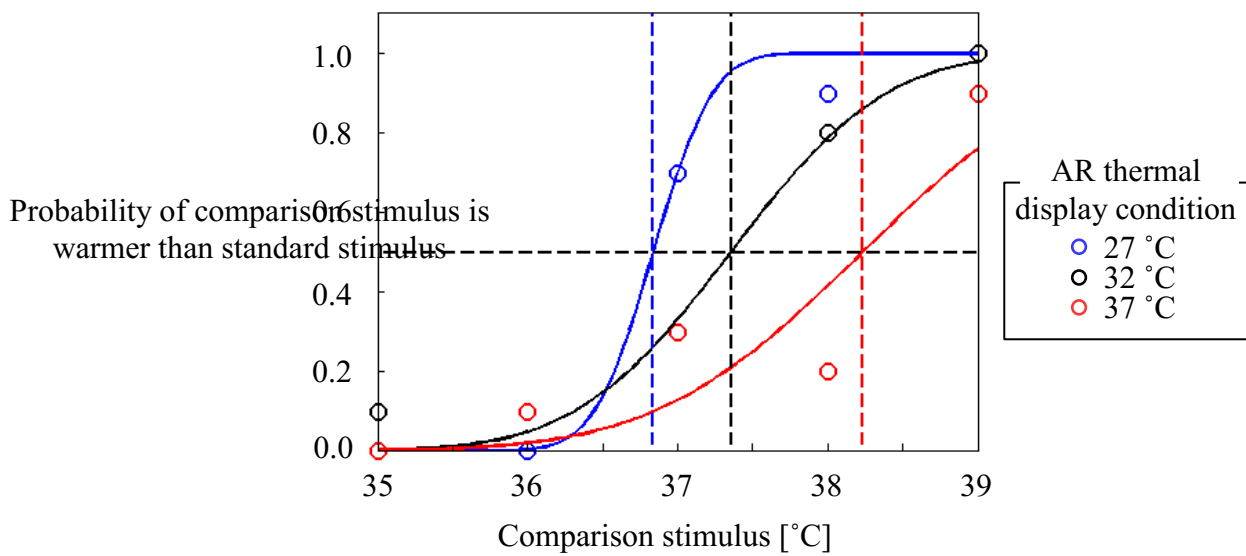


(b) Participant 2

Figure 5.37 Probability of comparison stimulus is warmer than standard stimulus

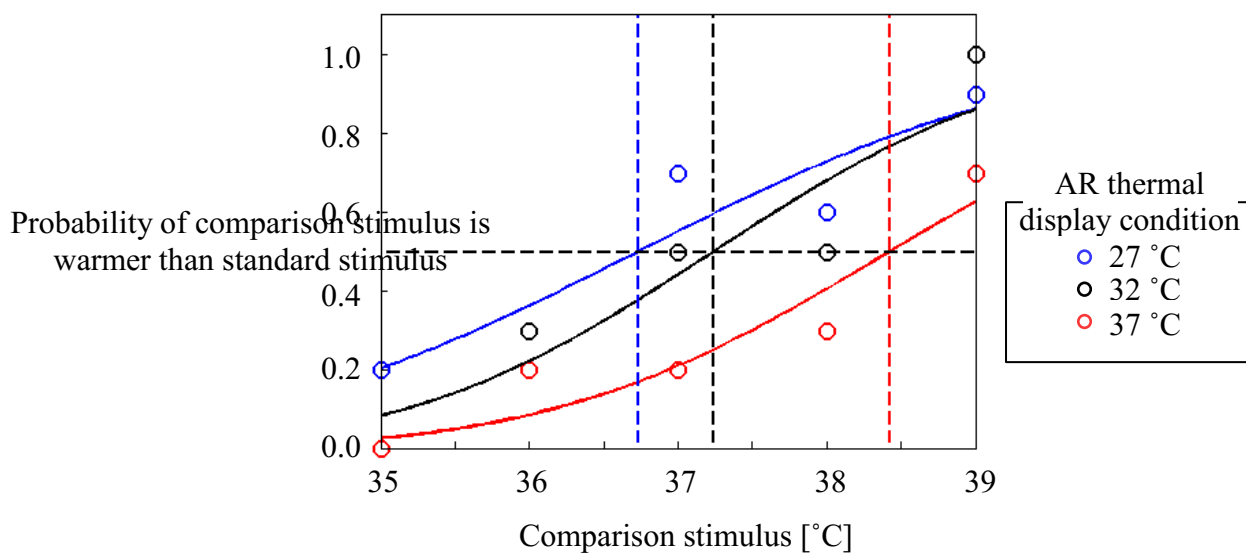


(c) Participant 3



(d) Participant 4

Figure 5.37 Probability of comparison stimulus is warmer than standard stimulus



(e) Participant 5

Figure 5.37 Probability of comparison stimulus is warmer than standard stimulus

Table 5.12 PSE values (Object: warm condition)

Participant	AR thermal display condition		
	27 °C	32 °C	37 °C
1	36.16	37.12	38.08
2	37.22	37.08	38.57
3	37.10	37.19	38.67
4	36.84	37.36	38.24
5	36.73	37.24	38.43
Mean	36.81	37.20	38.40
Standard deviation	0.413	0.108	0.243

unit: °C

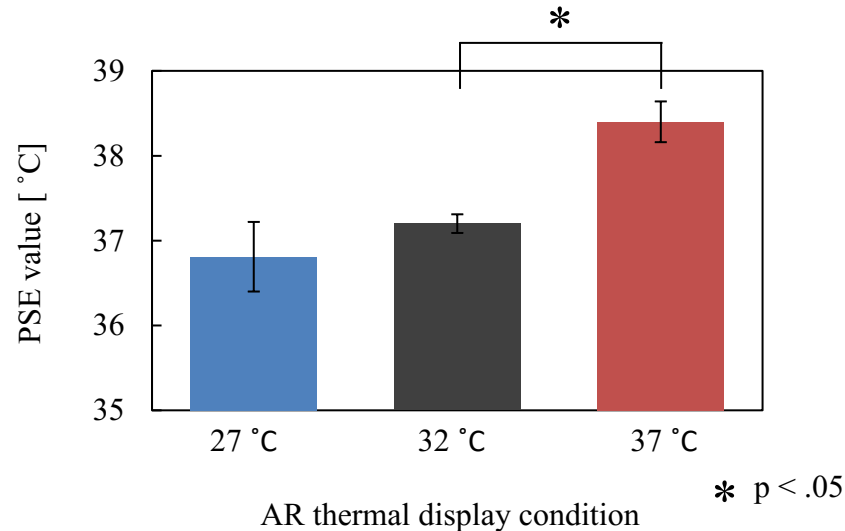


Figure 5.38 Mean of PSE values (Object: warm condition)

Furthermore, the mean difference of PSE values between the conditions of 37 °C and 32 °C was 1.20 °C, which was not statistically significant, $t(4) = 9.37, p < 0.05$. This result showed that the mean of PSE value for 37 °C to be significantly higher than 32 °C. Therefore, this result proved that, when the back of the hand was warming, the thermal perception of palm became higher; the object felt warmer than actual temperature.

As shown in Figure 5.36, when the back of hand was cooled, the thermal perception of the palm was shifted 0.99 °C towards lower temperature. Stevens et al. found that when the skin of the thenar eminence is maintained at 33 °C, the differential threshold for cooling is 0.11 °C at the rate of 1.9 °C (J. C. Stevens & Choo, 1998). Thus, by cooling the back of hand, the user can discriminate objects touched by palms although they are same in temperature.

However, there was no significant effect to thermal perception of the palm when the back of hand was warmed. In human cutaneous system, thermoreceptors are divided into two; warm and cold receptors. Due to this, the operation of one sensation may not apply equally well to each other. Here, the warm receptors were triggered on the back of hand, however, the cold receptors were triggered at the palm. Both warm and cold sensation did not summate each other well.

Table 5.13 Result conclusion

Object	AR thermal display	Augmented thermal perception	Spatial summation
Cool	Cool	Cooler *	○
	Warm	Cooler	×
Warm	Cool	Cooler	×
	Warm	Warmer *	○

*p < .05

5.4 Discussions

As shown in Figure 5.38, the thermal perception of the palm was significantly shifted at 1.20 °C towards higher temperature when the back of the hand was warmed. Stevens et al. also found that when the skin of the thenar eminence is maintained at 33 °C, the differential threshold for warming is 0.20 °C at the rate of 2.1 °C (J. C. Stevens & Choo, 1998). Thus, by warming the back of the hand, the user can discriminate warm objects although they have the same temperature.

On the other hand, there was no significant effect on the thermal perception of the palm when the back of the hand was cooled. There was a common characteristic when both receptors were triggered either on the back of the hand or on the palm, which is the decrease of PSE value, the decrease in the thermal perception of the palm. Thus, this condition needs further investigation.

Therefore, from this experiment can conclude that a cold object can be augmented to be colder than the actual, and a warm object can be augmented to be warmer than its actual temperature (see Table 5.13).

Chapter 6

CONCLUSION

In this research, works in tactile rendering and sensing have been presented to improve product development in the manufacturing industry. First, a method to quantitative hierarchically model of human tactile sensation based on human perception was proposed. The takeaways from the study are summarized in the following points:

1. A novel quantification method of human tactile sensation was proposed and developed. The objects were limited to door armrests and fabrics. The proposed idea is to replace the conventional evaluation method of product quality which is by using sensory evaluation. Hence, by measuring physical quantities, product manufacturers may evaluate their product which could be done in a quick time.
2. Tactile sensation is hierarchically classified; (1) low-order of tactile sensation (LTS) is a group of adjectives that directly describe the texture/property of the object, in other words, tactile-related adjectives, (2) high-order of tactile sensation (HTS) is a group of adjectives that describe the object by associating LTS adjectives with psychological impressions and past experiences, (3) desired tactile sensation (DTS) means adjectives that are related to one's preference which majorly affect the purchase decision-making process.
3. Two types of physical quantities are proposed to be used in the quantification. (1) the physical properties of objects that represent the characteristics or properties of the objects, (2) the physical quantities which represent the physical effects of the skin from skin-object interaction, such as deformation, vibration, thermal effects, etc.
4. Sensory evaluation was conducted by hand and forearm. Then, principal component analysis was performed to extract the common potential principal components of adjectives from each group, i.e., LTS and HTS. After that, multiple regression analysis was used to determine and examine the relationship between all principal components in

LTS and each principal component in HTS, and between all principal component in HTS and each adjective in DTS.

5. For door armrests, there were 6 LTS principal components extracted; “dampness”, “coldness”, “micro-roughness”, “macro-roughness”, “hardness” and “hollowness”. Then there were 4 HTS principal components extracted; “embracingness”, “refreshingness”, “excitingness”, and “excitingness”.
6. For fabrics when touched by hand, there were 4 LTS principal components extracted; “surface texture”, “dryness”, “downiless” and “coolness”. Then, there were 2 HTS principal components extracted; “refreshingness” and “relaxation”. For fabrics when touched by forearm, there were 3 LTS principal components extracted; “surface texture”, “softness” and “downiless”. Then, there were 3 HTS principal components extracted; “refreshingness”, “relaxation” and “elegant”.
7. The group of subjects and the dominant principal components regarding the tactile sensation of underwear knitted fabric are clarified by modeling the tactile perception system using a hierarchical structure using principal component analysis and multiple regression analysis. As a result, although the understanding of the meaning of the evaluation word pair representing the psychophysical response is common to all subjects, understanding the meaning of the evaluation word pair representing the emotional response and preference differs depending on the subjects.

To conclude, the proposed method successfully enables us to evaluate the textures of any unknown sample of door armrests and fabrics. The models developed from this research are not tested whether they are applicable to objects other than door armrests and fabrics. However, the approach proposed in this research is applicable to quantify tactile sensation for other materials too.

As for future works, linking the physical quantities with the product designing parameters may help the manufacturer to design the product’s tactile sensation before manufacturing the product. Besides, the investigation on the non-linear effect for the regression analysis between the hierarchical groups can be one of the novel findings for the future.

On top of that, the effect of spatial summation for augmentation of thermal sense was investigated in AR thermal display applications. An AR thermal display was designed and manufactured to test the phenomena of spatial summation. The proposed display was used as an AR tool to delude the material identification so that the users can experience various materials without changing the material of an object. From the overall development of the research, a few key points can be summarized;

1. As the method of display, spatial summation of symmetrical sites is proposed. The AR thermal display is placed on the back of hand in order that there is no obstruction on the palm. When the back of hand is warmed or cooled, the thermal perception of palm is augmented, so that the touched object can be deluded as a different material.
2. To confirm the phenomenon of spatial summation, two experiments were conducted. In the first experiment, the back of hand was stimulated in advance before touching the objects. On the other hand, in the second experiment, the back of hands were stimulated simultaneous with touching the objects.
3. From the first experiment, the thermal perception of palm was not significantly augmented when the back of hand was cooled or warmed. In the second experiment, the thermal perception of palm had a significant different when the object and the back of hand was cooled or warmed.
4. From the second experiment, spatial summation is confirmed to take place when the same type of receptor is triggered on the back of hand and the palm. Moreover, the experiment proved that the AR thermal display is effective for augmentation of thermal sense; cooling a cool object and warming a warm object.

In brief, the concept of spatial summation can be used as the method of display to augment the thermal sense on palm. The resting temperature of the skin on the hand is usually higher than the temperature of material encountered in the environment (Verrillo et al., 1998). Thus, if the touched objects do not have their own heat source, the result from this research can

be used to delude the material identification. Furthermore, the experiments showed that the proposed AR thermal display needs to display thermal stimulus when the user touched an object. Therefore, a sensor that can detect the touch operation of the user and a thermal display with a good response time are needed for the realization of this AR thermal display.

REFERENCES

- 3D Systems: Scanners and Haptics. (2017). Retrieved from <https://www.3dsystems.com/scanners-haptics>
- A. Gescheider, S. J. B. K. G. (2001). The frequency selectivity of information-processing channels in the tactile sensory system. *Somatosensory & Motor Research*, 18(3), 191-201. doi:10.1080/01421590120072187
- Ando, H., Watanabe, J., Inami, M., Sugimoto, M., & Maeda, T. (2007). A fingernail-mounted tactile display for augmented reality systems. *Electronics and Communications in Japan (Part II: Electronics)*, 90(4), 56-65. doi:10.1002/ecjb.20355
- Asaga, E. (2012). *Development of tactile evaluation method based on human tactile perception mechanism (in Japanese)*. (Master Thesis), Keio University, Yokohama, Japan.
- Asaga, E., Takemura, K., Maeno, T., Ban, A., & Toriumi, M. (2013). Tactile evaluation based on human tactile perception mechanism. *Sensors and Actuators A: Physical*, 203, 69-75. doi:10.1016/j.sna.2013.08.013
- Banks, W. P. (1973). Reaction time as a measure of summation of warmth. *Perception & psychophysics*, 13(2), 321-327. doi:10.3758/BF03214147
- Bau, O., & Poupyrev, I. (2012). REVEL: tactile feedback technology for augmented reality. *ACM transactions on graphics*, 31(4), 1-11. doi:10.1145/2185520.2185585
- Bau, O., Poupyrev, I., Israr, A., & Harrison, C. (2010). *TeslaTouch: electrovibration for touch surfaces*. Paper presented at the Symposium on User Interface Software and Technology.
- Behery, H. M. (2005). *Comparison of fabric hand evaluation in different cultures*: Woodhead Publishing Limited.
- Berg, S. L. (1978). Magnitude Estimates of Spatial Summation for Conducted Cool Stimuli along with Thermal Fractionation and a Case of Secondary Hyperalgesia. In: ProQuest Dissertations Publishing.
- Bergamasco, M., Allotta, B., Bosio, L., Ferretti, L., Parrini, G., Prisco, G. M., . . . Sartini, G. (1994). An arm exoskeleton system for teleoperation and virtual environments applications. In (pp. 1449-1454 vol.1442): IEEE Comput. Soc. Press.
- Bergmann Tiest, W. M. (2010). Tactual perception of material properties. *Vision Research*, 50(24), 2775-2782. doi:10.1016/j.visres.2010.10.005

- Bergmann Tiest, W. M., & Kappers, A. M. L. (2009). Cues for haptic perception of compliance. *IEEE Transactions on Haptics*, 2(4), 189-199. doi:10.1109/TOH.2009.16
- Bianchi, G., Knörlein, B., Székely, G., & Harders, M. (2006). *High Precision Augmented Reality Haptics*. Paper presented at the EuroHaptics'06.
- Bluman, A. G. (2014). *Elementary statistics - A step by step approach* (9 ed.). New York: McGraw-Hill Education.
- Caldwell, D. G., Lawther, S., & Wardle, A. (1996). *Tactile perception and its application to the design of multi-modal cutaneous feedback systems*.
- Cantin, I., & L. Dubé, L. (1999). Attitudinal Moderation of Correlation between Food Liking and Consumption. *Appetite*, 32(3), 367-381. doi:10.1006/appe.1998.0220
- Charles, E. O. (2003). What are Physical Properties and Changes? *Virtual Chembook, Elmhurst College*. Retrieved from <http://www.elmhurst.edu/~chm/vchembook/104Aphysprop.html>
- Chen, X., Barnes, C. J., Childs, T. H. C., Henson, B., & Shao, F. (2009). Materials' tactile testing and characterisation for consumer products' affective packaging design. *Materials & Design*, 30(10), 4299-4310. doi:10.1016/j.matdes.2009.04.021
- Chen, Y., Yang, Z., & Lian, L. (2005). On the development of a haptic system for rapid product development. *Computer aided design*, 37(5), 559-569. doi:10.1016/j.cad.2004.08.004
- Citrin, A. V., Stem, D. E., Spangenberg, E. R., & Clark, M. J. (2003). Consumer need for tactile input. *Journal of business research*, 56(11), 915-922. doi:10.1016/S0148-2963(01)00278-8
- Cudeck, R., & O'Dell, L. L. (1994). Applications of standard error estimates in unrestricted factor analysis: Significance tests for factor loadings and correlations. *Psychological Bulletin*, 115(3), 475-487. doi:10.1037//0033-2909.115.3.475
- Dargahi, J., & Payandeh, S. (1998, 20 March 1998). *Surface texture measurement by combining signals from two sensing elements of a piezoelectric tactile sensor*. Paper presented at the Sensor Fusion: Architectures, Algorithms, and Applications II, Orlando, FL, USA.
- Darian-Smith, I., & Johnson, K. O. (1977). Thermal Sensibility and Thermoreceptors. *Journal of Investigative Dermatology*, 69(1), 146-153. doi:10.1111/1523-1747.ep12497936
- Darian-Smith, I., Johnson, K. O., & Dykes, R. (1973). "Cold" fiber population innervating palmar and digital skin of the monkey: responses to cooling pulses. *J Neurophysiol*, 36(2), 325-346. doi:10.1152/jn.1973.36.2.325
- Dyck, P. J., Curtis, D. J., Bushek, W., & Offord, K. (1974). Description of "Minnesota Thermal Disks" and normal values of cutaneous thermal discrimination in man. *Neurology*, 24(4), 325-330. doi:10.1212/WNL.24.4.325

- Ekman, G., & Akesson, C. (1965). Roughness, smoothness, and preference. A study of quantitative relations in individual subjects. *Scandinavian journal of psychology*, 6(4), 241-253. doi:10.1037/h0021985
- Fernando, C. L., Furukawa, M., Kurogi, T., Kamuro, S., Sato, K., Minamizawa, K., & Tachi, S. (2012). *Design of TELESAR V for transferring bodily consciousness in telexistence*. Paper presented at the IEEE/RSJ International Conference on Intelligent Robots and Systems.
- Force Dimension: Products. (2017). Retrieved from <http://www.forcedimension.com/products>
- Fukumoto, M., & Sugimura, T. (2001). *Active click: tactile feedback for touch panels*. Paper presented at the Conference on Human Factors in Computing Systems.
- Gescheider, A., Bolanowski, S. J., & Hardick, K. R. (2001). The frequency selectivity of information-processing channels in the tactile sensory system. *Somatosensory & Motor Research*, 18(3), 191-201. doi:10.1080/01421590120072187
- Gescheider, G. A. (1985). *Psychophysics: Method, Theory, and Application* (2 ed.). United States of America: Lawrence Erlbaum Associates, Inc.
- Green, B., & Cruz, A. (1998). "Warmth-insensitive fields": evidence of sparse and irregular innervation of human skin by the warmth sense. *Somatosensory & Motor Research*, 15(4), 269-275. doi:10.1080/08990229870682
- Green, B. G., & Zaharchuk, R. (2001). Spatial variation in sensitivity as a factor in measurements of spatial summation of warmth and cold. *Somatosensory & Motor Research*, 18(3), 181-190. doi:10.1080/01421590120072178
- Greenspan, J. D., & Kenshalo, D. R. (1985). The Primate as a Model for the Human Temperature-sensing System: 2. Area of Skin Receiving Thermal Stimulation (Spatial Summation). *Somatosensory research*, 2(4), 315-324.
- Grohmann, B., Spangenberg, E. R., & Sprott, D. E. (2007). The influence of tactile input on the evaluation of retail product offerings. *Journal of retailing*, 83(2), 237-245. doi:10.1016/j.jretai.2006.09.001
- Guest, S., Essick, G., Dessirier, J. M., Blot, K., Lopetcharat, K., & McGlone, F. (2009). Sensory and affective judgments of skin during inter- and intrapersonal touch. *Acta Psychologica*, 130(2), 115-126. doi:<https://doi.org/10.1016/j.actpsy.2008.10.007>
- Guest, S., Mehrabyan, A., Essick, G., Phillips, N., Hopkinson, A., & McGlone, F. (2012). Physics and tactile perception of fluid-covered surfaces. *Journal of Texture Studies*, 43(1), 77-93. doi:10.1111/j.1745-4603.2011.00318.x

- Hannaford, B., Wood, L., McAfee, D. A., & Zak, H. (1991). Performance evaluation of a six-axis generalized force-reflecting teleoperator. *IEEE transactions on systems, man, and cybernetics*, 21(3), 620-633. doi:10.1109/21.97455
- Haption: Products. (2017). Retrieved from <https://www.haption.com/en/products-en.html>
- Hardy, J. D., & Oppel, T. W. (1937). Studies in Temperature Sensation. III. The Sensitivity of the Body to Heat and the Spatial Summation of the end Organ Responses. *Journal of Clinical Investigation*, 16(4), 533-540. doi:10.1172/JCI100879
- Harry, F. H. (1959). Love in Infant Monkeys. *Sci Am*, 200(6), 68-75. doi:10.1038/scientificamerican0659-68
- Hayashi, K., Tomita, M., & Tanaka, Y. (2008). Rotation of axes for principal component analysis (in Japanese). *Keisanki Tokei Gaku*, 19(2), 89-101. doi:10.20551/jscswabun.19.2_89
- Hellier, J. L. (2016). *The Five Senses and Beyond: The Encyclopedia of Perception*. Westport: Westport: ABC-CLIO, LLC.
- Hensel, H. (1973a). Cutaneous Thermoreceptors. In D. Albe-Fessard, K. H. Andres, J. A. V. Bates, J. M. Besson, A. G. Brown, P. R. Burgess, I. Darian-Smith, M. v. Düring, G. Gordon, H. Hensel, E. Jones, B. Libet, O. Oscarsson, E. R. Perl, O. Pompeiano, T. P. S. Powell, M. Réthelyi, R. F. Schmidt, J. Semmes, S. Skoglund, J. Szentágothai, A. L. Towe, P. D. Wall, G. Werner, B. L. Whitsel, Y. Zotterman, & A. Iggo (Eds.), *Somatosensory System* (pp. 79-110). Berlin, Heidelberg: Springer Berlin Heidelberg.
- Hensel, H. (1973b). *Somatosensory System* (Vol. 2). Berlin, Heidelberg: Springer Berlin Heidelberg.
- Ho, H.-N., & Jones, L. a. (2006). Contribution of thermal cues to material discrimination and localization. *Perception & psychophysics*, 68(1), 118-128. doi:10.3758/BF03193662
- Ho, H.-N., & Jones, L. A. (2007). Development and evaluation of a thermal display for material identification and discrimination. *ACM Transactions on Applied Perception*, 4(2), 13-13. doi:10.1145/1265957.1265962
- Ho, H.-N., & Sato, K. (2014). Perception characteristic of thermal sensation (in Japanese). In M. Shimojo, T. Maeno, H. Shinoda, & A. Sano (Eds.), (Revised ed., pp. 89-99). Tokyo: S & T Publisher.
- Hollins, M., Aldowski, R. F., Rao, S., & Young, F. (1993). Perceptual dimensions of tactile surface texture : A multidimensional scaling analysis. 54(6).
- Hu, J. (2004). *Structure and Mechanics of Woven Fabrics*. New York: Woodhead Publishing.

- Hu, J. (2008). *Fabric Testing (Woodhead Publishing Series in Textiles No. 76)* (1 ed.). North America: Woodhead Publishing.
- Iwata, H. (2008). History of haptic interface. In *Human Haptic Perception: Basics and Applications* (pp. 355-361). Basel: Birkhäuser Basel.
- Jones, L. A., & Berris, M. (2003, 2003). *Material discrimination and thermal perception*.
- Jones, L. a., & Ho, H. N. (2008). Warm or cool, large or small? The challenge of thermal displays. *IEEE Transactions on Haptics*, 1(1), 53-70. doi:10.1109/TOH.2008.2
- Kajimoto, H. (2012). Immobile Haptic Interface Using Tendon Electrical Stimulation. In *Advances in Computer Entertainment* (pp. 513-516). Berlin, Heidelberg: Springer Berlin Heidelberg.
- Kandel, E., Schwartz, J., Jessell, T., Siegelbaum, S., & Hudspeth, A. J. (2012). *Principle of Neural Science* (5 ed.). United States: McGraw-Hill.
- Kawabata, S. (1980). Fabric Hand and Clothing. -An Introduction. *Sen'i Kikai Gakkaishi (Journal of the Textile Machinery Society of Japan)*, 33(2), 136-142. doi:10.4188/transjtmsj.33.2_P136
- Kayseri, G. Ö., Özdil, N., & Mengüç, G. S. (2012). Sensorial Comfort of Textile Materials. In H.-Y. Jeon (Ed.), (pp. 236-266): InTech.
- Kemp, S. E., Hollowood, T., & Hort, J. (2009). *Sensory Evaluation: A Practical Handbook*. Hoboken: Hoboken: John Wiley & Sons, Incorporated.
- Kenshalo, D. R. (1970). Psychophysical Studies of Temperature Sensitivity¹ 1Much of the research reported here was supported by USPHS Grant No. NB-02992 and NSF Grant No. GB-2473. Many of the experiments were done in collaboration with J. P. Nafe, Barbara Brooks, W. W. Dawson, D. D. Duncan, Kay Fite, E. S. Gallegos, Judy McCoy, D. M. Scott, H. A. Scott, Jr., and C. E. Rice. Special appreciation to Drs. F. A. Geldard, H. Hensel, and J. C. Stevens for their critical reviews and comments on the manuscript. In W. D. Neff (Ed.), *Contributions to Sensory Physiology* (Vol. 4, pp. 19-74): Elsevier.
- Kenshalo, D. R., Decker, T., & Hamilton, A. (1967). Spatial summation on the forehead, forearm, and back produced by radiant and conducted heat. *Journal of Comparative and Physiological Psychology*, 63(3), 510-515. doi:10.1037/h0024610
- Khoudja, M., & Hafez, M. (2004). VITAL: A vibrotactile interface with thermal feedback. *IRCICA International Scientific Workshop, Lille, France* 1-7.
- Kitaguchi, S., Kumazawa, M., Morita, H., Endo, M., Sato, T., & Sukigara, S. (2015). Fabric hand, quality, aesthetic and preference of textiles through sensory evaluation. *Journal of Textile Engineering*, 61(3), 31-39. doi:10.4188/jte.61.31

- Klatzky, R. L., Pawluk, D., & Peer, A. (2013). Haptic perception of material properties and implications for applications. *Proceedings of the IEEE*, *101*(9), 2081-2092. doi:10.1109/JPROC.2013.2248691
- Lan, H. (2009). Web-based rapid prototyping and manufacturing systems: A review. *Computers in industry*, *60*(9), 643-656. doi:10.1016/j.compind.2009.05.003
- Lawless, H. T., & Heymann, H. (2010). Sensory evaluation of food. In *Sensory evaluation of food - principles and practices* (pp. 433-449). New York, NY: New York, NY: Springer New York.
- Lederman, S. J. (1974). Tactile roughness of grooved surfaces: The touching process and effects of macro- and microsurface structure. *Perception & psychophysics*, *16*(2), 385-395. doi:10.3758/BF03203958
- Lederman, S. J. (1983). Tactual Roughness Perception: Spatial and Temporal Determinants. *Canadian Journal of Psychology*, *37*(4), 498-511.
- Lederman, S. J., & Klatzky, R. L. (1987). Hand movements: A window into haptic object recognition. *Cognitive Psychology*, *19*(3), 342-368. doi:10.1016/0010-0285(87)90008-9
- Lederman, S. J., Loomis, J. M., & Williams, D. a. (1982). The role of vibration in the tactual perception of roughness. *Perception & psychophysics*, *32*(2), 109-116. doi:10.3758/BF03204270
- Maeno, T., Kobayashi, K., & Yamazaki, N. (1998). Relationship between the Structure of Human Finger Tissue and the Location of Tactile Receptors. *JSME International Journal Series C*, *41*(1), 94-100. doi:10.1299/jsmec.41.94
- Mäkinen, M., Meinander, H., & Mag, N. (2005, 2005). *Influence of Physical Parameters on Fabric Hand*. Paper presented at the Proceedings of the HAPTEX'05 workshop on haptic and tactile perception of deformable objects, Hanover, Germany.
- Marks, L. E., & Stevens, J. C. (1973). Spatial Summation of Warmth: Influence of Duration and Configuration of the Stimulus. *The American Journal of Psychology*, *86*(2), 251-267. doi:10.2307/1421436
- Marks, L. E., Stevens, J. C., & Tepper, S. J. (1976). Interaction of spatial and temporal summation in the warmth sense. *Sensory processes*, *1*(1), 87-98.
- McCabe, D. B., & Nowlis, S. M. (2003). The effect of examining actual products or product descriptions on consumer preference. *Journal of Consumer Psychology*, *13*(4), 431-439. doi:10.1207/S15327663JCP1304_10
- McGlone, F., & Reilly, D. (2010). The cutaneous sensory system. *Neuroscience & Biobehavioral Reviews*, *34*(2), 148-159. doi:10.1016/j.neubiorev.2009.08.004

- Milgram, P., & Kishino, F. (1994). A Taxonomy of Mixed Reality Visual Displays. *IEICE Transactions on Information Systems*, *E77D*(12), 1321-1329.
- Miyaoka, T. (2010a). Tactile information processing in the touch receptors and peripheral (in Japanese). In *Tactile Perceptive Mechanism and Its Application - Tactile Sensor and Tactile Display* - (1 ed., pp. 3-18). Tokyo: S & T Publisher.
- Miyaoka, T. (2010b). Tactile information processing in the touch receptors and peripheral (in Japanese). In (1 ed., pp. 3-18). Tokyo: S & T Publisher.
- Moody, W., Morgan, R., Dillon, P., Baber, C., & Wing, A. (2001). *Factors Underlying Fabric Perception*. Paper presented at the 1st Eurohaptics Conference Proceedings, Birmingham.
- Mudit Ratana, B., Harsh Vardhan, B., & Anand Vardhan, B. (2010). Haptic Technology: An Evolution towards Naturality in Communication. *International journal of advanced research in computer science*, *1*(4).
- Nagano, H., Okamoto, S., & Yamada, Y. (2014). Semantically layered structure of tactile textures. *Lecture Notes in Computer Science (including subseries Lecture Notes in Artificial Intelligence and Lecture Notes in Bioinformatics)*, *8618*, 3-9. doi:10.1007/978-3-662-44193-0_1
- Niwa, M. (1975). Hand evaluation by instrumentation. *Sen'i Kikai Gakkaishi (Journal of the Textile Machinery Society of Japan)*, *28*(9), P503-P518. doi:10.4188/transjmsj.28.9_P503
- Okamoto, S., Nagano, H., Kidoma, K., & Yamada, Y. (2016). Specification of individuality in causal relationships among texture-related attributes, emotions, and preferences. *International Journal of Affective Engineering*, *15*(1), 1-9.
- Okamoto, S., Nagano, H., & Yamada, Y. (2013). Psychophysical dimensions of tactile perception of textures. *IEEE Transactions on Haptics*, *6*(1), 81-93. doi:10.1109/TOH.2012.32
- Okamura, A. M., Richard, C., & Cutkosky, M. R. (2002). Feeling is Believing: Using a Force-Feedback Joystick to Teach Dynamic Systems. *Journal of engineering education (Washington, D.C.)*, *91*(3), 345-349. doi:10.1002/j.2168-9830.2002.tb00713.x
- Ong, S. K., Yuan, M. L., & Nee, A. Y. C. (2008). Augmented reality applications in manufacturing: a survey. *International Journal of Production Research*, *46*(10), 2707-2742. doi:10.1080/00207540601064773
- Pan, N. (2007). Quantification and evaluation of human tactile sense towards fabrics. *International Journal of Design and Nature*, *1*(1), 48-60. doi:10.2495/D&N-V1-N1-48-60

- Patapoutian, A., Peier, A. M., Story, G. M., & Viswanath, V. (2003). Sensory systems: ThermoTRP channels and beyond: mechanisms of temperature sensation. *Nature Reviews Neuroscience*, 4(7), 529-539. doi:10.1038/nrn1141
- Peck, J., & Childers, T. L. (2002). To have and to hold: the influence of haptic information on product judgments. *Journal of marketing*, 66(4), 35.
- Peck, J., & Childers, T. L. (2003). Individual Differences in Haptic Information Processing: The “Need for Touch” Scale. *The Journal of consumer research*, 30(3), 430-442. doi:10.1086/378619
- Peck, J., & Childers, T. L. (2006). If I touch it I have to have it: Individual and environmental influences on impulse purchasing. *Journal of business research*, 59(6), 765-769. doi:10.1016/j.jbusres.2006.01.014
- Pingjun, X. (2016). Haptics for Product Design and Manufacturing Simulation. *IEEE Trans Haptics*, 9(3), 358-375. doi:10.1109/TOH.2016.2554551
- Rekimoto, J. (1997). NaviCam: A Magnifying Glass Approach to Augmented Reality. *Presence: Teleoperators and Virtual Environments*, 6(4), 399-412. doi:10.1162/pres.1997.6.4.399
- Rózsa, A. J., & Kenshalo, D. R. (1977). Bilateral spatial summation of cooling of symmetrical sites. *Perception & psychophysics*, 21(5), 455-462. doi:10.3758/BF03199502
- Sakamoto, M., & Watanabe, J. (2017). Exploring Tactile Perceptual Dimensions Using Materials Associated with Sensory Vocabulary. *Frontiers in Psychology*, 8(April), 1-10. doi:10.3389/fpsyg.2017.00569
- Sarakoglou, I., Garcia-Hernandez, N., Tsagarakis, N. G., & Caldwell, D. G. (2012). A High Performance Tactile Feedback Display and Its Integration in Teleoperation. *IEEE Trans Haptics*, 5(3), 252-263. doi:10.1109/TOH.2012.20
- Saville, B. P. (1999). *Physical Testing of Textiles*. North America: Woodhead Publishing.
- Schmidt, R. F. (1986). *Fundamentals of Sensory Physiology* (Third, Revised and Expanded Edition. ed.). Berlin, Heidelberg: Springer Berlin Heidelberg : Imprint: Springer.
- Schmitt, R., Falk, B., Stiller, S., & Heinrichs, V. (2015). *Human Factors in Product Development and Design*. Paper presented at the Advances in Production Technology, Cham.
- Seeram, R., Lingling, T., Charlene, W., Susan, L., & Wee Eong, T. (2015). Medical devices : regulations, standards and practices. In *8 - Product development overview* (pp. 177-188): Elsevier Ltd.
- Shen, Y., Pomeory, C., Xi, N., & Chen, Y. (2006). Quantification and verification of automobile interior textures by a high performance tactile-haptic interface. *2006 IEEE/RSJ*

- International Conference on Intelligent Robots and Systems*, 3773-3778. doi:10.1109/IROS.2006.281762
- Shimoga, K. B. (1993). A survey of perceptual feedback issues in dexterous telemanipulation. I. Finger force feedback. In (pp. 263-270): IEEE.
- Shimojo, M. (2014). Basic of tactile sensor: Overview of sensor, and its structure and function (in Japanese). In M. Shimojo, T. Maeno, H. Shinoda, & A. Sano (Eds.), (Revised ed., pp. 191-222).
- Shirado, H., & Maeno, T. (2014). Psychological Properties of Tactile Sensation (in Japanese). In M. Shimojo, T. Maeno, H. Shinoda, & A. Sano (Eds.), *Tactile Perceptive Mechanism and its Application - Tactile Sensor and Tactile Display* - (Revised ed., pp. 100-143). Tokyo: S & T Publisher.
- Shirado, H., Maeno, T., & Nonomura, Y. (2006, 2006). *Realization of human skin-like texture by emulating surface shape pattern and elastic structure*. Paper presented at the IEEE Virtual Reality Conference (VR'06).
- Shishoo, R. L. (1995). Importance of mechanical and physical properties of fabrics in the clothing manufacturing process. *International Journal of Clothing Science and Technology*, 7(2/3), 35-42. doi:10.1108/09556229510087137
- Smith, a. M., Scott, S. H., Smith, M., & Scott, S. H. (1996). Subjective scaling of smooth surface friction. *Journal of neurophysiology*, 75(5), 1957-1962.
- Spray, D. (1986). Cutaneous Temperature Receptors. *Annual Review of Physiology*, 48(1), 625-382. doi:10.1146/annurev.physiol.48.1.625
- Stevens, J. C., & Choo, K. K. (1998). Temperature sensitivity of the body surface over the life span. *Somatosensory & Motor Research*, 15(1), 13-28. doi:10.1080/08990229870925
- Stevens, J. C., & Marks, L. E. (1971). Spatial summation and the dynamics of warmth sensation. *Perception & psychophysics*, 9(5), 391-398. doi:10.3758/BF03210236
- Stevens, J. C., & Marks, L. E. (1979). Spatial summation of cold. *Physiology and Behavior*, 22(3), 541-547. doi:10.1016/0031-9384(79)90023-4
- Stone, H., Bleibaum, R., & Thomas, H. A. (2012). *Sensory Evaluation Practices* (4th ed. ed.). Burlington: Elsevier Science.
- Taylor, M. M., Lederman, S. J., & Gibson, R. H. (1973). Tactual perception of texture. In E. Carterette & M. Friedman (Eds.), (Vol. III, pp. 251-271). New York: Academic Press.
- Tsetserukou, D., Sato, K., & Tachi, S. (2010). *ExoInterfaces: novel exoskeleton haptic interfaces for virtual reality, augmented sport and rehabilitation*. Paper presented at the ACM International Conference Proceeding Series.

- Tuorila, H., Huotilainen, A., Lähteenmäki, L., Ollila, S., Tuomi-Nurmi, S., & Urala, N. (2008). Comparison of affective rating scales and their relationship to variables reflecting food consumption. *Food Quality and Preference*, *19*(1), 51-61. doi:10.1016/j.foodqual.2007.06.007
- Vallbo, A. B., & Johansson, R. S. (1984). Properties of cutaneous mechanoreceptors in the human hand related to touch sensation. *Human neurobiology*, *3*(1), 3-14.
- Verrillo, R. T., Bolanowski, S. J., Checkosky, C. M., McGlone, F. P., Francis, C., & McGlone, F. P. (1998). Effects of hydration on tactile sensation. *Somatosensory and Motor Research*, *15*(2), 93-108. doi:10.1080/08990229870826
- Xie, X., & Livermore, C. (2016). A pivot-hinged, multilayer SU-8 micro motion amplifier assembled by a self-aligned approach. *Proceedings of the IEEE International Conference on Micro Electro Mechanical Systems (MEMS), 2016-Febru(February)*, 75-78. doi:10.1109/MEMSYS.2016.7421561
- Xie, X., & Livermore, C. (2017). Passively self-aligned assembly of compact barrel hinges for high-performance, out-of-plane mems actuators. *Proceedings of the IEEE International Conference on Micro Electro Mechanical Systems (MEMS)*, 813-816. doi:10.1109/MEMSYS.2017.7863532
- Xie, X., Zaitsev, Y., Velásquez-García, L. F., Teller, S. J., & Livermore, C. (2014). Scalable, MEMS-enabled, vibrational tactile actuators for high resolution tactile displays. *Journal of Micromechanics and Microengineering*, *24*(12), 125014-125014. doi:10.1088/0960-1317/24/12/125014
- Yamauchi, T., Okamoto, S., Konyo, M., Hidaka, Y., Maeno, T., & Tadokoro, S. (2010). Real-time remote transmission of multiple tactile properties through master-slave robot system. In (pp. 1753-1760): IEEE.
- Yarnitsky, D., & Ochoa, J. L. (1991). Warm and cold specific somatosensory systems : psychophysical thresholds, reaction times and peripheral conduction velocities. *Brain*, *114*(4), 1819-1826. doi:10.1093/brain/114.4.1819
- Zhao, Z., Huang, P., Lu, Z., & Liu, Z. (2017). Augmented reality for enhancing tele-robotic system with force feedback. *Robotics and Autonomous Systems*, *96*, 93-101. doi:10.1016/j.robot.2017.05.017

APPENDIX

A. Advance Modeling of Tactile Sensation for Fabrics

A.1 New Concept for Modeling of Tactile Sensation

The tactile perception system is a complex system with multiple inputs and multiple outputs (Taylor et al., 1973). According to Taylor et al., not only the physical characteristics and shape of the object, but also the movement and force of the hand during touch, the movement of the object, and the physical characteristics of the skin are inputs for the perception of tactile sensation (Taylor et al., 1973). Physical quantities such as skin vibration, skin deformation, and heat transfer effect when the object comes into contact with the hand are perceived by tactile receptors, transmitted to the brain through nerves, and then the texture is analyzed. Tactile sensation is expressed in various terms and becomes an output (Taylor et al., 1973). The terms of tactile expression are diverse, and the conversion of tactile receptor responses to tactile terms in the brain is extremely complex and non-linear.

For such complicated inputs and outputs relationships, as mentioned in Section 3.1.2, this research proposes to organize and understand tactile sensation hierarchically (refer Figure 3.6) (X. Chen et al., 2009; Kitaguchi et al., 2015). By modeling the complex tactile perception process actually performed by humans with a three-layer structure system, it becomes easier to understand the relationship between the evaluation terms.

For the advanced modeling of tactile sensation, the methods used to model tactile sensation are the same as the previous sections; principal component analysis is used to group similar evaluation terms (adjectives), and multiple regression analysis is used to formulate the relationship between the layers of tactile sensation. As an addition to the advanced modeling of tactile sensation, this research proposes to group subjects/participants based on their interpretation of the highest hierarchy of tactile sensation, i.e., desired tactile sensation (DTS). This is because the interpretation of the meaning of a wide variety of evaluation terms depends on the attributes of the subjects. Therefore, it is necessary to construct a tactile sensation model

with the above three-layer structure for each group of subjects with common attributes. In this research, a cluster analysis of the subjects will be performed in advance using the evaluation scores of the sensory evaluation experiment.

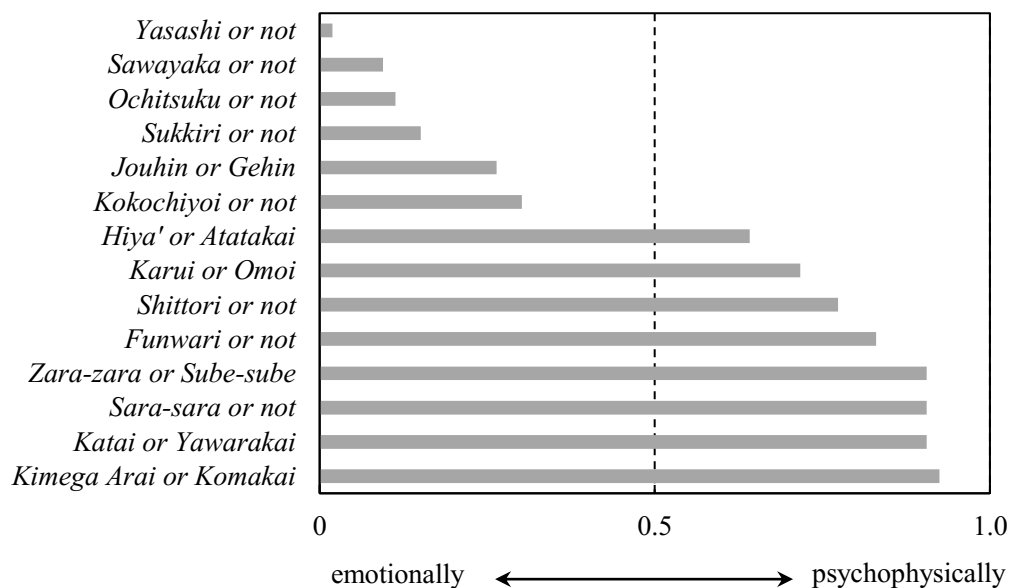


Figure A.1 Grouping of tactile sensory evaluation terms

Table A.1 Classification of evaluation term pairs

Evaluation term pairs		Evaluation term pairs	
DTS	<i>Kokochiyoi or not</i>	LTS	<i>Sube-sube or Zara-zara</i>
			<i>Kimega komakai or Arai</i>
HTS	<i>Sukkiri or not</i>		<i>Yawarakai or Katai</i>
	<i>Sawayaka or not</i>		<i>Hiya' or Atataakai</i>
	<i>Jouhin or Gehin</i>		<i>Sara-sara or not</i>
	<i>Yasashi or not</i>		<i>Funwari or not</i>
	<i>Ochitsuku or not</i>		<i>Shittori or not</i>
			<i>Karui or Omoi</i>

A.2 Classification of Adjectives

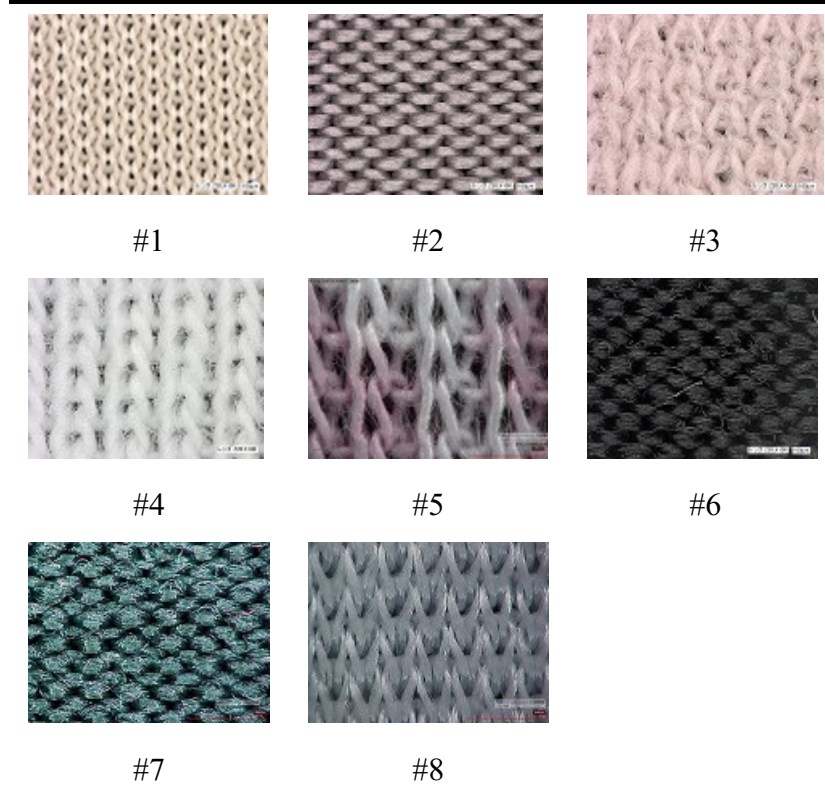
As mentioned previously, there are a wide variety of terms that express the tactile sensation of objects to be touched, not limited to knitted fabrics. Hence, 14 tactile evaluation terms are used and investigated which of the terms are related to the object's texture or related to the object with the inclusion of human emotions. The subjects were 53 adult men and women. The results are as shown in Figure A.1 and Table A.1.

A.3 Sensory Evaluation

In this section, a sensory evaluation is carried out. Eight types of knitted fabrics with

Table A.2 List of fabric samples' material, knitted method and picture

(a) Material and knitted method				
#	Material	Knitted method	Thickness [mm]	Weight [g/m ²]
1	Polyester 100 %	Interlock stitch	0.32	108
2	Cupro 93 %, Polyurethane 7 %	Plain stitch	0.49	175
3	Cotton 75 %, Nylon 20 %, Polyurethane 5 %	Half Milano rib	0.57	103
4	Cotton 100 %	Rib stitch	0.70	157
5	Acryl 100 %	Rib stitch	0.52	110
6	Cupro 59 %, Nylon 34 %, Polyurethane 7 %	Plain stitch	0.53	155
7	Cupro 53 %, Nylon 39 %, Polyurethane 8 %	Plain stitch	0.51	148
8	Cupro 60 %, Nylon 30 %, Polyurethane 10 %	Rib stitch	0.61	149

Table A.2 List of fabric samples' material, knitted method and picture(b) Picture of fabrics ($\times 100$ magnification)

different materials and knitting parameters were prepared. Table A.2 shows the materials of the selected knitted samples, the parameters of the knitting method, and the pictures. The selected knitted fabric is generally used as innerwear. Although some samples are colored, the sensory evaluation will not be affected because the visual information is blocked.

Tactile evaluation experiments were performed using the 14 evaluation word pairs (LTS: 8, HTS: 5, DTS: 1). The subjects were 40 adult females (10s: 3, 20s: 23, 30s: 7, 40s: 7). This sensory evaluation limits the subjects to women to minimize the differences in tactile perception evaluation between gender. The environment for tactile evaluation was a temperature of $25^{\circ}\text{C} \pm 1^{\circ}\text{C}$ and a humidity of $50\% \pm 5\% \text{RH}$.

Figure A.2 shows the setup of the sensory evaluation experiment. In order to eliminate the visual effect, the subjects were blindfolded and instructed to touch the sample hung on the hanger in the vertical direction (knitting direction of the sample). Prior to the evaluation, the



Figure A.2 Picture of sensory evaluation experiment

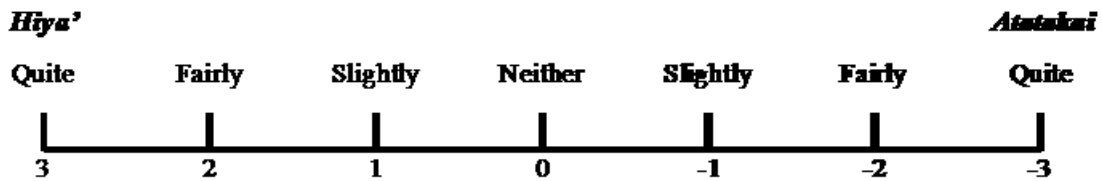


Figure A.3 Scoring of evaluation term pair

subjects were instructed to touch all the samples and recognize the difference in the tactile sensation of the evaluation target. Furthermore, in order to minimize the order effect, the evaluation was performed as follows. All the evaluation terms were evaluated in the order of LTS, HTS, and then DTS for one sample, but the evaluation terms in each hierarchy were randomly presented for each subject and each sample. The evaluation was performed using the SD method (semantic differential method) on a seven-point scale. However, the evaluation of “*Hiya'* or *Atatakai*” is considered to be affected by the time. Thus the evaluation term is asked first whenever the sample changed. Figure A.3 shows an example of the evaluation items. As can be seen from the figure, the answers to each evaluation term were scored from -3 to +3.

A.3.1 Cluster Analysis

In order to examine whether there is a common perception of DTS among the subjects, the subjects are classified and the evaluation score of "*Kokochiyoi* or not" for all the samples is used. A cluster analysis is performed by using Ward's method and squared Euclidean distance.

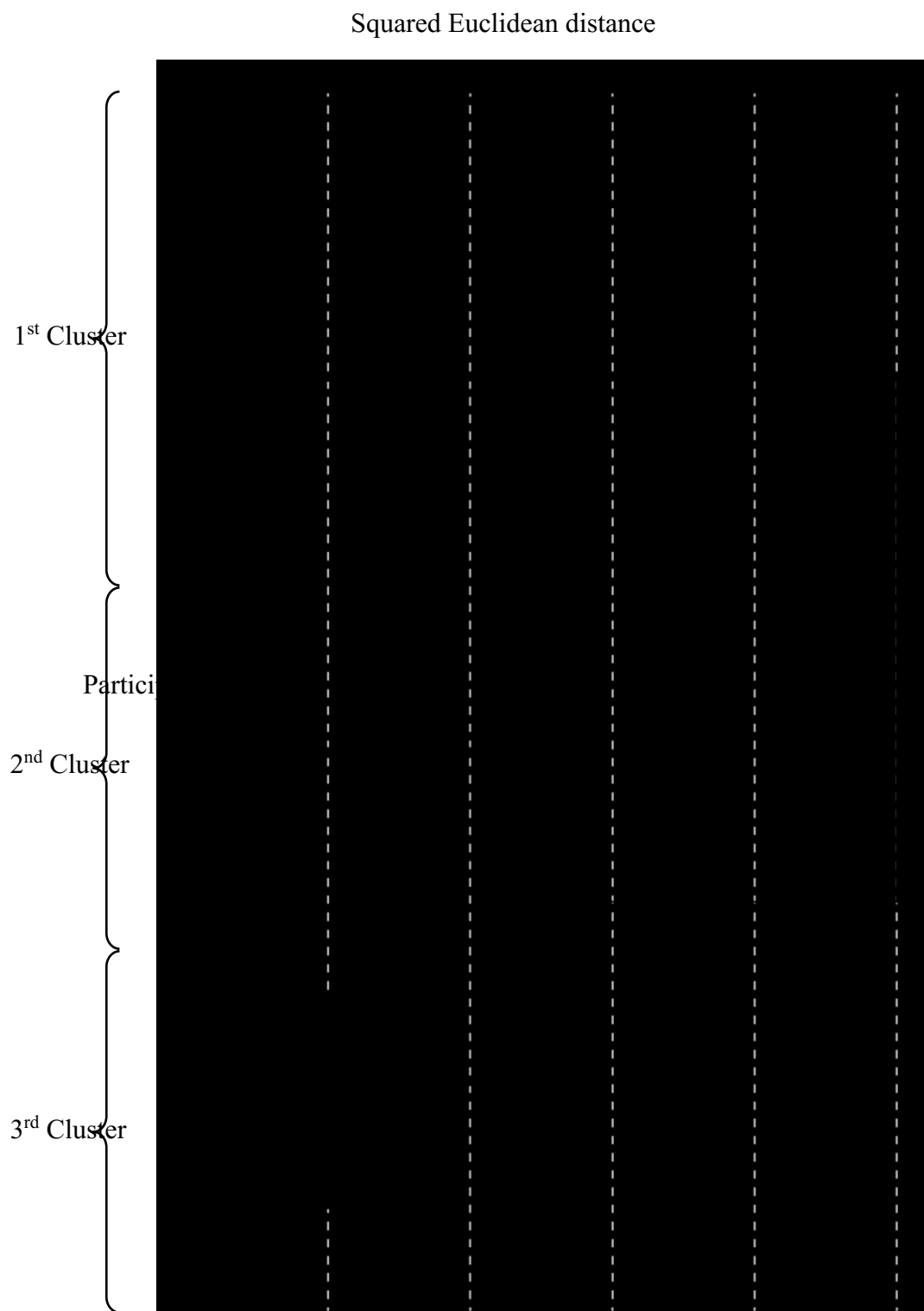


Figure A.4 Grouping of participants according to evaluation of “*Kokochiyoi*”

The result is as shown in Figure A.4. Based on the result, this research propose to classify the subjects into three groups, 1st, 2nd and 3rd clusters where there is 16 subjects, 12 subjects and 12 subjects respectively.

A.3.2 Principal Component Analysis and Multiple Regression Analysis

In order to extract the dominant tactile principal components in each cluster of subjects classified in previous section, principal component analysis is performed, and the hierarchical structure of tactile perception is constructed using multiple regression analysis. The procedures are as explained below.

First, in order to correct the variability in the tendency of responses among subjects, the scores of each subject's responses are standardized by subtracting the overall average responses scores and dividing the value by its standard deviation. Next, principal component analysis with varimax rotation is performed on the evaluation word pairs for each layer of LTS and HTS. Varimax rotation was performed on the result of the principal component analysis is to facilitate the understanding of the extracted principal components (Hayashi, Tomita, & Tanaka, 2008). However, the number of principal components are extracted until the cumulative contribution rate is 75% or more.

Then, based on the results of the principal component analysis, the average value of the principal component scores of each hierarchy was calculated. Since the evaluation word pair for DTS is " *Kokochiyoi* or not" only, the evaluation score in the tactile evaluation experiment is directly used. Finally, in order to formulate the relationship between the layers, multiple regression analysis is performed with stepwise method using the calculated principal component scores.

i) 1st Cluster's Tactile Sensation Model

Table A.3 and A.4 show the results of principal component analysis of the evaluation word pairs for LTS and HTS using the responses of the subjects that belongs to the 1st cluster. From Table A.3, four main components were extracted for LTS. In the evaluation word pair in the table, the term on the left side is on the positive score side, and the term on the right side is

Table A.3 Result for principal component analysis of 1st cluster's LTS

	Principal Component, PC			
	1	2	3	4
<i>Sube-sube</i> or <i>Zara-zara</i>	.840	.138	-.038	.133
<i>Kimega komakai</i> or <i>Arai</i>	.774	.106	.158	.301
<i>Yawarakai</i> or <i>Katai</i>	.591	.028	.420	.443
<i>Hiya'</i> or <i>Atataikai</i>	-.006	.896	.049	-.213
<i>Sara-sara</i> or not	.248	.771	-.103	.343
<i>Funwari</i> or not	.008	.000	.892	.227
<i>Shittori</i> or not	.577	-.080	.636	-.234
<i>Karui</i> or <i>Omoi</i>	.254	-.009	.124	.853
Eigenvalue	3.046	1.487	.970	.778
Contribution rate	26.414	17.936	17.899	16.261
Cumulative contribution rate	26.414	44.350	62.249	78.510

Table A.4 Result for principal component analysis of 1st cluster's HTS

	Principal Component, PC		
	1	2	3
<i>Sukkiri</i> or not	.835	-.020	-.037
<i>Sawayaka</i> or not	.825	.006	-.094
<i>Jouhin</i> or <i>Gehin</i>	.208	.853	-.068
<i>Yasashi</i> or not	-.264	.770	.213
<i>Ochitsuku</i> or not	-.086	.078	.984
Eigenvalue	1.659	1.333	.861
Contribution rate	29.964	26.525	20.567
Cumulative contribution rate	29.964	56.490	77.057

on the negative score side. Considering the contribution rate of each term to each component, the first principal component (PC 1) is "*Sube-sube/Kimega komakai/Yawarakai*", the second principal component (PC 2) is "*Hiya'/Sara-sara*", the third principal component (PC 3) represents "*Funwari/Shittori*", and the fourth principal component (PC 4) represents "*Funwari*". However, "*Yawarakai or Katai*" and "*Shittori or not*" contribute significantly to the first and third principal components, respectively, but they also show a relatively large contribution to other principal components.

On the other hand, three main components were extracted for HTS as shown in Table A.4. PC 1 is "*Sukkiri/Sawayaka*", PC 2 is "*Jouhin/Yasashi*", and PC 3 is "*Ochitsuku*". From the contribution rate, each evaluation word pair shows a large contribution rate for one principal component.

Multiple regression analysis was performed based on the above results of principal component analysis. The results are shown in Figure A.5. The straight line in the figure shows the explanatory variables extracted when estimating the preference from the main component of the lower tactile sensation to the main component of the higher tactile sensation and from the main component of the higher tactile sensation. It corresponds to the size of the standardized partial regression coefficient. The solid line shows a positive contribution, and the broken line

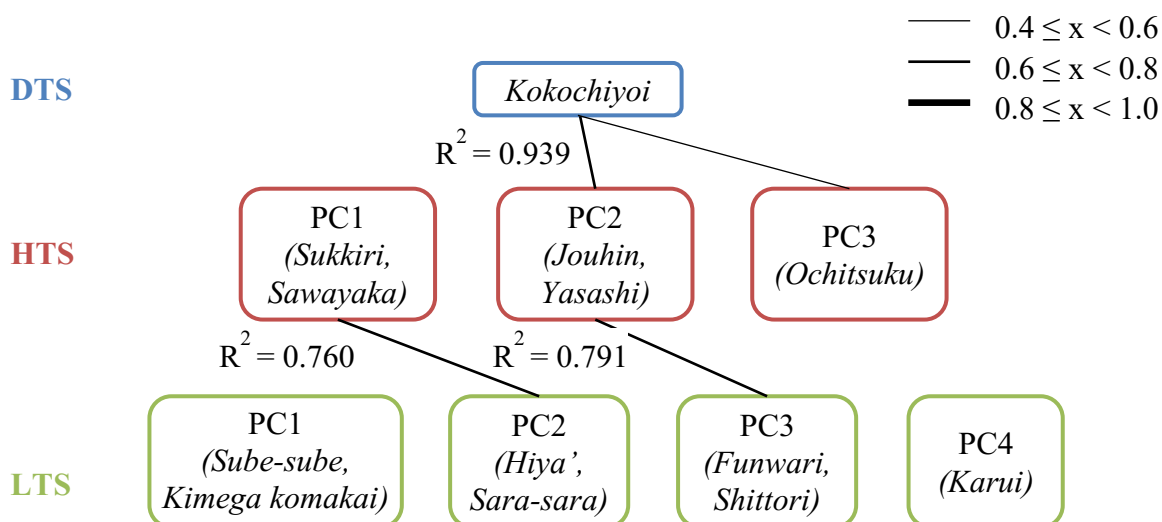


Figure A.5 1st cluster's tactile perception structure

shows a negative contribution. Each component can be expressed as the equations below.

$$D_{kokochiyoi} = (6.788 \times 10^{-1} \times H_{PC2}) + (7.959 \times 10^{-1} \times H_{PC3}) + 4.460 \times 10^{-2} \quad (\text{A.1})$$

$$H_{PC1} = (7.444 \times 10^{-1} \times L_{PC2}) \quad (\text{A.2})$$

$$H_{PC2} = (6.469 \times 10^{-1} \times L_{PC3}) \quad (\text{A.3})$$

Here, D is the sensory evaluation score of "Kokochiyoi or not", H is the principal component score of HTS, L is the principal component score of LTS, and the coefficient represents the partial regression coefficient.

According to the tactile sensation structure of the 1st cluster, "Kokochiyoi" has a strong relationship to "Jouhin/Yasashi" and "Ochitsuku" consecutively. Furthermore, the HTS of "Jouhin/Yasashi" has strong relationship to LTS of "Funwari/Shittori"

Table A.5 Result for principal component analysis of 2nd cluster's LTS

	Principal Component, PC			
	1	2	3	4
<i>Sara-sara</i> or not	.884	-.082	.076	.132
<i>Sube-sube</i> or <i>Zara-zara</i>	.723	.308	-.049	.234
<i>Kimega komakai</i> or <i>Arai</i>	.600	.386	.196	.292
<i>Yawarakai</i> or <i>Katai</i>	.530	.259	.270	.486
<i>Shittori</i> or not	.134	.945	.035	.113
<i>Funwari</i> or not	.183	.130	.893	-.016
<i>Hiya'</i> or <i>Atataikai</i>	.593	.250	-.599	.032
<i>Karui</i> or <i>Omoi</i>	.205	.091	-.089	.936
Eigenvalue	3.372	1.302	.822	.724
Contribution rate	30.657	16.347	15.911	14.827
Cumulative contribution rate	30.657	47.004	62.915	77.742

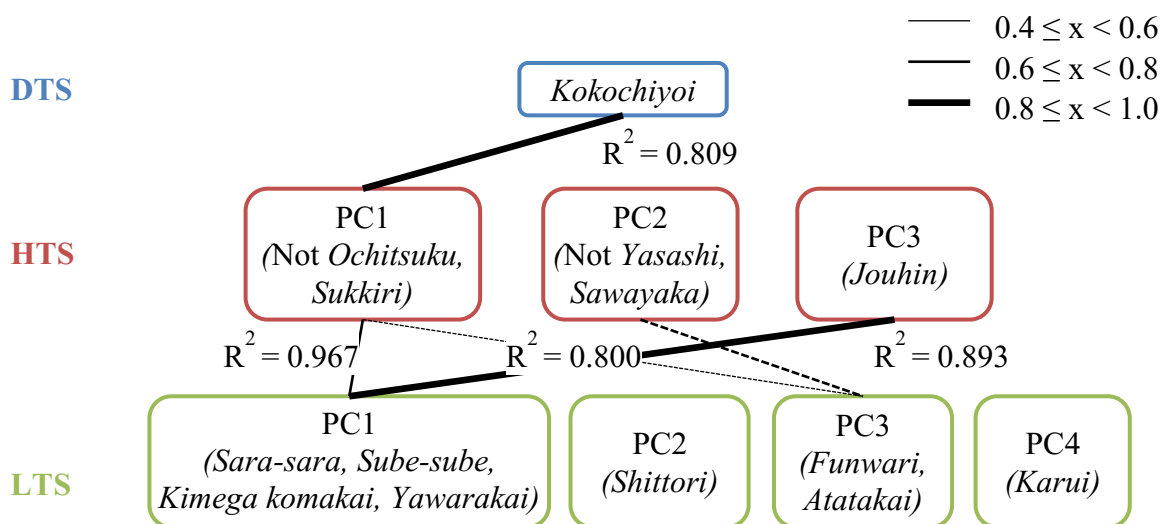
Table A.6 Result for principal component analysis of 2nd cluster's HTS

	Principal Component, PC		
	1	2	3
<i>Ochitsuku</i> or not	-.871	.021	.040
<i>Sukkiri</i> or not	.727	.267	.199
<i>Yasashi</i> or not	.010	-.912	.033
<i>Sawayaka</i> or not	.416	.633	.217
<i>Jouhin</i> or <i>Gehin</i>	.078	.054	.978
Eigenvalue	1.961	.949	.909
Contribution rate	29.314	26.138	20.923
Cumulative contribution rate	29.314	55.451	76.374

ii) 2nd Cluster's Tactile Sensation Model

Table A.5 and A.6 show the results of principal component analysis using the responses of subjects that belongs to the 2nd cluster.

As shown in Table A.5, four principal components for LTS were extracted, PC 1 is “*Sara-sara/Sube-sub/Kimega komakai/Yawarakai*”, PC 2 is “*Shittori*”, PC 3 is “*Funwari/Atatakai*” and PC 4 is “*Karui*”. However, “*Yawarakai* or *Hard*” and “*Hiya*’ or

**Figure A.6** 2nd cluster's tactile perception structure

Atataikai" contribute significantly to the second and third principal components, respectively, but they also show a relatively large contribution to other principal components.

On the other hand, three main components for HTS were extracted as shown in Table A.6. PC 1 is "*Not Ochitusku/Sukkiri*", PC 2 is "*Not Yasashi/Sawayaka*", and PC 3 is "*Jouhin*". However, "*Sawayaka or not*" contributes significantly to the second principal component, but it also shows a relatively large contribution to the first principal components.

Figure A.6 shows the result of multiple regression analysis based on the above results of principal component analysis. Each component can be expressed as the equations below.

$$D_{kokochiyoi} = (5.537 \times 10^{-1} \times H_{PC1}) + 4.842 \times 10^{-1} \quad (\text{A.4})$$

$$H_{PC1} = (5.047 \times 10^{-1} \times L_{PC1}) + (-5.260 \times 10^{-1} \times L_{PC3}) \quad (\text{A.5})$$

$$H_{PC2} = (-5.395 \times 10^{-1} \times L_{PC3}) \quad (\text{A.6})$$

$$H_{PC3} = (6.422 \times 10^{-1} \times L_{PC1}) \quad (\text{A.7})$$

Here, D is the sensory evaluation score of "*Kokochiyoi or not*", H is the principal component score of HTS, L is the principal component score of LTS, and the coefficient represents the partial regression coefficient.

According to the tactile sensation structure of the 2nd cluster, "*Kokochiyoi*" has a strong relationship to "*Not Ochitsuku/Sukkiri*". Furthermore, the HTS of "*Not Ochitsuku/Sukkiri*" has strong relationship to LTS of "*Sara-sara/Sube-sub/Kimega komakai/ Yawarakai*" and "*Funwari/Atataikai*".

iii) 3rd Cluster's Tactile Sensation Model

Table A.7 and A.8 show the results of principal component analysis using the responses of subjects that belongs to the 3rd cluster.

As shown in Table A.7, four principal components for LTS were extracted. PC 1 is "Sara-sara/Kimega komakai/Sube-sube", PC 2 is "Karui/Yawarakai", PC 3 is "Funwari" and PC 4 is "Shittori". However, "Hiya' or Atataikai" contribute significantly to the third principal components, respectively, but they also show a relatively large contribution to other principal components.

Table A.7 Result for principal component analysis of 3rd cluster's LTS

	Principal Component, PC			
	1	2	3	4
<i>Sara-sara</i> or not	.852	.224	-.056	.058
<i>Kimega komakai</i> or <i>Arai</i>	.807	.233	.103	.094
<i>Sube-sube</i> or <i>Zara-zara</i>	.751	.313	.056	.328
<i>Karui</i> or <i>Omoi</i>	.283	.880	-.028	-.013
<i>Yawarakai</i> or <i>Katai</i>	.258	.626	.246	.388
<i>Funwari</i> or not	.205	.056	.869	.170
<i>Hiya'</i> or <i>Atataikai</i>	.528	-.060	-.646	.156
<i>Shittori</i> or not	.155	.094	.054	.944
Eigenvalue	3.413	1.374	.841	.659
Contribution rate	30.422	17.306	15.667	15.194
Cumulative contribution rate	30.422	47.727	63.395	78.589

Table A.8 Result for principal component analysis of 3rd cluster's HTS

	Principal Component, PC		
	1	2	3
<i>Sawayaka</i> or not	.849	.061	.034
<i>Sukkiri</i> or not	.838	.061	-.034
<i>Jouhin</i> or <i>Gehin</i>	.203	.840	.002
<i>Ochitsuku</i> or not	-.072	.775	.270
<i>Yasashi</i> or not	.007	.177	.971
Eigenvalue	1.728	1.364	.741
Contribution rate	29.376	26.892	20.372
Cumulative contribution rate	29.376	56.268	76.641

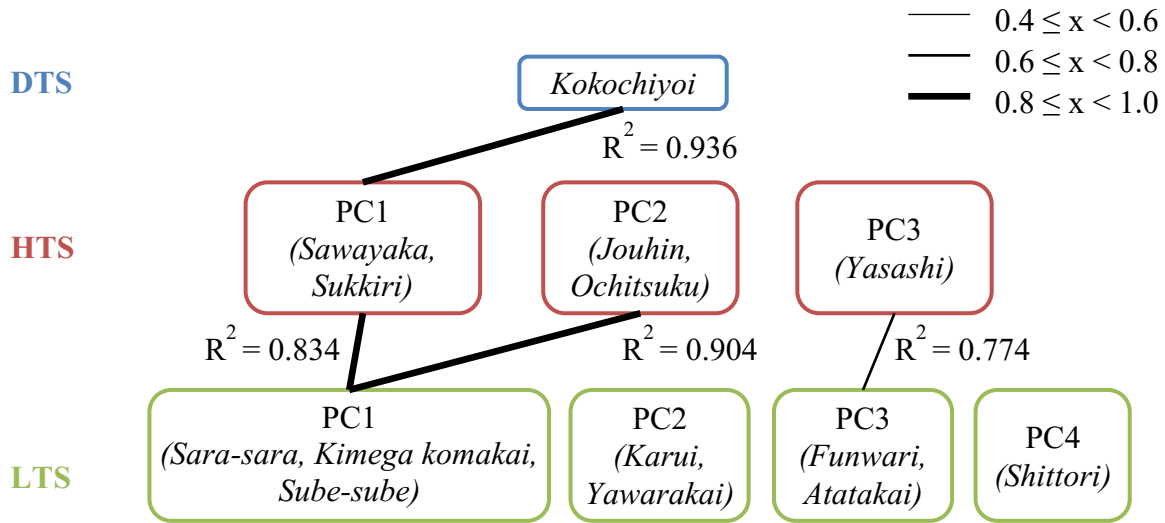


Figure A.7 3rd cluster's tactile perception structure

On the other hand, three main components for HTS were extracted, as shown in Table A.8. PC 1 is "Sawayaka/Sukkiri", PC 2 is "Jouhin/Ochitsuku", and PC 3 is "Yasashi".

Figure A.7 shows the results of multiple regression analysis based on the above results of principal component analysis. Each component can be expressed as the equations below.

$$D_{kokochiyoi} = (1.136 \times H_{PC1}) - 5.500 \times 10^{-3} \quad (\text{A.8})$$

$$H_{PC1} = (6.093 \times 10^{-1} \times L_{PC1}) \quad (\text{A.9})$$

$$H_{PC2} = (3.035 \times 10^{-1} \times L_{PC1}) \quad (\text{A.10})$$

$$H_{PC3} = (4.914 \times 10^{-1} \times L_{PC3}) \quad (\text{A.11})$$

Here, D is the sensory evaluation score of "Kokochiyoi or not", H is the principal component score of HTS, L is the principal component score of LTS, and the coefficient represents the partial regression coefficient.

According to the tactile sensation structure of the 3rd cluster, "Kokochiyoi" has a strong relationship to "Sawayaka/Sukkiri". Furthermore, the HTS of "Sawayaka/Sukkiri" has a strong relationship to LTS of "Sara-sara /Kimega komakai/Sube-sube".

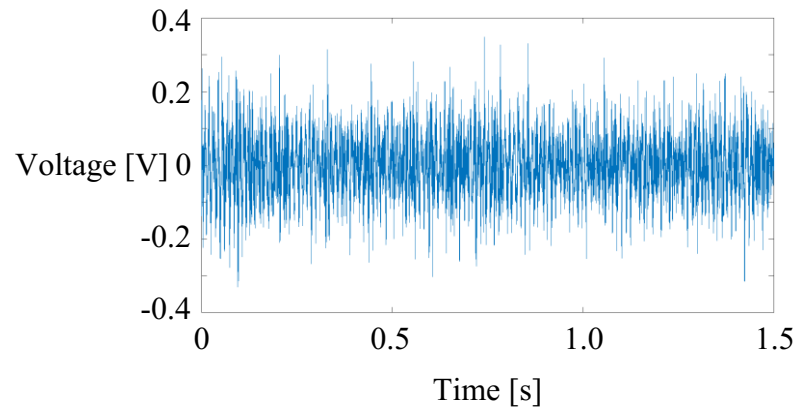
Table A.9 Dominant component for HTS and LTS for each cluster.

	1 st Cluster	2 nd Cluster	3 rd Cluster
HTS	<i>Jouhin</i>	Not <i>Ochitsuku</i>	<i>Sawayaka</i>
	<i>Yasashi</i>	<i>Sukkiri</i>	<i>Sukkiri</i>
LTS	<i>Funwari</i>	<i>Sara-sara</i>	<i>Sara-sara</i>
	<i>Shittori</i>	<i>Sube-sube</i>	<i>Kimega komakai</i>
		<i>Kimega komakai</i>	<i>Sube-sube</i>
		<i>Funwari</i>	
		<i>Hiya'</i>	

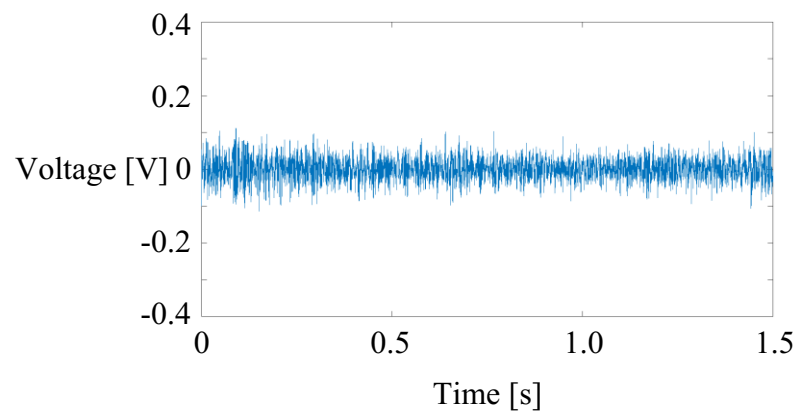
A.4 Discussions

From the previous section, each cluster shows differences in the dominant components of HTS and LTS that are related to “*Kokochiyoi*”. The differences are summarized in Table A.9. Dominant components of HTS are different in 2nd and 3rd clusters, but the dominant components of LTS are mostly similar. The cluster analysis results (refer Figure A.4) also shows that when the squared Euclidean distance is at 11, 2nd and 3rd cluster can be combined to form a single cluster. In other words, there is a large difference between the tactile perception structure of the 1st cluster and the 2nd/3rd cluster, but there is a similarity in the tactile perception structure of the 2nd cluster and the 3rd cluster.

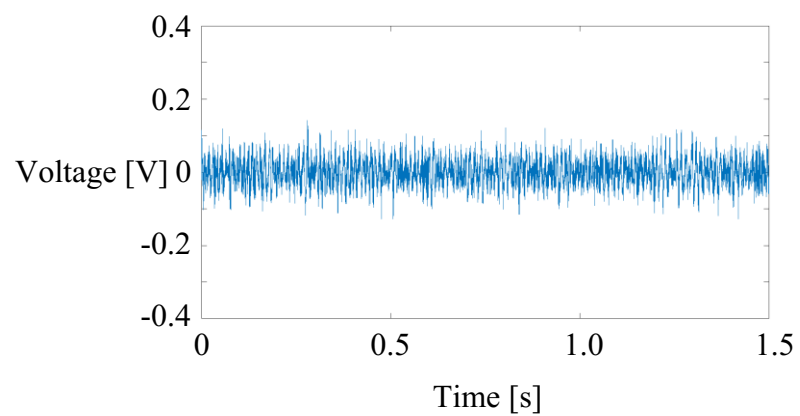
B. Vibration Measuring Results in Chapter 4, Section 4.2.1



(a) Sample #1

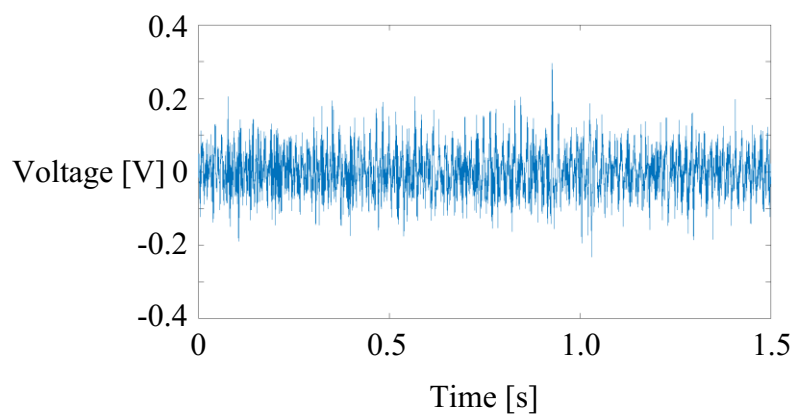


(b) Sample #2

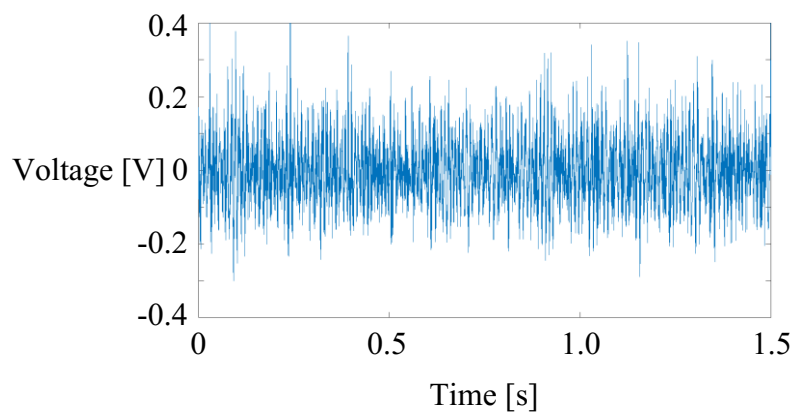


(c) Sample #3

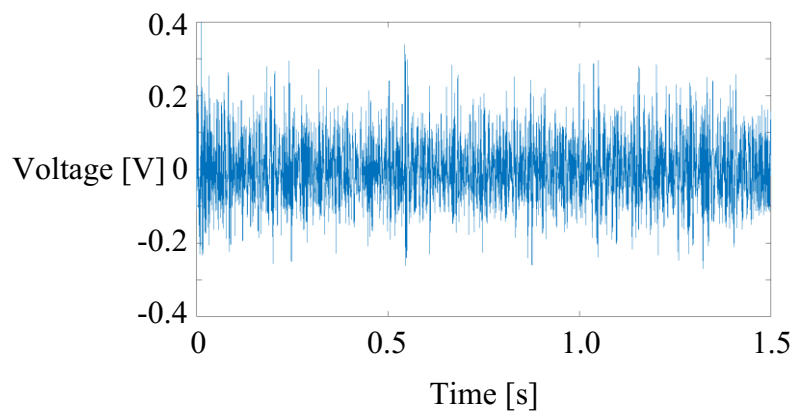
Figure B.1 Vibration measuring results



(d) Sample #4



(e) Sample #5



(f) Sample #6

Figure B.1 Vibration measuring results (continued from previous page)

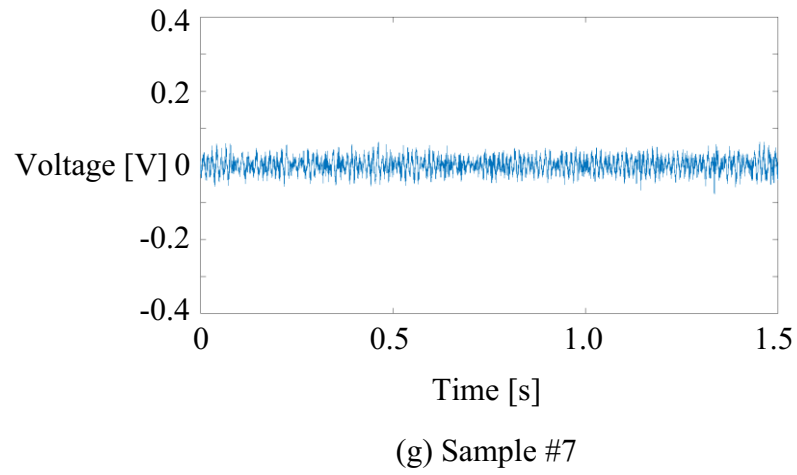
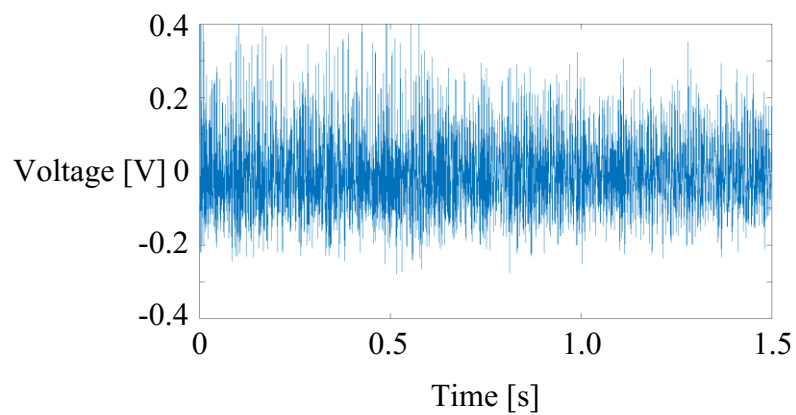
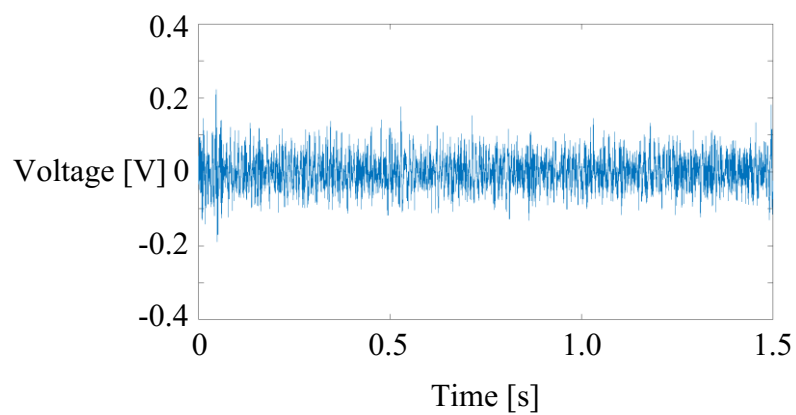


Figure B.1 Vibration measuring results (continued from previous page)

C. Vibration Measuring Results in Chapter 4, Section 4.2.2 and Section 4.2.3



(a) Sample #8



(b) Sample #9

Figure C.1 Vibration measuring results for verification test

D. Programming for Thermal Feedback Control in Chapter 5, Section 5.2.3

```
#define PWM1 (7)      // PWM1 connected to digital pin 7
#define PWM2 (6)      // PWM2 connected to digital pin 6

const int analogInPin = A5; // Output sensor connected to A0
double Vout = 0; // Initial value of sensor voltage

//SET A//
double Tc = 0; // Initial value of current temperature
double Ts = 37; // Initial value of set temperature

// Gain for P control
int Kp = 90;

//Gain for I control
int Ki = 20;
int PWMvalue = 0; // PWM's value
float dt=0.01;
float error;
float integral = 0;

void setup() {
  pinMode(PWM1, OUTPUT); // initialize the D7 as an output
  pinMode(PWM2, OUTPUT); // initialize the D6 as an output
  pinMode(analogInPin1, INPUT); // initialize the A0 as an input
  Serial.begin(9600); // initialize serial communications
}
```

```
void loop() {  
  
  // Detect the current temperature//  
  //SET A//  
  Vout1 = analogRead(analogInPin1);  
  Vout1 = Vout1*5/1023;  
  Tc1 =    -0.01393*Vout1*Vout1*Vout1*Vout1*Vout1  
+0.35720*Vout1*Vout1*Vout1*Vout1  
-3.58061*Vout1*Vout1*Vout1  
+18.04735*Vout1*Vout1  
-51.54273*Vout1+84.22417;  
  Serial.println(Tc );  
  
  //Calculate error  
  error=Ts-Tc;  
  
  //Integration  
  if(abs(error)>0.01 && abs(error)<1.2){  
    integral = integral + error*dt;  
  }  
}
```

```
//Calculate PWM's value

PWMvalue1 = Kp*error1 + Ki*integral1;

//Thermal Feedback//

//SET A//

// if Peltier's temperature is colder than the set temperature
if (PWMvalue1>0){
    if(PWMvalue>255)PWMvalue = 255;
    analogWrite(PWM1, PWMvalue);
    analogWrite(PWM2, 0);
}

// if Peltier's temperature is hotter than the set temperature
else if(PWMvalue<0){
    PWMvalue = -1*PWMvalue;
    if(PWMvalue1>255)PWMvalue1 = 255;
    analogWrite(PWM1, 0);
    analogWrite(PWM2, PWMvalue);
}

delay(10);

}
```

Figure D.1 Programming for Thermal Feedback Control